

# **Sub-Optimum Day-Ahead Power Dispatch for a Mixed Generation System considering Emission and Energy Storage for Semi-Liberalized Power Market**

**Banghao Zhou**

**A thesis presented in fulfillment of the requirements for the degree  
*of Doctor of Philosophy***

**Department of Electronic and Electrical Engineering**

**University of Strathclyde, Glasgow, UK**

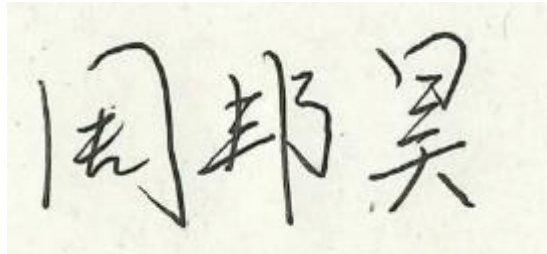
**September 2022**

# Declaration of Author's Right

This thesis is the result of the author's original research. It has been composed by the author and has not been previously submitted for the examination which has led to the award of a degree.

The copyright of this thesis belongs to the author under the terms of the United Kingdom Copyright Acts as qualified by the University of Strathclyde Regulation 3.50. The due acknowledgement must always be made of the use of any material contained in, or derived from, this thesis.

Signed:

A photograph of a handwritten signature in black ink on a light-colored background. The signature consists of three Chinese characters: 周 (Zhou), 邦 (Bang), and 昊 (Hao), which together read 'Zhou Banghao'.

Date: 2022/09/1

# Acknowledgements

I would like to express a deep sense of gratitude to the following people, without whom I would not have been able to complete this Ph.D. program, and without whom I would not have made it through my life in the UK.

First and foremost, I would like to thank my supervisor Professor Kwok Lo for his continuous support, encouragement, and guidance. His immense knowledge, motivation, enthusiasm, and patience contribute tremendously to the accomplishment of my Ph.D. in time. Moreover, his rigorous research attitudes, innovative ideas, and efficient research methods benefit me throughout my lifetime, which also illuminates my career life.

Grateful acknowledgement is made to my friends, Lingxi Zhang, Su Wang, Kai Huang, Haijie Qi, and for all concerns and companies in the past time.

Finally, I would like to express my most gratitude to my family for their support and understanding during my life in the UK.

# Abstract

This thesis concentrates on the development of a modified 15-minute interval and cost-based model using dynamic programming (DP) for resolving the day-ahead optimization dispatch schedule of thermal unit commitment (UC) problem including emission, renewable energy resources (RES) costs, and battery energy storage system to mitigate greenhouse gas emissions at minimal possible operation cost under special China semi-liberalized power market.

Besides this, a novel modelling approach of Double Cubic power curve of wind turbine is developed to express the relationship between the output power of the wind turbine with the wind speed based on considering the inflection point in the nonlinear portion of the wind power curve.

A novel model of forecasting wind speed is developed based on using Weibull method and adding two types of forecasting correction values based on white noise generated by a random number generator to stochastically simulate forecasting wind speeds.

The proposed models are tested on a China provincial power network with some unavailable data supplemented from IEEE standard test system.

# Contents

<b>ACKNOWLEDGEMENTS</b> .....	<b>3</b>
<b>ABSTRACT</b> .....	<b>4</b>
<b>CONTENTS</b> .....	<b>5</b>
<b>LIST OF FIGURES</b> .....	<b>8</b>
<b>LIST OF TABLES</b> .....	<b>10</b>
<b>LIST OF ABBREVIATIONS</b> .....	<b>12</b>
<b>LIST OF SYMBOLS</b> .....	<b>14</b>
<b>CHAPTER 1 INTRODUCTION</b> .....	<b>19</b>
1.1 BACKGROUND OF POWER SYSTEM AND MARKET IN CHINA .....	19
1.1.1 <i>Two Rounds of Power Sector Reform in China</i> .....	21
1.1.2 <i>Power Issues in China Market</i> .....	24
1.1.3 <i>Further Motivation for the New Reform</i> .....	28
1.2 OBJECTIVES .....	29
1.3 ORIGINAL CONTRIBUTIONS .....	32
1.4 THESIS STRUCTURE .....	34
1.5 PUBLICATION.....	36
<b>CHAPTER 2 LITERATURE REVIEW</b> .....	<b>37</b>
2.1 INTRODUCTION.....	37
2.2 REVIEW OF MODELLING METHODOLOGY .....	38
2.2.1 <i>Renewable Energy Source Models</i> .....	38
2.2.2 <i>Unit Commitment Problem Model</i> .....	44
2.2.3 <i>Battery Energy Storage System Model</i> .....	48
2.3 REVIEW OF UNIT COMMITMENT.....	49
2.3.1 <i>Unit Commitment Problem Formulation</i> .....	49
2.3.2 <i>Unit Commitment Environment and Objective</i> .....	51
2.3.3 <i>Unit Commitment Constraints</i> .....	52
2.3.4 <i>Unit Commitment Problem Solving Techniques</i> .....	55
2.4 SUMMARY.....	62
<b>CHAPTER 3 WIND ENERGY AND POWER CURVE MODELLING</b> .....	<b>64</b>
3.1 INTRODUCTION.....	64
3.2 OVERVIEW OF WIND ENERGY.....	65
3.2.1 <i>Background</i> .....	65
3.2.2 <i>Development</i> .....	65
3.2.3 <i>Technology</i> .....	67

3.3	WIND POWER CURVE.....	70
3.3.1	<i>Theoretical Wind Power Output</i> .....	70
3.3.2	<i>Wind Turbine</i> .....	70
3.3.3	<i>Power Curve</i> .....	73
3.3.4	<i>Power Curve Modelling</i> .....	75
3.4	PROPOSED MODELLING METHOD .....	79
3.4.1	<i>Modelling Issue of Cubic Approach</i> .....	79
3.4.2	<i>Double Cubic Power Curve</i> .....	81
3.4.3	<i>Results Demonstration</i> .....	91
3.5	CASE STUDY AND DISCUSSION .....	92
3.6	SUMMARY.....	96
<b>CHAPTER 4 FORMULATION AND PROPOSED SOLUTION TO THERMAL UNIT COMMITMENT PROBLEM .....</b>		<b>97</b>
4.1	INTRODUCTION.....	97
4.2	FORMULATION AND MODELLING OF UNIT COMMITMENT PROBLEM .....	98
4.2.1	<i>Total Operation Cost Function</i> .....	98
4.2.2	<i>System Constraints of Unit Commitment</i> .....	100
4.3	UNIT COMMITMENT SOLUTION BY MODIFIED DYNAMIC PROGRAMMING .....	103
4.3.1	<i>Dynamic Programming</i> .....	103
4.3.2	<i>Optimization Methods</i> .....	105
4.3.3	<i>Unit Commitment by Proposed Dynamic Programming</i> .....	107
4.4	CASE STUDY AND DISCUSSION .....	112
4.4.1	<i>Background Data Description</i> .....	112
4.4.2	<i>Case I with Conventional Dynamic Programming</i> .....	119
4.4.3	<i>Case II with Sequential Dynamic Programming</i> .....	120
4.4.4	<i>Case III with Different Level of Spinning Reserves</i> .....	122
4.4.5	<i>Case Study Discussion</i> .....	124
4.5	SUMMARY.....	126
<b>CHAPTER 5 MODELLING CONSTRUCTION OF RENEWABLE ENERGY SOURCES AND BATTERY ENERGY STORAGE SYSTEM .....</b>		<b>127</b>
5.1	INTRODUCTION.....	127
5.2	SOLAR POWER MODELLING .....	129
5.2.1	<i>Modelling Approach of Photovoltaic Module</i> .....	129
5.2.2	<i>A Novel Modelling Approach of Forecasting Solar Irradiance</i> .....	131
5.2.3	<i>Simulation Results Demonstration of Solar Irradiance</i> .....	135
5.3	WIND SPEED AND WIND POWER COST MODELLING .....	139
5.3.1	<i>Weibull Method for Wind Speed</i> .....	139
5.3.2	<i>A Novel Modelling Approach of Forecasting Wind Speed</i> .....	141
5.3.3	<i>Simulation Model Demonstration of Wind Speed</i> .....	152

5.3.4	<i>Modelling of Wind Power Cost</i> .....	155
5.4	STORAGE SYSTEM .....	157
5.4.1	<i>Modelling Approach of Battery Energy Storage System Cost</i> .....	157
5.4.2	<i>Simulation Model Demonstration of Battery Energy Storage System</i> .....	160
5.5	SUMMARY.....	162
<b>CHAPTER 6 CASE STUDY .....</b>		<b>164</b>
6.1	INTRODUCTION .....	164
6.2	CASE STUDY DESCRIPTION .....	165
6.2.1	<i>Case Model Description</i> .....	165
6.2.2	<i>Base System Description</i> .....	167
6.3	CASE STUDY RESULTS AND ANALYSIS .....	180
6.3.1	<i>Simulation Results</i> .....	181
6.3.2	<i>Discussion of Cases A, B, C and D Results</i> .....	191
6.4	SUMMARY.....	201
<b>CHAPTER 7 CONCLUSION AND FURTHER WORK.....</b>		<b>202</b>
7.1	CONCLUSION .....	202
7.2	FURTHER WORK.....	209
<b>APPENDIX .....</b>		<b>211</b>
<b>REFERENCES .....</b>		<b>219</b>

# List of Figures

FIGURE 1.1: ELECTRICITY CONSUMPTION OF CHINA'S WHOLE SOCIETY IN 2015 – 2020 .....	19
FIGURE 1.2: POWER MIX IN CHINA .....	20
FIGURE 2.1: IMPACT OF THE TIME INTERVAL ON THE COST CALCULATION .....	47
FIGURE 3.1: WORLD INSTALLED WIND POWER CAPACITY AND GROWTH RATES, 2000-2020.....	66
FIGURE 3.2: THE POWER CURVE WITH ITS ASSOCIATED CP CURVE FOR AN ENERCON E-126 EP4 / 4.2 MW WIND TURBINE.....	72
FIGURE 3.3: TYPICAL POWER CURVE OF A REGULATED WIND TURBINE .....	74
FIGURE 3.4: STRUCTURE CHART OF PROPOSED POWER CURVE OF A REGULATED WIND TURBINE .....	79
FIGURE 3.5: STRUCTURE CHART OF POWER CURVE OF WIND TURBINE WITH ITS ASSOCIATED CP CURVE .....	80
FIGURE 3.6: POWER CURVE OF CUBIC MODEL FOR A REGULATED WIND TURBINE .....	81
FIGURE 3.7: EXAMPLE CHART OF CUBIC CURVES.....	82
FIGURE 3.8: EXPLANATION CHART OF COMBINED CURVE BASED ON THE APPROACH OF DOUBLE CUBIC POWER CURVE .....	83
FIGURE 3.9: DOUBLE CUBIC POWER CURVE AND SEGMENTS OF COMBINED CURVES FOR AN ENERCON E-126 EP4 / 4.2 MW WIND TURBINE.....	83
FIGURE 3.10: EXPLANATION CHART BASE OF HOW THE NEW REGION 3 CURVES COME FROM .....	86
FIGURE 3.11: EXPLANATION CHART 1 OF HOW THE NEW REGION 3 CURVES COME FROM.....	87
FIGURE 3.12: EXPLANATION CHART 2 OF HOW THE NEW REGION 3 CURVES COME FROM.....	88
FIGURE 3.13: EXPLANATION CHART 3 OF HOW THE NEW REGION 3 CURVES COME FROM.....	89
FIGURE 3.14: EXPLANATION CHART 4 OF HOW THE NEW REGION 3 CURVES COME FROM.....	90
FIGURE 3.15: COMPARED GRAPHS OF POWER CURVE BASED ON PROPOSED DOUBLE CUBIC METHOD AND MANUFACTURER'S DATA FOR AN ENERCON E-126 EP4 / 4.2 MW WIND TURBINE.....	91
FIGURE 3.16: COMPARED GRAPH OF POWER CURVES BASED ON PROPOSED METHOD, MANUFACTURER'S DATA AND 5 POLYNOMIAL METHODS FOR AN ENERCON E-82 E4 / 3 MW WIND TURBINE .....	94
FIGURE 3.17: COMPARED GRAPH OF POWER CURVES BASED ON PROPOSED METHOD, MANUFACTURER'S DATA AND 5 POLYNOMIAL METHODS FOR AN ENERCON E-126 EP4 / 4.2 MW WIND TURBINE .....	95
FIGURE 4.1: UNIT CATEGORIES BLOCK DIAGRAM WITH LOAD CURVE.....	108
FIGURE 4.2: FLOW CHART OF UNIT COMMITMENT BY PROPOSED DYNAMIC PROGRAMMING.....	110
FIGURE 4.3: EXAMPLE DIAGRAM OF SEARCHING PATHS IN DYNAMIC PROGRAMMING.....	111
FIGURE 4.4: FUEL COST CURVES OF 6 GENERATORS IN DP CASE .....	113
FIGURE 4.5: EMISSION COST CURVES OF 6 GENERATORS IN DP CASE .....	115
FIGURE 4.6: TOTAL COST CURVES OF PRODUCTION AND EMISSION OF 6 GENERATORS IN DP CASE .....	116
FIGURE 4.7: SYSTEM DEMAND.....	118
FIGURE 4.8: COST IMPACTS OF THE SPINNING RESERVE .....	123
FIGURE 5.1: LIVE AND FORECAST SOLAR IRRADIANCE DATA FOR EASTERN AUSTRALIA FROM FREE OPEN SOURCE OF 'SOLCAST API TOOLKIT' .....	131
FIGURE 5.2: SIMULATED EXAMPLE OF SOLAR IRRADIANCE DEVIATION BASED ON DOUBLE BETA METHOD.....	134

FIGURE 5.3: EXAMPLE GRAPHS OF ACTUAL 5-MINUTE SOLAR RADIATION AT PITTSTOWN .....	136
FIGURE 5.4: SIMULATED 15-MINUTE SOLAR IRRADIANCE RESULTS .....	137
FIGURE 5.5: COMPARED GRAPH OF DIRECTLY GENERATED AND AVERAGE GENERATED WIND SPEED .....	148
FIGURE 5.6: EXAMPLES OF SIMULATED WIND SPEED REFERENCES .....	150
FIGURE 5.7: EXAMPLES OF SIMULATED WIND SPEED DEVIATIONS .....	151
FIGURE 5.8: EXAMPLES OF OVERALL SIMULATION OF WIND SPEED (SIMILARITY OBSERVATION).....	154
FIGURE 5.9: EXAMPLE OF OVERALL SIMULATION OF WIND SPEED (DEVIATION AND REFERENCE).....	155
FIGURE 5.10: EXAMPLES OF CHARGE/DISCHARGE PROCESS OF BESS .....	161
FIGURE 6.1 MODIFIED ONE LINE DIAGRAM OF 330-kV NETWORK IN PROVINCE CASE .....	169
FIGURE 6.2: SOLAR IRRADIANCE REFERENCE IN PROVINCE CASE STUDY.....	173
FIGURE 6.3: HYDRO POWER IN PROVINCE CASE STUDY .....	175
FIGURE 6.4: FORECASTING LOAD DEMAND AND TEMPERATURE IN PROVINCE CASE STUDY .....	178
FIGURE 6.5: ACTUAL POWER OUTPUT OF SOLAR AND WIND FARMS IN PROVINCE CASE STUDY.....	178
FIGURE 6.6: FORECASTING POWER OUTPUT OF SOLAR AND WIND FARMS IN PROVINCE CASE STUDY.....	180
FIGURE 6.7: THERMAL GENERATION OUTPUT IN PROVINCE CASE A (RADAR CHART) .....	182
FIGURE 6.8: THERMAL GENERATION OUTPUT IN PROVINCE CASE A (AREA CHART).....	183
FIGURE 6.9: WIND FARMS OUTPUT IN PROVINCE CASE A (AREA CHART) .....	184
FIGURE 6.10: SOLAR FARMS OUTPUT IN PROVINCE CASE A (AREA CHART).....	185
FIGURE 6.11: TRANSMISSION LINE LOAD RATE IN PROVINCE CASE A .....	186
FIGURE 6.12: WIND POWER COST IN PROVINCE CASE A.....	187
FIGURE 6.13: MONEY COST OF INDEPENDENT AND COMBINED STRATEGIES TO WIND FARMS IN PROVINCE CASE STUDY.....	195
FIGURE 6.14: RENEWABLE POWER OUTPUT DIFFERENCES BETWEEN PREDICTED AND ACTUAL IN PROVINCE CASE STUDY.....	196
FIGURE 6.15: BESS OPERATION SITUATION IN PROVINCE CASE A (AREA CHART) .....	197
FIGURE 6.16: WIND POWER OUTPUT STOCHASTIC SIMULATION .....	199
FIGURE 6.17: SOLAR POWER OUTPUT STOCHASTIC SIMULATION .....	200

# List of Tables

TABLE 3-1: GLOBAL COST REDUCTION POTENTIAL FOR WIND POWER, 2010-2020 .....	67
TABLE 3-2: ROUGHNESS OF DIFFERENT TERRAINS.....	73
TABLE 3-3: EXPRESSIONS OF PARAMETRIC MODELS.....	77
TABLE 3-4: EXPRESSIONS OF DOUBLE CUBIC CURVE MODEL.....	85
TABLE 3-5: MANUFACTURER’S DATASHEET OF ENERCON E-82 E4 / 3 MW AND E-126 EP4 / 4.2 MW WIND TURBINE.....	93
TABLE 3-6: COMPARED DATA OF POWER CURVES BASED ON PROPOSED METHOD, MANUFACTURER’S DATA AND 5 POLYNOMIAL METHODS FOR AN ENERCON E-82 E4 / 3 MW WIND TURBINE .....	94
TABLE 3-7: COMPARED DATA OF POWER CURVE BASED ON PROPOSED METHOD, MANUFACTURER’S DATA AND 5 POLYNOMIAL METHODS FOR AN ENERCON E-126 EP4 / 4.2 MW WIND TURBINE.....	95
TABLE 4-1:FUEL COST COEFFICIENTS IN DP CASE .....	113
TABLE 4-2: FUEL CONSUMPTION COEFFICIENTS IN DP CASE .....	114
TABLE 4-3: EMISSION FACTOR OF UNITS IN DP CASE .....	114
TABLE 4-4: CARBON TAX AND EMISSION ALLOWANCE IN DP CASE.....	115
TABLE 4-5: GENERATOR CONSTRAINTS IN DP CASE.....	117
TABLE 4-6: GENERATOR START UP AND SHUT DOWN COST AND PARAMETERS IN DP CASE.....	117
TABLE 4-7: SYSTEM DEMAND IN DP CASE .....	118
TABLE 4-8: CASE I RESULTS OF CONVENTIONAL DYNAMIC PROGRAMMING WITH QUADRIC OPTIMIZATION METHOD .....	119
TABLE 4-9: CASE I RESULTS OF CONVENTIONAL DYNAMIC PROGRAMMING WITH MIXED-INTEGER LINEAR OPTIMIZATION METHOD.....	120
TABLE 4-10: CASE I RESULTS OF CONVENTIONAL DYNAMIC PROGRAMMING WITH LINEAR OPTIMIZATION METHOD .....	120
TABLE 4-11: CASE II RESULTS OF SEQUENTIAL DYNAMIC PROGRAMMING WITH QUADRATIC OPTIMIZATION METHOD .....	121
TABLE 4-12: CASE II RESULTS OF SEQUENTIAL DYNAMIC PROGRAMMING WITH MIXED-INTEGER LINEAR OPTIMIZATION METHOD.....	121
TABLE 4-13: CASE II RESULTS OF SEQUENTIAL DYNAMIC PROGRAMMING WITH LINEAR OPTIMIZATION METHOD .....	122
TABLE 4-14: CASE III RESULTS OF COST IMPACT OF DIFFERENT LEVELS OF SPINNING RESERVES.....	122
TABLE 4-15: FINAL COMPARED RESULTS OF OPERATION COST BY DIFFERENT PROGRAMMING TECHNIQUES	124
TABLE 5-1: PARAMETER SETTINGS OF DIFFERENT WEATHERS .....	138
TABLE 5-2: EXPLANATION EXAMPLES OF STOCHASTIC VARIABLES AND CONTINUOUS VARIABLES .....	153
TABLE 5-3: PARAMETERS OF COST COEFFICIENTS FOR WIND FARM .....	157
TABLE 5-4: PARAMETERS OF EXAMPLE BESS .....	160
TABLE 6-1: PARAMETERS OF THERMAL UNITS IN PROVINCE CASE STUDY .....	170
TABLE 6-2: PARAMETERS OF WIND FARMS IN PROVINCE CASE STUDY.....	171

TABLE 6-3: PARAMETERS OF SOLAR FARMS IN PROVINCE CASE STUDY.....	174
TABLE 6-4: PARAMETERS OF BESS STATIONS IN PROVINCE CASE STUDY .....	174
TABLE 6-5: FORECASTING HYDRO POWER OUTPUT IN PROVINCE CASE STUDY .....	176
TABLE 6-6: FORECASTING LOAD POWER DEMAND IN PROVINCE CASE STUDY.....	176
TABLE 6-7: FORECASTING TEMPERATURE IN PROVINCE CASE STUDY .....	179
TABLE 6-8: ACTUAL AND FORECASTING POWER OUTPUT OF SOLAR AND WIND FARMS IN PROVINCE CASE STUDY.....	179
TABLE 6-9: SOLUTION RESULTS OF OUTPUT AND COST OF ALL GENERATORS IN PROVINCE CASE STUDY.....	188
TABLE 6-10: EMISSION OUTPUT AND COST OF ALL GENERATORS IN PROVINCE CASE STUDY .....	192

# List of Abbreviations

ACSA	Ant Colony Search Algorithm
ANN	Artificial Neural Network
B&B	Branch and Bound
BESS	Battery Energy Storage System
CDP	Conventional Dynamic Programming
DP	Dynamic Programming
DSM	Demand Side Management
EP	Evolutionary Programming
ES	Expert System
ESS	Energy Storage System
FL	Fuzzy Logic
GA	Genetic Algorithm
GENCO	Generation Companies
ISO	Independent System Operators
LR	Lagrangian Relaxation
MILP	Mixed-Integer Linear Programming
NRMSE	Normalized Root Mean Square Error
PBUC	Price-Based Unit Commitment
PL	Priority Listing
PSO	Particle Swarm Optimization
RES	Renewable Energy Sources
RMSE	Root Mean Square Error
SA	Simulated Annealing
SBUC	Security-Based Unit Commitment

SDP	Sequential Dynamic Programming
SGC	State Grid Corporation
SOC	State of Charge
TPC	Total Production Cost
TS	Tabu Search
TSR	Tip Speed Ratio
UC	Unit Commitment
VRE	Variable Renewable Energy

# List of Symbols

$\pi_{BESS}$	Coefficient of battery energy storage system cost (US\$)
$\rho_{air}$	Density of the air ( $kg/m^3$ )
$\tau_i$	Cooling time constant of the unit $i$
$\lambda$	Tip speed ratio
$A_{upper-lim}^S$	Solar irradiance deviation limitation towards increment ( $W/m^2$ )
$A_{upper-lim}^W$	Fluctuation setting of upside limit of wind speed random variable
$A_{eq}$	Left linear equality constraints
$B_{lower-lim}^S$	Solar irradiance deviation limitation towards decrement ( $W/m^2$ )
$B_{lower-lim}^W$	Fluctuation setting of downside limit of wind speed random variable
$B_{eq}$	Right linear equality constraints
$C_{oe,i,t}$	Overestimated cost for wind farm $i$ in $t$ period
$C_{op,i,t}$	Direct operation cost for wind farm $i$ in $t$ period
$C_{ue,i,t}$	Underestimated cost for wind farm $i$ in $t$ period
$C_{hot,i}$	Hot start-up cost of the unit $i$
$C_{Capacity,i,t}^{BESS}$	Current value of capacity of BESS $i$ at time point $t$
$C_{cold,i}$	Cold start-up cost of the unit $i$
$C_{i,t}^{BESS}$	Operation cost of BESS $i$ at time point $t$
$C_{i,t}^{prod}$	Production cost of the thermal unit $i$ at time point $t$
$C_{i,t}^W$	Wind cost for farms $i$ in $t$ period
$C_{ini,i,t}^{BESS}$	Initial value of the capacity of BESS $i$ at time point $t$
$C_p$	Power coefficient of wind turbine
$C_{tax}$	Carbon tax
$c$	Scale parameter of the Weibull distribution of wind speed
$DR_n$	Ramping down rate of the unit $n$

$DT_n^{off}$	Down time (turn off) of the unit $n$
$D_t$	Power demand at time point $t$
$E_{cost}(K, I)$	Emission Cost for State $(K, I)$
$E_{wind}$	Wind energy (m/s)
$F_{COST}(K, I)$	Least Total Cost to Arrive at State $(K, I)$
$ef_{co2,i}$	Fuel emission factors of $co_2$ of thermal unit $i$
$ef_{no2,i}$	Fuel emission factors of $no_2$ of thermal unit $i$
$F_n^t$	Fuel cost for the unit $n$ at time point $t$
$FF$	Fill factor
$f$	Frequency of rotation (Hz)
$H_s$	Atmospheric transparency coefficient
$I_{sc}$	Short-circuit current (A)
$I_{MPP}$	Current at maximum power point (A)
$K_i$	Current temperature coefficient ( $A/^\circ C$ )
$K_v$	Voltage temperature coefficient ( $V/^\circ C$ )
$k_{oe}$	Reserve cost coefficients for the wind farm $i$
$k_{op}$	Available cost coefficients for the wind farm $i$
$k_{ue}$	Penalty cost coefficients for the wind farm $i$
$k$	Shape parameter of the Weibull distribution of wind speed
$lb$	Lower bound
$MDT_n$	Minimum down time (turn off) of the unit $n$
$MUT_n$	Minimum up time (turn on) of the unit $n$
$m_{air}$	Mass of air (kg)
$N_{OT}$	Nominal operating temperature of PV cell ( $^\circ C$ )
$N_{pan}$	Nitrogen emission allowance cost
$\eta_{Efficiency}^{charge}$	Charge efficiency

$\eta_{Efficiency}^{discharge}$	Discharge efficiency
$P_{BESS,i,t}^{charge}$	Power charge for BESS $i$ at time point $t$
$P_{BESS,i,t}^{discharge}$	Power discharge for BESS $i$ at time point $t$
$P_{MAX}(i, t)$	Maximum power generation limit of thermal unit $i$ at time point $t$
$P_{MIN}(i, t)$	Minimum power generation limit of thermal unit $i$ at time point $t$
$P_{cost}(K, I)$	Production Cost for State $(K, I)$
$P_{load-dev}$	Randomly generated load power demand deviation
$P_{load-r}$	Load demand reference
$P_{load-s}$	Simulated load power demand
$Pmax_n^t$	Maximum active power output for the unit $n$ at time point $t$
$Pmin_n^t$	Minimum active power output for the unit $n$ at time point $t$
$P_r$	Rated power output of the wind turbine
$P_{wind}$	Wind power (J/s)
$p_{Loss}(l, t)$	Power loss of the transmission $l$ at time $t$
$p_n^t$	Power generated of the unit $n$ at time point $t$
$p(i, t)$	Power generated by the thermal unit $i$ at time point $t$
$\overrightarrow{(R)}$	Continuous superposition function of $R$
$\overleftarrow{(R)}$	Reverse order of $\overrightarrow{(R)}$ in time axis
$r_s(i, t)$	Spinning reserve of thermal unit $i$ at time $t$
$r$	Radius of the rotor (m)
$S_a$	Average solar irradiance ( $kW/m^2$ )
$SD_n^t$	Shut-down cost for the unit $n$ at time point $t$
$SOC_{Limit}^{lower}$	Lower state of charge limitations
$SOC_{Limit}^{upper}$	Upper state of charge limitations
$SOC_{i,t}$	State of charge of BESS $i$ at time point $t$
$SR_t$	Spinning reserve at time point $t$

$SU_n^t$	Start-up cost for the unit $n$ at time point $t$
$S_{a-predict}$	Average predicted solar irradiance ( $W/m^2$ )
$State(K,I)$	Combination $I$ of Units at Time $K$
$T_A$	Ambient temperature ( $^{\circ}C$ )
$TP_l^{max}$	Maximum transmission power of line $l$
$TP_l^t$	Transmission power of line $l$ at time point $t$
$T_c$	Cell temperature ( $^{\circ}C$ )
$T_{dev}$	Randomly generated temperature deviation
$T_{factor}$	Power demand difference factor caused by temperature
$T_{initial}$	Initial temperature
$T_{off}(i)$	Minimum shut-down time of thermal power unit $i$
$T_{on}(i)$	Minimum start-up time of thermal power unit $i$
$\Delta T$	Temperature difference
$UR_n$	Ramping up rate of the unit $n$
$UT_n^{on}$	Up time (turn on) of the unit $n$
$U_n^t$	Unit $n$ at time point $t$
$u(i, t)$	On/Off status of thermal unit $i$ at time point $t$
$ub$	Upper bound
$V_{oc}$	Open-circuit voltage ( $V$ )
$V_{MPP}$	Voltage at maximum power point ( $V$ )
$V_b^{max}$	Maximum voltage limits of bus $k$
$V_b^{min}$	Minimum voltage limits of bus $k$
$V_b^t$	Voltage magnitude of the bus $k$ at time point $t$
$v_{a-Weibull}$	Average 15 minutes wind speed based on Weibull method ( $m/s$ )
$v_{ci}$	Cut-in speed for the turbine ( $m/s$ ),
$v_{co}$	Cut-out speed for the turbine ( $m/s$ ),
$v_{dev}^w$	Simulated deviation between predicted and actual wind speed

$v_g$	Wind speed at the inflection point of wind power curve
$v_{local-ref}$	Simulated wind speed reference of local wind farm (m/s)
$v_r$	Rated speed for the turbine (m/s).
$\omega$	Angular velocity (rad/s)
$X_{off}(i, t)$	Duration time for unit $i$ has remained off at time $t$
$X_{on}(i, t)$	Duration time for unit $i$ has remained on at time $t$
$z$	Wind shear exponent

# Chapter 1 Introduction

## 1.1 Background of Power System and Market in China

The electric power system is a complex operational system, which consists of the generation, distribution, transmission, and utilization of electrical energy. Generally, the works of economic operation and power dispatch are controlled and managed by the Independent System Operator (ISO) which is an independent organization that handles the power grid operation, power market management, and power system planning. In China, this role is played by the State Grid Corporation (SGC).

Since the 21<sup>st</sup> century, it is reported [1] that China's power system has entered a stage of rapid development, achieving annual generation growth rates of 12% in the first decade and 7% in the second decade. At the same time, this growth rate for the world average is 2.5%. Details of recent annual generation growth for China [2, 3] are shown in Figure 1.1.

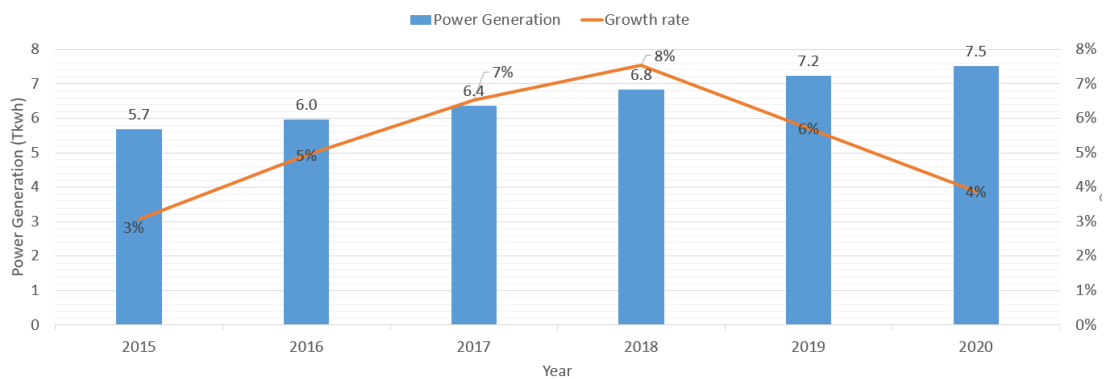


*Figure 1.1: Electricity Consumption of China's Whole Society in 2015 – 2020*

In 2020, annual power generation was 7511 TWh in China and a total of 25865 TWh in the world. However, as a country with a large growth in electricity demand,

China's power market mechanism is still in its infancy. And its power mix [4] is heavily coal-dependent, with about 61% in 2020 as Figure 1.2 shows.

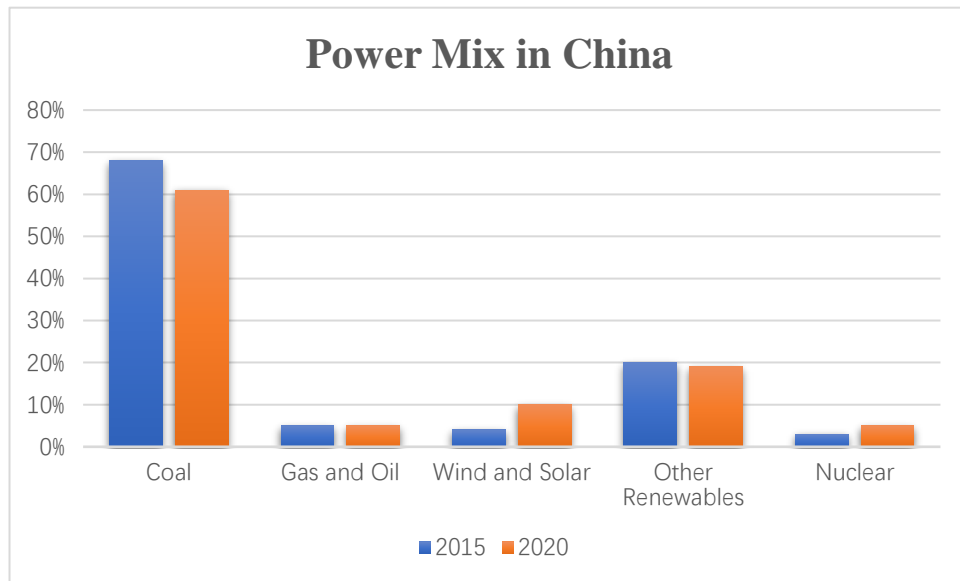


*Figure 1.2: Power Mix in China*

Fossil energy refers primarily to coal, oil, and natural gas which are formed from organic material over the course of millions of years. Since the first Industrial Revolution, fossil energy has boosted global economic development over the past centuries. Global fossil energy consumption is still growing now, but it will exhibit a decreasing trend since the global energy transformation.

China's electricity market mechanism has undergone two rounds of reforms. As early as 2002, China launched the first round of power sector reform to shift the power industry from 'vertical integration' to 'single buyer' [5] which means the separation of power plants and grids to break the monopoly.

'Single buyer' model is just one step away from the fully centralized approach and 'Single buyer' here refers to the State Grid Corporation of China which is the only

one in charge of purchasing electricity and selling it to consumers at regulated prices at that time.

Even through this round of reform changed a lot of power mechanisms and enhanced the development of the power market, there are still many problems that hinder the development of power industries in China such as low energy efficiency and serious curtailment of renewable energy.

Hence, China issued the ‘Several Opinions on Further Deepening Electricity System Reform’, which is commonly known as ‘Document No.9’, to launch the second round of power sector reform in 2015 [6]. Since the new reform, it was reported that the last province of Hainan had set up its own power exchange sectors for power market trading on the 25<sup>th</sup> of December 2017. This event marked that the market for electricity trading had been completely open.

Up to the end of 2018, China was under the reform stage of further power market construction, and it was reported [7] that the sum of all market-based electricity transactions in the wholesale forward market was 2065 TWh, accounting for 30.2% of the total China electricity consumption. So far, there are still many issues remained such as legal and regulatory barriers for power markets and market participation rules to integrate renewable energy.

### **1.1.1 Two Rounds of Power Sector Reform in China**

#### **i) First round of reform in 2002**

Before the year 2002, China’s power sector is a vertically integrated monopoly corporation, and the electricity prices were strictly regulated. During this period, the power supply issue of shortages often happened in the provinces. But this phenomenon was relieved since the government expanded power investment.

To break the monopoly of the vertically integrated models, the power sector planned to separate the power plants and grids in the first round of reform in 2002. [8] noticed that the former State Power Corporation was split into two power grid companies that State Grid Corporation of China and China Southern Power Grid, and five power generation groups consisting of China Datang Corporation, China Huaneng Group Corporation, China Huadian Corporation, China Guodian Corporation, and State Power Investment Corporation.

The grid corporation is responsible for purchasing electricity from the generator corporation and selling it to consumers at regulated prices. At the same time, the power dispatch, transmission, and distribution are all managed by the grid corporation. The generator corporation is allowed to select large industrial consumers to sign the bilateral agreement contract. However, during this period of reform, the price and quantity of power were still strictly regulated even through the number of electricity purchasing channels had increased.

Generally, the government highly regulates and controls the on-grid electricity prices and the quantity of power generated by the power plants. The problem here is that the power quantity generated by all the power plants using different technologies and costs must be dispatched in a ‘fair’ manner [9] sharing similar capacity factors. This rule was established in the 1980s when the monopoly model was ended in order to protect the old and inefficient generators. However, this traditional rule that causes low efficiency is still in use in many provinces in China now. The details of this issue ‘fair’ dispatch rule will be discussed in the following sub-section 1.1.2 (Power Issues in China Market).

The lack of a market-based pricing mechanism and the regulated on-grid electricity prices hindered the transactions among the provinces since there were not

enough pricing signals to guide the power trades. Therefore, with these various problems, the second round of reform in 2015 was carried out to support more efficient pricing and investment by policies.

ii) Second round of reform in 2015

China launched the second round of reform in 2015 which is aiming to improve the efficiency of the power market system and control the investment of generator plants based on using the price orientation of the electricity market. During this period, electricity transaction is mainly managed through the power exchange sector.

The other two major changes are that the retail corporation was built and allowed to purchase the electricity from the generator corporation. Transmission and distribution networks are open to all market participants so as to lower high transmission and distribution costs. However, for the protection of residents, agriculture production, public services, and some special consumers, the power supply and price still remain highly regulated.

Benefits from the second round of power market reform, spot market, forward market, ancillary market, and capacity market are built-in and open to the market participants in the trial provinces. Various market functions are also showing their advantages during this period such as frequency regulation, peak regulation, and market competition.

Unlike the early power market with limited power transactions, it was reported that [10, 11] up to the end of 2020 the total amount of market-based transacted electricity this year in the provincial power markets has reached 2476 TWh, accounting for 40.2% of the total amount sales of transacted electricity, which reduced the customer electricity bill of 55 billion Yuan, about 8.5 billion US dollars. Although

the reform of China's power market is still in its infancy in comparison with the West and many market mechanisms and rules that need to be changed and promoted, positive results of reform have gradually emerged.

### **1.1.2 Power Issues in China Market**

Fossil energy is an energy source with extremely high carbon density, and its carbon emissions have already caused climate change. According to an ongoing temperature analysis conducted by NASA's Goddard Institute, the global temperature has increased by 1 °C since 1880 with increasing carbon emissions. And it causes the Arctic Sea ice disappears by more than 70,000 km<sup>2</sup> every year [12].

Based on the case of the Renewable Energy Road Map [13] to 2050 proposed by international renewable energy agency, fossil fuel use for energy would fall to one-third of today's levels by 2050. Coal and Oil would decline by 85% and 70%, respectively. However, fossil fuels still accounted for an estimated 84% of the world's primary energy consumption in 2019 [3].

China, as the world's largest coal-fired power generation country, its coal-fired power generation account for more than half of the world's total in 2020 [4]. Under this situation, China must ensure that coal-fired power generation will decrease significantly in the next ten years to achieve its goal of limiting global warming.

In order to cope with the major strategic goal of carbon neutrality in the world, the China State Council issued the notice of the "Carbon Peaking Action Plan by 2030" on October 24, 2021. Therefore, developing renewable energy and insisting on safe carbon reduction have become important goals of the power industries in China.

The proportion of thermal power in China is large, more than 65%, and 61% of which is heavily coal-dependent in 2020. Since the fuel cost is a major cost component,

it can be particularly significant in deals that the dispatch and operation schedules of these thermal plants. It is reported that reducing the fuel cost by little as 0.5% can result in savings of millions of dollars per year for large utilities [14, 15].

China aims at reducing the emissions produced by the traditional thermal power plants and increasing the utilization of renewable energy sources (RES). The integration of wind and solar energy sources also causes intermittent and volatile characteristics but no pollution. These characteristics will lead to an additional cost of managing the intermittency for the dispatch department.

It is widely accepted that RES are essential to mitigate greenhouse gas emissions and reduce global warming. Wind power and solar power are technologies that can be used as the main sources of RES to achieve the goal that ‘Notice State Council of the Action Plan for Carbon Dioxide Peaking Before 2030’ [16].

In 2020, wind power and solar power generation accounted for one-tenth of China's total power generation. The use of RES is particularly successful in China and the government department uses different incentives to encourage the installation of renewable energy. China now is switching away from fossil fuels and toward pollution-free and sustainable energy sources.

However, the dramatic growth of RES capacity brings a lot of problems in balancing management in the short-term schedule for power system operation to the dispatch department. Especially the problems of consumption of RES, the majority come from wind and solar energy sources, their output depends on the weather condition cannot be fully controlled as the thermal plant can.

Although two rounds of reforms enhanced the development of the power market, China's power market is still semi-liberalized. China, as a large government-directed

regulatory regime, its parts of power generation, consumption, dispatch, and electricity price are still centrally planned and regulated now.

The disadvantages of this semi-liberalized market and planned economy have been gradually magnified under the influence of the Coronavirus (COVID-19) pandemic.

With electricity and coal shortages across China, the northeast provinces of China still looked for the purchase and transport of high-cost coal from other provinces to generate electricity and then dispatched electricity to other provinces to complete its planned economy tasks of power generation. The reason why these tasks were planned last year was that the government decided to protect the planned profit of old and inefficient generation units in the northeast provinces by curtailing the amount of power generation of other provinces and then gifted this quota to the northeast provinces.

But these behaviors of actively delivering power to the outside were contradictory under the situation of electricity and coal shortages that caused both the waste of energy transmission and serious environmental problems.

This type of planning problem cannot be solved quickly and timely is because of the lack of economic methods of power regulation and the completed power market construction. Various problems cannot be reflected in the price signal in time, and this lack of guidance from the price signal results in insufficient ancillary service resources and power contract transfer.

This planned economy is efficient when the development direction is clear or large-scale reforms needed to make. However, under the current semi-liberalized market where the structure of electricity development is becoming more and more

complex, planning arrangements are also becoming more and more complex and difficult, resulting in the government's planning results becoming inefficient. Therefore, the existing power planning and dispatching rules need to be gradually changed.

In a developing country, such as China, the development of power market in each province varies greatly. A specific province as the object of the case study in this thesis, the development of its electricity market is also relatively backward compared with other provinces. In particular, its prediction of renewable energy output is even directly drawn by the dispatching operator based on personal experience and the weather conditions of the next day.

Under China's existing traditional power market, power generation, consumption, and dispatch are centrally planned and regulated. The government strictly controls power supply, power generation, and the electricity price, to ensure the balance of supply and demand in the market, as well as the safe and stable operation of the power grid. In terms of power generation, all units are ensured to generate a planned and fixed amount of power based on the 'fair' dispatch rule with sharing similar capacity factors which is usually determined and regulated by the local provincial commission of the economy and informatization [17].

Following this quota rule, the total amounts of assessed electricity consumption next year are allocated into a planned generation amount to each power plant based on approximately similar capacity factors. Then, the generators could sign the annual generation contract based on the planned generation amount at the regulated on-grid prices. However, this approach disadvantages thermal power plants with lower operation costs because a similar capacity factor is allocated.

This is also the reason why the thermal power flexible system has developed slowly in some of China's provinces. Most generation plants with different technologies and operation cost only pursue a larger thermal power scale instead of improving the flexibility of their own unit. Because owning a larger power scale in China means more power allocations based on that quota dispatch rules discussed just now. As for flexibility improvement of generators, it can neither help them obtain more power generation quotas nor allow them to obtain short-term profits.

Besides this, another issue is that the generation space for adjustment in real-time operation is small to integrate variable renewable energy because the regulated and fixed dispatching schedule must be finished based on the 'fair' dispatch rule in a month.

### **1.1.3 Further Motivation for the New Reform**

The Chinese power mix is heavily coal-dependent, but now its focus is going to switch away from fossil fuels and toward pollution-free and sustainable energy sources, such as wind and solar energy. To achieve the goals of sustainable development, the government has formulated many policies to support renewable energy [18]. The goal is set at annual additions of 55 GW of wind capacities until 2030. In terms of solar energy, it is required to achieve a total of 854 GW of solar capacities in 2030 [19]. Therefore, an important goal of the new reform is to build a renewable energy-friendly power system, maximizing integration and minimizing curtailment.

As stated above Chinese power mix is heavily coal-dependent, and the promotion of the generator efficiency of thermal power units is particularly important. However, at the moment, it is reported that in one of China's provinces the capacity factor of thermal generators was only 44% in 2018 [20]. It is far lower than the United States of about 55% capacity factor. The reason for this phenomenon is the lack of power market price signals causing excessive investment in unsuitable time or in the wrong

area. Therefore, another important goal of the new reform is to provide a competitive market environment and price incentives for the investment of thermal power units.

As discussed in previous sub-sections, the original intention of the ‘fair’ dispatch rule with sharing similar capacity factors is to protect the less efficient thermal power units. It is good to support them with a rated power generation space. But at the same time, obviously, it hinders the development of new thermal power units, and it also hurts the profits of high-efficiency units and causes the waste of resources. Therefore, the target to reduce energy consumption and emission has also been added to the new reform.

## **1.2 Objectives**

The main objective of this thesis is to develop an overall cost-based and 15-minute interval model of thermal units, wind farms and solar farms for resolving the day-ahead schedule problem of the power dispatch and this model is based on unit commitment problem incorporating with the energy storage system and emission cost. The proposed model is tested on an actual China provincial power network system in a semi-liberalized electricity market. This provincial system is simplified to a 58 nodes test system and because some of the data are not in the open domain, they are supplemented with IEEE standard test system data.

The objectives of this thesis are realized by addressing these four main research problems, which are outlined below:

***Problem 1: How to achieve the day-ahead dispatching schedule based on the unit commitment problem for the thermal units with emission costs in the semi-liberalized electricity market unique to China?***

Reviewing the UC theory to find suitable solutions to the UC problem, this solution method should also fit with the further simplified case of the actual Province Power Grid system in China, which is a large-scale system.

Reviewing the power market in China to understand special rules of power dispatch of thermal units and renewable energy units in the semi-liberalized electricity market unique to China.

Selecting the suitable modelling method to code the emission cost into the thermal UC problem. The generator physical constraints and system operational constraints should also be included in the model.

***Problem 2: How to model the power output of renewable energy resources and their related operation cost?***

It is necessary to include the operation cost of renewable energy resources in solving the electrical power systems economic dispatch problem.

Modelling the wind turbine to convert the data of wind speed to wind power output based on the wind power curve method. Wind power costs can be achieved based on the proposed method of underestimation and overestimation of the wind power output between the forecast and actual values.

Modelling the solar operation module to convert the data of solar irradiance to solar power output based on the module specifications. Unlike wind power cost, due to the lack of a unified pricing mechanism for forecasting the deviation cost of solar power in China's semi-liberalized market, only a local fixed operation cost of solar power to each solar farm will be considered in the model.

There is yet no existing large-scale battery energy storage system in the province test system, but with the operator's request energy storage stations will be added to the case study. A battery energy storage system model that complies with the basic charging and discharging rules will be developed, and its related operation cost is depending on how much charging power is used or discharging power is released at a local fixed price for each storage station.

***Problem 3: How to model the stochastic data of forecasting wind speed and solar irradiance to achieve their simulation results of power output?***

Due to the lack of open public data on wind speed and solar irradiance in the China Province, their stochastic data will be generated based on the limited data acquired and their related forecasting and simulating methods.

The solar power output can be achieved based on modelling the construction of the photovoltaic module. The output power of the photovoltaic module can be calculated once the data of solar irradiance, ambient temperature, and characteristics of the module are determined based on related equations.

The wind power output can be achieved based on modelling the construction of the wind turbine. The output power of the wind turbine can be calculated once the data of wind speed, characteristics and power curve of the wind turbine are determined based on related equations.

***Problem 4: How to model the power generation system as the case study, which focuses on the power output of generators and composition of network?***

First of all, this case study of mixed power generation system should include the generation units of wind farms, solar farms, thermal plants, hydro plants, and battery energy storage system (BESS) system. Secondly, lots of the publicly available data

from the power grid company can be found and used to construct a simplified network system.

Unfortunately, some of the data still has to be estimated, and the generator data are also replaced by the data of common generator units used in formal published papers. The remaining data are supplemented by IEEE standard test system data. But the final total simulated power generations and demands in China's province case are close estimates of the actual system.

### **1.3 Original Contributions**

The main original contributions of the thesis are listed as:

***Contribution 1:*** An overall cost-based and a 15-minute interval model of thermal units, wind farms, solar power farms, and battery energy storage systems for resolving the day-ahead UC problem of the power dispatch is developed based on the simplified case of actual Province Power Grid system in semi-liberalized electricity market unique to China.

***Contribution 2:*** A novel model of Double Cubic power curve of wind turbine and its related calculation equations are developed by the author to express the relationship between the output power of the wind turbine with wind speed based on considering the inflection point in the nonlinear portion of the wind power curve.

***Contribution 3:*** A novel stochastic model of forecasting wind speed was developed by considering Weibull method by adding two types of stochastic forecasting corrections of wind speed. These two types of stochastic forecasting corrections of wind speed are designed as the white noise sequence of mathematic expectation mean value of zero. This white noise sequence is generated by a random

number generator based on the novel approach of continuous superposition developed by the author.

**Contribution 4:** A novel stochastic model of forecasting solar irradiance was developed through stochastic generating the output data of solar irradiance in the forecasting range of next day based on the forecasting data extracted from the free open source ‘SOLCAST API Toolkit’ [21]. This model is designed to generate forecasting solar irradiance by adding the stochastic and corrections into the data of forecasting solar irradiance curve supported by the ‘SOLCAST API Toolkit’. These stochastic and corrections are generated based on the method of uniformly distributed random variables combining the Beta function by using the software MATLAB.

**Contribution 5:** A model of battery energy storage system with two different proposed operation strategies, performance priority, and lifetime priority, is developed to investigate its relative impacts on renewable energy integration and battery lifetime.

**Contribution 6:** A cost-based model of wind power output is proposed to estimate their related cost in China’s province case. This model not only considers the operation cost of wind power but also provides a new penalty strategy for forecasting overestimation and underestimation, which makes each wind farm operator actively participate in wind power forecasting.

**Contribution 7:** Based on the results of the cost-based model of wind power output, a combined strategy of wind power operation is proposed to save further penalty costs of forecasting overestimation and underestimation. The theory of this combined strategy is also applicable to the forecasting of renewable energy.

## 1.4 Thesis Structure

This thesis consists of seven chapters and the contents are organized as follows:

*Chapter 2* provides the reviews of modelling methodologies of power generation models of wind farms, solar farms, thermal units, BESS and the reviews of unit commitment formation, environment, and objectives. The UC constraints and their corresponding equations are also briefly introduced. Finally, the various solutions to the UC problem with their characteristics are described in detail.

*Chapter 3* presents a novel method of Double Cubic to model the power curve of the wind turbine. Firstly, this chapter gives an overview of wind energy from the aspects of background, and development to their technology. Secondly, the wind power curve with developed modelling methods are introduced and discussed to propose a novel method of Double Cubic developed by the author followed by the details of its mathematical formulation. Finally, the results of two modelling cases are used to demonstrate the improvements of this novel method.

*Chapter 4* introduces the model details of formulation and proposed solution of the thermal unit commitment problem including emission cost and corresponding system constraints used in the research. After this, a modified dynamic programming approach is introduced in detail. Finally, this method is employed in solving the UC problems with corresponding optimization methods implemented on a test system including 6 thermal power generators and to discuss their performances and results.

*Chapter 5* investigates two novel models developed by the author to stochastic generate the forecasting solar irradiance and wind speed. Beside this, a proposed method of modelling wind power cost is introduced which considers the relative penalty cost when the forecasting underestimation or overestimation of wind power

forecasting output occurs. At last, a model of battery energy storage system with two storage strategies of performance priority and lifetime priority respectively are introduced.

*Chapter 6* applies one simplified case model of China's province power generation system with the 330-kV network of 58 node buses based on all approaches and concepts discussed in previous chapters to illustrate renewable-based UC problems and the analysis of their results.

*Chapter 7* summarizes the conclusions of the thesis and discusses possible further works.

The data of branches and buses of the simplified network of 58 node test system are listed in Appendix (A).

The test solution results of case study of power output dispatching of solar farms, wind farms and thermal generators are complementally listed in Appendix (B).

## 1.5 Publication

Based on the results of the research work reported in this thesis, the following papers have been published:

Banghao Zhou and K.L.Lo, “A Summary Study of Wind Turbine with Related Control” Energy and Power Engineering Vol. 9 No. 4B, April 6, 2017, DOI: 10.4236/epe.2017.94B032

Banghao Zhou and K.L.Lo, “A Novel Modelling Approach of Double Cubic Power Curve of Wind Turbine”, under preparation for IET journal submission (expected submission date: January 2023)

Banghao Zhou and K.L.Lo, “A Novel Stochastic Model of Forecasting Wind Speed”, under preparation for Engineering Technology conference 2023 submission (expected submission date: February 2023)

# Chapter 2 Literature Review

## 2.1 Introduction

Unit Commitment (UC), as an important problem in the electrical power industry, has been researched for several decades with thousands of related published articles. However, there are still researchers working in this field to find a new hybrid method to make the problem more realistic.

The task of UC is to find an optimal schedule of on/off statuses and generation output for each generating unit at a possible minimized cost of operation and production over a given time period in the power system based on their specific generational, environmental, and technical constraints to meet the varying load demands.

Depending on the different objectives, the formulation environments of the UC functions and its corresponding generator physical and system operational constraints will change accordingly. Generally, UC environments are divided into three main categories of profit-based UC (traditional UC), price-based UC (PBUC), and security-constrained UC (SBUC).

To address UC problems, various methodologies of classical heuristic approaches and modern meta-heuristic approaches have been proposed to solve this time-dependent problem.

However, due to three main impacts of higher penetration integration of intermittent renewable energy sources (RES) and the requirements of China's electricity market reform and emission policy of 'carbon neutrality', it is important to have corresponding modelling methodologies to construct the UC problem which

includes the thermal units, wind farms, solar farms, and battery energy storage system (BESS).

To achieve this objective, this chapter focuses on the reviews of modelling methodology of mixed generation system, UC theory and its related solving approaches.

Section 2.2 gives a review of methodology of renewable energy modelling, wind speed simulation, wind power curve modelling, solar irradiance simulation, UC problems, optimizing approach, and BESS.

Section 2.3 gives a review of UC formulations, objective functions, and their constraints. To address UC problems, two categories of solving methods of deterministic and meta-heuristic approaches are mainly discussed with its individual advantages and disadvantages.

## **2.2 Review of Modelling Methodology**

### **2.2.1 Renewable Energy Source Models**

It is widely accepted that renewable energy source (RES) is essential to mitigate greenhouse gas emissions and reduce global warming. Now, wind power and solar power as the main sources of RES are used to achieve the goals of ‘Notice State Council of the Action Plan for Carbon Dioxide Peaking Before 2030’ [16], and ‘low-carbon mix for 2030’ [22].

The generation of RES is characterized as high variability, uncertainty, and intermittency [23]. These features will make RES generation behavior completely different with conventional generation sources. Appropriate forecasting of RES plays an important role to ensure stable and uninterrupted energy supply. Therefore, it is

necessary to require a long term weather data in order to obtain accurate RES forecasting generation.

The modelling methods of RES forecasting basically can be categorized into two types of physical approach [24] and statistical approach [25]. The physical approach requires the detailed physical description to model the conditions of the site by using numerical weather prediction data [26]. Statistical approach uses previous historical data to build statistical model.

However, the previous historical data are not easily available because of the cost of measuring devices and the difficulty in accessibility of the measuring sites, especially in China RES sites where most of the data are not in the open domain. Then, it is difficult to estimate the accurate power generations in solar and wind farms of China without the majority data of solar irradiance and wind speed at corresponding sites.

Therefore, the uncertainty modelling of renewable energy forecasting models with less amount requirement of historical data and simpler calculation of model parameters are selected for researching simulation models of RES generation in China. Compared with deterministic forecasting, uncertain forecasting can not only provide information, but also reflect the uncertainty of renewable energy power from the aspects of change interval, the probability of occurrence, and the possible scenarios [27].

Uncertainty model techniques includes interval approach [28], probabilistic approach [29], possibilistic approach [30]. Interval approach is based on the interval that the predicted object may change in the future, providing the fluctuation range of the predicted object. Probabilistic approach is based on the probability density function

(PDF) of the input variables. Possibilistic approach is based on a membership function which is assigned for modeling uncertain parameters.

Generally, the speed of wind is uncertain and stochastic variable, and its simulation models can be divided into probability distribution models [31-34] and time-series models [35-39]. The wind speed probability distribution model is a type of data analysis method which is used to characterize the distribution characteristics of wind speed probability. Probability distribution models include the Weibull distribution [32, 40, 41], Rayleigh distribution [42-44], normal distribution [34, 45, 46], and lognormal distribution [31, 45, 47]. The time series model is a type of model which is used to describe the wind speed dynamic changes at time horizon. The wind speed series has both the characteristics of probability distribution and dynamic changes. Time series models include the Autoregressive (AR) [48], Autoregressive Moving Average (ARMA) [49, 50], and Autoregressive Integrated Moving Average (ARIMA) [51, 52] models.

Weibull distribution is generally considered as a probability model with a simple form and a good fitting ability into the real distribution of wind speed [53-56]. However, the forecasting wind speed cannot be represented effectively by the Weibull PDF at hourly or shorter time scales [57, 58] because the Weibull PDF is not a time-dependent but a static distribution, it cannot represent the frequent short-term wind speed fluctuations that take place inside the hour [58].

However, this thesis is devoted to establishing a research model at time scale of 15-minute intervals that will be discussed in latter paragraph. Beside this, the sufficient historical data of wind speed is not available in China to each wind farm that the corresponding PDF of wind speed are difficult to define. Because, in China

Provincial power dispatch department, the open data of wind speed is only supported for a larger area but not a certain place which the wind farm locates at.

Therefore, based on these two reasons, one selection to represent the uncertainty wind speed corresponding to each wind farm in China is using the hybrid approach that combining Weibull approach and adding forecasting corrections. These forecasting corrections can be represented based on other uncertainty modelling techniques, interval approach, probabilistic approach or possibilistic approach, which is dependent on the known historical data.

Power curve modelling methods, such as deterministic, probabilistic, parametric, non-parametric, and stochastic methods [59] are representing the relationship between relative wind speed and wind power.

For a deterministic power curve model, each value of wind speed corresponds to a fixed value of output power [60]. However, in practice at a wind farm, the same type of turbines may produce different amounts of power even if the wind speed is the same.

Hence, the approach of probabilistic power curve model is used to cope with the issue that each value of wind speed corresponds to a probabilistic or accidental value of output power [61]. The probabilistic approach requires large numbers of historical data to improve the results' accuracy [62].

A parametric model defines the relationship between input and output parameters of a wind turbine by a set of mathematical polynomial approximations.

Unlike parametric methods, non-parametric models establish a model and simulate it in a way to minimize the deviations between observed data and outputs without searching for a mathematical relationship, such as neural networks, fuzzy clustering centers, and data mining methods [63, 64].

The stochastic method characterizes the output power performance of the turbine by evaluating its dynamic response against the wind speed inputs [65].

The simulation approaches with features of wide application and fast estimation of parametric models are simple to use such as linear [66], quadratic [67], cubic [68], Weibull [66], double exponential [69], and high degree powers of speed [70]. However, these polynomial expressions ignore the important inflection point variation characteristics in the simulation curve [65, 69, 71]. In most real power curves, there is an inflection point on the curve at which its curvature changes sign.

Therefore, it is necessary to propose a new approach in which simulation inflection point [69-72] is considered and it should be simple to use, limited data required, parameter calculation is easy, and can be used to calculate the power output of wind turbines.

An important aspect in modeling wind energy is to evaluate the accuracy of the developed model using statistical error approaches such as the mean absolute percentage error (MAPE), mean bias error (MBE) and root mean square error (RMSE) [73]. RMSE provides information on the short-term performance of the model and is a measure of the variation of the predicted values around the measured data. A large positive RMSE value implies a big deviation in the predicted value from the measured value.

For the part of solar energy, solar irradiance data provide information on how much of the sun's energy obtained per unit area by a given surface. Solar irradiation is a measure of the solar power over all wavelengths per unit area incident on the Earth.

Solar power output can be achieved based on modelling the construction of the photovoltaic modules [74, 75]. Based on this approach, the conversion output results

of solar power can be obtained based on the data of forecasting solar irradiance. The output power of the photovoltaic module is generally dependent on the solar irradiance and ambient temperature of the site as well as the specification of the module itself.

The commonly used solar energy models developed in the past are based on linear models [73, 76-79] and nonlinear models [80-84]. These models give a correlation between solar energy on a horizontal surface and some meteorological variables such as sunny hours, ambient temperature, and relative humidity. The linear models use simple linear function while the nonlinear models use polynomial function of the third or fourth degree. Beside this, artificial neural network models (ANN) [85-88] and fuzzy logic models [89, 90] are also used in solar energy modelling. [91] gives a comparison of the forecasting accuracy among the solar energy modeling techniques of linear, nonlinear, ANN and fuzzy logic models. The ANN model is the most accurate model for solar energy forecasting in which the RMSE value for ANN based global solar energy models is 7.37% and the RMSE values of linear, nonlinear, and fuzzy logic models are 9.32%, 8.73% and 8.8%, respectively.

[92, 93] state that it is difficult to derive deterministic models for solar irradiance considering it as a time-dependent phenomenon in which there are many unknown factors, especially focusing on the local scale that they may lack great accuracy because of the complexity of the addressed atmospheric phenomenon. Therefore, [92, 93] proposed to use stochastic models approach to provide solution to the solar irradiance variability problems.

Because it is mainly to achieve the uncertainty modelling of RES, uncertainty model techniques of wind speed and solar irradiance are similar except the corresponding distribution characteristics are different or some other different characteristic to each. For example, the characteristic of strong production of solar

energy in the noon of the day corresponding to the beta function is a good fitting into the actual distribution of solar irradiance.

Unlike wind speed, the free open-source ‘SOLCAST API Toolkit’ [21] supports the historical and forecasting data for solar irradiance based on a latitude and longitude in anywhere on earth. SOLCAST API Toolkit operates a global cloud tracking and forecasting system, using near-real-time satellite imagery from 11 weather satellites, and weather data from 7 numerical weather prediction models. This solar irradiance toolkit supports deterministic historical data and 90/10 probability values of forecast data which means there is a 90 percent chance that the forecasting data is correct.

So, as similar as the uncertainty modelling of wind speed, one selection to represent the uncertainty solar irradiance corresponding to each solar farm in China is using the hybrid approach that combining forecast data supported by SOLCAST API Toolkit and adding forecasting corrections. These forecasting corrections can be represented based on uncertainty modelling techniques discussed in previous.

### **2.2.2 Unit Commitment Problem Model**

Recently, lots of developing countries are using RES to replace the thermal energy power generation [94]. But the integration of solar and wind energy sources causes intermittent and volatile characteristics that requires higher level ability of dispatching of thermal units. These characteristics will lead to an additional cost of managing the intermittency for the dispatch department. Therefore, both the forecasting and addition of RES have a decisive impact on the day-ahead scheduling of thermal power units that leads the changes of unit commitment (UC) and economic dispatch (ED) models.

The dramatic growth of RES capacity brings operational problems in managing balancing in the short-term schedule for power system operation. Especially the problems of consumption of RES, the majority of which come from wind and solar energy sources, their output depends on the weather condition, and it cannot be fully controlled as the thermal plant can.

The lack of renewable power output forecasting and corresponding operation rules has caused a huge stagnation in the integration and development of renewable energy resources in some provinces of China. As the share of wind and solar power rapidly increases, it is necessary to include their power operation costs in solving the ED problem in electrical power system.

Therefore, the forecasting results discussed in previous paragraph of the once deterministic power output of these uncertainty forecasting models at different RES sites can be further used to determine the problem of unit commitment (UC) and generation dispatching optimization of thermal power units in the power system of targeted case in China.

The techniques used to meet these targets of optimal resource dispatch tasks are named as UC and ED problem [95]. The UC problem aims to determine the start-up and shut-down schedule of units by considering security constraints that ramping limits and minimum on/off time to meet the system load demand and reserve requirements. Once the UC problem has been solved the purpose of ED is to allocate the system demand among the operating units while minimizing the operation cost [96].

There are many research working on optimizing the power system operation. A parallel implementation of Lagrangian relaxation (LR) for solving stochastic unit commitment subject to uncertainty in renewable power supply was studied in [97]. a

robust optimization approach to accommodate wind output uncertainty providing a unit commitment schedule for the thermal generators in the day-ahead market under the worst wind power output scenario was proposed in [98]. In [99], the author of the paper proposed a hybrid approach of combining branch and bound algorithm with a dynamic programming algorithm to coordinate the problem of wind and thermal generation scheduling. [100] decided to solve day-ahead UC problem by formulating fuzzy optimization models based on solving method of mixed integer linear programming (MILP) technique. Furthermore, there are still many methods to solve the UC problems, such as exhaustive enumeration [101, 102], the dynamic programming (DP) method [103, 104], the artificial neural network (ANN) method [105], the genetic algorithm (GA) methods [106-109], the ant colony search algorithm [110] and the particle swarm optimization method [111-113].

The proportion of thermal power in China is large, more than 65%, and 61% of which is heavily coal-dependent in 2020 [4]. Since the fuel cost is a major cost component, it can be particularly significant when dealing with dispatch and operation schedules of these thermal plants. It is reported that reducing the fuel cost by little as 0.5% can result in savings of millions of dollars per year for large utilities [14, 15]. Therefore, China now is aiming at reducing the emissions produced by the traditional thermal power plants and increasing the utilization of RES at minimal possible operation cost.

However, a lot of previous UC research works did not consider the emission issue and operation cost of RES at same time [14, 15, 107, 114-119]. Beside this, most of these models are only based on the operating time scale of hourly interval [116, 120-125]. However, in China's practical power dispatch and market, the time interval of decision-making was planned at 15-minute intervals [6].

For the country of China, with a large proportion of thermal power and rapid development of RES, these omissions that ignoring emission cost will have a critical impact on the solution results of UC and ED problem.

For the time interval scale, the advantage of using smaller interval is that it will support closer approximation results of the practical production cost calculation than using larger interval as Figure 2.1 shows.

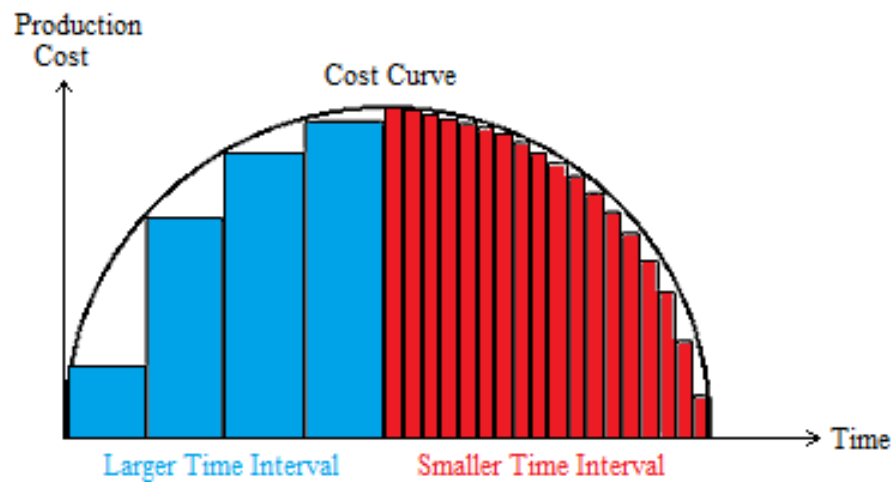


Figure 2.1: Impact of the Time Interval on the Cost Calculation

Similar to the calculation of the cumulative value of the integral of the curve area. Total production costs can be represented by the cumulative summation of the area of the corresponding columns in Figure 2.1. The smaller the time interval is, the closer area of the cost amount can be represented accurately. For example, calculating the half area of the cost curve, it can be seen that the area of red is larger than the area of blue and the area of red is closer to the half area of the cost curve.

Although UC model and its corresponding solution approaches are numerous, its complex programming makes it not easy to add cost-based RES, emission, and BESS functions into original programming formulation. Therefore, it is necessary to find a

method that is suitable and compatible with the various objectives of this thesis to formulate the model of UC and ED problems.

The DP method [103] is based on searching for the minimal cost solution by consistently sorting solutions of each unit's status to each simpler sub-problem. This status is known as a combination of generation units. Since all sub-problems are built and evaluated systematically as a "logic decision tree", this programming will suffer from the "curse of dimensionality" when the problem size increases [126] which may result in unacceptable solution time. So various approaches [127-129] have been developed to reduce the dimension and it is suggested to combine with the priority list technique [117].

DP can maintain the solution feasibility at the same time that it is easily modified to model generation units [130], add different constraints [131], and overcome the difficulty of non-convexity and non-linearity of large-scale systems [104]. Hence it is accepted and preferred by many researchers throughout the world.

Therefore, DP can be selected as a suitable and compatible approach which is not heavily rely on an extensive domain knowledge of programming to match the adding designs of emission cost, RES cost, and battery energy storage system (BESS). The addition of these designs allows for clearer research of corresponding impacts of these adding conditions on the optimization process to analyze how the problems of emission, integration of RES and total operation cost are affected.

### **2.2.3 Battery Energy Storage System Model**

At last, to reduce fluctuation of the RES, a BESS is proposed to be integrated into a renewable energy generation system [132]. The use of BESS is accepted gradually to achieve peak load leveling. BESS can be used to mitigate the variation between the

predicted and actual power output of RES and to smooth their fluctuations in the power system.

The BESS models are divided into two types of economic and power system stability studies [133]. This thesis is focused on modelling the BESS from the operation cost point of view at time scales.

Generally, for the part of economic, it is mainly concerned on capital cost and operation cost of the BESS [134]. However, as the scale of the energy storage system gradually increases, the optimization problem is also concerned with the battery life and battery sizing [135].

BESS models also can be summarized as generic models and dynamic models. The generic model monitors the change in the state of charge (SOC) of BESS due to power charging or discharging of the battery. The dynamic model monitors current and voltage characteristics including transients which is similar to the modelling of equivalent circuits [133]. Basic modeling of the BESS model should also consider the SOC upper and lower boundaries, charging and discharging efficiency, maximum charging and discharging rate.

## **2.3 Review of Unit Commitment**

### **2.3.1 Unit Commitment Problem Formulation**

It is noticed that the unit commitment problem has commonly been formulated as a non-convex, large-scale, nonlinear, and mixed-integer combinatorial optimization problem with constraints [136]. For example, the non-convexity and non-linearity are caused by the binary nature of the on/off statuses and non-linear cost curves for generation units. All these variability and constraints are typically created by using

unit commitment models. Even though different UC models and related algorithms have been developed in the past decades, researchers are still working in this field to find new hybrid algorithms to solve the problem more efficiently.

Since the significant increase of renewable energy sources integration into the power system, the impact of their intermittent nature causes variability and uncertainty in power system operations schedule. To cope with these effects, there is a growing need to promote the traditional thermal unit commitment to adapt to the new requirements such as fast and more ramping adjustments.

For the traditional UC problem, the first step towards the optimal schedule solution is to decide the on-off states of the generation units in every hourly period for a given planning period (normally one day or one week) [137]. They are the discrete variables that determine whether each generation unit is on or off service at any specific time.

$$U_n^t \in \{0,1\} \quad (2-1)$$

Where,  $U_n^t$  means the unit  $n$  at hour  $t$ . 1 means the unit is “on-line” and 0 means the unit is “off-line”.

The solution should serve the load demand and spinning reserve considering the units’ constraints, minimized start-up time, and minimized shut-down time.

The next step toward the economic dispatch solution is to allocate the system demand and the spinning reserve capacity among the operating units during the operation period at a minimum total production cost (TPC) which includes the fuel cost, start-up cost, and shut-down cost.

$$\text{mini } TPC = \sum_{t=1}^T \sum_{n=1}^N (F_n^t + SU_n^t + SD_n^t) \quad (2-2)$$

Where, T is the total time horizon, N is the total number of generation units and  $F_n^t$  is the fuel cost for the unit  $n$  at hour  $t$ .  $SU_n^t$  and  $SD_n^t$  are the start-up cost and shut-down cost for the unit  $n$  at hour  $t$ .

Generally, the fuel cost is expressed as a second-order function of every unit output as following:

$$F_n^t = a_n + b_n * p_n^t + c_n * (p_n^t)^2 \quad (2-3)$$

Where,  $p_n^t$  is the power generated of the unit  $n$  at time  $t$ .  $a_n, b_n, c_n$  are production cost function coefficients of unit  $n$ .

### 2.3.2 Unit Commitment Environment and Objective

As introduction previous, UC environments are divided into three main categories of profit-based UC (traditional UC), price-based UC (PBUC), and security-constrained UC (SBUC) [138]. Generally, traditional UC is looking for a solution with possible minimized generation cost in a vertically integrated utility environment [139]. PBUC emphasizes the importance of price signals that satisfying load is no longer an obligation and the objective would be to maximize the profit. The Security now is unbundled from energy, and it is priced as ancillary services [138]. The objective of SCUC is not only the economic scheduling of generating units but also to meet the temporal and operational limits of generation and transmission equipment [140].

In fact, some individuals have the misconception that maximizing profit is the same as minimizing cost. Profit is defined as the revenue minus cost that profit would

not only depend on cost but also on revenue. If the incremental revenue is larger than the incremental cost, it prefers to generate more energy for making profits.

In solving the UC problem, it is important to select the appropriate objective function for all power system operators. Traditionally, there are three common objectives of minimization of total production cost, minimization of the total emissions, and maximization of reliability and security to solve the UC problem. However, in the modern power system, the objective of maximization of reliability and security is applied as a constraint rather than an objective [117].

In general, the objective of minimization of total production cost is the main objective for UC scheduling to achieve as much profit as possible since the cost of fuel is a major economic concern [141]. Due to the low carbon context of future power systems, more and more researchers are focusing on the minimization of emissions. Even though it is reported that these two objectives are conflicting ones [141], a multi-objective approach has been achieved to search for a sub-optimal solution that leads to a saving of cost with lower fuel consumption and emission [142].

### **2.3.3 Unit Commitment Constraints**

A variety of UC problems are related to lots of constraints of generator physical constraints and system operational constraints. Depending on the different requirements of the system, the constraints can be one or more of the following constraints.

- i) Power balance constraint [143]

Equality constraint of power balance is the most important constraint that output power of online committed units must satisfy the load demand for each hour.

$$\sum_{n=1}^N P_n^t = D_t \quad (2-4)$$

Where,  $P_n^t$  is the power generated of the unit  $n$  at time  $t$ .  $D_t$  is the total demand at time  $t$ .

The following are the inequality constraints.

ii) Generation unit limit constraint [144]

The upper and lower limits of generation for the units make the units to operate within the requirements.

$$Pmin_n^t < P_n^t < Pmax_n^t \quad (2-5)$$

Where,  $Pmin_n^t$  and  $Pmax_n^t$  are the minimum and maximum active power output for the unit  $n$  at hour  $t$  respectively.

iii) Minimum up and down time constraints [145]

The reason why the setting up of minimum up time constraint for the generation unit is because that the unit is economical only when it is required to run for a certain minimum number of hours continuously.

The unit must be off-line for a minimum down time before it is re-committed to generate power again.

$$\begin{aligned} UT_n^{on} &> MUT_n \\ DT_n^{off} &> MDT_n \end{aligned} \quad (2-6)$$

Where,  $UT_n^{on}$  and  $DT_n^{off}$  are the total up-time and down time of the unit  $n$ .  $MUT_n$  and  $MDT_n$  are the minimum up time and minimum down time of the unit  $n$ .

iv) Ramp up and down rate constraint [146]

The electrical power output cannot be adjusted instantly because of the confines of thermal stress and mechanical characteristics of a generation unit [147], and this change is restricted by the ramp rate limit of the unit concerned.

$$\begin{aligned} P_n^t - P_n^{t-1} &\leq UR_n \\ P_n^{t-1} - P_n^t &\leq DR_n \end{aligned} \quad (2-7)$$

Where,  $P_n^{t-1}$  is the power generated of the unit  $n$  at the previous interval time  $t$ .  $UR_n$  and  $DR_n$  are the ramping up rate and ramping down rate of the unit  $n$ .

v) Transmission constraint [118]

To satisfy the steady-state operation of the power system, the transmission capacity constraints and bus voltage constraints are added to the system security constraints.

$$\begin{aligned} |TP_l^t| &\leq TP_l^{max} \\ V_b^{min} &\leq V_b^t \leq V_b^{max} \end{aligned} \quad (2-8)$$

Where,  $TP_l^t$  is the transmission power of line  $l$  at time  $t$ .  $TP_l^{max}$  is the maximum transmission power of line  $l$ .  $V_b^t$  is the voltage magnitude of the bus  $k$  at time  $t$ .  $V_b^{min}$  and  $V_b^{max}$  are the minimum and maximum voltage limits of bus  $k$ .

vi) Spinning reserves constraint [148]

The spinning reserve is online but unloaded capacity used to supply the sudden loss of a loaded generation unit [147].

$$\sum_{n=1}^N P_n^t \geq (D_t + SR_t) \quad (2-9)$$

Where,  $SR_t$  is the spinning reserve at time  $t$ .

### 2.3.4 Unit Commitment Problem Solving Techniques

The UC problem belongs to the class of complex combinational optimization problems, and it is the time-dependent problem of determining the schedule of generation units in the power system under the constraints of the unit and operation. Various optimization approaches have been applied to search for the solution to the thermal UC problem and they have been classified into three main categories, the classical heuristic approach based on mathematical methods, the non-classical approach based on metaheuristic methods and the hybrid algorithm approach.

The classical heuristic technique based on the mathematical method follows deterministic transition rules in moving from one solution to another one. The non-classical technique based on the metaheuristic method includes randomness and the use of the stochastic approach in moving from one solution to another [104].

#### A) Classical Heuristic Approach

The classical heuristic approaches include exhaustive enumeration, priority listing (PL), dynamic programming (DP), Lagrangian relaxation (LR), branch and bound (B&B), and mixed-integer linear programming (MILP).

##### i) Exhaustive enumeration

The exhaustive enumeration is an early and simplest solving method that evaluates the optimal solution by sorting the least operation cost based on enumerating all possible combinations of the generation units [101, 102]. This method can support an accepted solution, but it is not suitable for a large-scale power system since its computational time is very huge [149].

#### ii) Priority listing

The priority listing method [150-152] is creating a priority list of committing generation units based on the order of the increasing operation cost. It means that the least cost units are first selected to operate until the system load and reserve requirements are satisfied. This method is still being used in many developing countries because of its simplicity and ease of application and understanding [117], but its result of the total cost could be away from the optimal solution compared with other advanced methods [153].

#### iii) Dynamic programming

The dynamic programming (DP) method [103] is based on searching for the minimal cost solution by consisting and sorting solutions of each unit's status to each simpler sub-problem. This status is known as a combination of generation units. Since all sub-problems are built and evaluated systematically as a "logic decision tree", this programming will suffer from the "curse of dimensionality" when the problem size increases [126] which may result in unacceptable solution time. So various approaches [127-129] have been developed to reduce the dimension and it is suggested to combine with the priority list technique [117].

DP can maintain the solution feasibility at the same time that it is easily modified to model generation units [130], add different constraints [131], and overcome the

difficulty of non-convexity and non-linearity of large-scale systems [104]. Hence it is accepted and preferred by many researchers throughout the world.

#### iv) Lagrangian relaxation

The Lagrangian relaxation (LR) method [154-156] is a problem conversion method based on adjoining the coupling constraints onto the cost objective expression by adding the Lagrange multipliers as the penalty factor. Then the original UC problem is converted to the relaxed problem to find the multipliers so that the solution is near the optimum. The LR method supports a faster solution, and its advantages are the same as the DP method in that it is easy to modify, model, and add constraints. However, there are two main issues with the LR method it suffers from slow numerical convergence [157] and the dual optimal solution seldom satisfies the once relaxed coupling constraints [158].

#### v) Branch and bound

The branch and bound method [159-161] is based on the principle that the total set of feasible solutions can be partitioned into smaller subsets of solutions by the upper and lower bounds obtained from employing linear function to represent cost and constraints expressions. Finally, these smaller subsets can then be evaluated systematically until the best or a near-optimal feasible commitment schedule is achieved [162]. The advantages of this method are that all time-dependent constraints can be included, and this method does not require a priority ordering of generation units. However, this method suffers exponential growth in execution time when the size of the UC problem increases [163].

#### vi) Mixed-integer linear programming

The mixed-integer linear programming [164-166] is an operational research method in which some of the variables are restricted to be integers in the formulation of unit commitment problems [167]. The advantage of a MILP formulation is that it gives feasible solutions with its flexible and accurate modelling, but this method results in longer programming running time because of its computational complexity [120].

## B) Meta-heuristic Approaches

The meta-heuristic approaches include expert system (ES), fuzzy logic (FL), artificial neural network (ANN), genetic algorithm (GA), tabu search (TS), simulated annealing (SA), evolutionary programming (EP), ant colony search algorithm (ACSA), and particle swarm optimization (PSO).

### i) Expert system

In the early form of the intelligent computer program, a rule-based expert system [168-170] combining the UC algorithm is only using experiences and inference procedures by human experts in the domain to adjust the program's parameters to schedule and modify unit commitments [117]. This method saves lots of computation time and does not need exact mathematical formulation. But the quality of solution performance is dependent on the knowledge of experienced operators [157].

### ii) Fuzzy logic

The fuzzy logic method [100, 171] is based on treating each type of cost as fuzzy variables in the unit commitment problem and it is based on the fuzzy sets method to select membership functions for each fuzzy input and output variable. Then the decisions can be made by forming various rules that relate the input variables to the output variable using If-Then (condition-consequence) statements. The details and

examples about how to formulate the UC problem based on a basic fuzzy logic method can be found in [115].

### iii) Artificial neural network

The artificial neural network method [146, 172-174] is creating complex network connections between different processing variables of input and output signals and is analogous to a single neuron in a biological brain [105]. This network is trained using a training set algorithm based on an internal weighting system to achieve the minimum total cost. During the UC model, this training process means changing possible combinations and dispatch schedules of generation units to acquire optimal results. This method can handle large and complex systems with nonlinear modelling, but with the increment of problem size, its computation time can be large.

### iv) Genetic algorithm

The genetic algorithm methods [106-109] are stochastic and adaptive search techniques based on the principles and mechanisms of natural selection and “survival of the fittest” derived from natural evolution [175]. During the UC problem, a population of potential solutions of the UC schedules is used to perform cost results through crossover, mutation, and selection to acquire a better ‘genetic’ which is a lower-cost solution located near the optimal solution. Finally, the best solution of minimum total cost could be achieved through this continuous iteration loop systematically. This method is very flexible in modelling both time-dependent and coupling constraints, but it may fail to converge to the optimal solution [107, 119].

### v) Tabu search method

The tabu search method [114, 176] is based on iteratively improving and promoting a feasible solution to the UC schedule by the method of the greedy

algorithm [177] to evaluate a better neighborhood solution each time until the solution to the cost function cannot be improved further. There is no limitation on the modelling of the cost function in this method. However, the major drawback is that it cannot guarantee the optimality of the provided solution since it may get stuck in the local minima [172].

vi) Ant colony search algorithm

The ant colony search algorithm [110] is based on the idea that a colony of ants can find the shortest path between the nest and food source by depositing, exploiting, and exchanging pheromone information on the path [178]. During the UC problem, it is to model a problem that searches for a minimum cost path. Then, using artificial ants to look for cost paths of UC schedules based on their ants' simple selection behaviors. As a result, pheromone will accumulate faster in the lower-cost path. Then, cheaper paths are found through the efforts of global cooperation among ants in the colony. It is reported that this method supports positive feedback accounts for the rapid discovery of good solutions [179] and its convergence is guaranteed [180], but its theoretical analysis is difficult, and its solution relies on a large number of iterations.

vii) Particle swarm optimization

The particle swarm optimization method [111-113] is similar in concept to the GA method and is based on creating a population of random solutions. The potential solutions, regarded as particles with position and velocity vectors, are promoted through the problem space by following the current optimal solution of each individual particle and global particle swarm. This method gives good precision and high-quality solution with stable convergence characteristics for the problems featuring non-linearity and non-differentiability [181]. In addition, this method is good at controlling the balance between the global and local exploration of the research space [182] by

appropriate selection of inertia weigh factor. However, its ability of local optimal search is weak since its slow convergence in the refined search stage [104].

### C) Hybrid Approaches

With the development of the power system, its modelling construction and constraints become more and more complex gradually. And a single algorithm is simple indeed but may cause suboptimal results. So, it is proposed to merge more than one algorithm and form a hybrid model to meet optimal requirements.

The hybrid approaches can obtain better and more accurate solutions by adding complicated constraints and integrating the advantages of different methods. The following will support some methodologies proposed based on the hybrid approaches with its feature.

References [183, 184] proved that the strategy of adaptive memory can be used to escape from the local optima by driving the search to different parts of the search space. The hybrid method of LR and GA for unit commitment is proposed by [185] to deal with large-scale power systems. Reference [186] used the priority list method to create the initial population based on the GA method to search the UC schedule decisions to reduce the computation time. Since the good compatibility feature of fuzzy set notations and errors in the forecasted hourly loads, a fuzzy logic combined with the DP method [187] for the UC problem is proposed to achieve a better optimal result. A two-step method [188] uses an artificial neural network creating typical commitment schedules to train and then follows modified dynamic programming to search for new combinations for the uncertain units.

## 2.4 Summary

This chapter firstly conducted reviews of modelling methodologies of various power generation unit types. This section discussed and compared the common modelling methods in order to select the suitable modelling methods to develop the power generation models of wind farms, solar farms, thermal units, and BESS for resolving the day-ahead UC problem of the power dispatch.

Secondly, this chapter conducted reviews of UC problem formulation, objective functions, and their constraints. To address UC problems, various approaches were introduced and discussed with their individual characteristics.

In general, classical methods have been used widely in solving the UC problem due to their efficiency and credible mathematical foundations. It follows deterministic transition rules in moving from one solution to the next but meta-heuristic methods do not. The randomness and stochastic approach in moving from one solution to the next can make the meta-heuristic methods avoid the local optimal solution.

Because the special background of China's semi-liberalized power market, power quota dispatch rules and policies, and uncertainties on renewable energy integration all cause the changes in UC problem formulation and result in the UC model being a non-convex and large-scale program. These particularities are summarized as follows. The power trading of inter-provincial and inter-regional are normally pre-determined by the government according to the national strategy. Even the dispatch rule takes into account the differences in capacity, operating efficiency of the thermal units, but there is little difference in the amount of power generation operation hours allocated by each unit eventually. The renewable energy farms have the highest priority in power scheduling even its operation cost is higher than the thermal units.

In order to adapt these special features in paragraph above, a part of power generations have been fixed based on the quota dispatch rules and policies during the power system operation. Then only the other power generations in mixed system can be scheduled and sub-optimized.

Besides, China is carrying out a digital technology-based power reform that combines economic management and a production model to improve decision-making efficiency and reduce generation costs.

The above issues and updates require flexibility that new models must have the ability to manage sub-problems in decomposition programs and maintain the solution feasibility. So, after the review previous, it is selected to use the dynamic programming optimization approach as a further solution method in this thesis due to its ability to overcome the difficulty of non-convexity and non-linearity of large-scale systems and also the dynamic variables. Besides, the additional sub-problems can be easily coded into the modelling programming without extensive domain knowledge.

# Chapter 3 Wind Energy and Power Curve Modelling

## 3.1 Introduction

Wind energy, as a source of zero-emission and inexhaustibility, can be the most efficient technology to produce power in a safe and environmentally sustainable manner.

In the past two decades, the application and large-scale development of wind power systems have made a non-negligible contribution to reducing energy pollution. However, the randomness and intermittency of wind lead to uncertainty in wind power generation and also challenges the power system of balancing and dispatching at the same time.

Therefore, the wind power curve, as an essential approach to representing the relationship between relative wind speed and wind power, has been discussed again and the researchers are mainly focused on the nonparametric methods of power curve modelling approaches, such as methods of Artificial neural networks [189], clustering [190], data mining [191].

These methods above can provide reliable results, but their model complexity and mathematical requirements make them lack a wide application and fast estimation. So, it is necessary to propose a new novel method that is simple to use and can be utilized for predicting the power output of turbines for sizing and cost optimization applications in which a good accuracy is not desired.

Therefore, a novel method of Double Cubic is proposed in section 3.4. Before that, this chapter firstly gives an overview of wind energy background, development, and technology to understand the basic wind energy concept in section 3.2. And then

wind power and its further curve related to the wind turbine and their modeling can be found in section 3.3. Finally, case studies are examined to prove the accuracy improvement based on the proposed Double Cubic power curve method in section 3.5.

## **3.2 Overview of Wind Energy**

### **3.2.1 Background**

Wind is a renewable and clean energy resource, which makes it suitable to satisfy the increasing energy demand of the world. The scale use of wind energy by early humans can be traced back to the agricultural era for grain milling and water pumping. Until 1887, Prof James Blyth at Anderson's College installed the first power generating windmill in the world, mentioned on page 65 of [192]. Before the 1980s, the technology is just mature to enable small-scale wind turbines to provide electricity for remote farms. However, with the rapid development of modern technology and the reduction of wind turbine costs in the 2000s, the development of wind power has rapid growth [193].

Electricity production from wind power, as pollution-free energy is one of the most rapidly growing fields among the renewable energy sources in the last decades [94]. As more and more conferences on global climate issues are held by developed countries, developing countries are also constantly participating. Now, it is time for both governments and ordinary citizens to join hands to make this world a better place to live in, not only for ourselves but also for future generations.

### **3.2.2 Development**

The improvement in wind power technology has made it one of the fastest-growing renewable energy technologies in the world.

### i) Capacity

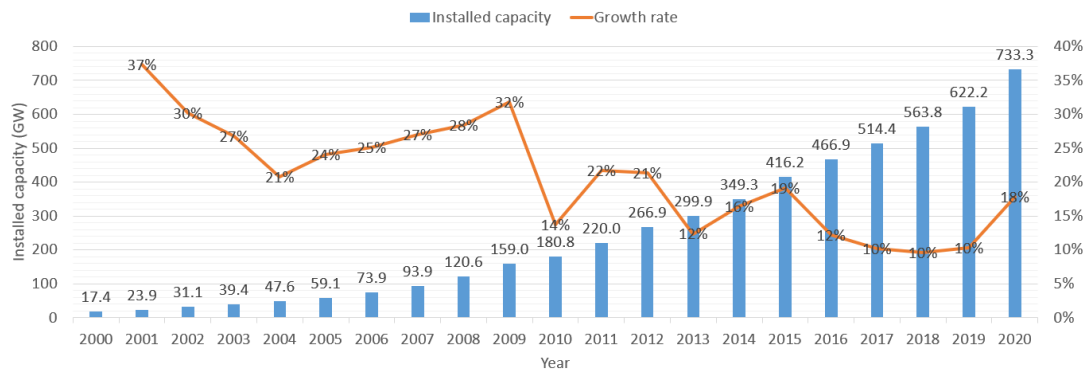


*Figure 3.1: World Installed Wind Power Capacity and Growth Rates, 2000-2020*

To cope with global climate problems, the majority of countries have declared goals to cut carbon emissions by 2050. Hence global installed wind generation capacity has grown dramatically in the past two decades, jumping from 17.4 gigawatts (GW) in 2000 to 733 GW by 2020 as Figure 3.1 shows [192] [194]. Not only it has doubled from 2014 to 2020, but also it will be expected to increase strongly in the coming years [195]. The roadmap [196] published on 18 May, calls for scaling up wind rapidly this decade to achieve carbon neutrality. The goal is set at annual additions of 390 GW of wind capacities by 2030 which is about a four-times to level set in 2020.

### ii) Economy

The major cost fields of wind energy are focused on investment costs, power generation costs, operation and maintenance costs, and grid-based consumption costs [192]. With improving economies of scale and technological advancement of wind technology, the global installed cost of both onshore and offshore wind farms declined by more than 30 %, and the global average cost of electricity from wind power fell by 56.2 % from onshore wind, and by 48.1 % from offshore wind between 2010 and 2020

as indicated in Table 3-1 [197, 198]. Depending on the table below shows and also falling cost trend, wind power generation will become more price-competitive compared with the new fossil fuel-fired power generation (0.057 USD /kWh in 2020 page 26 in [198] ).

*Table 3-1: Global Cost Reduction Potential for Wind Power, 2010-2020*

Cost reduction potential for wind power, 2010-2020				
	Installed costs			
	(USD/kW)			
	2010	2015	2020	Total percent change
Onshore wind	1971	1560	1355	31.3%
Offshore wind	4706	4650	3185	32.3%
	Levelized cost of electricity			
	(USD/kWh)			
	2010	2015	2020	Total percent change
Onshore wind	0.089	0.07	0.039	56.2%
Offshore wind	0.162	0.18	0.084	48.1%

### **3.2.3 Technology**

Wind power technology is briefly introduced here by focusing on three topics wind resources, wind turbines, and their power integration.

#### *i) Wind resource*

The assessment and forecasting of wind energy resources require highly accurate wind data. This high-quality wind data is an essential basis for the construction and investment of wind farms [199]. By two illustrating cases of Norway and Scotland, [200] helps to understand the impact assessment and gives a clearer definition of the criteria to be used for sustainable wind power planning. [23] give an overview of new and current developments in wind forecasting.

In China, the majority of focused attention on the early research for wind resources is in the wind resources assessment and long-term wind forecasting (more than one day [201]). However, it was not until the issue of large-scale curtailment [202] of wind power occurs in 2015 that research institutes return to focus on short-term (30 seconds to 6 hour time horizon) wind power forecasting to support the technique for wind power curtailment and balancing. [203] shows the economic benefit of using short-term forecasting in integrating higher levels of wind energy into the electricity market. In general, since the twenty-first century, wind energy has gradually entered a new stage of mature technology, research on wind resources has become more in-depth, and wind forecasting has become more accurate [204].

*ii) Wind turbine*

Modern wind turbines mainly consist of two basic configurations, the horizontal axis, and the vertical axis. [205] describes how machines and systems extract energy from wind in various fields and it introduces different types of wind turbines. The wind turbine technology is mainly divided into two aspects, the increment of the maximum rated power capacity of a single-unit wind turbine and the increasing maturity of the control technology for the wind turbine.

The rated power capacity of a single-unit wind turbine grows from 75 kilowatts in 1980 to 5000 kilowatts in 2020 [206]. In the future, this rated number may be improved to 10000 kilowatts, and even 20000 kilowatts [206]. This continued growth not only has contributed to utilization efficiency but also increases the space requirement of wind farms.

Typically, the wind gust is a strongly random process, variable both in time and in space and these changes would cause fluctuation of power output which affects the power quality and the system stability [207]. Hence, it is necessary to control wind

turbines to support constant power. [208] gives a review on wind turbine control methods.

The control methods are divided into three main control systems, pitch control, generator torque control, and grid integration control. In general, the pitch angle and the generator torque are the main targets to be controlled in the wind turbine control system. The pitch angle control enables a smooth power output through the pitch system controlling the wind input torque [209, 210]. The generator torque control is to extract much power from wind through the rotor speed system tracking the maximum power point [211, 212]. The grid integration control [213] is to cope with the power system oscillations through frequency relay disconnecting the wind generator after a frequency disturbance [214, 215]. With the gradual development of wind turbine control technology, the applications of wind energy have been more stable, safer, and more efficient.

### *iii) Power integration*

Due to the high stochastic volatility and intermittent nature of wind energy, many institutes have established wind power integration studies for load balancing, grid safety, power quality, and so on. [216] gives a review on the evolution of wind power integration studies. Generally, a basic system-friendly wind farm should carry on these features at least, a forecasting system of short-term and ultrashort-term for dispatching adjustment [217, 218], an active and reactive power regulation system to support the stability of the grid [219-221], and low voltage ride-through to cope with fluctuation of grid [222-224].

## 3.3 Wind Power Curve

### 3.3.1 Theoretical Wind Power Output

The energy contained in the wind is the kinetic energy of moving air. It can be described by the kinetic energy of the particles in the air:

$$E_{wind} = \frac{1}{2} * m_{air} * v^2 \quad (3-1)$$

Where,  $E_{wind}$  is the energy content in the mass of air,  $m_{air}$  in kilograms (kg).  $v$  is the wind speed in meters per second (m/s).

The power of wind can be described as follows:

$$P_{wind} = \frac{1}{2} * \rho_{air} * A * v^3 \quad (3-2)$$

Where,  $P_{wind}$  is the kinetic energy in the wind crossing the circular ring per second in watts (J/s).  $\rho_{air}$  is the density of the air in kilograms per cubic meter ( $\text{kg}/\text{m}^3$ ).  $A$  is the swept area crossed by the wind in square meters ( $\text{m}^2$ ).

### 3.3.2 Wind Turbine

Wind turbines work by converting the kinetic energy of wind into kinetic energy of the blade of the turbine. Turbines blades around the rotor turn the generator to produce electricity. The main conversion energy depends on the speed of the wind, the swept area of the blade, and air density.

Besides, this conversion energy also depends on how well they match the angular velocity of the rotor of the wind turbine to the wind speed. Because the rotor of the wind turbine turns too slowly, most of the wind will pass without action through the

openings between the blades with little power extraction. And if the rotor turns too fast, the rotating blades act as a solid wall obstructing the wind flow, again reducing the power extraction.

The power coefficient is defined as the power extracted by the wind turbine relative to that available in the wind stream:

$$C_p = \frac{P_{WT}}{P_{avail}} = \frac{P_{WT}}{\frac{1}{2} * \rho_{air} * A * v^3} \quad (3-3)$$

The values of  $C_p$  are different among the wind turbines, which are depending on the turbine designs and the rotor blades. Therefore, according to Betz Limit Law, the theoretical maximum value of  $C_p$  is 0.593. Generally, wind turbines with three blades have a maximum  $C_p$  value between 0.4 to 0.5, whose the mechanical and electrical losses are included [225].

So, the wind turbine should be designed to operate at its optimal wind tip speed ratio to extract power from the wind stream as much as possible. The wind tip ratios depend on the wind turbine design, the number of blades, and the rotor airfoil profile [226]. For grid-connected wind turbines with three rotor blades, the optimal wind tip speed ratio is reported as 7, with values over the range from 6 to 8 [226].

The relationship between the wind speed and the rate of rotation of the rotor is characterized by a non-dimensional factor, known as the Tip Speed Ratio (TSR):

$$\lambda = \frac{\text{speed of rotor tip}}{\text{wind speed}} = \frac{\omega * r}{V_{wind}} = \frac{2\pi f * r}{V_{wind}} \quad (3-4)$$

Where,  $\lambda$  is the tip speed ratio,  $\omega$  is the angular velocity in radians per second (rad/s),  $r$  is the radius of the rotor in meters (m) and  $V$  is the wind speed in meters per second (m/s).  $f$  is the frequency of rotation in  $Hz$  or  $sec^{-1}$ .

Figure 3.2 here is an example graph of the power curve with its associated  $C_p$  curve for an ENERCON E-126 EP4 [227] wind turbine with a rated power of 4.2 Megawatts, rotor diameter,  $D_{rotor}$ , of 127 meters, and rotational speed of 3 – 11.6 revolutions per minute. This new E-126 EP4 concept combines innovative technology and intelligent modular design for more efficiency and reliability.

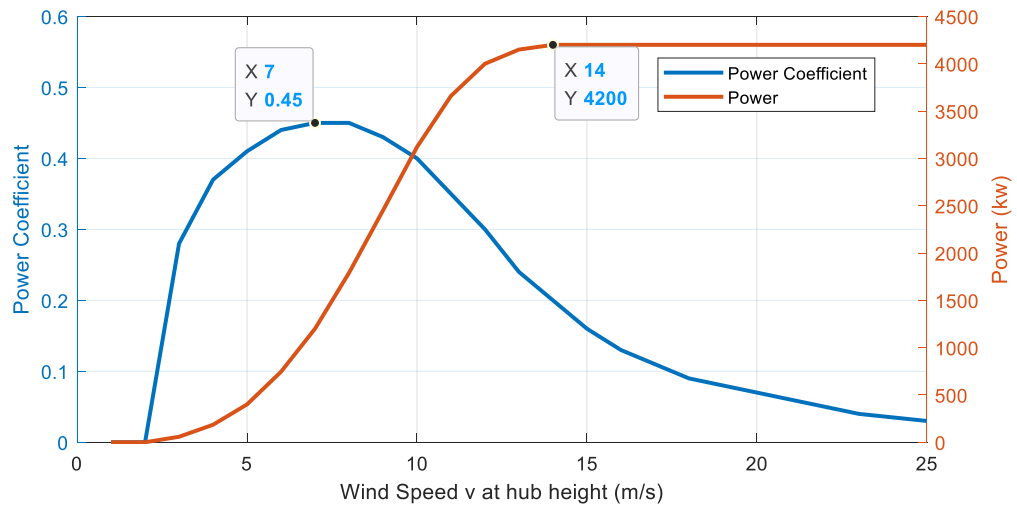


*Figure 3.2: The Power Curve with its associated  $C_p$  Curve for an ENERCON E-126 EP4 / 4.2 MW Wind Turbine*

Figure 3.2 shows the maximum  $C_p$  is 0.45 and the corresponding wind speed is 7 m/s. This point is named the maximum  $C_p$  point. It is easy to find that, from the cut-in speed point to maximum  $C_p$  point the value of  $C_p$  is increasing, but from the point of maximum  $C_p$  to the point of cut-out speed the value of  $C_p$  is decreasing. By considering the slope changes around this point, the modelling of the power curve can be promoted compared with the parametric models using polynomial approximations to model wind power curve models. The proposed method can be found in sub-section 3.4.2 (Double Cubic Power Curve).

To calculate wind power production from historical wind data, the hub height of the wind turbine should be considered. The wind shear function is used to modify the measured wind data to the desired height:

$$\frac{v_2}{v_1} = \left(\frac{h_2}{h_1}\right)^z \quad (3-5)$$

Where  $v_1$  is the measured wind speed at the height  $h_1$ ,  $v_2$  is the calculated wind speed at the hub height  $h_2$ .  $z$  is the wind shear exponent and it is dependent on the ground roughness [66].

The researched results of parameters  $z$  for different types of terrain come from the following table [228].

*Table 3-2: Roughness of Different Terrains*

Type of Terrain	Roughness Class	$z$
Water Areas	0	0.01
Open Country, few surface features	1	0.12
Farmland with buildings and hedges	2	0.16
Farmland with many trees, forests, villages	3	0.28

### 3.3.3 Power Curve

The Power curve of a wind turbine shows the relationship between the output power of the turbine with the wind speed. It is a good method to represent the performance of the wind turbine.

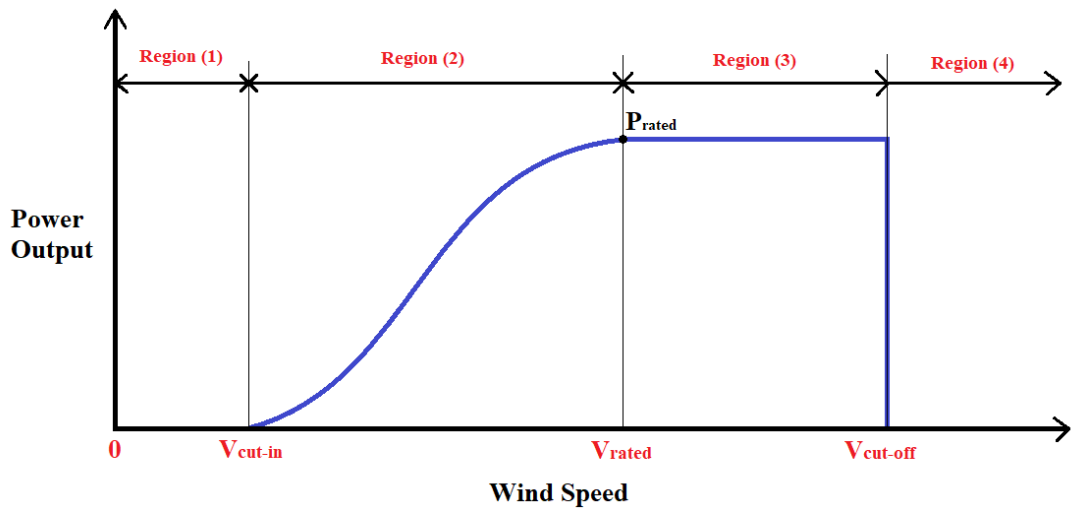


*Figure 3.3: Typical Power Curve of a Regulated Wind Turbine*

Generally, the generator of a wind turbine has not enough torque to generate power when the wind speed is below the cut-in speed since this speed is not sufficient to support the blades to rotate.

With the wind speed increase over the value of cut-in speed, the wind turbine first starts to rotate and generates power. In Region 2 as Figure 3.3 shows, the output of electrical power increase rapidly with the wind speed rising.

Until the wind speed reaches the rated wind speed, the generator begins to deliver the rated power. During the Region 3 between rated and cut-out wind speeds, the power output is maintained constant at the rated value.

Because of the risk of damage to the rotor, if the wind speed exceeds the cut-out wind speed, the wind turbine will shut down by a braking system or other control methods.

So, the wind power output generated by a typically regulated wind turbine could be written as the following equations:

$$P = \begin{cases} 0 & v \leq v_{ci} \\ P_{(v)} & v_{ci} \leq v \leq v_r \\ P_r & v_r \leq v \leq v_{co} \\ 0 & v_{co} \leq v \end{cases} \quad (3-6)$$

Where,  $P$  is the wind power output in watt (W),  $P_r$  is the rated power output of the wind turbine,  $v$  is the wind speed in meters per second (m/s),  $P_{(v)}$  is the power output of the wind turbine under the wind speed of  $v$ ,  $v_{ci}$  is the designed cut-in speed for the turbine in meters per second (m/s),  $v_{co}$  is the designed cut-out speed for the turbine in meters per second (m/s), and  $v_r$  is the designed rated speed for the turbine in meters per second (m/s).

### 3.3.4 Power Curve Modelling

#### i) Classification

There are many power curve modelling methods, such as deterministic, probabilistic, parametric, and non-parametric, and stochastic methods. A detailed review [59] of current power curve modelling techniques is presented from many perspectives.

For a deterministic power curve model, each value of wind speed corresponds to a fixed value of output power [60]. However, in practice at a wind farm, the same type of turbines may produce different amounts of power even if the wind speed is the same.

Hence, the method of probabilistic power curve model is used to cope with the issue that each value of wind speed corresponds to a probabilistic or accidental value of output power [61]. The probabilistic method requires large numbers of historical data to improve the results' accuracy [62].

A parametric model defines the relationship between input and output parameters of a wind turbine by a set of mathematical equations.

Unlike parametric methods, non-parametric models establish a model and simulate it in a way to minimize the deviations between observed data and outputs without searching for a mathematical relationship, such as neural networks, fuzzy clustering centers, and data mining methods [63, 64].

It is reported [65] that the stochastic method characterizes the output power performance of the turbine by evaluating its dynamic response against the wind speed inputs. The dynamic power output is separated into a deterministic stochastic part in its model.

#### ii) Parametric models

Parametric models have three main advantages, simple to construct and use, limited data requirement, and their parameters are easy to calculate. However, the accuracy is insufficient, and it is only suitable for power estimation and prediction in the early wind resource assessment.

Review [65] introduces various approaches for modelling wind turbine power curves in detail. Since the proposed modelling approach by the author belongs to the type of polynomial of the parametric method, this sub-section is focused on the discussion of parametric models.

Generally, parametric models are based on the polynomial approximations to represent the relationship between power output and wind speed of wind turbines as equation (3-6) expressed. The power output of the wind turbine under the wind speed of  $v$ ,  $P_{(v)}$ , in equation (3-6) at Region (2) of Figure 3.3, can be estimated by various functions using polynomial expressions.

Different models of linear [66], quadratic [67], cubic [68], Weibull [66], double exponential [69], and high degree powers of speed [70] are used to model the power curve or any other approaches.

These models in Table 3-3 below use the wind turbine specifications of cut-in speed ( $v_{ci}$ ), cut-off speed ( $v_{co}$ ), rated wind speed ( $v_r$ ), and rated power ( $P_r$ ) to determine the equations for the power curve. However, these modes do not consider the inflection point on the power curves. An example of this point is marked in Figure 3.4.

*Table 3-3: Expressions of Parametric Models*

Model	Expressions of $P_{(v)}$	Parameters
Linear	$P_{(v)} = P_r \frac{v - v_{ci}}{v_r - v_{ci}}$	—
Quadratic	$P_{(v)} = P_r \left( \frac{v - v_{ci}}{v_r - v_{ci}} \right)^2$	—
Binomial	$P_{(v)} = (a + bv + cv^2)$	$a = \frac{1}{(v_{ci} - v_r)^2} \left[ v_{ci}(v_{ci} + v_r) - 4v_{ci}v_r \left( \frac{v_{ci} + v_r}{2v_r} \right)^3 \right]$
		$b = \frac{1}{(v_{ci} - v_r)^2} \left[ 4(v_{ci} + v_r) \left( \frac{v_{ci} + v_r}{2v_r} \right)^3 - 3v_{ci} - v_r \right]$
		$c = \frac{1}{(v_{ci} - v_r)^2} \left[ 2 - 4 \left( \frac{v_{ci} + v_r}{2v_r} \right)^3 \right]$
Cubic	$P_{(v)} = av^3 - bP_r$	$a = \frac{P_r}{v_r^3 - v_{ci}^3}$
		$b = \frac{v_{ci}^3}{v_r^3 - v_{ci}^3}$
Weibull	$P_{(v)} = a + bv^k$	$a = \frac{P_r v_{ci}^k}{v_{ci}^k - v_r^k}$
		$b = \frac{P_r}{v_r^k - v_{ci}^k}$

### iii) Inflection point

The inflection point is where a curve changes from Concave upward to Concave downward. Concave upward is when the slope increases and Concave downward is when the slope decreases.

In most real power curves, models which consider this inflection point can describe the actual shape of the curve more accurately than the above models in Table 3-3. And an example inflection point can be found in Figure 3.4.

The reference [71] proposes a new formula for power curve interpolation which considers the inflection point on the curve. And another reference [69] uses a double exponential model to fit the data in two inflection zones using a single equation.

The models of four-parameter logistics [70] and five-parameter logistics [72] are also used for modelling the wind turbine power curve by considering the inflection point on the curve.

Although these methods above can provide reliable results, their model complexity and mathematical requirements make them lack a wide application and fast estimation since their parameter estimation is difficult [65].

So, it is necessary to develop a new novel method based on the polynomial models with the merits of simplicity, limited data required, parameter calculation is easy, and inflection point consideration.

### 3.4 Proposed Modelling Method

This section will introduce the developed modelling method in this thesis. It is based on the polynomial model of the cubic approach by considering the inflection point to improve the simulation accuracy.

#### 3.4.1 Modelling Issue of Cubic Approach

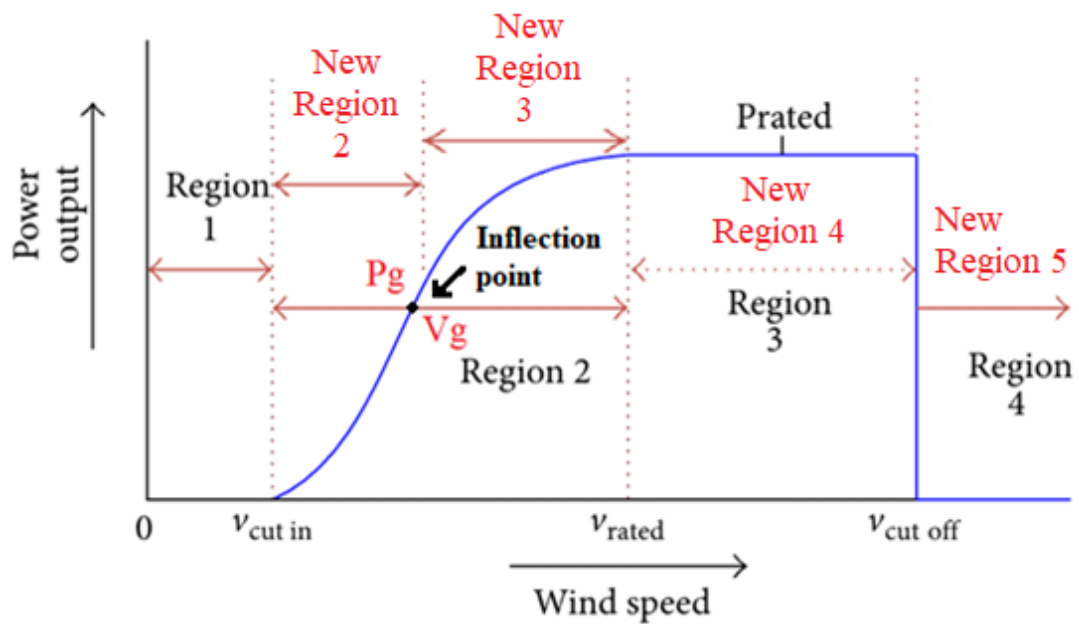


Figure 3.4: Structure chart of proposed Power Curve of a Regulated Wind Turbine

The proposed method is going to divide the original Region 2 (bold prints in Figure 3.4 between  $v_{cut\ in}$  and  $v_{rated}$ ) into two parts consisting of New Region 2 and New Region 3 (red words) by adding an inflection point. And then modelling these curves in the two New Regions based on the polynomial model of cubic in Table 3-3.

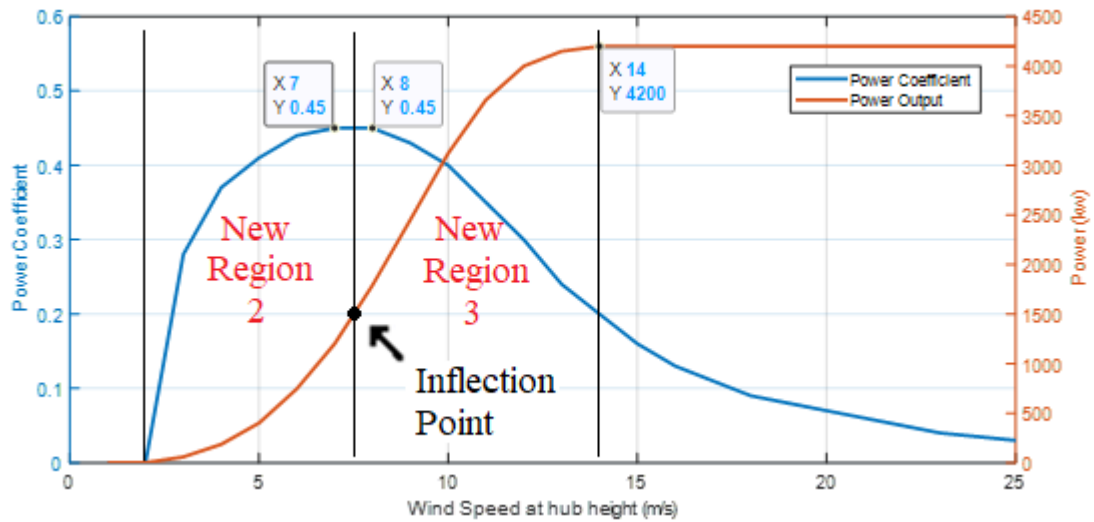
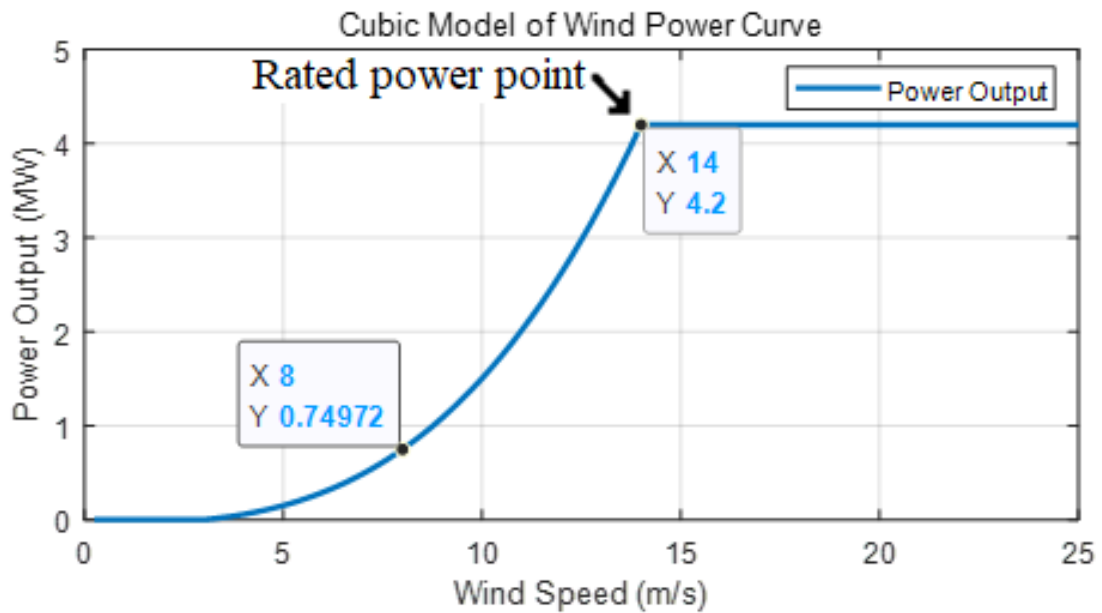


Figure 3.5: Structure Chart of Power Curve of Wind Turbine with its associated  $C_p$  Curve

It is noticed that the inflection point is where a curve changes from Concave upward to Concave downward. Concave upward is when the slope increases and Concave downward is when the slope decreases.

Figure 3.5 shows an example power curve of a wind turbine, and it is easy to find that, the curve value of the power output increase with the value increase of wind speed in New Region 2 and New Region 3. But this curve changes from concave upward to concave downward at the inflection point and it reaches its largest value of power coefficient corresponding.

Hence, the modelling issue comes. It is not exactly that, for the polynomial method of the cubic model, its slop value of power output always increases no matter in the New Region 2 or the New Region 3 as shown in Figure 3.6 which keeps increasing until it reaches the point of rated power.



*Figure 3.6: Power Curve of Cubic Model for a Regulated Wind Turbine*

Another feature is that the rising and falling trend of the power coefficient is approximately similar to the slope of the power output curve. When the slope of power output begins to decrease, the value of power coefficient begins to fall at a similar wind speed which is close to the inflection point as Figure 3.5 shows.

Therefore, combining these features the method of the Double Cubic Power Curve is developed by the author in this thesis to cope with these modelling issues.

### **3.4.2 Double Cubic Power Curve**

#### **i) Introduction**

The Double Cubic power curve is a modelling approach by combining two segments of the cubic curves to simulate the wind power curve. New Region 2 uses the segment of the curve with an increasing slope and New Region 3 uses the segment of the curve with decreasing slope. And this curve is still acquired based on the original

equation of the polynomial cubic method in Table 3-3, but the values of parameters are changed.

Figure 3.7 supports a simple example of cubic curves,  $y = kx^3 - b$ , based on the same polynomial structure of expressions of the cubic model approach,  $P_{(v)} = av^3 - bP_r$ .

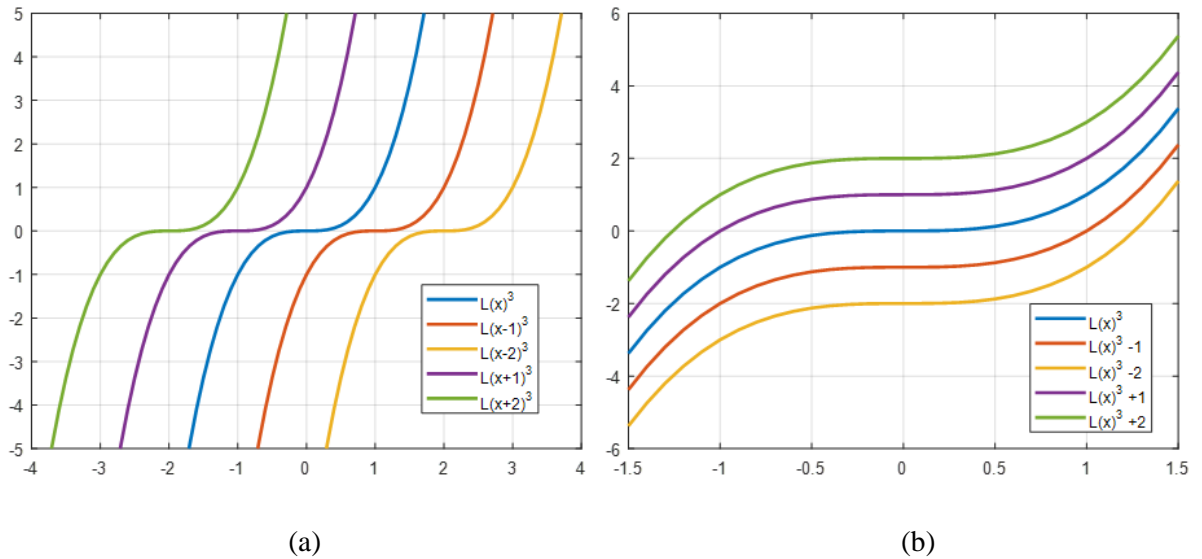


*Figure 3.7: Example Chart of Cubic Curves*

As Figure 3.7 shows, this structure type of polynomial curve can move the position of the curve on the coordinate axis by changing the polynomial parameters without slope changes at each point, such as the left and right movement of the curve in Figure 3.7 (a) or up and down movement of the curve in Figure 3.7 (b).

Based on this method, by referring Figure 3.8 (a) and (b), one segment of the cubic curve (Figure 3.8 (a)) generated by the cubic equation Table 3-3 can be moved to the target area (Figure 3.8 (b)) combining with another segment of the cubic curve to generate a new segment of the curve. This new combined curve (circled area in

Figure 3.8 (b)) is named the Double Cubic Curve which can be used to simulate the nonlinear portion of the wind power curve.

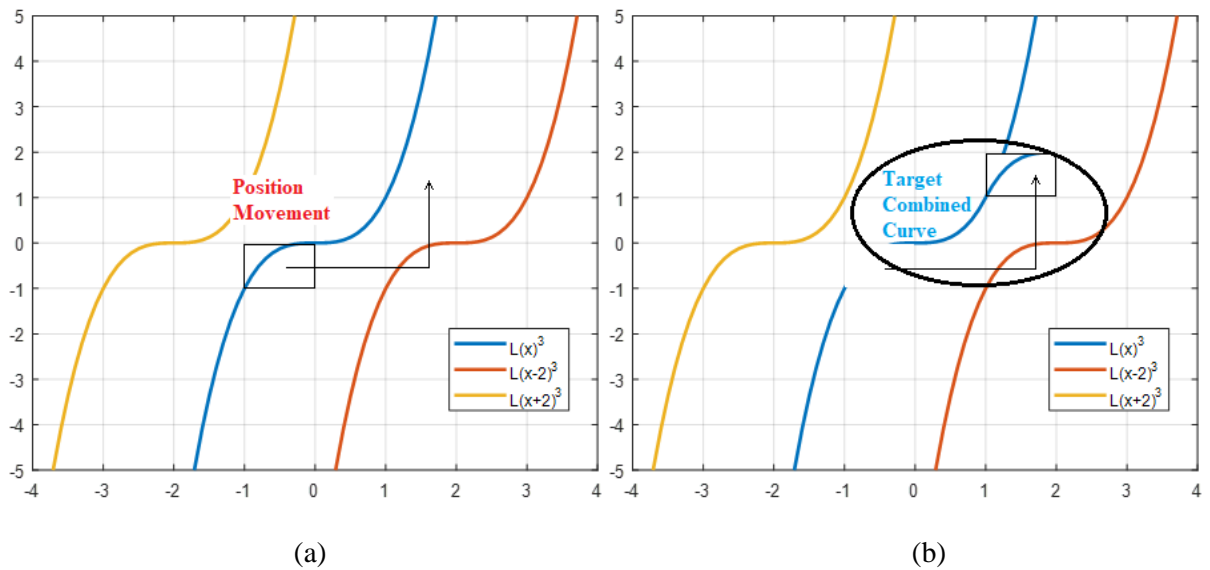


Figure 3.8: Explanation Chart of Combined Curve based on the approach of Double Cubic Power Curve

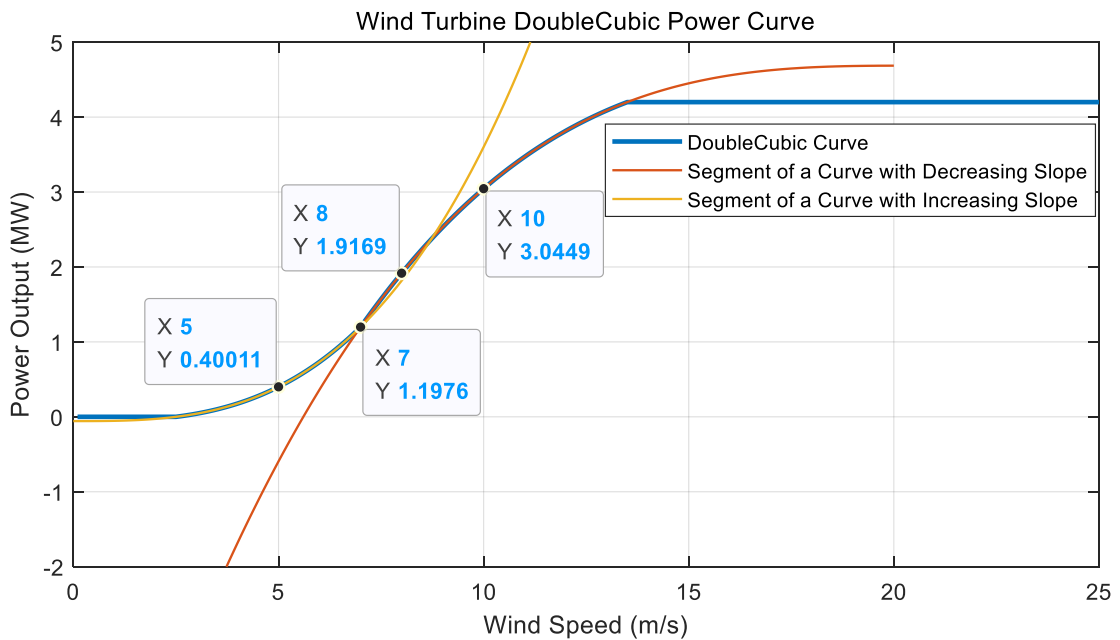


Figure 3.9: Double Cubic Power Curve and segments of Combined Curves for an ENERCON E-126 EP4 / 4.2 MW Wind Turbine.

As an example of Figure 3.9, the Double Cubic power curve for an ENERCON E-126 EP4 turbine is generated, and its nonlinear portion of the wind power curve consists of two segments of the cubic curve.

New Region 2 uses a segment of the yellow curve with an increasing slope to express, and New Region 3 uses a segment of the red curve with decreasing slope to express. And these curves are generated based on the equation of the polynomial cubic method in Table 3-3 but their parameters are different. These parameters will be introduced in the following sub-section of mathematical formulation.

*ii) Mathematical formulation*

The amended formula  $P_{(Region\ 3)}$  of the cubic polynomial is written below: and its target is to make the segment of the curve move to the target position as Figure 3.8 (a) to (b) shows.

$$\begin{aligned}
 P_{(New\ Region\ 3)} &= A_2 * (v - v_g - v_r)^3 - B_2 * (P_r - P_g) \\
 &\quad - \left[ A_2 * (v_g - v_g - v_r)^3 - B_2 \right. \\
 &\quad \left. * (P_r - P_g) \right] + A_1 v_g^3 - B_1 P_g \\
 &= A_2 * ((v - v_g - v_r)^3 + v_r^3) + A_1 v_g^3 - B_1 P_g
 \end{aligned} \tag{3-7}$$

Where,  $v_g$  is the wind speed at the point where it reaches its maximum value of power coefficient, and its corresponding power is  $P_g$ .

Table 3-4 list the expressions of equations for modelling the Double Cubic curve of wind power.

Table 3-4: Expressions of Double Cubic Curve Model

Double Cubic Curve	
Expression of $P_{(v)}$	$P_{(New\ Region\ 2)} = A_1 v^3 - B_1 P_r$
	$P_{(New\ Region\ 3)} = A_2 * ((v - v_g - v_r)^3 + v_r^3) + A_1 v_g^3 - B_1 P_g$
Parameters	$A_1 = \frac{P_g}{v_g^3 - v_{ci}^3}$
	$A_2 = \frac{P_r - P_g}{v_r^3 - v_g^3}$
	$B_1 = \frac{v_{ci}^3}{v_g^3 - v_{ci}^3}$
	$B_2 = \frac{v_g^3}{v_r^3 - v_g^3}$

iii) Explanation of how the equation  $P_{(New\ Region\ 3)}$  is achieved

As discussed in previous sub-section, the polynomial cubic curve can move to a different position corresponding to the coordinate axes by changing the polynomial parameters without changing the slope at each point.

The figures from Figure 3.10 to Figure 3.14 in this sub-section support the demonstration of the equation of evolution, and how the final equation  $P_{(New\ Region\ 3)}$  is achieved by amending the equation of the cubic method  $P_{(v)} = av^3 - bP_r$ .

First, using the cubic method to form the blue curve in New Region 3 and the equation has been amended as  $P_{(v)} = A_2 v^3 - B_2 (P_r - P_g)$  because in New Region 3 the value increment of the y axis is only  $(P_r - P_g)$  from the point of New  $v_g$  to the point of New  $v_r$ . As for the value increment of the x axis, it is correspondingly changed to  $(v_r - v_g)$  from the point of New  $v_g$  to the point of New  $v_r$ .

The second step is moving the position of the segment of the blue cubic curve. Figure 3.10 shows the final target is to move the position of blue curve from the coordinate axis to the position of the red curve.

After the position movement, part of the red curve segments will partially overlap with the yellow curve segments. And this overlapping segment of the curve is the achieved curve which is used to form the curve in New Region 3. This is also the segment of the red curve in the New Region 3 of Figure 3.5.

From Figure 3.10 to Figure 3.14, the yellow curve is the reference curve that is generated based on the equations of the Double Cubic method directly in Table 3-4. It is also the target of position movement of the blue curve in these figures.

As the result of position movement, the original point of  $-v_r$  will locate at the point of New  $v_g$  and the point of  $-v_{ci}$  will locate at the point of New  $v_r$  in Figure 3.10. So, the whole process of curve position movement has been achieved.

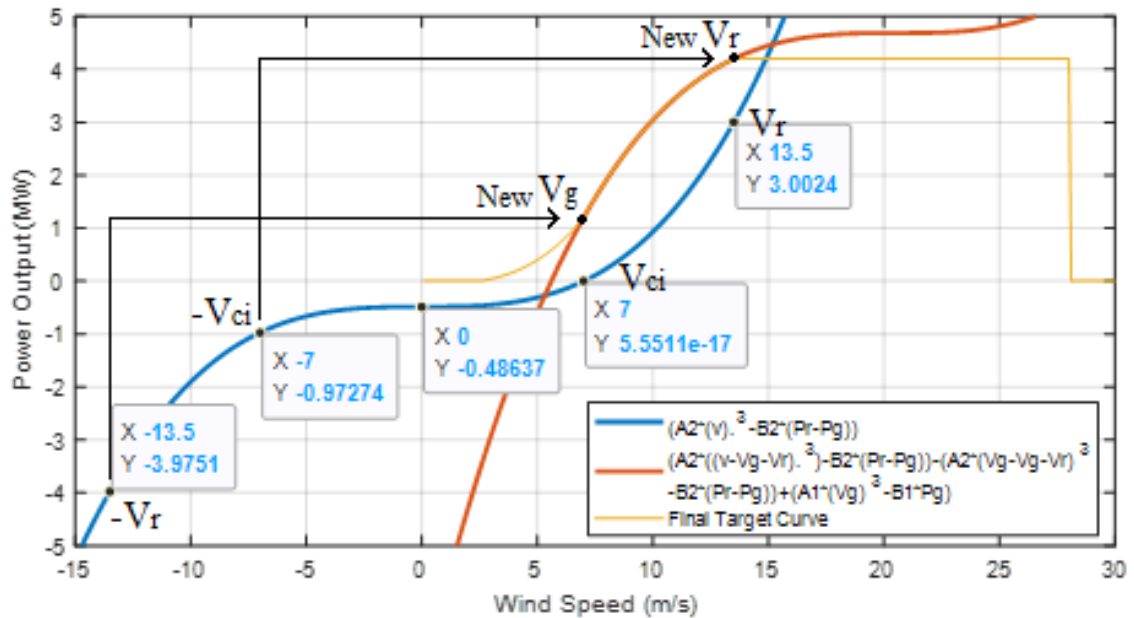


Figure 3.10: Explanation Chart Base of How the New Region 3 Curves Come From

Next, it is introduced that how the blue curve in Figure 3.10 forms the proposed Double Cubic curve through the position movement based on the related mathematical expression changes step by step.

Next correctness of all involved changes of mathematical expressions from Figure 3.10 to Figure 3.14 has been verified by the software MATLAB. The verification method is based on whether the moving curve is overlapped with the final target yellow curve in New Region 3 in Figure 3.10.

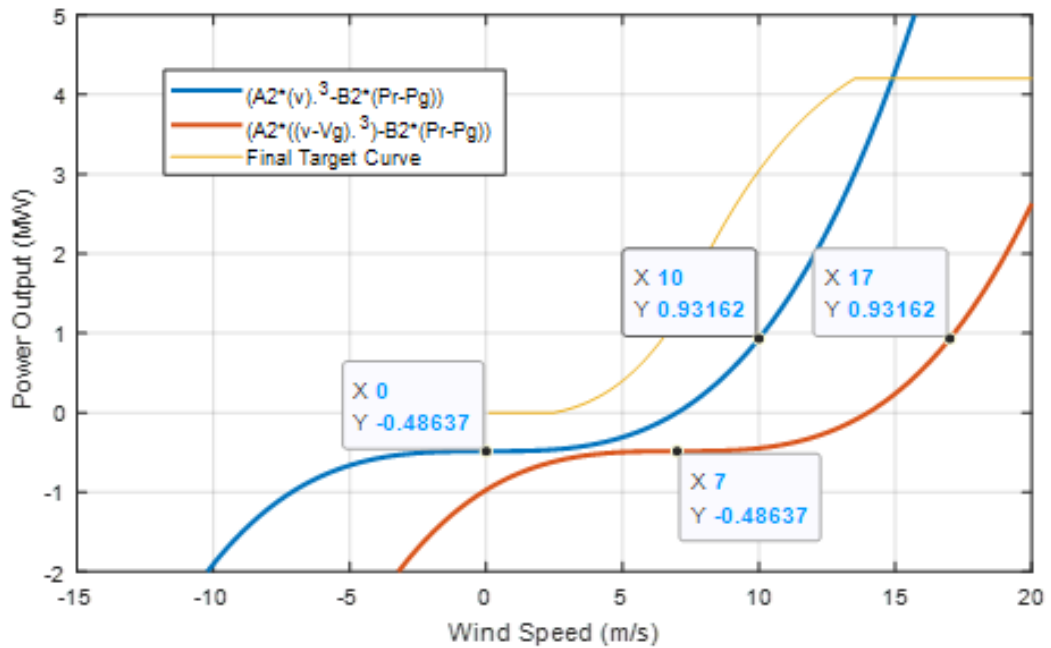


Figure 3.11: Explanation Chart 1 of How the New Region 3 Curves Come From

In the first step, the position of the blue line is moved from the left to the position of the red line by a distance  $v_g$  of horizontal axis, referencing Figure 3.11.

The corresponding mathematical expression changes are:

From:

$$A_2 * (v)^3 - B_2 * (P_r - P_g)$$

To:

$$A_2 * (v - v_g)^3 - B_2 * (P_r - P_g)$$

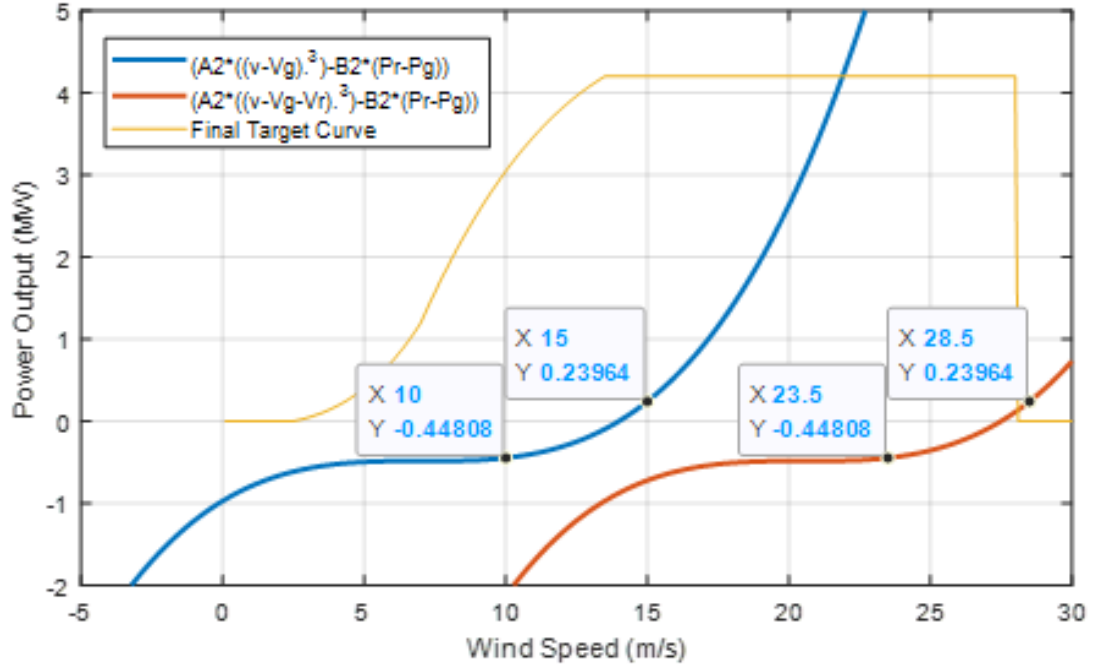


Figure 3.12: Explanation Chart 2 of How the New Region 3 Curves Come From

In the second step, the position of the blue line is moved from the left to the position of the red line by a distance  $v_r$  of horizontal axis, referencing Figure 3.12.

The corresponding mathematical expression changes are:

From:

$$A_2 * (v - v_g)^3 - B_2 * (P_r - P_g)$$

To:

$$A_2 * (v - v_g - v_r)^3 - B_2 * (P_r - P_g)$$

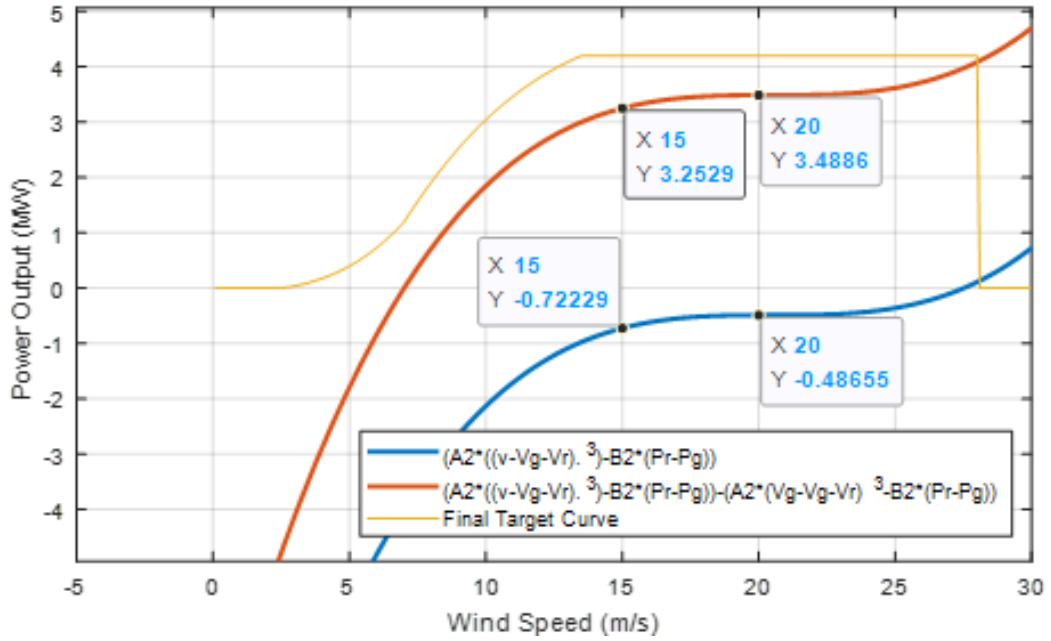


Figure 3.13: Explanation Chart 3 of How the New Region 3 Curves Come From

In the third step, the position of the blue line is moved from bottom to the position of the red line by a distance  $-\left[A_2 * (v_g - v_g - v_r)^3 - B_2 * (P_r - P_g)\right]$  of vertical axis, referencing Figure 3.13. The value of  $\left[A_2 * (v_g - v_g - v_r)^3 - B_2 * (P_r - P_g)\right]$  is the corresponding value of the point of  $-v_r$  at the vertical axis in Figure 3.10. (**Hint: The value of  $\left[A_2 * (v_g - v_g - v_r)^3 - B_2 * (P_r - P_g)\right]$  is a negative number which is approximately equal to -3.97519.**)

The corresponding mathematical expression changes are:

From:

$$A_2 * (v - v_g - v_r)^3 - B_2 * (P_r - P_g)$$

To:

$$A_2 * (v - v_g - v_r)^3 - B_2 * (P_r - P_g) - \left[A_2 * (v_g - v_g - v_r)^3 - B_2 * (P_r - P_g)\right]$$

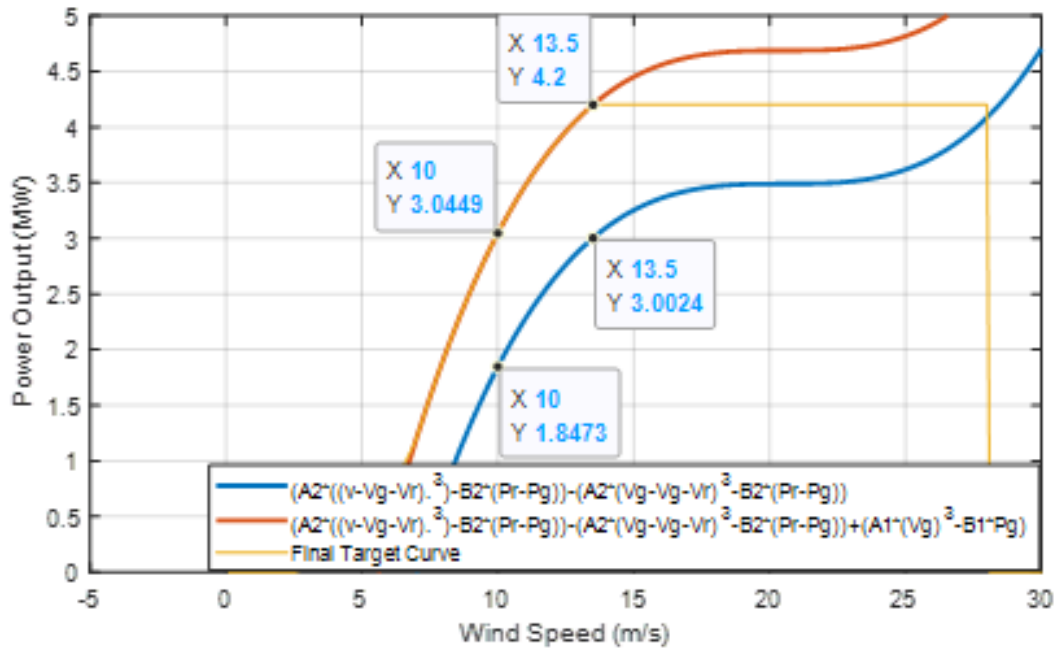


Figure 3.14: Explanation Chart 4 of How the New Region 3 Curves Come From

In the final step, the position of the blue line is moved from bottom to the position of the red line by a distance  $A_1 v_g^3 - B_1 P_g$  of vertical axis, referencing Figure 3.14. The value of  $A_1 v_g^3 - B_1 P_g$  is the corresponding value of the point of New  $v_g$  at the vertical axis in Figure 3.10.

The corresponding mathematical expression changes are:

From:

$$A_2 * (v - v_g - v_r)^3 - B_2 * (P_r - P_g) - [A_2 * (v_g - v_g - v_r)^3 - B_2 * (P_r - P_g)]$$

To:

$$\begin{aligned} P_{(Region\ 3)} &= A_2 * (v - v_g - v_r)^3 - B_2 * (P_r - P_g) \\ &\quad - [A_2 * (v_g - v_g - v_r)^3 - B_2 * (P_r - P_g)] + A_1 v_g^3 - B_1 P_g \\ &= A_2 * ((v - v_g - v_r)^3 + v_r^3) + A_1 v_g^3 - B_1 P_g \end{aligned}$$

### 3.4.3 Results Demonstration

Figure 3.15 gives the compared graphs of the power curve based on the proposed Double Cubic method (Figure 3.15 (a)) and manufacturer's data (Figure 3.15(b)) for an ENERCON E-126 EP4 / 4.2 MW wind turbine. This Double Cubic method can be applied to other types of wind turbines based on the wind turbine specifications of cut-in speed ( $v_{ci}$ ), cut-off speed ( $v_{co}$ ), rated wind speed ( $v_r$ ), inflection point wind speed ( $v_g$ ), and rated power ( $P_r$ ) to determine the equations for the power curve.

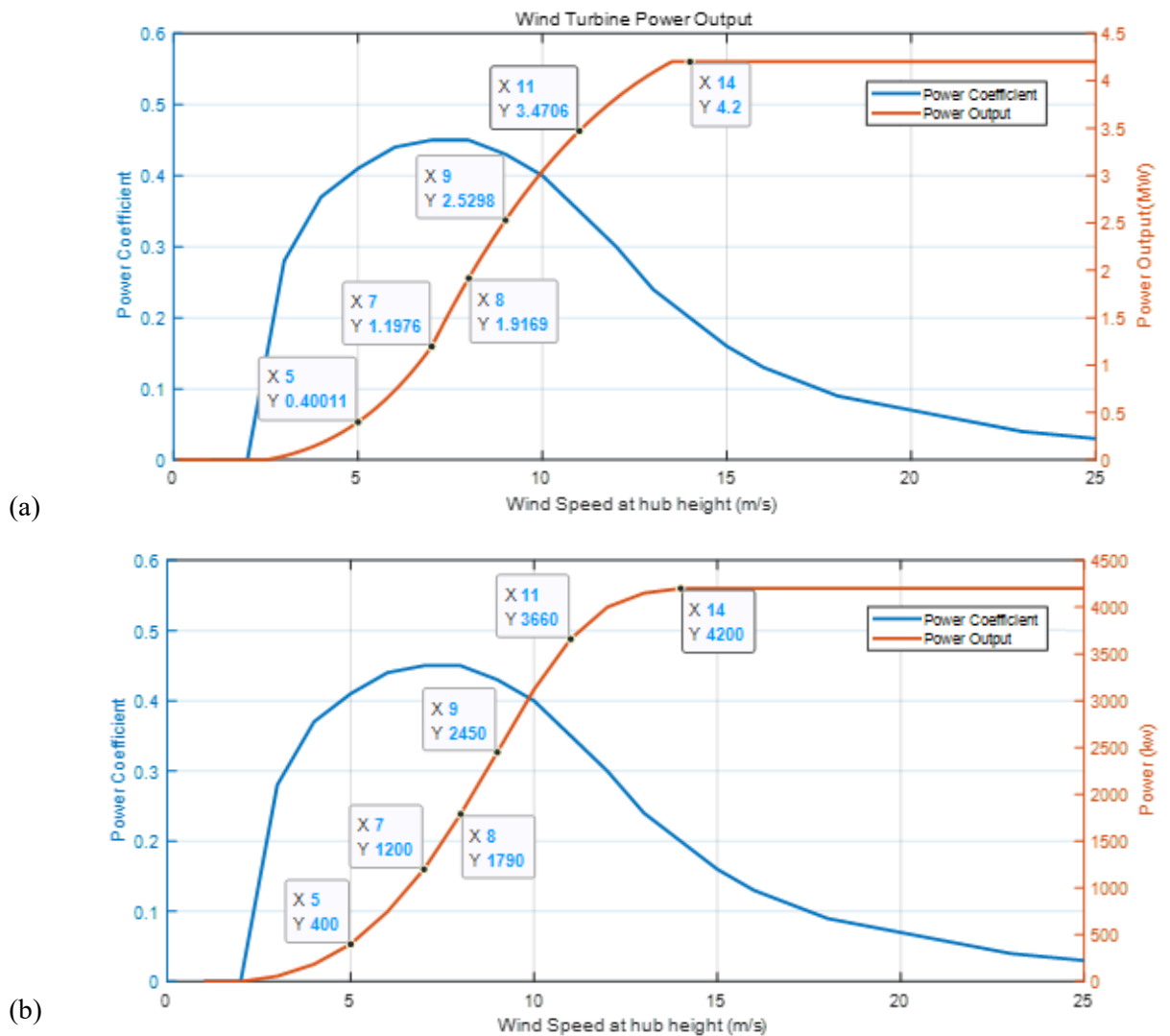


Figure 3.15: Compared Graphs of Power Curve based on Proposed Double Cubic Method and Manufacturer's Data for an ENERCON E-126 EP4 / 4.2 MW Wind Turbine

It is found that the simulated results of the power curve are close to the manufacturer's data and show a similar increment trend in Figure 3.15. The detailed comparison of data and accuracy will be illustrated in the next section 3.5 (Case Study and Discussion).

Generally, the exact position of the inflection point is dependent on the curve of power coefficient as Figure 3.5 shows. And the maximum value of the power coefficient is dependent on the turbine design and its optimal rotor tip speed ratio which has been introduced in sub-section 3.3.2 (Wind Turbine). Further introduction of optimal rotor tip speed ratio and how this parameter affects the power coefficient can be found in the reference [226].

So far, the modelling issue of original polynomial methods that its slope value of power output keeps increasing until it reaches the point of rated power, shown in Figure 3.6, has been solved by adding the inflection point to improve its modelling accuracy based on the Double Cubic model. This method can determine the wind power curves in a fast estimation because only basic specification of cut-in speed, cut-off speed, rated wind speed, inflection point wind speed, and rated power are needed.

### **3.5 Case Study and Discussion**

To find out which of the proposed parameter models is appropriate to represent power curves, it is necessary to compare these models with manufacturer power curve data. The parameters of their manufacturer's datasheet are listed in Table 3-5.

So, this section compares the simulation accuracy of power curves among the common five polynomial models, linear, quadratic, binomial, cubic, and Weibull, and proposed Double Cubic model based on two cases of ENERCON E-82 E4 /3MW and E-126 EP4 / 4.2 MW wind turbines [227].

Table 3-5: Manufacturer's Datasheet of ENERCON E-82 E4 / 3 MW and E-126 EP4 / 4.2 MW Wind Turbine

	$v_{ci}$	$v_g$	$v_r$	$P_r$	Maximum power coefficient	Rotor diameter
E-82 E4	3 m/s	8 m/s	16 m/s	3MW	0.483	82 m
E-126 EP4	3 m/s	7 m/s	14 m/s	4.2MW	0.45	127 m

The method of root mean square error (RMSE) [229] is used to measure the differences between simulated values and the manufacturer's data. And the method of normalized root mean square error (NRMSE) [229] is used to evaluate the simulation accuracy of models. The smaller the RMSE, the closer model follows the target data. The equations are given:

$$RMSE = \sqrt{\frac{1}{n} \sum_{i=1}^n (MPC_i - P_{fi})^2} \quad (3-8)$$

Where,  $MPC_i$  are the values of the manufacturer power curve, and  $P_{fi}$  are the simulated values by the models corresponding to wind speed bin  $i$ .  $n$  is the number of bins at range from  $v_{ci}$  to  $v_r$ .

$$NRMSE = \frac{RMSE}{MPC_{max} - MPC_{min}} \quad (3-9)$$

Where,  $MPC_{max}$  and  $MPC_{min}$  are the maximum and minimum values of the manufacture power curve respectively.

The obtained power output curves and results of the case of ENERCON E-82 E4 /3MW are shown in Figure 3.16 and Table 3-6 respectively. The obtained power output curves and results of the case of E-126 EP4 / 4.2 MW are shown in Figure 3.17 and Table 3-7 respectively.

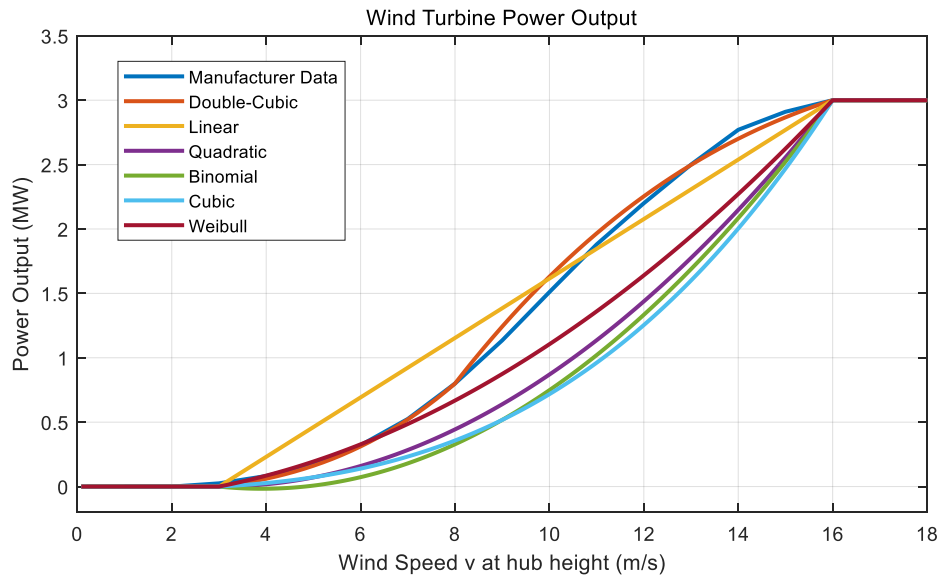


*Figure 3.16: Compared Graph of Power Curves based on Proposed Method, Manufacturer's Data and 5 Polynomial Methods for an ENERCON E-82 E4 / 3 MW Wind Turbine*

*Table 3-6: Compared Data of Power Curves based on Proposed Method, Manufacturer's Data and 5 Polynomial Methods for an ENERCON E-82 E4 / 3 MW Wind Turbine*

	Manufacturer Data	Double Cubic	Linear	Quadratic	Binomial	Cubic	Weibull
4 m/s	0.082	0.061024	0.23077	0.017751	0.000911	0.027279	0.08502
5 m/s	0.174	0.16163	0.46154	0.071006	0.007459	0.072254	0.19433
6 m/s	0.321	0.31172	0.69231	0.15976	0.073108	0.13935	0.32794
7 m/s	0.525	0.52118	0.92308	0.28402	0.18004	0.23298	0.48583
8 m/s	0.8	0.79991	1.1538	0.44379	0.32825	0.35758	0.66802
9 m/s	1.135	1.2425	1.3846	0.63905	0.51774	0.51757	0.87449
10 m/s	1.51	1.6299	1.6154	0.86982	0.7485	0.71738	1.1053
11 m/s	1.88	1.9656	1.8462	1.1361	1.0206	0.96142	1.3603
12 m/s	2.2	2.2535	2.0769	1.4379	1.3339	1.2541	1.6397
13 m/s	2.5	2.4972	2.3077	1.7751	1.6885	1.5999	1.9433
14 m/s	2.77	2.7004	2.5385	2.1479	2.0844	2.0032	2.2713
15 m/s	2.91	2.8668	2.7692	2.5562	2.5216	2.4684	2.6235
RMSE	/	0.059926	0.242263	0.504084	0.588767	0.623533	0.350688
NRMSE	/	0.015114	0.0611	0.127133	0.148491	0.157259	0.088446

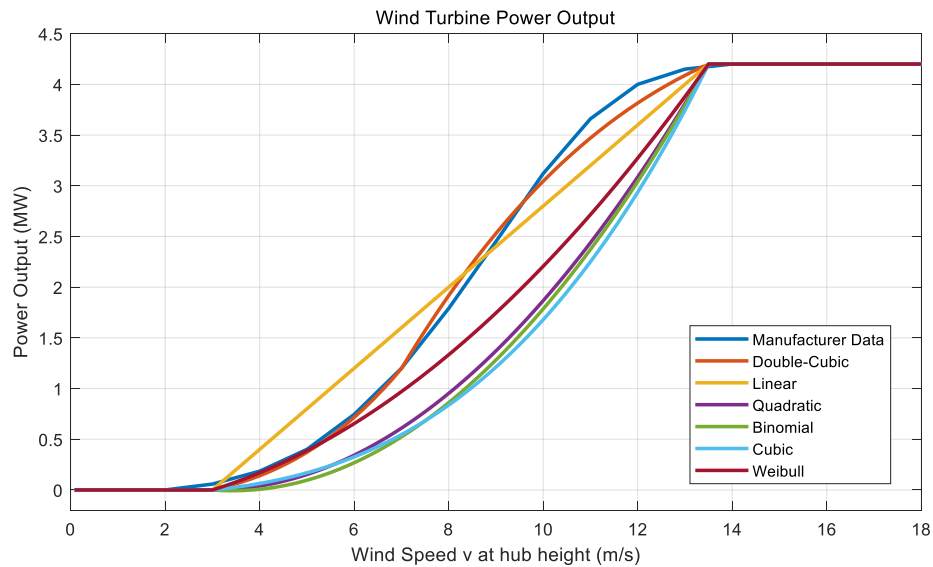


*Figure 3.17: Compared Graph of Power Curves based on Proposed Method, Manufacturer's Data and 5 Polynomial Methods for an ENERCON E-126 EP4 / 4.2 MW Wind Turbine*

*Table 3-7: Compared Data of Power Curve based on Proposed Method, Manufacturer's Data and 5 Polynomial Methods for an ENERCON E-126 EP4 / 4.2 MW Wind Turbine*

	Manufacturer Data	Double Cubic	Linear	Quadratic	Binomial	Cubic	Weibull
4 m/s	0.185	0.14022	0.4	0.038095	0.006571	0.063862	0.1697
5 m/s	0.4	0.37141	0.8	0.15238	0.09597	0.16915	0.38788
6 m/s	0.745	0.71628	1.2	0.34286	0.2682	0.32621	0.65455
7 m/s	1.2	1.1976	1.6	0.60952	0.52325	0.54542	0.9697
8 m/s	1.79	1.9169	2	0.95238	0.86113	0.83711	1.3333
9 m/s	2.45	2.5298	2.4	1.3714	1.2818	1.2117	1.7455
10 m/s	3.12	3.0449	2.8	1.8667	1.7854	1.6794	2.2061
11 m/s	3.66	3.4706	3.2	2.4381	2.3717	2.2507	2.7152
12 m/s	4	3.8155	3.6	3.0857	3.0409	2.9359	3.2727
13 m/s	4.15	4.0882	4	3.8095	3.7929	3.7454	3.8788
RMSE	/	0.102712	0.3341182	0.804609	0.867488	0.920363	0.556495
NRMSE	/	0.025905	0.0842669	0.202928	0.218786	0.232122	0.140352

Figure 3.16 and Figure 3.17 compared power curves of polynomial models, linear, quadratic, binomial, cubic, Weibull, and proposed Double Cubic with power curve of manufacturer data to find out which is the most appropriate for modelling wind turbine power curves. It can be seen that the Double Cubic based model in two cases both gives the closest curve to the manufacturer data curve.

From the two cases results based on further accuracy evaluation methods in Table 3-6 and Table 3-7, the Double Cubic based model can not only give the lowest values of RMSE and NRMSE, but also is far lower than the values of these common polynomial models. Thus, the proposed model of Double Cubic can be considered a good method to model the nonlinear portion of the wind power curve among the presented parameter models.

### **3.6 Summary**

This chapter presented the development of wind energy from the aspects of capacity and economics. Then the main wind technology of assessment, forecasting, turbine, control methods, and power integration were also briefly introduced.

Power curve, as one of the most essential tools to estimate the power output of wind turbine was discussed to propose the novel method of Double Cubic curve by considering the inflection point in the nonlinear portion of the wind power curve.

Finally, the two cases with real data of wind turbines were used to compare six polynomial models to evaluate the simulation accuracy of proposed method and other main parametric models. From the results, the proposed modelling method of the Double Cubic power curve is the most accurate model due to its least values of RMSE and NRMSE. The RMSE value is relatively reduced by a factor of about 3 to 10. While the NRMSE value is relatively reduced by a factor of about 4 to 10.

# Chapter 4 Formulation and Proposed Solution to Thermal Unit Commitment Problem

## 4.1 Introduction

The unit commitment and economic dispatch are two integrated operations in the short-term planning of the power system. The early definition of the unit commitment is the selection of the available units in the system which would be put into service to meet the demand and system constraints. The economic dispatch is to determine the allocation of the generation among the already committed units to find the optimum operating schedule. Sometimes, economic dispatch can be considered as the following sub-problem in the solving process of a unit commitment problem.

The objective function of the unit commitment consists of operation cost, unit start-up and shut-down costs, and the proposed emission cost. The operation costs of the thermal plants include fuel cost, labor cost, and maintenance cost. The fuel cost is the major cost of the operating cost. Labor and maintenance costs are usually assumed as a fixed percentage of the total cost.

However, due to impacts of higher penetration integration of intermittent renewable energy sources, quota rules of generation allocation in China's special semi-liberalized market, and emission policy of 'carbon neutrality' to protect the climate change recently, both the formulation and solution approaches to the thermal unit commitment problem should be replaced or upgraded by corresponding modifications to meet these new requirements.

In this chapter, the method of dynamic programming optimization approach with adding carbon tax cost and NO<sub>2</sub> penalty cost to the original UC problem is proposed

because the DP method can manage sub-problems of further renewable energy sources in decomposition programs and maintain the solution feasibility which is discussed in section 2.3 (Review of Unit Commitment).

Thus, to achieve the above modifications, this chapter is organized as follows. Section 4.2 introduces the modified UC problem with problem formulation including emission cost and corresponding system constraints. Section 4.3 provides a modified dynamic programming approach employed in solving the UC optimization problems. Section 4.4 presents case study results based on the proposed method of UC formulation and solution.

## **4.2 Formulation and Modelling of Unit Commitment Problem**

To the UC problem, the first step towards the optimal solution is to decide the on-off states of the generation units based on the different cost and constraints functions. They are discrete variables that determine whether each generation unit is on or off at any given time [137], and different types of energy sources of coal, gas, and oil are formulated in the unit commitment problem. The cost function of the unit can be represented by the mathematical relationship between its input and output characteristics. Emission cost can also be formulated into the programming.

### **4.2.1 Total Operation Cost Function**

#### **i) Production cost**

The production cost of a thermal unit mainly consists of fuel cost, which is assumed as a function of the power generated by the unit.

$$C_{i,t}^{prod} = \alpha_{i,t} + b_{i,t}p(i,t) + c_{i,t}p(i,t)^2 \quad (4-1)$$

$C_{i,t}^{prod}$  is the production cost of the thermal unit  $i$  at time  $t$

$p(i,t)$  is the power generated by the thermal unit  $i$  at time  $t$

$\alpha_i, b_i, c_i$  are production cost function coefficients of thermal unit  $i$

### ii) Emission Cost

The reason why the nitrogen dioxide emission penalty is also coded in the model is because carbon dioxide and nitrogen dioxide are the common fuel burning emissions of the traditional thermal unit in China.

$$C_{i,t}^{emission} = C_{tax} * ef_{co2,i} * [fa_i + fb_i p(i,t) + fc_i p^2(i,t)] + N_{pan} * ef_{no2,i} * [fa_i + fb_i p(i,t) + fc_i p^2(i,t)] \quad (4-2)$$

$C_{tax}$  and  $N_{pan}$  are the carbon tax and nitrogen emission allowance cost

$ef_{co2,i}$  is fuel emission factors of  $co_2$  of thermal unit  $i$

$ef_{no2,i}$  is fuel emission factors of  $no_2$  of thermal unit  $i$

$p(i,t)$  is the power generated of the thermal unit  $i$  at time  $t$

$fa_i, fb_i$  and  $fc_i$  are the fuel consumption coefficients of the unit  $i$

### iii) Start-up and Shut-down Cost

The shut-down cost of the thermal units, caused by the fuel consumed during the shut-down time, is assumed as a fixed cost in this programming. However, the start-up cost of the thermal units is modeled as an exponential cost curve [230]. This

variable start-up cost depends on the duration time,  $T_{off}$ , which is the thermal unit  $i$  has been switched off prior to the start-up.

$$C_{i,t}^{start} = C_{hot,i} + C_{cold,i} \left( 1 - e^{-\frac{T_{off,i}}{\tau_i}} \right) \quad (4-3)$$

$C_{hot,i}$  is the hot start-up cost of the unit  $i$

$C_{cold,i}$  is the cold start-up cost of the unit  $i$

$\tau_i$  is the cooling time constant of the unit  $i$

For the unit undergoing cooling or heating, the thermal time constant is the time to reach the temperature difference equals 63.21 % of the initial temperature.

$$\Delta T = 63.21\% * T_{initial} \quad (4-4)$$

$\Delta T$  is the temperature difference

$T_{initial}$  is the initial temperature

## 4.2.2 System Constraints of Unit Commitment

System constraints of unit commitment are applied in the power system operation cost objective function to keep the system working within the range of planned limits of stability and to meet security requirements. The constraints below are all applied to the unit commitment problem to satisfy the system security.

### i) Active Power Balance

The total power output of the units of the system must satisfy the load demand as well as the transmission losses. The load balance equation is formulated as:

$$\sum_t \sum_i p_{Gen}(i, t) - \sum_t \sum_b p_{Demand}(n, t) - \sum_t \sum_b p_{Loss}(l, t) = 0 \quad (4-5)$$

$p_{Gen}(i, t)$  is the power generated by the thermal unit  $i$  at time  $t$

$p_{Demand}(n, t)$  is the power load demand of the bus  $n$  at time  $t$

$p_{Loss}(l, t)$  is the power loss of the transmission  $l$  at time  $t$

#### ii) Generation Limit

Generally, the thermal unit must operate between its minimum and maximum output power limit to remain stable.

$$P_{MIN}(i, t) \leq P(i, t) \leq P_{MAX}(i, t) \quad (4-6)$$

$P_{MIN}(i, t)$  is the minimum power generation limit of thermal unit  $i$  at time  $t$

$P_{MAX}(i, t)$  is the maximum power generation limit of thermal unit  $i$  at time  $t$

#### iii) Ramp Up and Down Rate Limit

The ramping constraint is important in the short-term schedule of generation and dispatching. It limits the capability of units to change production over the given short period.

$$\begin{aligned} P(i, t) - P(i, t - 1) &\leq U_{R.up}(i) \\ P(i, t) - P(i, t - 1) &\geq -U_{R.down}(i) \end{aligned} \quad (4-7)$$

$p(i, t)$  is the power generated by the thermal unit  $i$  at time  $t$

$U_{R.up}(i)$  is the power output ramp up rate of thermal unit  $i$

$U_{R.down}(i)$  is the power output ramp down rate of thermal unit  $i$

iv) Minimum Start-up or Shut-down time Limit

Each unit must be kept on-line for a certain time before it can be shut down to avoid high maintenance cost once the unit is committed. A certain elapse time must remain before the unit can be started up again if it is shut down.

$$\begin{aligned} [X_{on}(i, t - 1) - T_{on}(i)] * [u(i, t - 1) - u(i, t)] &\geq 0 \\ [X_{off}(i, t - 1) - T_{off}(i)] * [u(i, t - 1) - u(i, t)] &\geq 0 \end{aligned} \quad (4-8)$$

$u(i, t)$  is the on/off status of thermal unit  $i$  at time  $t$

$T_{on}(i)$  is the minimum start-up time of thermal power unit  $i$

$T_{off}(i)$  is the minimum shut-down time of thermal power unit  $i$

$X_{on}(i, t)$  is the duration time for unit  $i$  has remained on at time  $t$

$X_{off}(i, t)$  is the duration time for unit  $i$  has remained off at time  $t$

v) Spinning Reserve Capacity Limit

The spinning reserve is the amount of unused capacity in online energy assets which can compensate for power shortages or frequency drops within a given time [231]. However, this additional capacity increases the system operation cost. Traditionally, the amount of spinning reserve is assigned as a fixed percentage of the total demand to avoid any transmission limitation and generator outage.

$$\sum_t \sum_i r_s \geq R_s(t) \quad (4-9)$$

$r_s(i, t)$  is the spinning reserve of thermal unit  $i$  at time  $t$

$R_s(t)$  is the total spinning reserve requirement at time  $t$

## **4.3 Unit Commitment Solution by Modified Dynamic Programming**

### **4.3.1 Dynamic Programming**

Dynamic programming was one of the earliest optimization-based method to be applied to the UC problem [141]. It has the advantage of being able to solve problems of a variety of sizes and to be easily modified to model characteristics of specific utilities such as adding constraints [232]. So, this method is selected to use and promote as the base program.

Dynamic Programming is a mathematical optimization technique, which systematically evaluates possible and interrelated decisions in a multi-stage problem. Usually, this multi-step problem is transformed into a series of smaller single-stage sub-problem based on the principle of optimality formulated by R. Bellman in 1957 [233].

Unlike the other mathematical programming techniques, generally, there does not exist a standard mathematical formulation of the dynamic programming problem. And it should be noticed that particular equations used in dynamic programming must be developed to fit each problem, such as the integer values required in the on-off state problem of unit commitment.

The reference [234] summarized the computational procedure for solving a problem with the dynamic programming approach in the following steps:

Step 1. Identify the decision variable and specify the objective function to be optimized under certain limitations.

Step 2. Decompose the given problem into several smaller sub-problems. Identify the state variables at each stage and write down the transformation function as a function of the state variables and decision variables at the next stage.

Step 3. Define a general recursive relationship for computing the optimal policy. Decide whether the forward or backward method is to be followed to solve the problem.

Step 4. Construct appropriate stages to show the required values of the return function at each stage.

Final Step. Determine the overall optimal policy or decisions and its value at each stage.

The typical dynamic programming recursive function can be expressed as follows [235]:

$$F(J, K, X) = Z[C(J, K, X), f_{J-1}(K')] \dots \dots \quad (4-10)$$

F: the cost function.

J: the stage of the problem.

K: the state of the system stage J.

X: the decision being evaluated at stage J.

Z: the return function of objective problem.

$C(J, K, X)$ : the immediate cost associated with making decision X at stage J when the state of the system is K.

$K'$ : the state of the system at  $J - 1$  stage resulting from decision X.

$f_{J-1}(K')$ : the cost associated with the optimal sequence of the decision at stage  $J - 1$  when the state is  $K'$ .

### 4.3.2 Optimization Methods

The optimization methods of quadratic programming, mixed-integer linear programming, and linear programming are used to calculate and find the solution to the sub-problem of the minimum production cost and emission cost of each state at each time point in the system. Note that, a suitable linearization of the cost curve of the units is required when using linear programming.

#### i) Quadratic Programming

Quadratic programming finds a minimum for a typical problem specified by:

$$\min_x \frac{1}{2} x^T H x + f^T x \quad (4-11)$$

Constraints:

$$\begin{cases} A * x \leq b, \\ Aeq * x = beq, \\ lb \leq x \leq ub. \end{cases}$$

Where,  $H$ ,  $A$  and  $Aeq$  are matrices, and  $f$ ,  $b$ ,  $beq$ ,  $lb$ ,  $ub$  and  $x$  are vectors.  $H$  is the quadratic objective term,  $f$  is a linear objective term,  $A$  and  $b$  are linear inequality constraints,  $Aeq$  and  $Beq$  are linear equality constraints,  $lb$  is the lower bound and  $ub$  is the upper bound.

#### ii) Mixed-integer Linear Programming

Mixed-integer linear programming finds a minimum for a typical problem specified by:

$$\min_x f^T x \quad (4-12)$$

Constraints:

$$\begin{cases} x \text{ are integers,} \\ A * x \leq b, \\ Aeq * x = beq, \\ lb \leq x \leq ub. \end{cases}$$

Where,  $A$  and  $Aeq$  are matrices, and  $f$ ,  $b$ ,  $beq$ ,  $lb$ ,  $ub$  and  $x$  are vectors.

### iii) Linear Programming

Linear programming is the same as the programming of mixed-integer linear except for the vector of  $x$ , which does not have to be integers.

### iv) Example of Quadratic Programming

Find the minimum of:

$$f(x) = \frac{3}{2}x_1^2 + 2x_2^2 - x_1x_2 - 3x_1 - 4x_2$$

Subject to the constraints:

$$\begin{cases} x_1 + 2x_2 \leq 4 \\ -x_1 + x_2 \leq 3 \\ 3x_1 + 2x_2 \leq 5 \end{cases}$$

This problem is to minimize:

$$f(x) = \frac{1}{2}x^T Hx + f^T x$$

where,

$$H = \begin{bmatrix} 3 & -1 \\ -1 & 5 \end{bmatrix} \quad f = \begin{bmatrix} -3 \\ -4 \end{bmatrix}$$

$$A = \begin{bmatrix} 1 & -1 & 3 \\ 2 & 1 & 2 \end{bmatrix} \quad b = \begin{bmatrix} 4 \\ 3 \\ 5 \end{bmatrix}$$

Using quadratic programming and solve the problem:

$$x = \begin{bmatrix} 0.9667 \\ 1.0500 \end{bmatrix}$$

$$\min f(x) = -4.5083$$

### 4.3.3 Unit Commitment by Proposed Dynamic Programming

In this modified dynamic programming, the unit commitment solution can be divided into two parts. The first covers the formation of the unit selection list, priority list (Priority DP) or complete enumeration (Conventional DP). The other part is the searching procedure which determines the optimal feasible schedules for the given units of the system during the scheduled period.

#### i) List Selection

The selection between priority list or complete enumeration is based on the amount  $N$  of the units in the system because the  $N$  units at each interval would result in  $2^N - 1$  possible combinations. So, it is difficult to use the method of complete enumeration for a large system since it may result in unacceptable solution time costs.

However, there is a method to control the size of the problem. The units in the system can be categorized into the type groups of base units, search range units, and peak units to schedule and dispatch due to the demand level, as illustrated in Figure 4.1 [235]. The early use of this method can be found in [103]. This procedure can

significantly reduce computational requirements, but it also may lead to a sub-optimal solution.

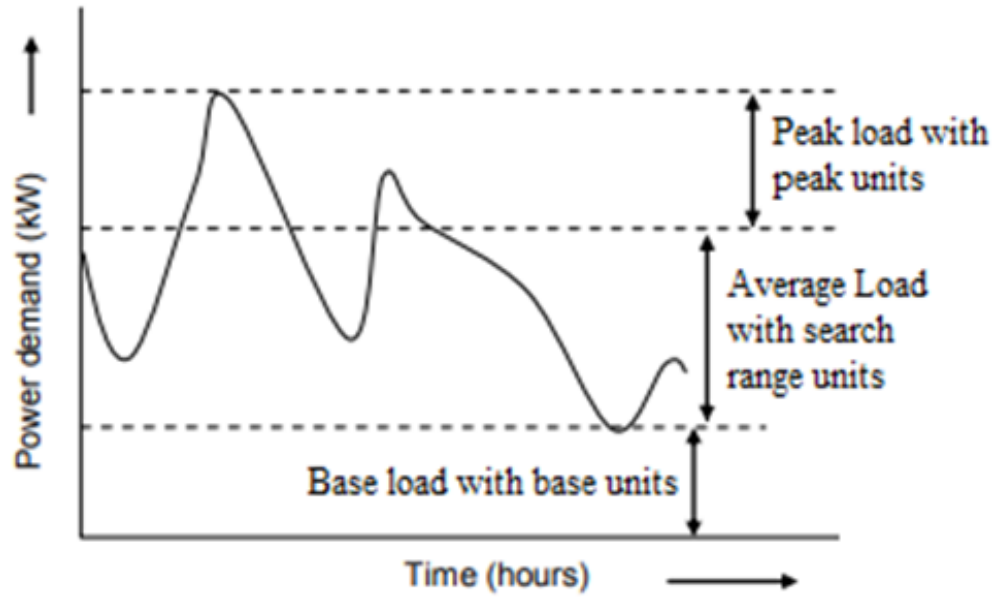


Figure 4.1: Unit Categories Block Diagram with Load Curve

ii) Objective function

A recursive algorithm to compute the minimum cost in  $K^{th}$  time points with  $I^{th}$  the combination is formulated as follows:

$$F_{COST}(K, I) = \min [P_{cost}(K, I) + E_{cost}(K, I) + S_{cost}(K - 1, L: K, I) + F_{cost}(K - 1, L)] \quad (4-13)$$

where

$State(K, I)$ : Combination  $I$  of Units at Time  $K$

$F_{COST}(K, I)$ : Least Total Cost to Arrive at State  $(K, I)$

$P_{cost}(K, I)$ : Production Cost for State  $(K, I)$

$E_{cost}(K, I)$ : Emission Cost for State  $(K, I)$

$S_{cost}(K - 1, L: K, I)$ : Transition Cost from State  $(K - 1, L)$  to State  $(K, I)$

### iii) Searching Procedure

The second part of the solution is to search for optimal commitment and their related generation amount during the given period. This procedure takes place after the first part is completed, then it starts to form the initial interval and then goes forward to the final stage of the problem. At each stage, the feasible combination of units and their lowest cost productions must be achieved. The flow chart for the dynamic programming method to solve the unit commitment problem is shown in Figure 4.2.

1. For each time point, the program finds the potential feasible combinations of the units' on-off states of thermal plants where demand and reserve should be supplied.

2. For each potential feasible combination, the program takes all feasible states from the previous time point and checks whether the transition from the previous time point to the current time point is possible based on the constraints of minimum up and down times.

3. For every successful transition path, the program calculates the total cost of start-up and the cost of shut-down and records all the results.

4. For the power generation with the corresponding minimum cost of each unit at the current time point, it is calculated due to the current demand based on using optimization methods introduced in sub-section 4.3.2 (Optimization Methods). And it

should consider the unit constraints of ramp-up or ramp-down rate by comparing the unit power generation at the previous time point.

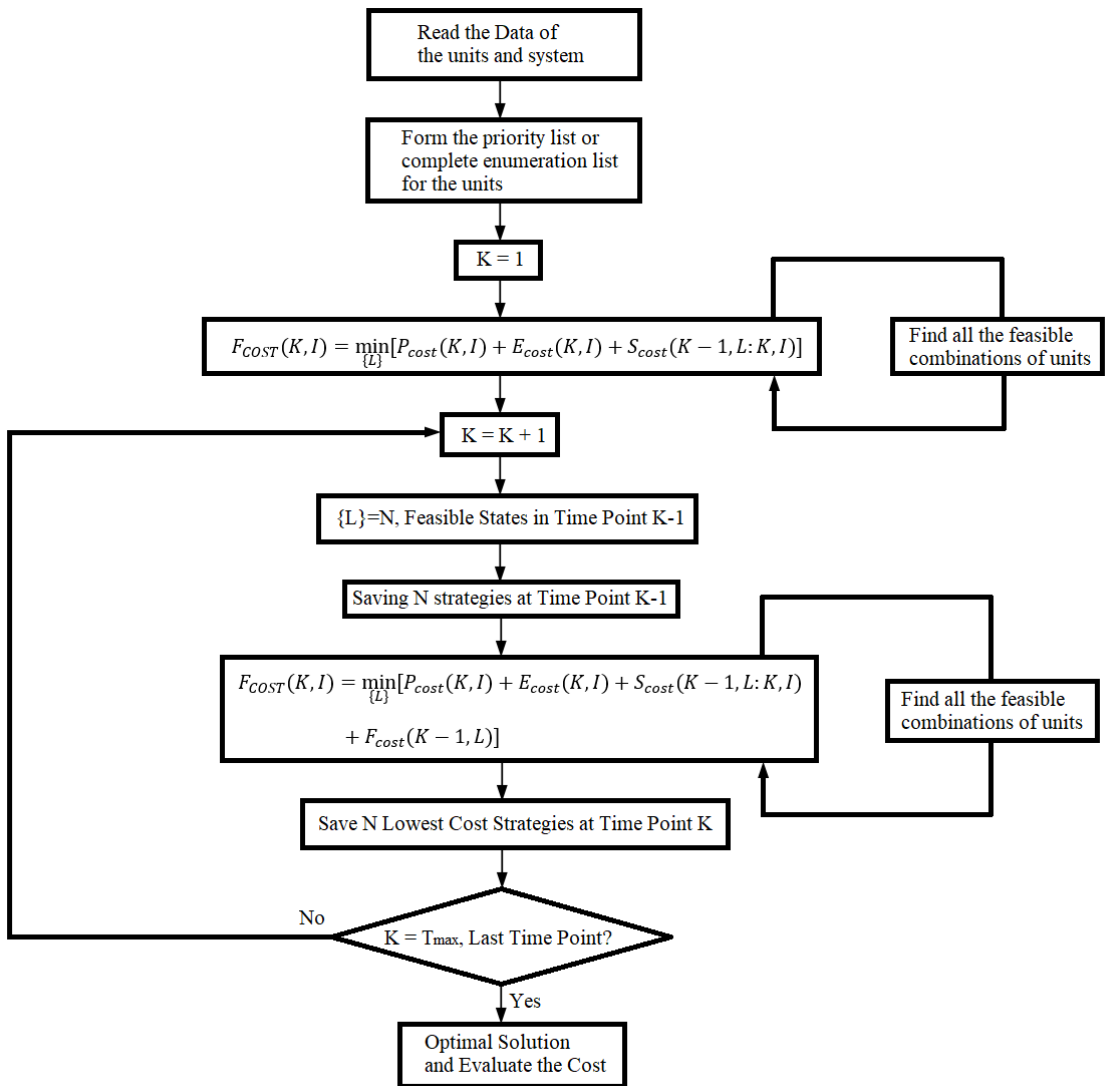


Figure 4.2: Flow Chart of Unit Commitment by Proposed Dynamic Programming

5. The costs include operation cost and emission cost to each unit for the current time point which is calculated based on corresponding cost functions of units. Emission cost is the combination of the carbon tax and pollution penalty.

6. The total cost in the current time point is the sum of the transition cost (start up or down cost), production cost (fuel cost), and emission cost (pollution and carbon tax).

7. Then this procedure is repeated and recorded until all the time points are calculated.

8. Finally, all possible schedules have been calculated and their cost results are used to sort to select the combinations associated with the minimum cost.

Then the minimum cost of commitment schedule and generation dispatch will be recorded as the solution result.

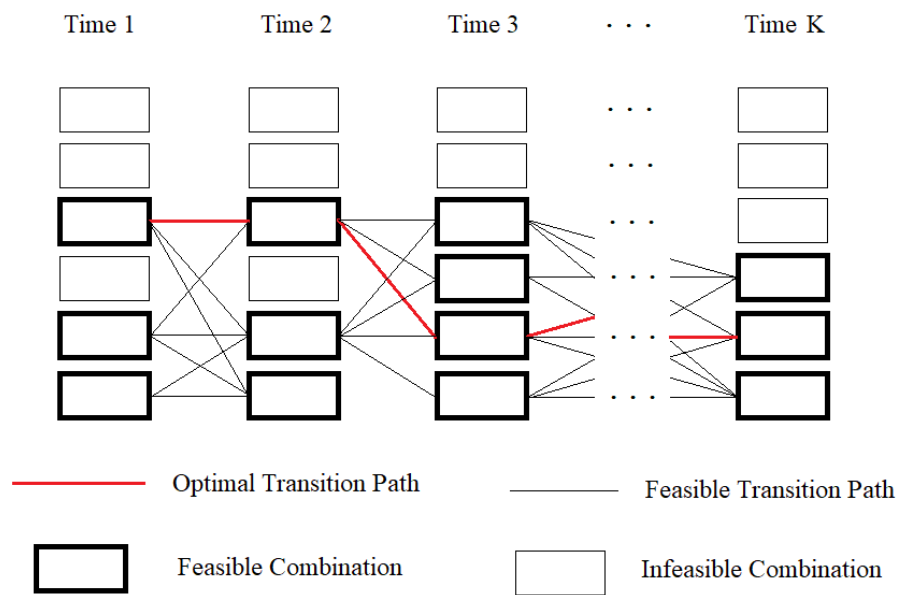


*Figure 4.3: Example Diagram of Searching Paths in Dynamic Programming*

The diagram in Figure 4.3 supports a procedure example of searching paths. Infeasible combinations of units and infeasible transition paths are caused by system constraints such as generation limit, ramping rate constraints and minimum start-up

time limit. All feasible combinations connected with feasible transition path are possible unit commitments and power dispatch schedules. The final optimal transition path can be selected based on the UC problem optimization approaches discussed in sub-section 2.3.4 (Unit Commitment Problem Solving Techniques). The main novel parts in this thesis are that the emission cost is added to the searching procedure to find optimal transition path and that the time interval of one hour is reduced to 15 minutes.

## **4.4 Case Study and Discussion**

The modified UC problem and its corresponding solving method are implemented on a test system including 6 thermal power generators, which consist of 3 coal fired units, 2 gas fired units and 1 oil fired unit. And this section is conducted as follows:

The data details are illustrated in sub-section 4.4.1 (Background Data Description). Three case results with corresponding brief introductions are listed: (a) in sub-section 4.4.2 (Case I with Conventional Dynamic Programming); (b) in sub-section 4.4.3 (Case II with Sequential Dynamic Programming), and (c) in sub-section 4.4.4 (Case III with Different Level of Spinning Reserves) respectively. Further discussion of above cases results is presented in sub-section 4.4.5 (Case Study Discussion).

### **4.4.1 Background Data Description**

#### **i) Production Cost Coefficient**

In this thesis, the production cost refers to fuel cost, and the fuel hourly cost coefficients for each unit are listed in Table 4-1.

Table 4-1: Fuel Cost Coefficients in DP case

Unit	$\alpha_i$ US\$	$b_i$ [US\$/MW]	$c_i$ [US\$/MW <sup>2</sup> ]
G1	2200	12	0.003
G2	2400	15	0.002
G3	6500	11	0.0022
G4	930.5	20	0.0032
G5	900	15	0.002
G6	130.2	20.5	0.004125

Figure 4.4 shows the fuel hourly cost curves of 6 thermal generators in the test system. It illustrates that the fuel cost of coal generator 3 is the most expensive unit if the power output is below 550 MW and the gas fired unit 5 is a good selection because of its lower fuel cost.

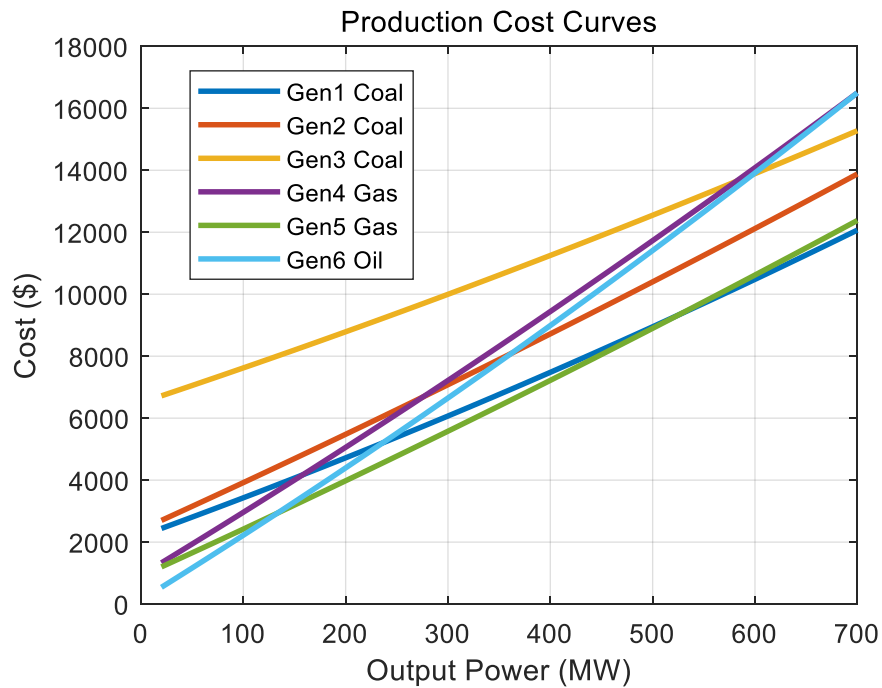


Figure 4.4: Fuel Cost Curves of 6 Generators in DP Case

ii) Emission Cost Coefficient

Table 4-2: Fuel Consumption Coefficients in DP case

Unit	$fa_i$	$fb_i$	$fc_i$
	$t \text{ or } m^3$	$t \text{ or } m^3/MW$	$t \text{ or } m^3/MW^2$
G1	45	0.3	0.00005
G2	50	0.25	0.00004
G3	90	0.14	0.00003
G4	2430.5	55	0.009
G5	2000	0.212	0.007
G6	1.248	0.334	0.0000342

Table 4-2 lists the fuel hourly consumption coefficients for the 6 thermal generators of the test system. The coefficient units of coal fired generators and oil-fired generators are in  $t$ ,  $t/MW$ ,  $t/MW^2$  respectively. The coefficient units of gas fired generators are in  $m^3$ ,  $m^3/MW$ ,  $m^3/MW^2$  respectively.

Table 4-3: Emission Factor of Units in DP case

Unit	Type	Unit Conversion	Emission Factor	
			$CO_2$	$NO_2$
G1	Coal	$Coal (t/t)$	3.1604	0.00129
G2	Coal	$Coal (t/t)$	3.1604	0.00129
G3	Coal	$Coal (t/t)$	3.1604	0.00129
G4	Gas	$Gas (t/m^3)$	0.00184	0.00000034
G5	Gas	$Gas (t/m^3)$	0.00184	0.00000034
G6	Oil	$Oil (t/t)$	2.8523	0.00033

In this case study,  $CO_2$  and  $NO_2$  are considered in the model. Table 4-3 lists the emission characteristics of the unit types, coal, gas, and oil. Combine these factors with fuel consumption, emissions of  $CO_2$  and  $NO_2$  in unit ton can be calculated.

The emission allowance prices are listed in Table 4-4. Combining these emission allowance prices, cost of emission can be calculated based on the equation (4-2).

Table 4-4: Carbon Tax and Emission Allowance in DP case

Emission Gas	CO <sub>2</sub> US\$/t	NO <sub>2</sub> US\$/t
Price	2	4500

Figure 4.5 shows the emission cost curves of 6 thermal generators in the test system. It is easy to find that the lower emission cost generator type is the gas fired unit and followed by the oil fired unit. Generally, the emission cost of coal fired unit is high.

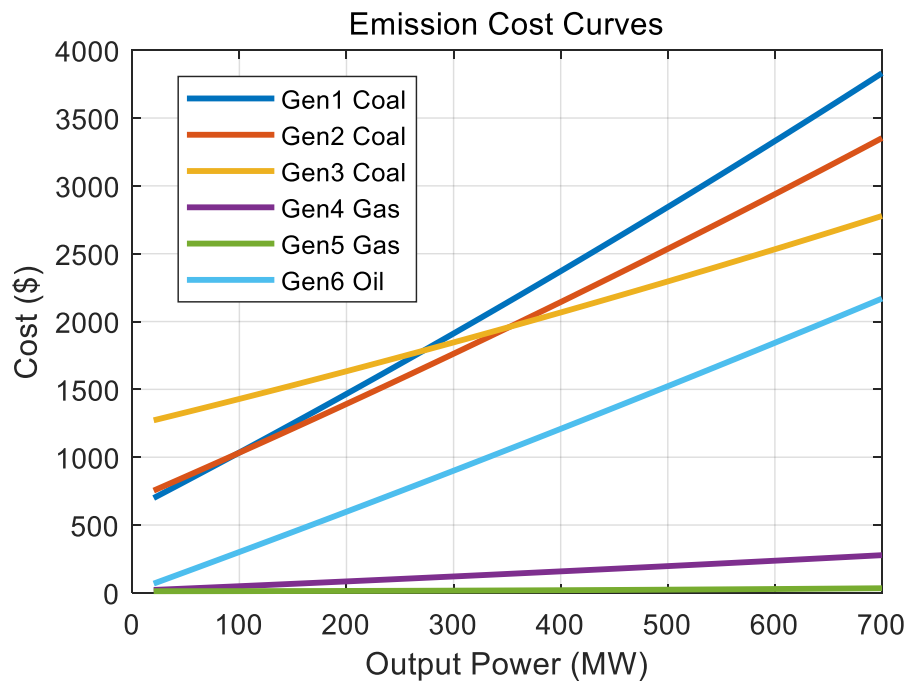


Figure 4.5: Emission Cost Curves of 6 Generators in DP Case

iii) Total Cost Coefficient of Production and Emission

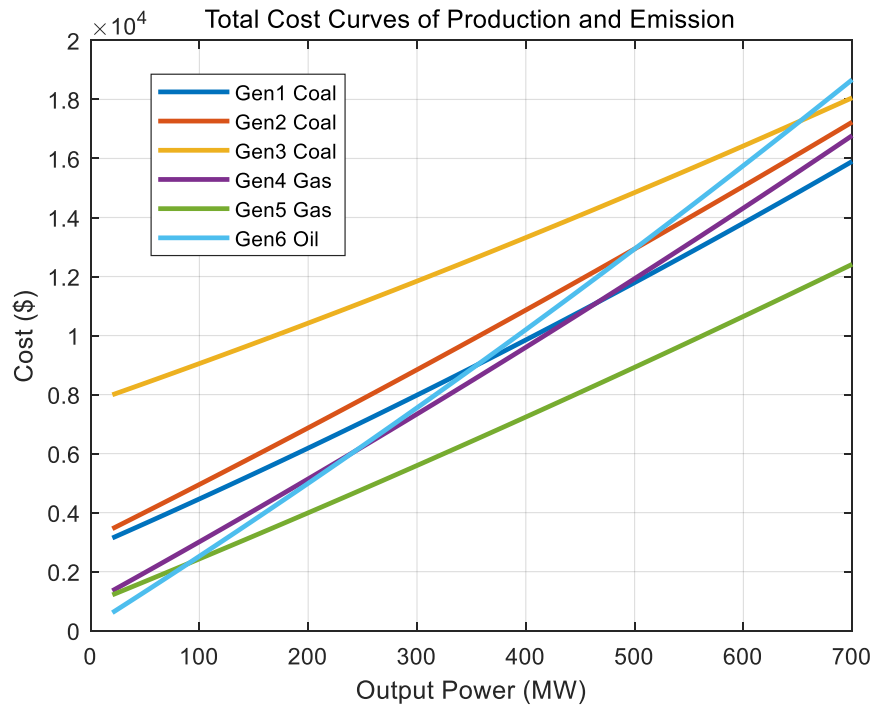


Figure 4.6: Total Cost Curves of Production and Emission of 6 Generators in DP Case

Figure 4.6 shows the total hourly cost curves of fuel and emission of 6 thermal generators in the test system. It illustrates that the best selection with the lowest cost is the generator 5 when the output power is more than 100 MW. Conversely, when the output is lower than 600MW the most expensive cost is the generator 3.

#### iv) Constraints

The parameters of generator constraints of generation minimum and maximum limit, ramp up and down rate limit, and minimum start-up or shut-down time limit are listed in Table 4-5. The cost coefficient and parameters of generator start up and shut down are listed in Table 4-6.

Table 4-5: Generator Constraints in DP Case

Unit	$P_{min}$	$P_{max}$	Ramp Up	Ramp Down	$T^{up}$	$T^{down}$
	<i>MW</i>	<i>MW</i>	<i>MW/h</i>	<i>MW/h</i>	<i>h</i>	<i>h</i>
G1	30	120	50	75	5	5
G2	20	110	40	60	4	3
G3	130	700	90	130	6	4
G4	100	500	150	130	4	3
G5	120	550	110	120	4	3
G6	45	210	75	82	3	4

Table 4-6: Generator Start Up and Shut Down Cost and Parameters in DP Case

Unit	Start Up (cold)	Start Up (Hot)	Shut Down	Cooling Constant	Initial Status
	<i>US\$</i>	<i>US\$</i>	<i>US\$</i>	<i>h</i>	<i>h</i>
G1	900	500	3200	4	-5
G2	780	360	3200	4	-6
G3	4800	2250	3200	4	-4
G4	7000	3600	3200	4	+1
G5	6600	3300	3200	2	+1
G6	4200	2230	3200	4	+3

The thermal time cooling constant is the time to reach the difference of temperature decrement equals to 63.21 % of the initial temperature. The initial status parameter,  $S_{Initial}^{time}$ , of '-5' means that the generator has been shut down for five hours. The opposite of '+3' means the generator has been activated for three hours.

#### v) Power Demand

The data of power demand in *MW* to each time point for a day are listed in Table 4-7 and the corresponding power curve is illustrated in Figure 4.7.

The time interval is a quarter of an hour and there is a total of 96 time points in the whole day.

Table 4-7: System Demand in DP case

Time	1	2	3	4	5	6	7	8	9	10
Demand	609	584	559	534	507	491	475	459	433	423
Time	11	12	13	14	15	16	17	18	19	20
Demand	413	403	397	395	393	391	388	395	402	409
Time	21	22	23	24	25	26	27	28	29	30
Demand	417	457	497	537	569	609	649	689	741	786
Time	31	32	33	34	35	36	37	38	39	40
Demand	831	876	927	977	1027	1077	1109	1169	1229	1289
Time	41	42	43	44	45	46	47	48	49	50
Demand	1359	1399	1439	1479	1510	1530	1550	1570	1600	1608
Time	51	52	53	54	55	56	57	58	59	60
Demand	1616	1624	1633	1613	1593	1573	1559	1539	1519	1499
Time	61	62	63	64	65	66	67	68	69	70
Demand	1478	1484	1490	1496	1503	1507	1511	1515	1519	1522
Time	71	72	73	74	75	76	77	78	79	80
Demand	1525	1528	1532	1515	1498	1481	1463	1423	1383	1343
Time	81	82	83	84	85	86	87	88	89	90
Demand	1293	1243	1193	1143	1081	1031	981	931	888	848
Time	91	92	93	94	95	96				
Demand	808	768	754	740	726	712				

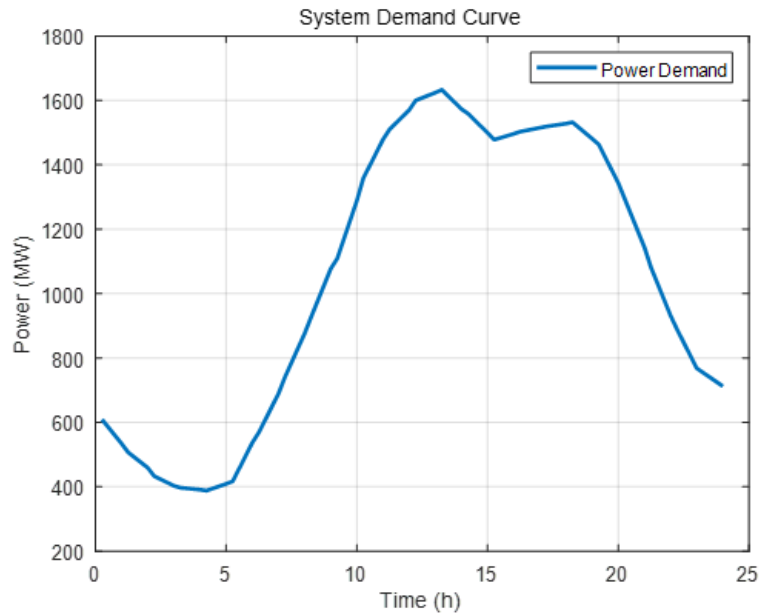


Figure 4.7: System Demand

#### 4.4.2 Case I with Conventional Dynamic Programming

In case I solution is based on the technique of conventional dynamic programming, all the possible combinations are tested during the search for the optimal solution. For a ‘N’ number of units system, there will be total  $2^N - 1$  possible computational states at each time point. This method gives the optimal result, but it takes more computational time. The spinning reserve is assigned as a fixed percentage 15% of the total demand.

*The conventional dynamic programming model with different optimization methods of quadratic programming, mixed-integer linear programming, and linear programming are tested on the system to calculate the production cost and emission cost of each state in each time interval. The simulation results are shown in Table 4-8,*

Table 4-9, and Table 4-10 with the computation time of 12 seconds, 55 seconds, and 227 seconds respectively.

*Table 4-8: Case I Results of Conventional Dynamic Programming with Quadric Optimization Method*

Unit	Power (MW)	Production Cost (US\$)	Emission Cost (US\$)	Start Up-Down Cost (US\$)
G1 (Coal)	0	0	0	0
G2 (Coal)	0	0	0	0
G3 (Coal)	33388	201948	32633	6852
G4 (Gas)	20352	126118	1795	3200
G5 (Gas)	42215	189997	446	0
G6 (Oil)	5235	30296	3378	0
Total	101190	548359	38252	10052
Overall Cost		596663		

*Table 4-9: Case I Results of Conventional Dynamic Programming with Mixed-integer Linear Optimization Method*

Unit	Power (MW)	Production Cost (US\$)	Emission Cost (US\$)	Start Up-Down Cost (US\$)
G1 (Coal)	2136	18134	4843	4545
G2 (Coal)	0	0	0	0
G3 (Coal)	31156	190057	30722	6886
G4 (Gas)	20835	128778	1833	3200
G5 (Gas)	42222	190035	446	0
G6 (Oil)	4841	28201	3137	0
Total	101190	555205	40981	14631
Overall Cost		610817		

*Table 4-10: Case I Results of Conventional Dynamic Programming with Linear Optimization Method*

Unit	Power (MW)	Production Cost (US\$)	Emission Cost (US\$)	Start Up-Down Cost (US\$)
G1 (Coal)	2030	17257	4608	4545
G2 (Coal)	0	0	0	0
G3 (Coal)	31298	190525	30795	6886
G4 (Gas)	20762	128380	1828	3200
G5 (Gas)	42284	190296	446	0
G6 (Oil)	4816	28070	3122	0
Total	101190	554528	40799	14631
Overall Cost		609958		

#### **4.4.3 Case II with Sequential Dynamic Programming**

In the case II, the technique of priority list, is used to generate the combinations so that there are only ‘N’ combinations to be tested at each time point. This method takes less computation time since it reduces the dimensionality of the problem, but it will cause a sub-optimal feasible result. The spinning reserve is set as 15%.

The Sequential dynamic programming (SDP) model based on the priority list approach is also tested on the system with three optimization methods respectively. The simulation results are shown in Table 4-11, Table 4-12, and Table 4-13 with the computation time of 1 second, 3.1 seconds, and 12 seconds respectively. Obviously, this method reduced the computation time.

*Table 4-11: Case II Results of Sequential Dynamic Programming with Quadratic Optimization Method*

Unit	Power (MW)	Production Cost (US\$)	Emission Cost (US\$)	Start Up-Down Cost (US\$)
G1 (Coal)	0	0	0	0
G2 (Coal)	0	0	0	0
G3 (Coal)	32606	199328	32223	6852
G4 (Gas)	21852	137227	1952	0
G5 (Gas)	41497	187087	441	0
G6 (Oil)	5235	30297	3379	0
Total	101190	553939	37995	6852
Overall Cost		598786		

*Table 4-12: Case II Results of Sequential Dynamic Programming with Mixed-integer Linear Optimization Method*

Unit	Power (MW)	Production Cost (US\$)	Emission Cost (US\$)	Start Up-Down Cost (US\$)
G1 (Coal)	2016	17213	4595	4555
G2 (Coal)	0	0	0	0
G3 (Coal)	32456	198834	32146	6852
G4 (Gas)	20881	131778	1874	0
G5 (Gas)	41373	186561	440	0
G6 (Oil)	4464	26220	2908	0
Total	101190	560606	41963	11407
Overall Cost		613976		

*Table 4-13: Case II Results of Sequential Dynamic Programming with Linear Optimization Method*

Unit	Power (MW)	Production Cost (US\$)	Emission Cost (US\$)	Start Up-Down Cost (US\$)
G1 (Coal)	2030	17257	4608	4555
G2 (Coal)	0	0	0	0
G3 (Coal)	32605	199328	32223	6852
G4 (Gas)	20668	130598	1856	0
G5 (Gas)	41419	186751	441	0
G6 (Oil)	4468	26244	2911	0
Total	101190	560178	42039	11407
Overall Cost		613624		

#### **4.4.4 Case III with Different Level of Spinning Reserves**

In case III, the model of Conventional Dynamic Programming (CDP) with a quadratic optimization method is used to test the cost impact of different levels of spinning reserves. The simulation results are shown in Table 4-14 with level specifications of spinning reserves from 15% to 35%. Here the amount of spinning reserve is set as a fixed percentage of the total demand in each certain time point. Its corresponding cost curves are shown in Figure 4.8.

*Table 4-14: Case III Results of Cost Impact of Different Levels of Spinning Reserves*

Spinning Reserve Level (%)	Production Cost (US\$)	Emission Cost (US\$)	Start Up-Down Cost (US\$)	Overall Cost (US\$)
15	548359	38252	10051	596663
16	548359	38252	10051	596663
17	548359	38252	10051	596663
18	548708	38238	10051	596999
19	548708	38238	10051	596999
20	548708	38238	10051	596999

21	557747	44188	14626	616562
22	558218	44639	14623	617481
23	558676	45211	14609	618497
24	558676	45211	14609	618497
25	557374	41371	14356	613102
26	557374	41371	14356	613102
27	558961	45631	14605	619199
28	568595	48344	18928	635868
29	568574	49004	18911	636490
30	568672	49220	18908	636802
31	568400	49262	18907	636570
32	568400	49262	18907	636570
33	568407	49553	18904	636864
34	568407	49553	18904	636864
35	Cannot find the feasible path since the total demand and reserve of 2192.4 MW is exceeding the maximum system ability of power generation of 2190 MW at time point 52 (real-time 13:00)			

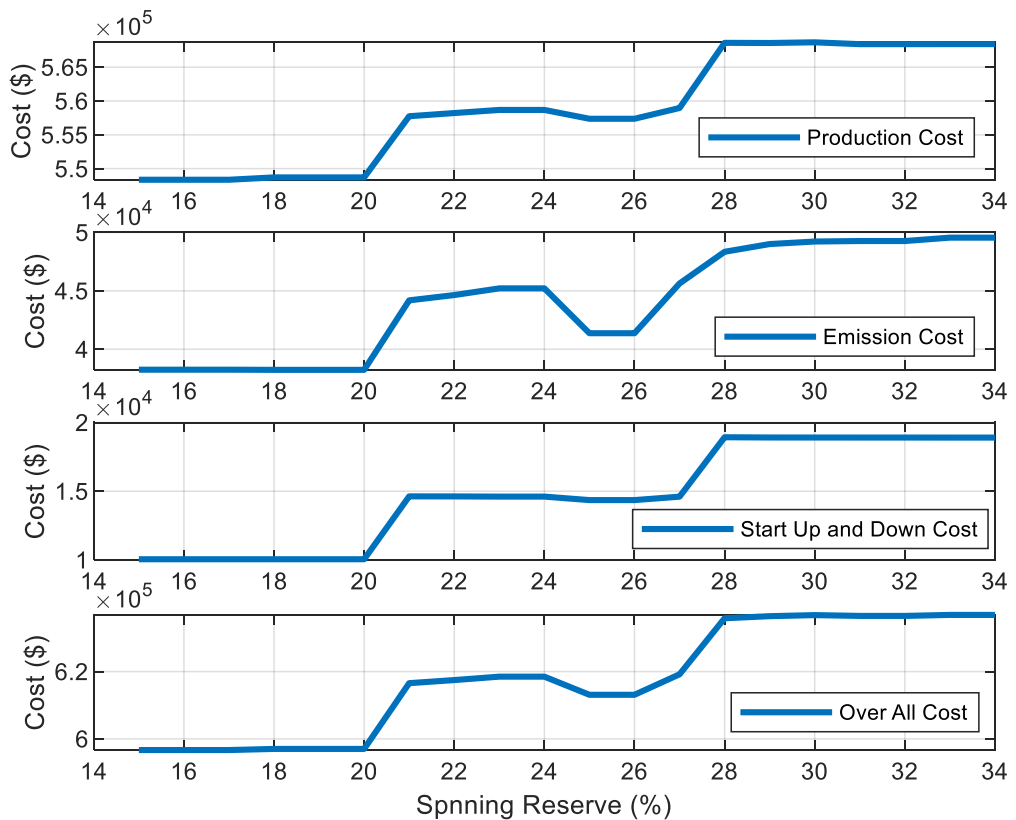


Figure 4.8: Cost Impacts of the Spinning Reserve

#### 4.4.5 Case Study Discussion

In conventional dynamic programming comparing one-hour intervals, and 15-minute intervals the latter can support more accurate cost calculation, and more system decision-making chances (feasible transmission paths) during the simulation programming.

Three optimization methods of quadratic programming, mixed-integer linear programming, and linear programming are used to minimize the production cost and emission cost of each state. The final results are listed below.

*Table 4-15: Final Compared Results of Operation Cost by Different Programming Techniques*

Method of Solution	Production Cost (US\$)	Emission Cost (US\$)	Start Up-Down Cost (US\$)	Overall Cost (US\$)	CPU Time (second)
CDP with Quadratic	548359	38252	10052	596663	12
SDP with Quadratic	553939	37995	6852	598786	1
CDP with MILP	555205	40981	14631	610817	55
SDP with MILP	560606	41963	11407	613976	3.1
CDP with Linear	554528	40799	14631	609958	227
SDP with Linear	560178	42039	11407	613624	12

It can be noted that the conventional dynamic programming with the quadratic optimization method has achieved the best results with the least overall cost of US\$596663 in solving the unit commitment problem of the small size power system. Based on this method, all combinations of units and the most of paths have been considered to find optimum schedule solutions but this method requires a lot of time to get the desired solution.

Because of the conventional dynamic programming is hard to solve the problem of a large-scale system due to the dimensionality problem, sequential dynamic programming with the priority list approach is used to overcome the dimensionality problem. However, priority list approach will result in a sub-optimal result due to its limited arrangement set of unit commitment combinations.

Spinning reserve allows system operators to compensate for unpredictable imbalances between load and generation. However, the over setting of the spinning reserve will increase the unnecessary operation cost.

By observing Figure 4.8, this cost increment is more like a stepwise increment. In example Case III with Table 4-14, the increment setting of the spinning reserve from 15% to 20% or from 28% to 34% has only a small effect on the cost.

So, for example, a higher reserve setting of 20% rather than 15% for the system according to this phenomenon can be selected, and at the same time, the increment of operating cost is small. And in China, a higher reserve setting also means more renewable energy can be integrated.

Besides, the interesting thing is that, with the cost decreasing from US\$618497 to US\$613102, the spinning reserve is increasing from its setting of 24% to 26% as Figure 4.8 shows.

The reason why this phenomenon happened is that with the increase of spinning reserve, the system starts up the shutdown generators earlier to release more low-cost power generation space so that the system can flexibly adjust the power generation schedule earlier and save further costs.

## 4.5 Summary

This Chapter developed modified dynamic programming to solve the problems of unit commitment and its operation economic optimization. The proposed model takes emission costs into account to reduce total emissions of thermal units. Besides this, the proposed model can provide any different time interval resolutions, such as one hour interval, 15 minutes interval, or even one minute interval.

Case studies were used to test the proposed modified dynamic programming and the results showed that the quadratic optimization approach is the most suitable technique for this test system with the lowest cost compared with the mixed-integer linear optimization approach and linear optimization approach.

Sequential dynamic programming with the priority list method is recommended to solve the problem of a large-scale system because its much less computation time. But it only supports a sub-optimal result due to its reduced combinations of unit commitment.

The increment of spinning reserve cost is like a stepwise increment. Therefore, the selection of a suitable reserve space can increase the capacity of the spinning reserve without increasing or only increasing a small amount of cost.

The cases in this chapter are only discussed the conventional systems. Modern power system including renewable energy sources and distributed generation will be demonstrated in the provincial case study in Chapter 6.

# **Chapter 5 Modelling Construction of Renewable Energy Sources and Battery Energy Storage System**

## **5.1 Introduction**

To arrange the schedule of power dispatching in a large-scale system with renewable energy and storage, a lot of time-series data of solar and wind forecasting output with the interval of 15 minutes are required. Therefore, the purpose of this chapter is to investigate models' constructions for these required input data. This chapter will introduce the simulation models of solar irradiance, wind speed and storage system, respectively.

[92, 93] state that it is difficult to derive deterministic models for solar irradiance and wind speed considering it as a time-dependent phenomenon in which there are many unknown factors, especially focusing on the local scale that they may lack great accuracy because of the complexity of the addressed atmospheric phenomenon. Therefore, [92, 93] proposed to use stochastic models approach to provide solution to the solar irradiance and wind speed variability problems. And the target case study involved in this thesis consists of a large number of renewable energy farms of different scales. So, the stochastic method is selected to generate the numerical results of forecasting solar irradiance and wind speed.

The model of solar power output is created based on modelling the construction of the photovoltaic module proposed in [74, 75]. Based on its approach and equations in sub-section 5.2.1, the conversion output results of solar power can be obtained based on the acquired data of solar irradiance from the proposed method of forecasting solar irradiance in sub-section 5.2.2.

The novel stochastic model of solar irradiance is developed by considering the more fluctuations and variations of forecasting solar irradiance because the solar fluctuations are directly related to the consideration of ramping rate of thermal plants. In sub-section 5.2.2, this model is developed by stochastic generating the output data of solar irradiance in forecasting next day range based on the free open-source ‘SOLCAST API Toolkit’ [21].

This model is designed to generate forecasting solar irradiance by adding the stochastic and correction variables into the data of forecasting solar irradiance curve supported by the ‘SOLCAST API Toolkit’. This toolkit supports the solar resource assessment and forecasting data for irradiance that is created using a global fleet of weather satellites.

In the section 3.3, the energy conversion from the wind speed to output power through the wind turbine curve has been discussed. Then, the next step is to develop a stochastic simulation model to generate the forecasting wind speed.

To simulate the wind speed of time interval of 15 minutes, in section 5.3 a novel stochastic model of forecasting wind speed is developed by considering Weibull method with adding two types of forecasting correction values of wind speed. The reason for adding these correction values is that the forecasting wind speed can be represented effectively by the Weibull PDF only over extended time periods and not at hourly or shorter time scales [57]. Because the Weibull PDF is not a time-dependent but a static distribution, it cannot represent the frequent short-term wind speed fluctuations that take place inside the hour [58].

Beside this, a proposed method of modelling wind power cost is introduced in sub-section 5.3.4 which considering the relative penalty cost when the underestimation or overestimation of wind power forecasting output occurs.

In section 5.4, the model of battery energy storage system (BESS) with two storage strategies of performance priority and lifetime priority is discussed because the BESS plays an important role to offset the deviations between the predicted and actual power output of the solar and wind energy in power dispatching schedule.

The strategy of lifetime priority may lose renewable integration power but extend the battery lifetime. The strategy of performance priority can reduce the power curtailment of renewable energy sources during operation but shorten battery lifetime.

## **5.2 Solar Power Modelling**

The output power of the photovoltaic module is dependent on the solar irradiance and ambient temperature of the site as well as the specification of the module itself. The data of ambient temperature is extracted from the local temperature monitoring reports.

### **5.2.1 Modelling Approach of Photovoltaic Module**

Solar irradiance means the amount of solar radiation obtained per unit area by a given surface ( $W/m^2$ ). Solar radiation means the electromagnetic radiation emitted by the sun. Solar irradiation is a measure of the solar power over all wavelengths per unit area incident on the Earth.

The output power of the photovoltaic module can be calculated once the data of solar irradiance, ambient temperature, and characteristics of the module are determined by using the following equations [74, 75].

$$P^{pv}(s) = N * FF * V(s) * I(s)$$

$$FF = \frac{V_{MPP} * I_{MPP}}{V_{oc} * I_{sc}}$$

$$V(s) = V_{oc} - K_v * T_c \quad (5-1)$$

$$I(s) = s_a * [I_{sc} + K_i(T_c - 25)]$$

$$T_c = T_A + s_a * \frac{N_{OT} - 20}{0.8}$$

where

$T_c$  is the cell temperature in  $^{\circ}C$

$T_A$  is the ambient temperature in  $^{\circ}C$

$K_v$  is voltage temperature coefficient  $V/^{\circ}C$

$K_i$  is current temperature coefficient  $A/^{\circ}C$

FF is the fill factor

$s_a$  is the average solar irradiance  $kW/m^2$

$I_{sc}$  is the short-circuit current in  $A$

$V_{oc}$  is the open-circuit voltage in  $V$

$I_{MPP}$  is the current at maximum power point in  $A$

$V_{MPP}$  is the voltage at maximum power point in  $V$

$N_{OT}$  is the nominal operating temperature of PV cell in  $^{\circ}C$

## 5.2.2 A Novel Modelling Approach of Forecasting Solar Irradiance

As mentioned before the data of forecasting solar irradiance to simulate the solar power generation are extracted from the free open-source ‘SOLCAST API Toolkit’ [21] as Figure 5.1 shows. This toolkit supports the solar resource assessment and forecasting data for solar irradiance that is created using a global fleet of weather satellites.

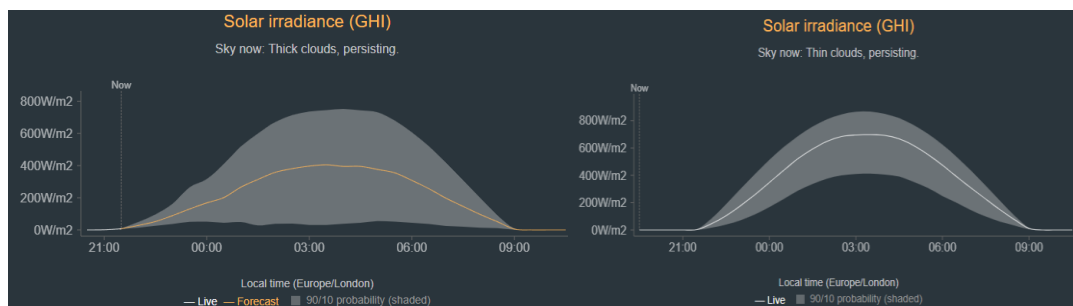


*Figure 5.1: Live and Forecast Solar Irradiance Data for Eastern Australia from Free Open Source of ‘SOLCAST API Toolkit’*

By observing Figure 5.1, the data provided by the software is the forecasting values of solar irradiance corresponding to the yellow curve. And the shaded area is the possible fluctuation range of the forecasting solar irradiance values. To simulate the possible forecasting values of solar irradiance in the shaded area caused by the uncertainty is also essential. Therefore, a novel model of stochastic generation method is proposed to simulate forecasting solar irradiance with the yellow line as the benchmark and the shaded area as the forecasting deviation limit based on the free open-source ‘SOLCAST API Toolkit’ [21] as shown in Figure 5.1.

Not only the uncertainty and variability of solar irradiance are proved by [236], but also [92, 93] proposed to use stochastic models to provide solution to the solar irradiance. Then, to simulate the possible forecasting result in the shaded area, the

author of this thesis proposed a new stochastic method to generate forecasting solar irradiance by adding the stochastic and correction deviation variables into the data of forecasting solar irradiance curve, such as the forecasting yellow curve in Figure 5.1. The definition of correction deviation variables here mean the forecasting differences between the yellow curve and possible values in shaded area at each certain time point supported by the ‘SOLCAST API Toolkit’.

These stochastic and correction deviation variables are designed to be generated based on the method of uniformly distributed random variables by the software of MATLAB. These generated variables are designed to be limited to a certain range, such as boundary of the shaded area in Figure 5.1. This shaded area is simulated based on the Beta function because the accumulation of the shaded area above or below the yellow curve in Figure 5.1 approximately conforms to the beta cumulative distribution.

The advantage of combining the Beta function to model the deviation is that the deviation variable corresponding to its range changes (shaded area in Figure 5.1) in each time point of solar irradiance can be simulated conforming the characteristic of strong production in the middle of the day that forecasting deviations are larger in the middle than on the sides in Figure 5.1.

In order to achieve the simulation of these stochastic forecasting deviations, the uniformly distributed [237] stochastic variables are selected, and they are generated as the first step based on distribution-dependent methods from random variables that are uniformly distributed on the range from 0 to 1.

The second step is to combine with the Beta distribution [238] random variables to convert the range of possible values from 0 to 1 generated by uniformly distributed in the first step into the possible corresponding values in the shaded area range.

[239] introduces that the stochastic variables generated based on Beta distribution-dependent method are parameterized by these two positive shape parameters, denoted by Alpha ( $\alpha$ ) and Beta ( $\beta$ ), that appear as exponents of the random variable and control the shape of the distribution.

$$f_b(x) = \frac{\Gamma(\alpha + \beta)}{\Gamma(\alpha) * \Gamma(\beta)} * x^{(\alpha-1)} * (1 - x)^{(\beta-1)} \quad (5-2)$$

where

$x$  is solar irradiance  $kW/m^2$  for  $0 \leq x \leq 1$

$f_b(x)$  is the Beta distribution function of  $x$   $kW/m^2$

$\alpha, \beta$  are the parameters of the Beta distribution function

[74] states the method to calculate the parameters of the Beta distribution function as follows:

$$\alpha = \frac{\mu * \beta}{1 - \mu} \quad (5-3)$$

$$\beta = (1 - \mu) * \left( \frac{\mu * (1 + \mu)}{\sigma^2} - 1 \right)$$

where

$\mu$  is the mean of the random variable  $x$

$\sigma$  is the standard deviation of the random variable  $x$

Based on the Beta distribution function, this study proposes to use two Beta distribution functions (regard as Double Beta method) to limit the forecasting range of solar irradiance stochastic deviations, like the shaded areas locate in the upside and downside of the forecasting yellow curve respectively in Figure 5.1. Because the

method of Double Beta method can make generated deviation variables locating in possible distribution more clearly like Figure 5.2 shows comparing with using only one beta distribution function, especially when the difference of shaded areas in the upper and lower is large.

Figure 5.2 below gives an example of deviation simulation result to understand this approach more clearly. The upside limit  $A_{upper-lim}^S$  and downside limit  $B_{lower-lim}^S$  are modelled based on the Double Beta method. The blue curve within the limits, consisted by stochastic deviation variables, are generated based on the method of uniformly distributed method combining with equation (5-4).

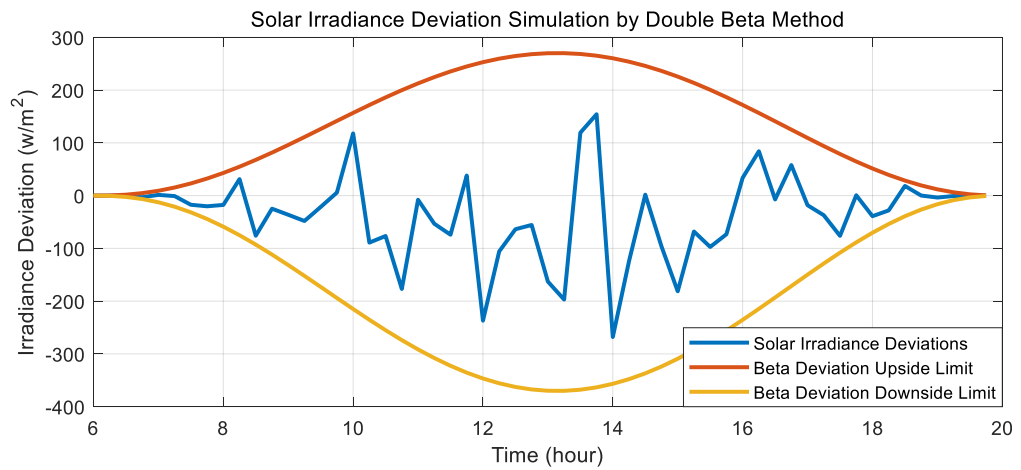


*Figure 5.2: Simulated Example of Solar Irradiance Deviation based on Double Beta Method*

The definition of atmospheric transparency,  $H_s$ , here is the ratio of the total amount of solar irradiance delivered to the surface of the solar farm to the total amount of solar irradiance delivered from atmospheric during that period.

The final simulation of forecasting solar irradiance at each time point with its uncertainty simulation variable based on the proposed method received at the solar farm,  $S_{overall} (W/m^2)$ , can be expressed as follows:

$$S_{overall} = \left\{ S_{base} + (R_{upper}^s * A_{upper-lim}^s - R_{lower}^s * B_{lower-lim}^s) * \frac{f_b(x)}{\max f_b(x)} \right\} * H_s \quad (5-4)$$

$S_{base}$  is the base value of forecasting solar irradiance extracted from the free open-source ‘SOLCAST API Toolkit’, such as the yellow forecasting curve in Figure 5.1  $W/m^2$

$A_{upper-lim}^s$  is the solar irradiance deviation limitation towards increment  $W/m^2$

$B_{lower-lim}^s$  is the solar irradiance deviation limitation towards decrement  $W/m^2$

$R_{upper}^s$  and  $R_{lower}^s$  are randomly generated variables range from 0 to 1 based on the method of uniformly distributed located in the upside limit  $A_{upper-lim}^s$  and downside limit  $B_{lower-lim}^s$  respectively

$f_b(x)$  is the Beta distribution function of  $x$   $kW/m^2$

$\max f_b(x_{day})$  is the maximum value of the Beta distribution function of  $x$   $kW/m^2$

$x$  is solar irradiance  $kW/m^2$  for  $0 \leq x \leq 1$

$H_s$  is the atmospheric transparency coefficient for  $0 \leq H_s \leq 1$

### 5.2.3 Simulation Results Demonstration of Solar Irradiance

In this work, a combined modeling process is used to represent the simulation of solar irradiance variation based on the statistical methods of Beta distribution and uniformly distributed stochastic variables. Simulated results based on this novel

proposed method present visual similarity to the obtained historical data under the different weathers as shown in Figure 5.3 and Figure 5.4.

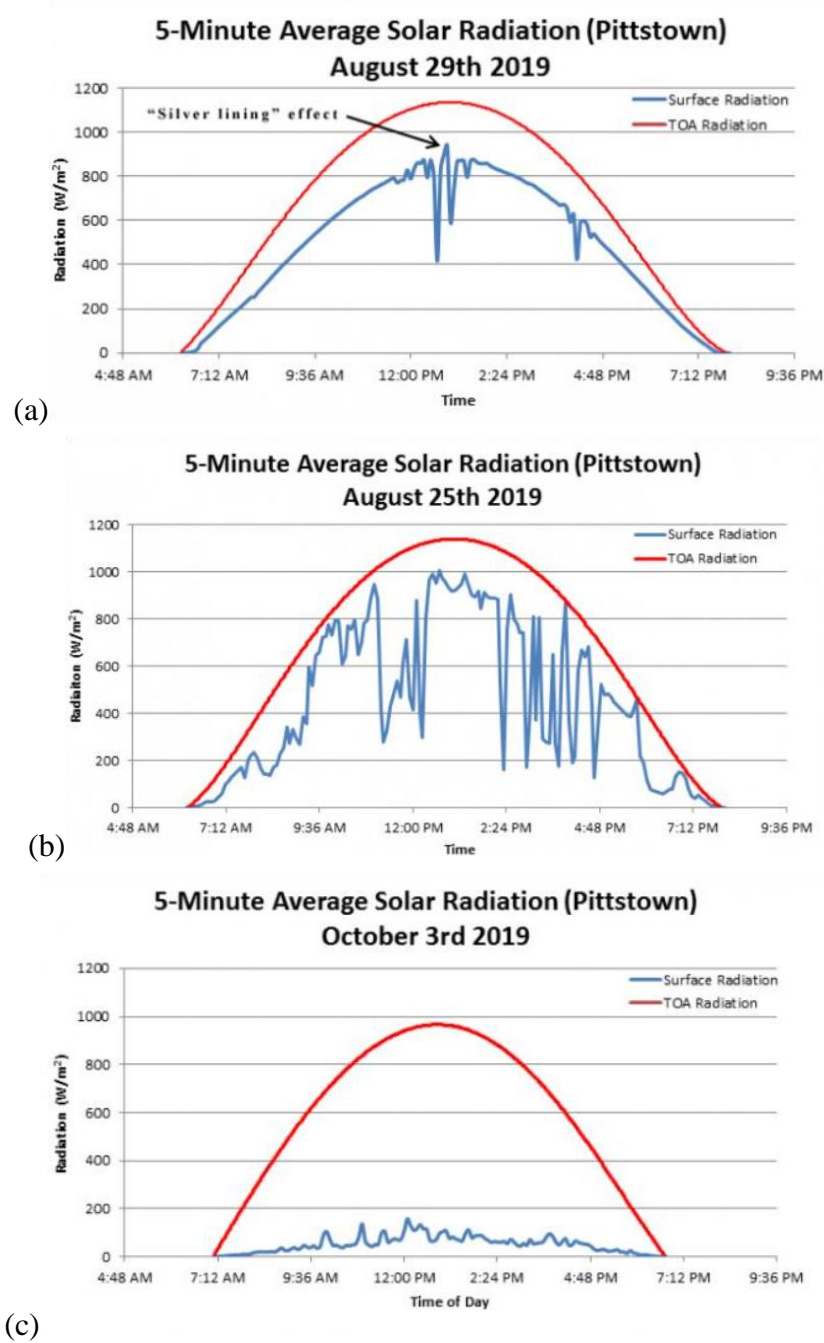


Figure 5.3: Example Graphs of Actual 5-minute Solar Radiation at Pittstown

The graphs in Figure 5.3 are extracted from the historical data in reference [240] and graphs in Figure 5.4 are generated based on the method mentioned in sub-section

5.2.2. The graphs (a, b, and c) in Figure 5.3 and Figure 5.4 respectively represent the solar irradiance under the weather of clear day (a), partly cloudy day (b), and heavily cloud-covered day (c), respectively.

The “silver lining” effect in Figure 5.3 (a) means the radiation is reflected off the sides of clouds from multiple directions and reaches the sensor that leading to the surface radiation coming close to top of the atmosphere (TOA) radiation [240].

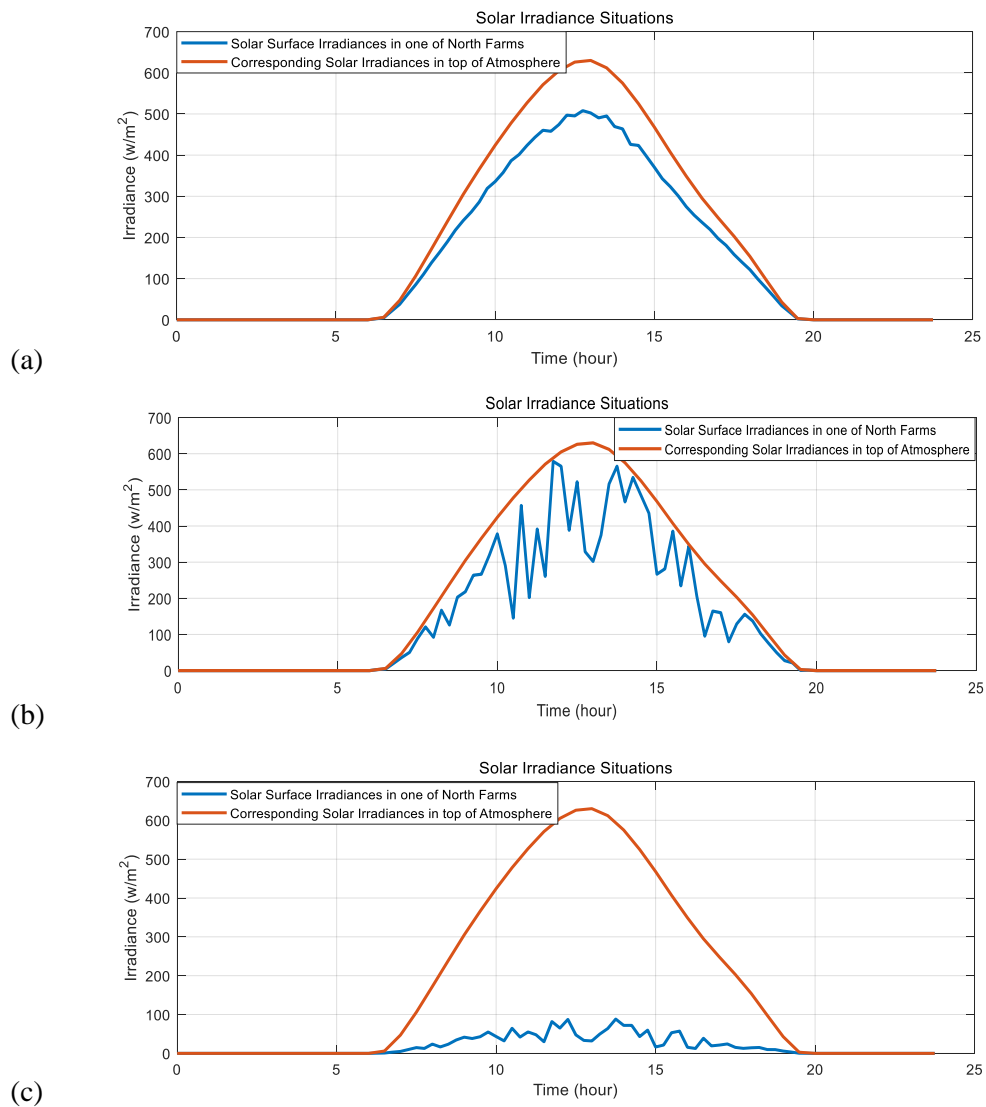


Figure 5.4: Simulated 15-minute Solar Irradiance Results

By adjusting the values of the variables,  $H_s$ ,  $A_{upper}^s$ ,  $B_{lower}^s$ ,  $\alpha$  and  $\beta$ , the solar irradiance variation in different seasons and atmospheric conditions can be represented. The value of  $H_s$  is dependent on the situation of atmospheric transparency.

The values of  $A_{upper}^s$ , and  $B_{lower}^s$  are dependent on the upside limit and downside limit of the shaded area in Figure 5.1. The values of  $\alpha$  and  $\beta$  are estimated based on the distribution of forecast solar irradiance values correspond to the time axis in Figure 5.1 according to the equation (5-3). Table 5-1 indicates the parameter settings to generate the simulated solar irradiance curves in Figure 5.4 (a), (b), and (c) respectively. These parameter settings are estimated by observing the changing trend of the solar irradiation curves in Figure 5.3.

*Table 5-1: Parameter Settings of Different Weathers*

	$H_s$	$A_{up}^s$	$B_{down}^s$	$\alpha$	$\beta$
clear day (a)	0.93	30	50	3.5	3.4
partly cloudy day (b)	0.8	50	430	3.5	3.4
heavily cloud-covered day (c)	0.2	70	270	3.5	3.4

By comparing graphs of (a) (b) and (c) in Figure 5.3 and Figure 5.4 respectively, it can be observed that the results generated by the proposed model can show the general characteristics of different weathers of magnitude and trend in solar irradiance changes.

This is why it was said before that they present a visual similarity. On clear days, the fluctuation of solar irradiance is smooth and stable as shown in Figure 5.3 and Figure 5.4 (a). In partly cloudy days, the fluctuation of solar irradiance is large and frequent as shown in Figure 5.3 and Figure 5.4 (b). In heavy cloudy weather, the solar

irradiance is being absorbed within the clouds or even by aerosols throughout the atmosphere. So, its value of atmospheric transparency coefficient is small as shown in Figure 5.3 and Figure 5.4 (c).

## **5.3 Wind Speed and Wind Power Cost Modelling**

The first stage of this section will introduce the novel wind speed model presented by the author and how its design logic is arrived step by step. The second stage of this section will introduce the proposed model of wind power cost supported by the reference [241].

This overall model of forecasting wind speed is developed by considering Weibull method with adding two different types of forecasting correction values of wind speed.

### **5.3.1 Weibull Method for Wind Speed**

The speed of wind is uncertain and stochastic variable, and its simulation models can be divided into probability distribution models [31-34] and time-series models [35-39]. Generally, Weibull distribution is generally considered as a probability model with a simple form and a good fitting ability into the real distribution of wind speed [53-56]. It is a widely used distribution model for the calculation in terms of wind power analyzing.

In this study, the variation of wind speed,  $v$  is modeled by using Weibull distribution function to represent the wind speed for each time point. This method of two parameters Weibull distribution function is widely used to describe wind speed data in many regions [42] and this method is based on a comparison of actual wind

speed profiles at different sites [242]. The characteristic function of the Weibull distribution is introduced as the following:

$$f_w(v) = \frac{k}{c} * \left(\frac{v}{c}\right)^{k-1} \exp \left[-\left(\frac{v}{c}\right)^k\right] \quad (5-5)$$

where

$v$  is the wind speed  $m/s$

$f_w(v)$  is the Weibull distribution function of  $v$

$k$  is the shape parameter of the Weibull distribution of wind speed

$c$  is the scale parameter of the Weibull distribution of wind speed

The credible approximation of the Weibull distribution parameters  $k$  and  $c$  can be obtained through a simple curve fitting procedure [243] which indicates that the shape parameter gives the description of wind behavior according to its value and the most sites have typically wind distribution at a shape parameter  $k$  equals to 2, known as the Rayleigh distribution.

These two parameters  $k$  and  $c$  also can be estimated using the equations depending on which wind statistics that are available. Reference [244] supports five methods for Weibull parameter estimation varying different types of wind statistics, such as the method of Least-squares fit and the method of Mean wind speed and standard deviation. Another method of the maximum likelihood method [245] is used to fit a Weibull distribution to a measured wind speed distribution to calculate the Weibull parameters. Beside to this, there are lots of papers that describe how to determine the Weibull parameters such as [246-250].

### 5.3.2 A Novel Modelling Approach of Forecasting Wind Speed

[38, 251-253] state that Auto-regressive Moving-Average ARMA model is the most widely used model for the description of a stable stochastic sequence. Wind speed, as a typically time sequence, featured by tendency, stochastic characters can be approximately boiled down to the certain Auto-regressive Moving-Average ARMA model. ARMR wind speed model usually label wind speed as the noise input for the system when wind speed is uncontrollable.

[57, 58] states that the forecasting wind speed cannot be represented effectively by the Weibull PDF in shorter time scales, especially less than hourly. [254] states that wind speed is a stochastic signal. The changing of wind speed can be regarded as an overlapping of different frequency components, each with its own amplitude. [255] states that a lot of research adopt the wind velocity model with a superposition of average wind velocity component and turbulence velocity component. [256] regards the changes of wind velocity caused by turbulence component as the stable stochastic process.

[257] states that in the medium time range (from several hours up to a day) the wind speed can be regarded as more or less stationary. Therefore, mean values and mean standard deviations of the wind speed can be determined over a range of hours. During this process, the fluctuations of this mean wind speed and the superimposed short-term wind-speed fluctuations can be examined and modelled, independent of each other. It is assumed that the "driving force" of wind speed is normally distributed white noise generated by a random number generator.

So, based on [38, 57, 58, 251-257] of the statements of the wind speed characteristics and the inspiration of the applications of methods, the novel model of forecasting wind speed presented by the author is designed to use Weibull method with

adding two types of forecasting correction values of wind speed as the white noise generated by a random number generator to stochastically simulate forecasting wind speeds with 15-minute intervals.

Based on the discussed theory of previous references of [57, 58, 255], the author of this thesis designs the model with a sum of average Weibull results of forecasting wind speed and two types of forecasting correction values of wind speed as the overall simulated forecasting wind speeds in shorter time intervals of 15 minutes. The two types of forecasting correction values of wind speed are designed as stochastic values because of previous reference discussions of [254-257]. The two types of forecasting correction values of wind speed are designed as the white noise sequence since the same idea used in [38, 251-253, 257]. Due to the inspiration of methods of Autoregressive Moving-Average ARMA model [38, 251-253], the white noise sequence are designed as a white noise sequence of mathematic expectation mean value of zero.

When the sample space is large, the addition of random numbers with mathematic expectation mean value of zero adding the base values generated by the Weibull method has minimal impact to the mean value of sample space. It will affect the overall variance value of base data of sample space a lot but just a little effect on mean value of base data of sample space. This is the reason why using a white noise sequence of mathematic expectation mean value of zero as the correction values.

Finally, these two types of correction values are designed to adapt the distribution characteristics of the wind farms such as the wind farms are distributed in several different regions of the province, and these wind farms in respective region are located in different places. Due to the lack of wind speed data in these wind farms, stochastic simulation methods have to be used to supplement the data.

In order to show the wind speed tendency changings in different regions and the wind speed amplitude changings in different wind farms respectively, the first type of correction value is designed as a stochastic reference value of wind speed for all wind farms in a certain region to follow. The second type of correction value is designed as a stochastic deviation value of wind speed for each wind farm in each region. For the convenience of understanding, the first type of correction value will be named as correction reference value. The second type of correction value will be named as correction deviation value.

The equation of novel model of forecasting wind speed presented by the author is given by:

$$v_{forecasting,t}^w = \{v_{avg-Weibull,t}^w + v_{correction-ref,t}^w + v_{correction-dev,t}^w\} \quad (5-6)$$

Where

$v_{avg-Weibull,t}^w$  is the average wind speed in each 15 minutes based on Weibull method at the time point  $t$   $m/s$

$v_{correction-ref,t}^w$  is the correction reference value of wind speed at the time point  $t$   $m/s$

$v_{correction-dev,t}^w$  is the correction deviation value of wind speed at the time point  $t$   $m/s$

In order to achieve the design purposes discussed previous in this sub-section, the establishment process with its related logic of this novel model is introduced by following six parties: i) white noise sequence, ii) two novel types of continuous superposition sequence, iii) average values of Weibull wind speed, iv) correction reference values, and v) correction deviation values respectively.

i) white noise sequence

The white noise sequence is designed as a white noise sequence of mathematic expectation mean value of zero and this white noise sequence is generated by a random number generator.

Firstly, the random number,  $R$ , generated at each time point,  $t$ , is designed based on the method of uniformly distributed random variables by through the software MATLAB. And the random number,  $R$ , is random generated by setting their upside and downside limitation values,  $A_{upper}^R$  and  $B_{lower}^R$  respectively. The value of the upper and lower limits depends on the upper and lower limits of the wind speed change during each simulation time interval.

Secondly, as the random numbers,  $R_t$ , are generated at each time point, they will form a set of numbers, and this simulated set of numbers will be used as the white noise sequence. When the limitation values of  $A_{upper}^R$  and  $B_{lower}^R$  are same, this white noise sequence consisting of random numbers  $R_t$ , will be a number sequence with a mathematical expectation of zero.

Finally, the calculation progress of equation (5-8) is referred as the continuous superposition in this thesis and its symbol is designed as the arrow symbol,  $\overrightarrow{v_t^{R-noise}}$ . Then, the white noise sequence,  $\overrightarrow{v_t^{noise}}$ , as the wind speed velocity correction value corresponding each time point is given by:

$$R_t = \{-B_{lower}^R + R * (A_{upper}^R + B_{lower}^R)\} \quad (5-7)$$

$$\overrightarrow{v_t^{R-noise}} = \sum_{t=1}^t R_t \quad (5-8)$$

Where

$R$  is the random number

$A_{upper}^R$  is the upside limitation value of  $R$

$B_{lower}^R$  is the downside limitation value of  $R$

$R_t$  is the random number generated at the time point  $t$

$\overrightarrow{v_t^{R-noise}}$  is the continuous superposition sequence values of  $R_t$

The reason why the values calculated by equation (5-8) are used as white noises instead of directly using randomly generated numbers is that the discrete random generated value,  $R_t$ , can be converted into a continuous form,  $v_t^{noise}$ . The reasons why using the continuous form relationship to simulate the relative forecasting wind speed acts on the turbine blade are these:

- 1) The wind speed simulated by this method are modeled as a continuous event, not a discrete event. For example, the latter value is obtained by superimposing the previous value step by step.

This conforms the change characteristic of wind speed in nature. The magnitude of the subsequent wind speed is closely related to the magnitude of the wind speed at the previous moment, especially in shorter time scale.

- 2) This continuous relationship is resembled to the inertia characteristic of rotational change for the turbine blade under the influence of wind speed, especially in models with short time interval.

For example, the increase or decrease of the wind speed will gradually affect the speed of the turbine blade as time proceeds, but it will not stop rotating

suddenly when the wind stops. So, the values of these deviation variables are gradually changed.

ii) two novel types of continuous superposition sequence

Based on the result,  $\overrightarrow{v_t^{R-noise}}$ , of equation (5-8), two novel types of continuous superposition sequence can be developed comparing with the white noise sequence generated directly by the random numbers.

Before the discussion of the two novel types of white noise sequence, a new concept should be clarified that the new arrow symbol of continuous superposition sequence of  $\overleftarrow{v_t^{R-noise}}$  is the reversed order of continuous superposition sequence of  $\overrightarrow{v_t^{R-noise}}$ .

Then, the two novel types of continuous superposition sequence are defined as:

$$\overleftarrow{v_t^{correction-ref}} = \left\{ \overrightarrow{v_t^{Ra-noise}} + \overleftarrow{v_t^{Rb-noise}} \right\} / 2 = v_{correction-ref,t}^w \quad (5-9)$$

$$\overrightarrow{v_t^{correction-dev}} = \left\{ \overrightarrow{v_t^{Rc-noise}} \right\} = v_{correction-dev,t}^w \quad (5-10)$$

Where

$\overrightarrow{v_t^{Ra-noise}}$  is the continuous superposition sequence values of  $R_t^a$

$\overrightarrow{v_t^{Rb-noise}}$  is the continuous superposition sequence values of  $R_t^b$

$\overleftarrow{v_t^{Rb-noise}}$  is the reversed order of  $\overrightarrow{v_t^{Rb-noise}}$

$\overrightarrow{v_t^{Rc-noise}}$  is the continuous superposition sequence values of  $R_t^c$

$\overrightarrow{v_t^{correction-ref}}$  is the first novel type of continuous superposition sequence that is regarded as the correction reference values of forecasting wind speed,  $v_{correction-ref,t}^w$  m/s

$\overrightarrow{v_t^{correction-dev}}$  is the second novel type of continuous superposition sequence that is regarded as the correction deviation values of forecasting wind speed,  $v_{correction-dev,t}^w$  m/s

iii) average values of Weibull wind speed

Firstly, the average values of Weibull wind speed in each 15 minutes is designed as the base value to achieve forecasting simulation wind speed as equation (5-6) shows. The average values of Weibull wind speed in each 15 minutes is given by:

$$v_{avg-Weibull,t}^w = \left\{ \sum_{n=15*(t-1)+1}^{15*t} v_{1-Weibull,n}^w \right\} / 15 \quad (5-11)$$

Where

$t$  is the time point and  $t = n$

$v_{avg-Weibull,t}^w$  is the average value of minutely Weibull wind speed in each 15 minutes at time point  $t$ , m/s

$v_{1-Weibull,n}^w$  is the Weibull wind speed with the interval of 1 minute at time point  $n$ , m/s

$v_{15-Weibull,n}^w$  is the Weibull wind speed with the interval of 15 minutes at time point  $n$ , m/s

Secondly, this research is designed to use a 15-minute average wind speed value instead of a single generated wind speed value based on the Weibull method to simulate the base wind speed. The reason why using average method is that the corresponding referenced database of wind speed in this research uses the average method as well.

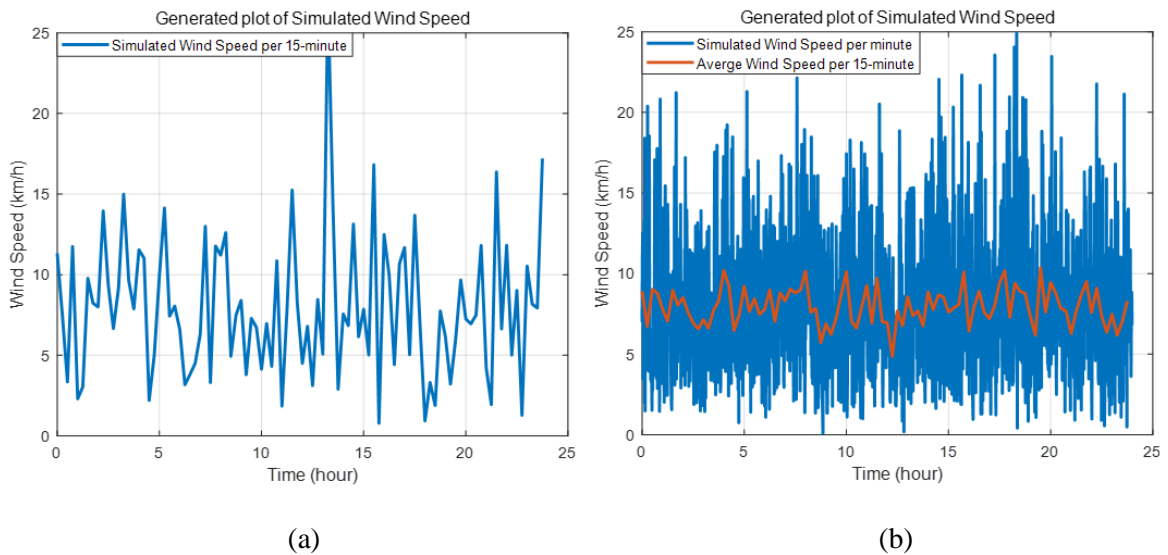


*Figure 5.5: Compared Graph of Directly Generated and Average Generated Wind Speed*

Based on the Weibull method, the wind speed simulation values corresponding to every 15-minute (blue curve in Figure 5.5 (a)) and every minute (blue curve in Figure 5.5 (b)) are generated. The value of the red curve is obtained from the average of the simulated values of the blue curve in Figure 5.5 (b) for every 15 minutes.

Thirdly, another reason is that the Weibull method shows an acceptable performance at the simulation of wind speed of the time interval of per day or even per hour, but not when the time interval is per 15-minute or per minute [57, 58]. For instance, the wind speed curves generated in a short period per 15-minute and per minute are too drastically between the upper and lower amplitude changes as blue curves in Figure 5.5 (a) and Figure 5.5 (b) show respectively.

However, the disadvantage due to the averaging method used is also obvious because this method makes the result variables concentrated in a range, such as the generated wind speed (red curve) ranges from 5 *m/s* to 10 *m/s* in Figure 5.5 (b). This is also the reason why to add the correction values to the base forecasting wind speed generated by the Weibull method.

The original design of this forecasting model is to simulate the different wind speeds of a large number of wind farms in different locations, so the stochastic wind speed generated by this model should not be designed to concentrate in a small range. It needs to increase the possibility of more variation.

So, it is necessary to utilize correction values in a new dimension to break through the range limitations. Beside to this, based on the previously designed method, the correction values of white noise sequence with mathematic expectation mean value of zero adding the base values generated by the Weibull method has minimal impact to the mean value of sample space when the sample space is large.

#### iv) correction reference values

Correction reference sequence is generated by simulating the daily random and continuous wind speed variables as the wind speed reference of wind farms in the different regions to follow.

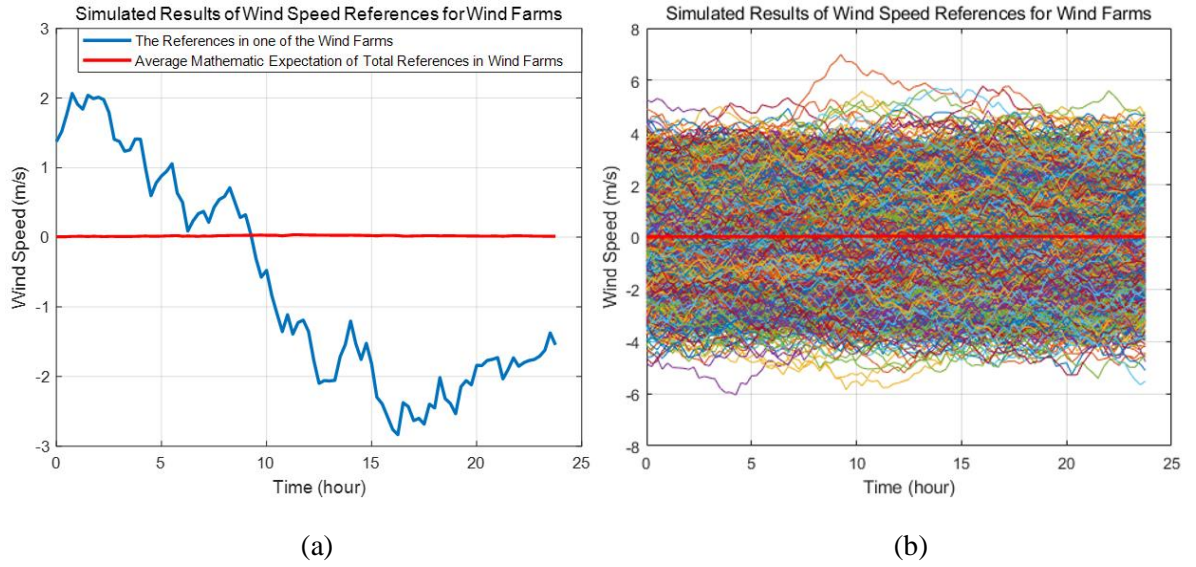


Figure 5.6: Examples of Simulated Wind Speed References

The blue curve in Figure 5.6 (a) is one result of stochastic correction reference sequences which is generated based on the equation (5-9). Its another 5000 times stochastic results are demonstrated in Figure 5.6 (b) to observe the simulated curves distributions, especially their approximate locations of maximum values. It can be observed that the upper and lower maximum amplitude trends of these stochastic results in Figure 5.6 (b) are basically at the same magnitude level. And the mathematic expectation mean value of these stochastic sequences is also well-designed to tend to zero.

The random variables,  $Ra_{ref,t}^w$ , and  $Rb_{ref,t}^w$ , are generated based on equation (5-7) by setting both their upside and downside limitation values,  $A_{upper-lim-ref}^w$  and  $B_{lower-lim-ref}^w$  equal to  $0.5 \text{ m/s}$  respectively.

The mathematic expectation mean value of these all samples, which is also the average value of the sum of these random variables, is relatively close to zero as the red curve shown in Figure 5.6 (a).

The reason why the equation (5-9) composed of the average value of two sets of correction reference values in reversed order is to increase the likelihood of a larger distribution of the correction value at the initial time point.

For example, in Figure 5.6 (a), the initial value of the sequence is about 1.4 m/s. But if for only one set of sequence values, its initial value will be limited to the limitation of the first random value, as shown in Figure 5.7, whose initial values are between  $-0.5$  m/s and  $0.5$  m/s.

v) correction deviation values

Correction deviation sequence is generated by simulating the stochastic deviation values of wind speed for each wind farm corresponding to each region. Its purpose is to demonstrate the variability of wind speed change of each wind farm.

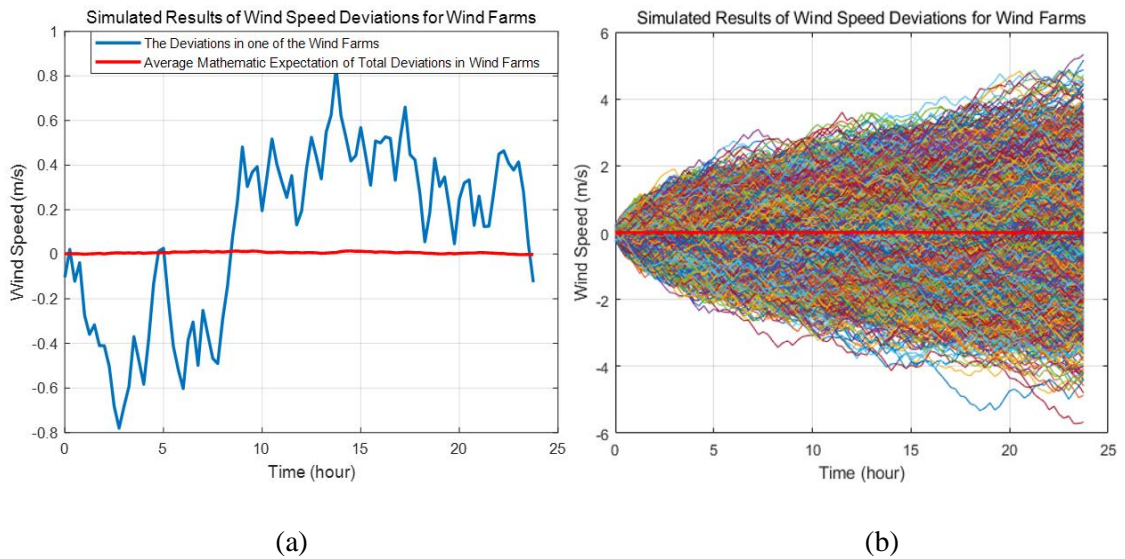


*Figure 5.7: Examples of Simulated Wind Speed Deviations*

The blue curve in Figure 5.7 (a) is one result of stochastic correction deviation sequences which is generated based on the equation (5-10). Its another 5000 times

stochastic results are demonstrated in Figure 5.7 (b) and the red curve is the mathematic expectation mean values of these all samples. The main difference between Figure 5.6 (b) and Figure 5.7 (b) is that the simulated value of the curves at the initial stage of Figure 5.7 (b) is designed smaller than that in Figure 5.6 (b) so that its overall change trend in Figure 5.6 (b) will be from small to large.

Comparing with Figure 5.6 (b), the maximum value trend of curves in Figure 5.7 (b) is becoming larger as the time axis goes on, which is caused by equation (5-8). The purpose of this design is to simulate the characteristic of wind speed forecasting that the forecasting of wind speed is relatively accurate at the beginning, but as the forecasting time increases, the forecasting deviation of wind speed will gradually become larger.

This characteristic can be formed because that the deviation amplitude will gradually increase with more deviation values from equation (5-8) are added as time proceeds.

### **5.3.3 Simulation Model Demonstration of Wind Speed**

In this work, the overall novel model proposed in sub-section 5.3.2 is used to show the simulation results of forecasting wind speed based on the statistics methods of continuous stochastic method and uniformly distributed random variables.

The parameters set of the novel model is listed in Table 5-2 as follows:

Since the output results in this sub-section are stochastic results, these listed parameters setting are for reference only. These 24 wind farms use a same simulated correction reference value but different correction deviation values because these 24 farms are locating in a same region but different places.

Table 5-2: Explanation Examples of Stochastic variables and Continuous variables

Weibull Parameters $k$	4.5
Weibull Parameters $c$	1.89
$A_{up-lim-ref}^w$ for Reference values	1 m/s
$B_{down-lim-ref}^w$ for Reference values	1 m/s
$A_{up-lim-dev}^w$ for Deviation values	0.5 m/s
$B_{down-lim-dev}^w$ for Deviation values	0.5 m/s
Total Number of Wind Farms	24

The simulated results of forecasting wind speed based on this proposed novel method also present visual similarity to the actual historical data as Figure 5.8 shows. Figure 5.8 (a) is the generated stochastic result of forecasting wind speed based on the novel method, Figure 5.8 (b) is the collected and actual historical data from Hong Kong Observatory, referencing from [258], and Figure 5.8 (c) is generated stochastic result of forecasting wind speed only based on the Weibull method. All these results are generated based on the time interval of 15 minutes.

Then comparing the result based on the Weibull method in Figure 5.8 (c) with the historical data in Figure 5.8 (b), it is easy to find that the result of the Weibull method almost concentrate in the same range of fluctuations and these fluctuations are too drastically. Almost every period will complete an amplitude fluctuation of about 7 km/h. Because insufficient historical data of wind speed in China wind farms. The proposed stochastic method prefer mainly simulating the trend and magnitude and cycle period of wind speed changes in time points. Therefore, comparing Figure 5.8 (a) and Figure 5.8 (b), their results can only show stronger visual similarity compared to Figure 5.8 (c) in the pattern of wind speed.

However, this better simulation of the trend and magnitude and cycle period of wind speed changes is necessary because these changes of wind speed is directly

related to the calculation of power ramping rate requirement and peaking balancing ability of thermal plants in the Unit Commitment optimization problem.

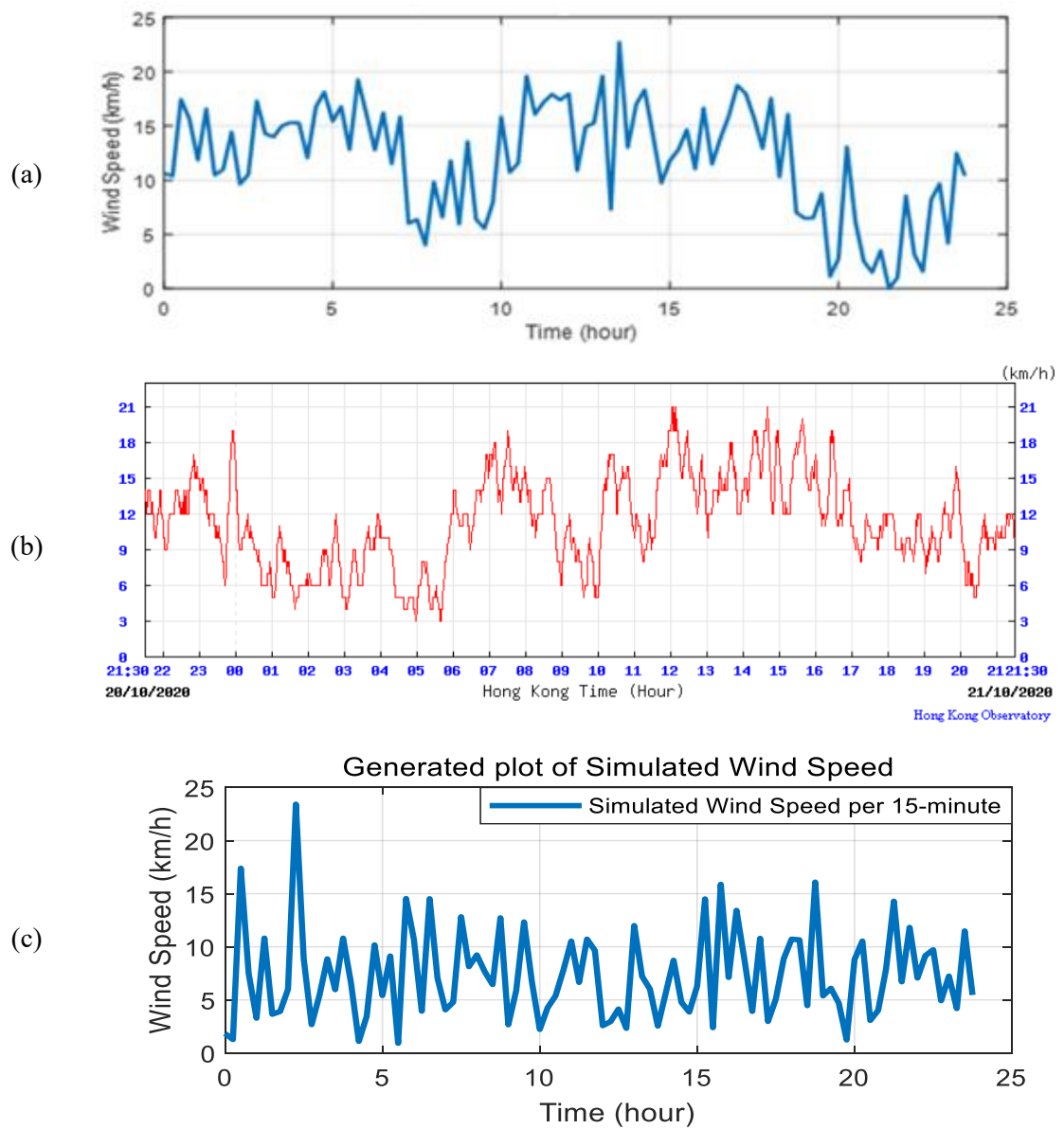
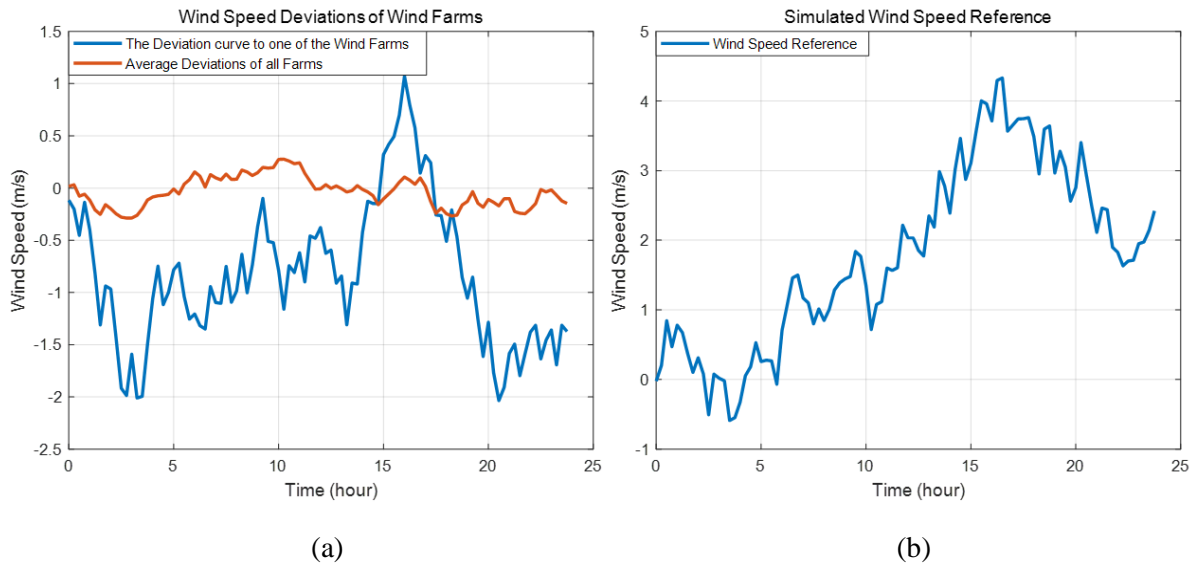


Figure 5.8: Examples of Overall Simulation of Wind Speed (Similarity Observation)

After the demonstration of overall result of the novel model, Figure 5.9 below will demonstrate the simulated results of correction reference value and correction deviation value respectively.



*Figure 5.9: Example of Overall Simulation of Wind Speed (Deviation and Reference)*

The red curve in Figure 5.9 (a) shows the curve of average correction deviation values of all 24 wind farms, and the blue curve is the generated correction deviation curve in one of the wind farms. The curve of corresponding generated correction reference value of wind speed following by these wind farms is shown in Figure 5.9 (b). These two figures show how the designed two types of correction values affecting the final simulated values of forecasting wind speed.

### **5.3.4 Modelling of Wind Power Cost**

As the share of wind power rapidly increases, it is necessary to include wind power operation cost in solving the electrical power systems economic dispatch problem even a lot of research regards this operation cost as zero. The reference [241] develops a model to include wind power operation costs and even penalty cost in the economic dispatch problem.

The penalty cost occurs when the underestimation and overestimation of its availability at any time because of the uncertainty of the availability of wind energy.

This is also the reason why it is necessary to simulate the forecasting wind speed in local wind farms in sub-section 5.3.2.

The model proposed in the reference [241] introduces that the cost can be associated with the use of wind energy by the wind farm  $i$  in each of the  $t$  periods, given by:

$$C_{i,t}^w = C_{op_{i,t}} + C_{ue_{i,t}} + C_{oe_{i,t}} \quad (5-12)$$

$$C_{op_{i,t}} = k_{op} * p_{w.sc_{i,t}} \quad (5-13)$$

$$C_{ue_{i,t}} = k_{ue} * p_{i,t}^{ue} = k_{ue} * (p_{w.av_{i,t}} - p_{w.sc_{i,t}}) \quad (5-14)$$

$$C_{oe_{i,t}} = k_{oe} * p_{i,t}^{oe} = k_{oe} * (p_{w.sc_{i,t}} - p_{w.av_{i,t}}) \quad (5-15)$$

where

$C_{i,t}^w$  is total wind cost for farms  $i$  in  $t$  period for the given system.

$C_{op_{i,t}}$  is direct operation cost for wind farm  $i$  in  $t$  period, it means the cost of renting the space of the wind farm or even expenses with its maintenance and implementation.

$C_{ue_{i,t}}$  is underestimated cost for wind farm  $i$  in  $t$  period, it means the penalty cost for not using all available power from the wind farm.

$C_{oe_{i,t}}$  is overestimated cost for wind farm  $i$  in  $t$  period, it means the penalty cost of the overestimation of the available wind power because of the uncertainty of wind power.

$p_{w.sc_{i,t}}$  and  $p_{w.av_{i,t}}$  are the scheduled wind power from the wind farm  $i$  in  $t$  period and available wind power from the wind farm  $i$  in  $t$  period.

$k_{op}$ ,  $k_{ue}$  and  $k_{oe}$  are the hourly cost coefficients of available, penalty, and reserve for the wind farm  $i$  respectively. Table 5-3 lists their values proposed to use according from the reference [241]. The advantage of this method considering the penalty cost of wind power forecasting underestimation and overestimation is to make each wind farm operator actively participate in wind power forecasting in order to avoid the extra penalty cost in real trade charge.

*Table 5-3: Parameters of Cost Coefficients for Wind Farm*

$k_{op}$	$k_{ue}$	$k_{oe}$
6	6	10

## 5.4 Storage System

In this research, battery energy storage system (BESS) can be used to mitigate the variation between the predicted and actual power output of the solar and wind energy and to smooth their fluctuations in the hybrid power system.

Besides this, the given BESS model are designed to support two storage strategies of performance priority and lifetime priority.

### 5.4.1 Modelling Approach of Battery Energy Storage System Cost

i) The operation cost of BESS can be expressed as:

$$C_{i,t}^{BESS} = \pi_{BESS} (|P_{BESS,i,t}^{discharge}| + |P_{BESS,i,t}^{charge}|) \quad (5-16)$$

$C_{i,t}^{BESS}$  is the operation cost of BESS  $i$  at time  $t$

$\pi_{BESS}$  is the hourly coefficient of battery energy storage system cost

$P_{BESS,i,t}^{charge}$  and  $P_{BESS,i,t}^{discharge}$  are power charge and discharge for BESS  $i$  at time  $t$

ii) BESS constraints are listed as following:

BESS charge/discharge power limits are:

$$0 \leq P_{BESS,i,t}^{charge} \leq P_{Rate,i}^{charge} \quad (5-17)$$

$$0 \leq P_{BESS,i,t}^{discharge} \leq P_{Rate,i}^{discharge}$$

$P_{BESS,i,t}^{charge}$  and  $P_{BESS,i,t}^{discharge}$  are power charge and discharge for BESS  $i$  at time  $t$

$P_{Rate}^{charge}$  and  $P_{Rate}^{discharge}$  are maximum charging and discharging rate

BESS storage constraints are:

$$SOC_{Limit,i}^{lower} \leq SOC_{i,t} \leq SOC_{Limit,i}^{upper} \quad (5-18)$$

$SOC_{i,t}$  are state of charge of BESS  $i$  at time  $t$

$SOC_{Limit}^{lower}$  and  $SOC_{Limit}^{upper}$  are the lower and upper state of charge limitations

iii) Energy capacity of the BESS can be expressed as:

$$C_{Capacity,i,t}^{BESS} = C_{ini,i,t}^{BESS} + P_{BESS,i,t}^{charge} * \eta_{Efficiency}^{charge} - P_{BESS,i,t}^{discharge} * \eta_{Efficiency}^{discharge} \quad (5-19)$$

$C_{Capacity,i,t}^{BESS}$  is the current value of capacity of BESS  $i$  at time  $t$

$C_{ini,i,t}^{BESS}$  is the initial value of the capacity of BESS  $i$  at time  $t$

$P_{BESS,i,t}^{charge}$  and  $P_{BESS,i,t}^{discharge}$  are power charge and discharge for BESS  $i$  at time  $t$

$\eta_{Efficiency}^{charge}$  and  $\eta_{Efficiency}^{discharge}$  are the charge and discharge efficiency

As stated before, it is presented that the BESS model is designed to support two storage strategies of performance priority and lifetime priority in this research.

The first strategy of lifetime priority will only charge or discharge until it reaches the state of charge upper or lower limit. This strategy may lose renewable integration power but extend the battery lifetime.

The key point to extend the battery lifetime is to minimize the deep charge/discharge cycles. For example, if the  $SOC_{Limit}^{lower}$  and  $SOC_{Limit}^{upper}$  are limited to between 20% and 80%, a deep charge or discharge ( $SOC > 80\%$  or  $SOC < 20\%$ ) will lead to permanent physical damage to the BESS and an exceedingly low cycle life [259].

The second storage strategy of performance priority does not require the BESS to charge or discharge until it reaches the SOC limit. This strategy allows BESS to change the state between charge and discharge at any time to mitigate the variability and uncertainty of renewable energy sources as much as possible between the predicted and actual power output.

So, this strategy can reduce renewable energy loss while operating but lose battery lifetime due to its operation flexibility of changing the state between charge and discharge frequently.

## 5.4.2 Simulation Model Demonstration of Battery Energy Storage System

In this work, a model that complies with the basic charging and discharging rules was created by the author based on the software MATLAB and to represent the process of power system charging and discharging. It also considers the previous two strategies of performance priority and lifetime priority that is rarely covered in some research on Unit Commitment problem.

Table 5-4 lists the relevant parameters of these two BESS with two different storage strategies and Figure 5.10 shows their simulation output results respectively:

*Table 5-4: Parameters of Example BESS*

Example	BES System (1)	BES System (2)
strategy	Performance Priority	Lifetime Priority
$P_{BESS}^{Max}$	500 MWh	100 MWh
$P_{BESS}^{Min}$	0 MWh	0 MWh
$C_{ini,t}^{BESS}$	100 MWh	70 MWh
$SOC_{Limit}^{lower}$	20%	20%
$SOC_{Limit}^{upper}$	80%	80%
$P_{Rate}^{charge}$	120 MWh/hour	40 MWh/hour
$P_{Rate}^{discharge}$	120 MWh/hour	40 MWh/hour
$\pi_{BESS}$	US\$25/MW · 15 minutes	US\$25/MW · 15 minutes
$\eta_{Efficiency}^{charge}$	0.83	0.83
$\eta_{Efficiency}^{discharge}$	0.83	0.83

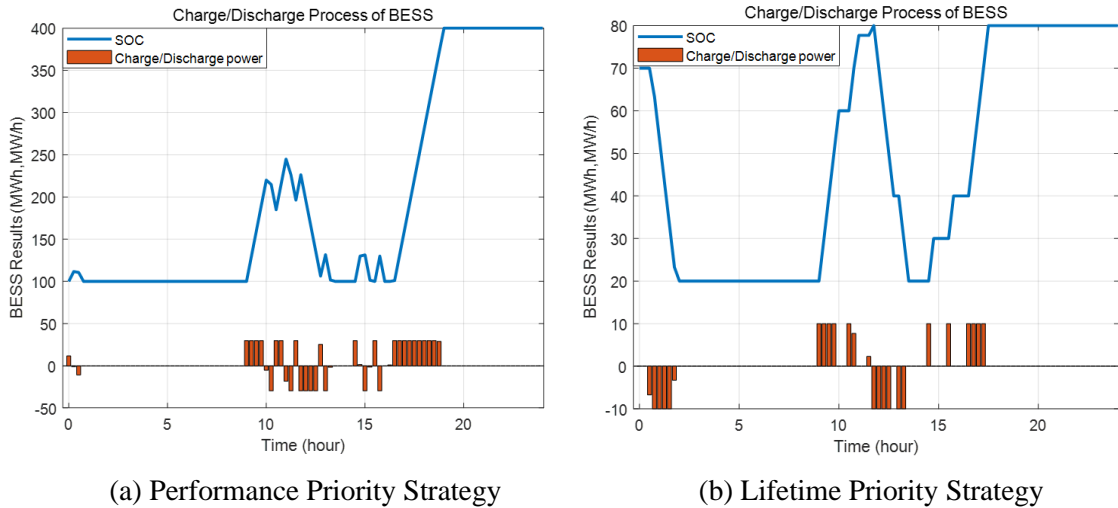


Figure 5.10: Examples of Charge/Discharge Process of BESS

For this example, two BESS systems are operating and cooperate with each other at the same time axis in one power system. It means that when the actual output of renewable energy source is higher (or lower) than the forecasting value, the two BESS will charge (discharge) energy at the same time following their own operation strategy rule. The BESS (1) has higher priority order to charge or discharge the power than BESS (2) when their coefficients of battery energy storage system cost,  $\pi_{BESS}$ , are the same.

For Figure 5.10, the blue curves represent the current value of energy capacity of BESS in the time axis. The red columns represent how much power charge or discharge at this certain time point.

Figure 5.10 (a) shows the BESS 1 operation results based on the strategy of performance priority and it is easy to see that this strategy can be allowed to change the state between charge and discharge at any time point without requiring the BESS to charge or discharge until it reaches the SOC limit.

However, for the BESS 2 operation results shown in Figure 5.10 (b), based on the strategy of lifetime priority, it is only allowed to change its state of charging or discharging until it reaches the SOC upper or lower limit, 80 *MW* or 20 *MW*.

## 5.5 Summary

This chapter introduced the simulation stochastic models of solar irradiance and wind speed presented by the author. The model of forecasting solar irradiance was developed based on the forecasting data extracted from the free open-source ‘SOLCAST API Toolkit’. And the model of forecasting wind speed was developed by considering Weibull method with adding two types of forecasting correction values of wind speed.

Beside this, a proposed method of modelling wind power cost was introduced which considers the relative penalty cost when the forecasting underestimation or overestimation of wind power forecasting output occurs. At last, a model of battery energy storage system with proposed two storage strategies of performance priority and lifetime priority was introduced.

The advantage of combining the Beta function to model the deviations of forecasting solar irradiance in the shaded area of forecasting data extracted from the free open-source ‘SOLCAST API Toolkit’ is that the deviation variables corresponding to its range changes in each time point of solar irradiance can be simulated conforming the characteristic of strong production in the middle of the day that forecasting deviations are larger in the middle than on the sides. Based on proposed model, by adjusting the setting parameters,  $H_s$ ,  $A_{upper}^s$ ,  $B_{lower}^s$ ,  $\alpha$  and  $\beta$ , the patterns of solar irradiance variations in different seasons and atmospheric conditions can be simulated.

The advantage of combining a white noise sequence with mathematic expectation mean value of zero as the correction values to add with base values generated by the Weibull method is that it can has minimal impact to the mean value of sample space. This method will affect the overall variance value of base data of sample space a lot but just a little effect on mean value of base data of sample space.

Another advantage of this continuous superposition method is that the generated correction deviation values are in line with the general characteristic of forecasting wind speed. For example, the forecasting of wind speed is relatively accurate at the beginning, but as the forecasting time increases, the forecasting deviation of wind speed will gradually become larger.

Overall, although the other existing commercial renewable power prediction methodologies and software can support the accuracy prediction results, they requires lots of historical data of each wind farms. However, for a region with insufficient historical data of wind speed of wind farms, its renewable power prediction results will become difficult. The proposed prediction method is not highly dependent on a large amount of historical data because this method prefer mainly simulating the trend and magnitude and cycle period of wind speed changes in time points.

At last, two storage strategies of performance priority and lifetime priority are also proposed to add in the BESS model to research its further impacts on the integration of renewable energy.

# Chapter 6 Case Study

## 6.1 Introduction

This section provides one selected case study of a China's province power generation system with 330-kV network to illustrate renewable-based UC problems and their results analyses. The models proposed in previous chapters are all coded into this case and based on the toolkit of MATLAB 2019a and MATPOWER.

The China province power network has been simplified into a 58 nodes test system by the advice of local dispatching operator, but because of data protection in China some of the data are not openly available, hence some of the system data are supplemented from those of IEEE standard test systems and some estimated data also added to the system. This simplified 58 nodes test system includes thermal generators, wind farms, solar farms, and hydro plants.

Because the hydropower plants in this case province affect the natural ecology of the upstream and downstream, and under China's unique planned economic system, the power generation scheduling of hydropower plants is strictly controlled and fixed, so the hydropower generation output in this case is simulated by using actual power output data of one day directly.

There is no large-scale battery energy storage system in this case province, but combined with further planning and the operator's proposal, three energy storage stations are added to this case. The storage stations in the overall model are proposed to locate in the areas near the RES units and in this case the assumed BESS is only designed to offset the deviations between predicted and actual power output of wind and solar farms.

Thus, this chapter is organized as follows. Section 6.2 will first give the description of proposed models and approaches used in the case study, such as the cost-based model of thermal units, simulation approaches of wind power output, and optimal solution method of the priority list. Secondly, a base system description will be introduced in sub-section 6.2.2. It describes the composition of the system and explains the parameters of the generator set. Section 6.3 provides the simulation results and further analysis respectively. The modelling data details of simplified 58 nodes test system of province power network supplemented from IEEE standard test systems are listed in Appendix (A).

## **6.2 Case Study Description**

### **6.2.1 Case Model Description**

The overall cost-based model of this case includes the UC cost-based problem of thermal units, integration cost-based problem of intermittent renewable energy sources, and schedule cost-based problem of battery energy storage system.

The model of the UC cost-based problem, discussed in sub-section 4.2.1 (Total Operation Cost Function), considers fuel cost, emission cost, startup and shut down cost. Emission cost includes carbon tax cost and nitrogen emission allowance cost. Besides, UC constraints are also included, discussed in sub-section 4.2.2 (System Constraints of Unit Commitment), which are power balance constraint, spinning reserve constraint, generator limit constraint, minimum up and down time constraint, and ramp rate constraint.

The model of renewable energy sources considers wind power costs and solar power costs. Wind power cost includes operation cost and penalty cost which are introduced in 5.3.4 (Modelling of Wind Power Cost). The penalty cost occurs when

the underestimation and overestimation of its availability at any time because of the uncertainty of the availability of wind energy. Unlike wind power cost, in this model, a fixed operation cost of solar power is applied and its related data is taken from [260].

The models of forecasting solar irradiance and wind speed are stochastically simulated based on the proposed novel methods discussed in sub-section 5.3.2 (A Novel Modelling Approach of Forecasting Wind Speed) and sub-section 5.2.2 (A Novel Modelling Approach of Forecasting Solar Irradiance) respectively.

Then the forecasting power generated by solar and wind farms are converted from forecasting solar irradiance and wind speed based on the models discussed in sub-section 5.2.1 (Modelling Approach of Photovoltaic Module) and sub-section 3.4.2 (Double Cubic Power Curve), respectively.

The model of BESS, discussed in sub-section 5.4.1 (Modelling Approach of Battery Energy Storage System Cost), considers the operation cost, storage capacity limit constraint, charging and discharging rate constraint, SOC limit, and charge and discharge efficiency.

The objective for the overall model is to determine the minimized cost schedule of thermal generating units while satisfying a set of system and unit constraints. At this optimization procedure, the renewable energy will be integrated as large as possible until the insufficient ramping rate of thermal power units or insufficient load capacity of transmission line occurs. The emission cost will be incorporated into operating costs to be considered together to achieve the final optimum total cost. And the BESS will minimize the power deviations between predicted and actual as much as possible.

The solution method of DP [103], is used to solve this case problem because the DP method can manage sub-problems in decomposition programs, maintain the solution feasibility, and so on, discussed in section 2.4 (Summary).

Priority list method [150-152] combining quadratic programming approach is selected to solve this province case problem due to its less computation time of a large-scale system and performance of the lowest cost result discussed in sub-section 4.4.5. The complete enumeration method [101, 102] is difficult to use because it causes the mathematical problem in this large-scale system problem and leads to an extremely long solution time requirement of several hours.

### **6.2.2 Base System Description**

This simulated case system includes a 58 nodes network system, 24 thermal units, 46 wind farms, 133 solar farms, 2 hydropower plants, and 3 BESS stations.

In this system, according to Figure 6.1, Page 169, wind and solar power farms are mainly concentrated in the north, hydropower plants are concentrated in the south, and the areas that mainly consume electricity are in the center.

#### **i) Power network**

A provincial power network of China has been simplified into a 58 nodes test system by the author. Because of data protection in China some of the data are not openly available, some of the system data are supplemented from those of IEEE standard test systems.

The final simplified network used in the case study includes 58 node buses with 98 transmission line branches. The one-line diagram of this network system is shown

in Figure 6.1. The modelling data details of simplified 58 nodes test system are listed in Appendix (A).

ii) Thermal power units

This case includes 24 thermal power units with approximately 23250 MW installed capacity totally. If all other thermal power units undergoing maintenance or upgrading are included, the total installed capacity will reach 33550 MW. The thermal unit characteristics and cost coefficients are listed in Table 6-1, Page 170.

iii) Wind farms

The total 46 wind farms are grouped into 8 large-scale wind power farms which are located at the bus 2 with 6 farms, bus 7 with 10 farms, bus 9 with 8 farms, bus 17 with 5 farms, bus 18 with 5 farms, bus 30 with 4 farms, bus 50 with 4 farms and bus 51 with 4 farms respectively.

A total of 24 wind farms located in bus 2, bus 7, and bus 9 are regarded as the North Wind Farms. A total of 10 wind farms located in bus 17 and bus 18 are regarded as Central Wind Farms. A total of 12 wind farms located in bus 30, bus 50, and bus 51 are regarded as Northwest Wind Farms.

The wind farms in these three regions use three different types of wind turbines and follow three different simulated correction reference values of wind speed, discussed in the paragraph of 'iv) correction reference values' in sub-section 5.3.2. And each farm owns its individual simulated correction deviation values of wind speed, discussed in the paragraph of 'v) correction deviation values' in sub-section 5.3.2. The total installed capacity of wind power is approximately 4055 MW. Further data details of wind farms are listed in Table 6-2, Page 171.

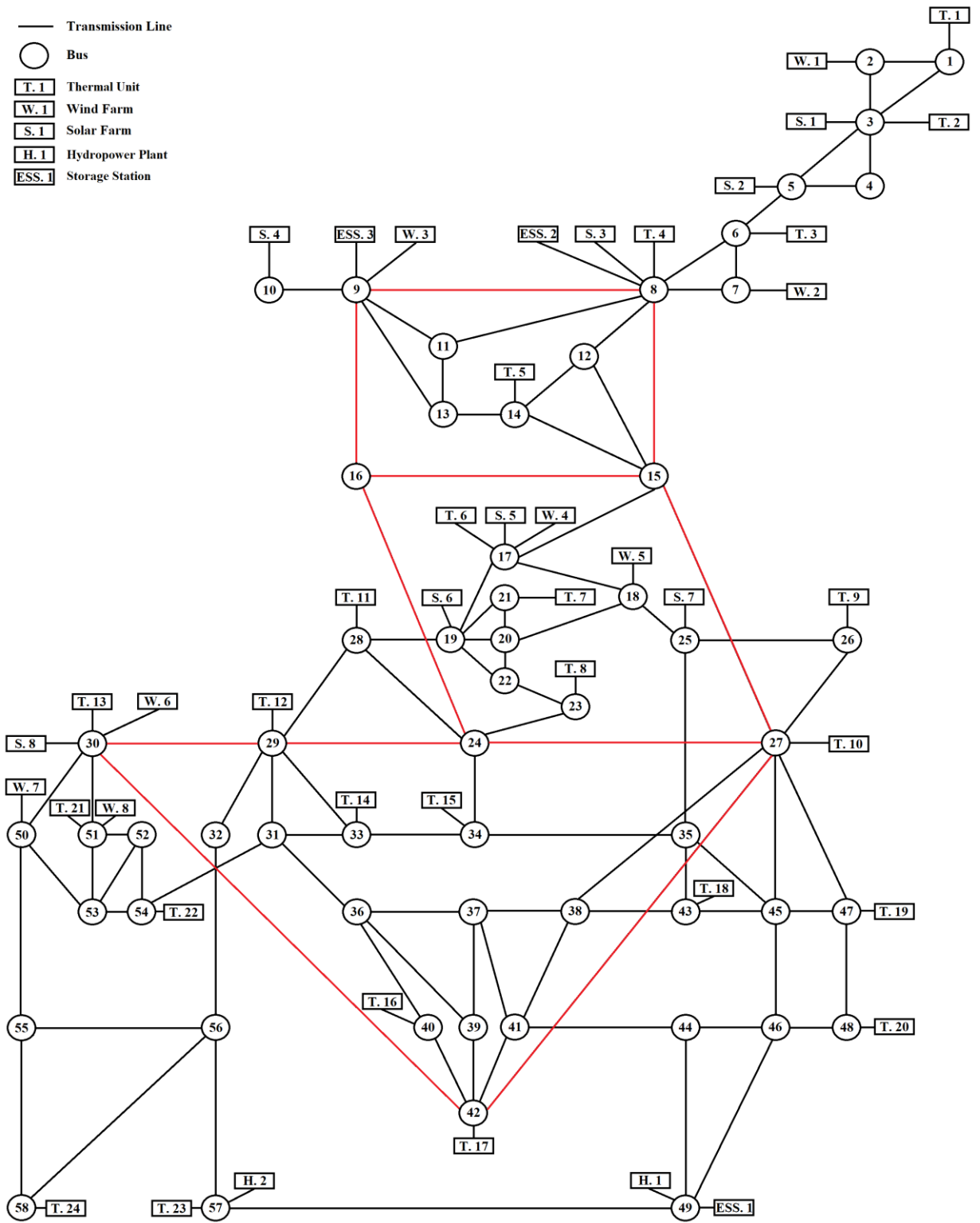


Figure 6.1 Modified One Line Diagram of 330-kV Network in Province Case

Table 6-1: Parameters of Thermal Units in Province Case Study

Unit	$P_{min}$	$P_{max}$	$U_{R.up}$	$U_{R.down}$	$T_{on}$	$T_{off}$	$C_{cold}$	$C_{hot}$	$C_{shut}$	$\tau_i$	$S_{Initial}^{time}$	$\alpha_i$	$b_i$	$c_i$	$fa_i$	$fb_i$	$fc_i$
	MW	MW	MW/h	MW/h	h	h	US\$	US\$	US\$	h	h	US\$	US\$/MW	US\$/MW <sup>2</sup>	t	t/MW	t/MW <sup>2</sup>
G1	300	600	150	210	6	6	1900	900	500	4	+8	2200	12	0.003	45	0.3	0.00005
G2	150	300	130	180	6	4	780	460	400	2	-8	2400	15	0.002	50	0.25	0.00004
G3	175	350	175	235	6	4	980	590	500	3	+5	2400	15	0.002	50	0.25	0.00004
G4	1600	3200	640	820	24	12	8800	4250	2000	8	+14	6000	11	0.0022	90	0.14	0.00003
G5	175	350	175	225	6	4	1000	400	500	3	+6	2000	10	0.002	45	0.3	0.00004
G6	150	300	150	200	6	4	900	500	500	2	+6	2200	12	0.003	45	0.3	0.00005
G7	175	300	140	190	6	4	900	420	500	3	-4	2200	12	0.003	45	0.3	0.00005
G8	675	1350	450	590	6	6	4780	2260	1200	6	+4	2400	15	0.002	50	0.25	0.00004
G9	1000	2000	500	650	24	10	7200	3230	1400	7	+10	2500	15	0.003	50	0.3	0.00005
G10	750	1500	480	630	8	8	4900	2640	1300	5	+6	2500	13	0.0025	44	0.25	0.00005
G11	800	1600	520	655	24	8	5800	2950	1700	6	+10	6000	11	0.0022	90	0.14	0.00003
G12	650	1300	430	570	8	6	4700	2540	1200	4	+6	6000	10	0.0018	80	0.12	0.00003
G13	800	1600	440	580	12	8	5200	2630	900	5	+12	5800	9	0.002	75	0.15	0.00025
G14	300	600	200	275	6	6	1300	640	600	3	-8	2200	12	0.003	45	0.3	0.00005
G15	750	1500	410	550	6	8	3200	1720	1300	5	+8	2000	10	0.002	90	0.14	0.00003
G16	300	600	210	285	6	6	1200	550	600	3	+8	6000	11	0.0022	90	0.14	0.00003
G17	600	1200	400	540	8	8	4780	2460	1100	4	+6	2000	10	0.002	50	0.25	0.00004
G18	350	700	240	320	6	6	2300	1530	700	3	+6	2000	10	0.0025	40	0.2	0.00004
G19	500	1000	310	410	6	6	3280	1560	900	4	+8	2400	15	0.002	50	0.25	0.00004

Unit	$P_{min}$	$P_{max}$	$U_{R.up}$	$U_{R.down}$	$T_{on}$	$T_{off}$	$C_{cold}$	$C_{hot}$	$C_{shut}$	$\tau_i$	$S_{Initial}^{time}$	$\alpha_i$	$b_i$	$c_i$	$fa_i$	$fb_i$	$fc_i$
	MW	MW	MW/h	MW/h	h	h	US\$	US\$	US\$	h	h	US\$	US\$/MW	US\$/MW <sup>2</sup>	t	t/MW	t/MW <sup>2</sup>
G20	450	900	300	395	8	6	3100	1400	800	4	+6	2400	15	0.002	50	0.25	0.00004
G21	375	650	220	300	6	6	2200	1730	600	4	+2	6000	11	0.0022	45	0.3	0.00005
G22	250	500	240	325	6	4	2000	1100	600	3	+4	2200	12	0.003	45	0.3	0.00005
G23	250	500	250	335	6	6	2100	1370	800	3	+4	2400	15	0.002	44	0.25	0.00005
G24	175	350	180	240	6	4	880	460	500	3	-6	2400	15	0.002	50	0.25	0.00004

Table 6-2: Parameters of Wind Farms in Province Case Study

Classify	Farms	Turbines	$k$	$c$	$\rho_{air}$	$D_{rotor}$	$z$	$h_{hub}$	$P_r$	$C_p$
					kg/m <sup>3</sup>	m		m	MW	
North	24	1080	4.5	1.89	1.106	82	0.1	90	2.3	0.45
Central	10	350	3.75	1.59	1.109	71	0.1	80	2	0.43
Northwest	12	396	4.3	1.71	1.116	82	0.1	90	2.2	0.45
Classify	$v_{ci}$	$v_r$	$v_{co}$	$k_{op}$	$k_{ue}$	$k_{oe}$	$A_{up-lim-dev}^w$	$A_{down-lim-dev}^w$	$A_{up-lim-ref}^w$	$A_{down-lim-ref}^w$
	m/s	m/s	m/s	US\$/MWh	US\$/MWh	US\$/MWh	m/s per 15 minutes			
North	3	8.8	19	8	3	10	0.5	0.5	1.1	1.1
Central	2.5	9.5	22	8	3	10	0.45	0.45	1	1
Northwest	3	8.6	19	8	3	10	0.4	0.4	0.9	0.9

#### iv) Solar farms

The total 133 solar farms are grouped into 8 large-scale solar power farms which are located at the bus 1 with 15 farms, bus 3 with 35 farms, bus 6 with 13 farms, bus 8 with 23 farms, bus 14 with 6 farms, bus 17 with 20 farms, bus 21 with 12 farms and bus 30 with 9 farms respectively.

A total of 86 solar farms in bus 1, bus 3, bus 6, and bus 8 are regarded as the North Solar Farms. A total of 38 solar farms in bus 14, bus 17, and bus 21 are regarded as Central Solar Farms. A total of 9 solar farms in bus 30 is regarded as Northwest Solar Farm.

The solar farms in these three regions use three different types of solar modules and follow three different solar irradiance references shown in Figure 6.2. And each solar farm owns its individual data of simulated forecasting solar irradiance generated based on the forecasting data result of free open-source 'SOLCAST API Toolkit' [21], discussed in sub-section 5.2.2 (A Novel Modelling Approach of Forecasting Solar Irradiance).

The total installed capacity of solar power is approximately 6594 MW. For analysis in the case study, this level can be achieved by using 160000 PV panels with each consisting of 6 modules in each solar farm to simulate. Further data details of solar farms and modules are listed in Table 6-3, Page 174.

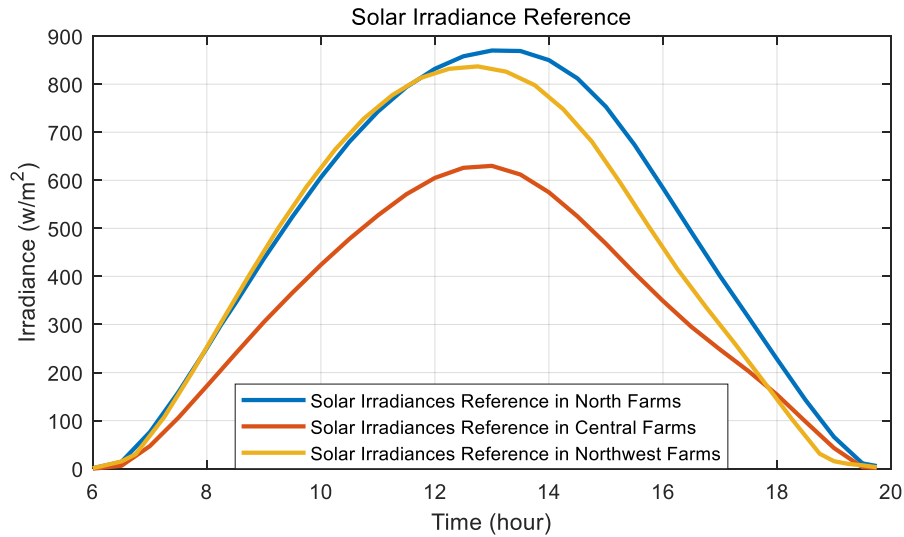


*Figure 6.2: Solar Irradiance Reference in Province Case Study*

v) BESS station

The three BESS stations are located in bus 49, bus 8, and bus 9 respectively. The relevant parameters of these BESS stations are listed in Table 6-4, page 174.

Generally, wind farm operators forecast wind power for the next hour. When the forecasting value is smaller than the actual power output, regarded as underestimation, the excess energy will be charged into BESS station. If the actual value is less than the forecasting value, regarded as overestimation, energy from the BESS station will discharge to support the system load demand.

So, the simulation of the overall model requires the actual data of solar and wind power output in the operation day, which will be listed in Table 6-8, page 179.

Table 6-3: Parameters of Solar Farms in Province Case Study

Classify	Farms	$H_s$	$\alpha$	$\beta$	$I_{sc}$	$V_{oc}$	$I_{MPP}$	$V_{MPP}$	$K_v$	$K_i$	$N_{OT}$	$A_{up-lim-dev}^s$	$B_{down-lim-dev}^s$	$\pi_{solar}$
					$A$	$V$	$A$	$V$	$mV/^\circ C$	$mA/^\circ C$	$^\circ C$	$W/m^2$ per 15 minutes		$US\$/MWh$
North	86	0.96	3.4	3.6	1.8	55.5	1.32	38	194	1.4	44	120	840	18
Central	38	0.93	3.5	3.4	3.4	21.7	3.05	17.4	88	1.5	43	110	730	20
Northwest	9	0.95	3.6	3.5	3.8	21.1	3.5	17.1	75	3.1	44	92	816	22

Table 6-4: Parameters of BESS Stations in Province Case Study

Classify	Location	Strategy	$P_{BESS}^{Max}$	$P_{BESS}^{Min}$	$C_{ini,i,t}^{BESS}$	$SOC_{Limit}^{lower}$	$SOC_{Limit}^{upper}$	$P_{Rate}^{charge}$	$P_{Rate}^{discharge}$	$\eta_{Efficiency}^{charge}$	$\eta_{Efficiency}^{discharge}$	$\pi_{BESS}$
	Bus	Priority	$MW$	$MW$	$MW$			$MW/h$	$MW/h$			$US\$/MWh$
BESS 1	49	Performance	500	0	100	30%	75%	120	140	0.80	0.81	96
BESS 2	8	Lifetime	200	0	70	20%	80%	60	60	0.83	0.84	108
BESS 2	9	Lifetime	100	0	30	20%	80%	40	40	0.84	0.85	112

vi) Hydropower plant

As mentioned in section 6.1 the hydropower plants in this province affect the natural ecology of the upstream and downstream, and under China's unique planned economic system, the power generation scheduling of hydropower plants is strictly controlled and fixed, so the hydropower generation output in this case is simulated by using forecasting power output data of one day directly, which is shown in Figure 6.3, page 175.

Hydro plant 1 is located in bus 49 and Hydro plant 2 is located in bus 50. Their hourly coefficient of hydro system cost,  $\pi_{hydro}$ , are set as 16 US\$/MWh and 24 US\$/MWh respectively. Exact data can be found in Table 6-5, page 176.

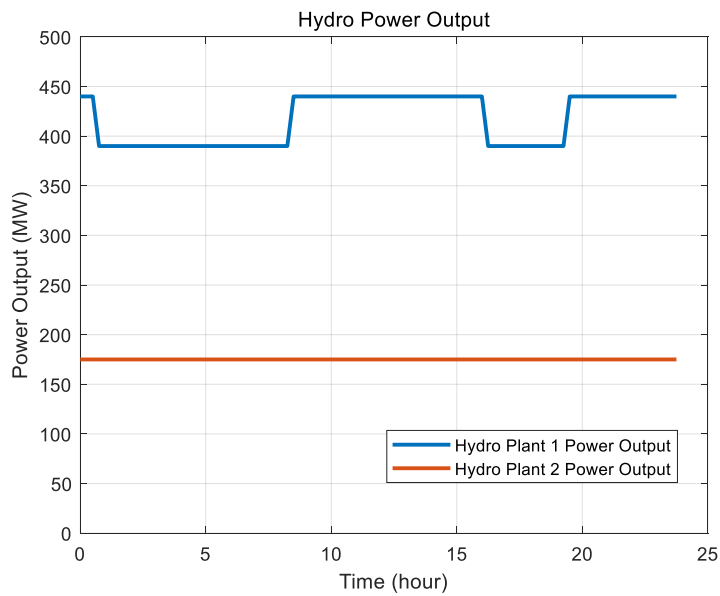


Figure 6.3: Hydro Power in Province Case Study

*Table 6-5: Forecasting Hydro Power Output in Province Case Study*

Time Point	1	2	3	4	5	6	7	8	9	10	11	12	13	14	15	16	17	18	19	20	21	22	23	24
Hydro 1	440	440	440	390	390	390	390	390	390	390	390	390	390	390	390	390	390	390	390	390	390	390	390	390
Hydro 2	175	175	175	175	175	175	175	175	175	175	175	175	175	175	175	175	175	175	175	175	175	175	175	175
Time Point	25	26	27	28	29	30	31	32	33	34	35	36	37	38	39	40	41	42	43	44	45	46	47	48
Hydro 1	390	390	390	390	390	390	390	390	390	390	440	440	440	440	440	440	440	440	440	440	440	440	440	440
Hydro 2	175	175	175	175	175	175	175	175	175	175	175	175	175	175	175	175	175	175	175	175	175	175	175	175
Time Point	49	50	51	52	53	54	55	56	57	58	59	60	61	62	63	64	65	66	67	68	69	70	71	72
Hydro 1	440	440	440	440	440	440	440	440	440	440	440	440	440	440	440	440	440	390	390	390	390	390	390	390
Hydro 2	175	175	175	175	175	175	175	175	175	175	175	175	175	175	175	175	175	175	175	175	175	175	175	175
Time Point	73	74	75	76	77	78	79	80	81	82	83	84	85	86	87	88	89	90	91	92	93	94	95	96
Hydro 1	390	390	390	390	390	390	440	440	440	440	440	440	440	440	440	440	440	440	440	440	440	440	440	440
Hydro 2	175	175	175	175	175	175	175	175	175	175	175	175	175	175	175	175	175	175	175	175	175	175	175	175

*Table 6-6: Forecasting Load Power Demand in Province Case Study*

Time Point	1	2	3	4	5	6	7	8	9	10	11	12	13	14	15	16	17	18	19	20	21	22	23	24
Actual Demand	14842	14728	14727	14630	14425	14363	14268	14319	14191	14149	14131	13991	13785	13728	13712	13716	13761	13773	13716	13843	14014	14093	14517	14853
Time Point	25	26	27	28	29	30	31	32	33	34	35	36	37	38	39	40	41	42	43	44	45	46	47	48
Actual Demand	15369	15605	15731	15677	15568	15544	15426	15647	15943	16189	16357	16271	16385	16445	16494	16574	16731	16841	17086	17150	17246	17369	17272	17073
Time Point	49	50	51	52	53	54	55	56	57	58	59	60	61	62	63	64	65	66	67	68	69	70	71	72
Actual Demand	16935	16690	16407	16453	16568	16548	16653	16824	16950	17014	17269	17284	17450	17340	17446	17568	17776	18110	18366	18497	18633	18621	18307	18053
Time Point	73	74	75	76	77	78	79	80	81	82	83	84	85	86	87	88	89	90	91	92	93	94	95	96
Actual Demand	17741	17512	17213	17135	17104	17197	17472	17903	18298	18403	18385	18150	18030	17772	17453	16824	16546	16225	15655	15315	15319	15294	15172	15074

vii) other data

In order to finish the simulation of power dispatch day-ahead of the simplified system of case study, some actual and forecasting data are still needed, such as forecasting demand, forecasting temperature, actual solar and wind power output in operation day. They are shown in Figure 6.4 (a), Figure 6.4 (b) and Figure 6.5 respectively. And their exact data are given in Table 6-6, Table 6-7, and Table 6-8 respectively.

The forecasting load demand of each bus  $i$ ,  $LD_t^{bus-i}$ , at time point,  $t$ , can be calculated through the data of forecasting load power demand of Table 6-6,  $FLD_t$ , and ratio of total power demand,  $Ratio_i$  based on equation (6-1):

$$LD_t^{bus-i} = FLD_t * \frac{Ratio_i}{25770} \quad (6-1)$$

The ratio of total power demand to each bus is listed in ‘ii) Bus data’ of Appendix (A).

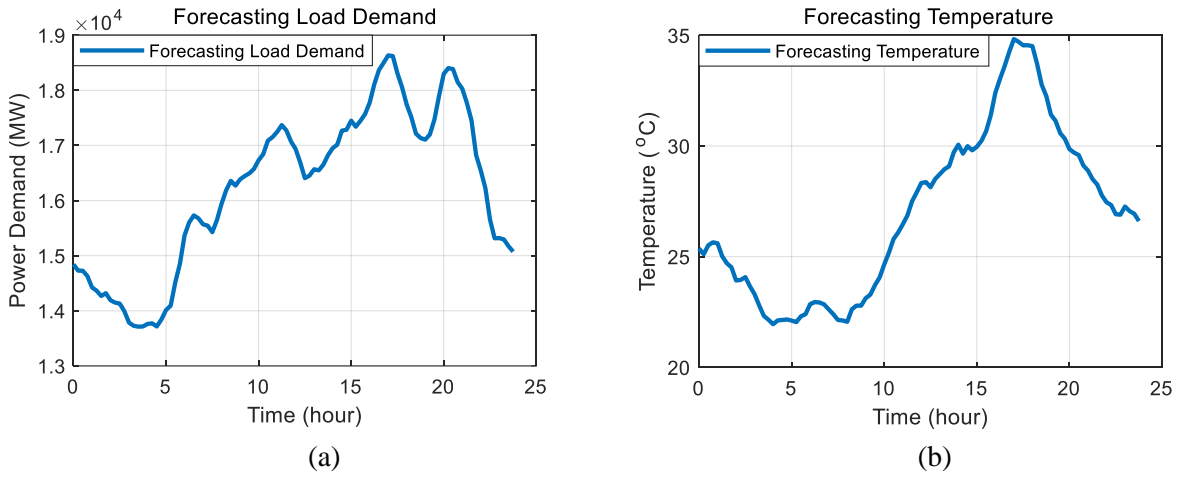


*Figure 6.4: Forecasting Load Demand and Temperature in Province Case Study*

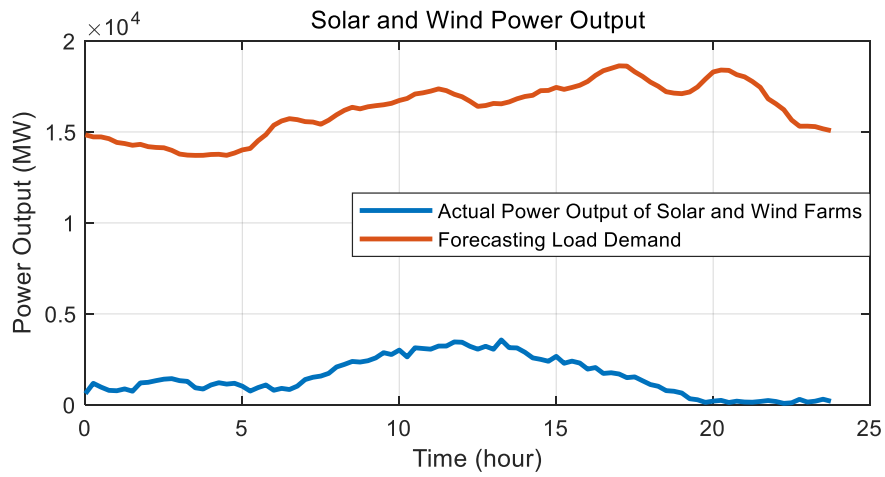


*Figure 6.5: Actual Power Output of Solar and Wind Farms in Province Case Study*

*Table 6-7: Forecasting Temperature in Province Case Study*

Time Point	1	2	3	4	5	6	7	8	9	10	11	12	13	14	15	16	17	18	19	20	21	22	23	24
Actual Temperature	25.4	25.1	25.5	25.6	25.6	25.0	24.7	24.5	23.9	24.0	24.1	23.7	23.3	22.8	22.3	22.1	21.9	22.1	22.1	22.2	22.1	22.0	22.3	22.4
Time Point	25	26	27	28	29	30	31	32	33	34	35	36	37	38	39	40	41	42	43	44	45	46	47	48
Actual Temperature	22.9	22.9	22.9	22.8	22.6	22.4	22.1	22.1	22.1	22.6	22.8	22.8	23.1	23.3	23.7	24.1	24.7	25.2	25.8	26.1	26.5	26.9	27.5	27.9
Time Point	49	50	51	52	53	54	55	56	57	58	59	60	61	62	63	64	65	66	67	68	69	70	71	72
Actual Temperature	28.3	28.4	28.1	28.5	28.7	29.0	29.1	29.7	30.1	29.7	30.0	29.8	30.0	30.2	30.7	31.4	32.4	33.0	33.6	34.3	34.8	34.7	34.5	34.6
Time Point	73	74	75	76	77	78	79	80	81	82	83	84	85	86	87	88	89	90	91	92	93	94	95	96
Actual Temperature	34.5	33.7	32.8	32.3	31.4	31.1	30.6	30.3	29.9	29.7	29.6	29.1	28.9	28.5	28.3	27.8	27.5	27.3	26.9	26.9	27.3	27.1	26.9	26.6

*Table 6-8: Actual and Forecasting Power Output of Solar and Wind Farms in Province Case Study*

Time Point	1	2	3	4	5	6	7	8	9	10	11	12	13	14	15	16	17	18	19	20	21	22	23	24
Actual Power Output of Solar and Wind Farms	616	1183	972	795	775	876	749	1206	1238	1330	1411	1441	1329	1290	938	870	1092	1215	1141	1184	1024	758	948	1092
Forecasting Power Output of Solar and Wind Farms	591	1238	1052	781	755	728	687	1008	1146	1356	1564	1458	1345	1461	1076	970	1097	1170	1059	1096	996	685	1027	973
Time Point	25	26	27	28	29	30	31	32	33	34	35	36	37	38	39	40	41	42	43	44	45	46	47	48
Actual Power Output of Solar and Wind Farms	801	905	842	1029	1391	1516	1582	1730	2081	2223	2385	2352	2424	2581	2867	2766	3011	2635	3135	3096	3060	3230	3232	3458
Forecasting Power Output of Solar and Wind Farms	654	866	773	835	1510	1572	1516	1522	2215	2246	2475	2448	2322	2694	2782	2862	3317	2899	3076	3169	3233	3701	3639	3532
Time Point	49	50	51	52	53	54	55	56	57	58	59	60	61	62	63	64	65	66	67	68	69	70	71	72
Actual Power Output of Solar and Wind Farms	3441	3217	3060	3220	3057	3566	3142	3129	2892	2582	2501	2395	2666	2285	2402	2298	1964	2050	1726	1763	1696	1495	1536	1323
Forecasting Power Output of Solar and Wind Farms	3446	3461	3337	3340	3268	3494	3410	3222	3103	3042	2863	2710	2681	2546	2516	2271	2058	1972	1775	1652	1533	1350	1366	1188
Time Point	73	74	75	76	77	78	79	80	81	82	83	84	85	86	87	88	89	90	91	92	93	94	95	96
Actual Power Output of Solar and Wind Farms	1115	1020	782	746	649	337	280	136	204	246	129	202	155	145	186	237	183	80	113	302	152	201	308	196
Forecasting Power Output of Solar and Wind Farms	1024	842	578	656	559	324	279	114	218	82	83	109	59	42	67	99	43	38	63	69	54	85	81	151

### 6.3 Case Study Results and Analysis

Figure 6.6 (a) shows the actual and stochastic simulation forecasting results of solar and wind power output compared with the forecasting load demand. And Figure 6.6 (b) shows relative actual penetration which is the ratio of the amount of power delivered to the grid from solar generation and wind generation to the total amount of power delivered to the grid from all sources during a given period.

The exact simulation result of total forecasting power output of solar and wind farms is listed in Table 6-8, page 179.

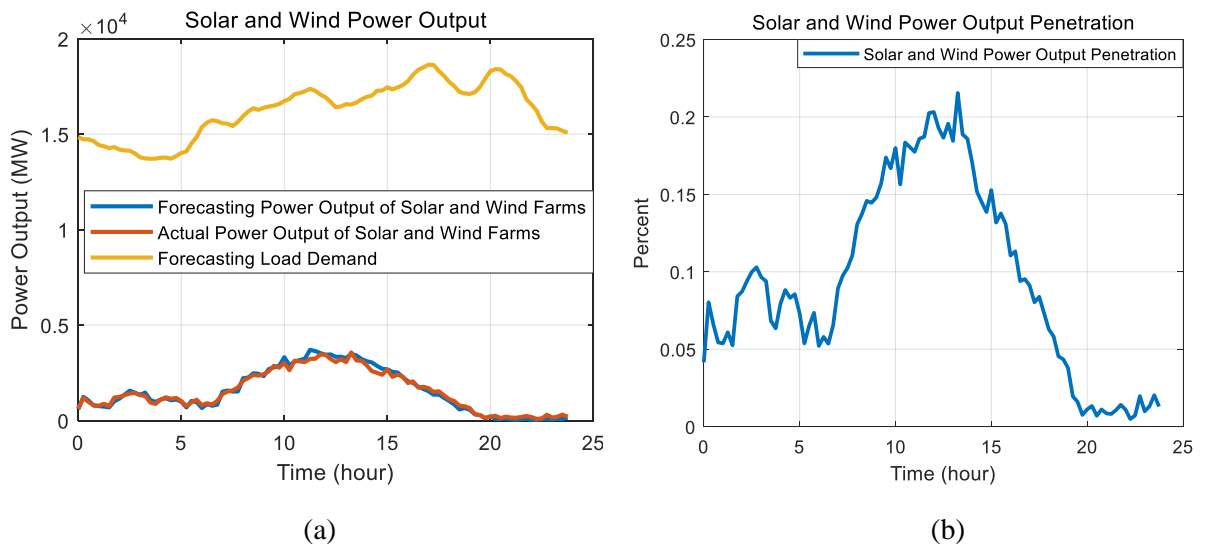


*Figure 6.6: Forecasting Power Output of Solar and Wind Farms in Province Case Study*

It can be seen that with the commitment of solar system, the penetration rate of renewable energy has a stage of rapid rise. Another stage of rapid decline occurs before the sun is about to set. These two stages of rapid change of penetration rate have a higher demand for the ramping ability of thermal power units.

### 6.3.1 Simulation Results

Due to the excessive amount of results data, a lot of these data are translated into charts only for analysis. Details of solution results of power output of 24 thermal units, 133 solar farms, and 46 wind farms at each time point are listed in Appendix (B).

Note that these solar farms and wind farms have been classified into 8 larger solar and wind farms that are located on different network node buses, discussed in sub-section 6.2.2 (Base System Description).

In this case study, the overall solution results of output and cost of all generators after spatial optimum day-ahead power dispatch are shown in Table 6-9. The power generation situation of all the thermal plants at each given time can be found in Figure 6.7 and Figure 6.8.

Table 6-9 shows four cases' cost results. In Case A, the model includes all renewable energy sources and considers the emission cost of thermal units. Case C is the same but represents results without considering the emission cost model. In Case B, all load demands rely only on thermal generation plants, and emission costs are also considered. But, in the Case D, only thermal plants are still committed to satisfy all load demands without considering the emission cost model.

Solar and wind and farms output in province Case A can be found in Figure 6.9 and Figure 6.10 respectively. The BESS operation situation is illustrated in Figure 6.15. Loading rates of all transmission lines are shown in Figure 6.11 and the mentioned lines with high load rates are highlighted. Figure 6.12 illustrates wind power costs based on the method of underestimation and overestimation.

Further analysis of results is discussed in next sub-section 6.3.2 (Discussion of Cases A, B, C and D Results).

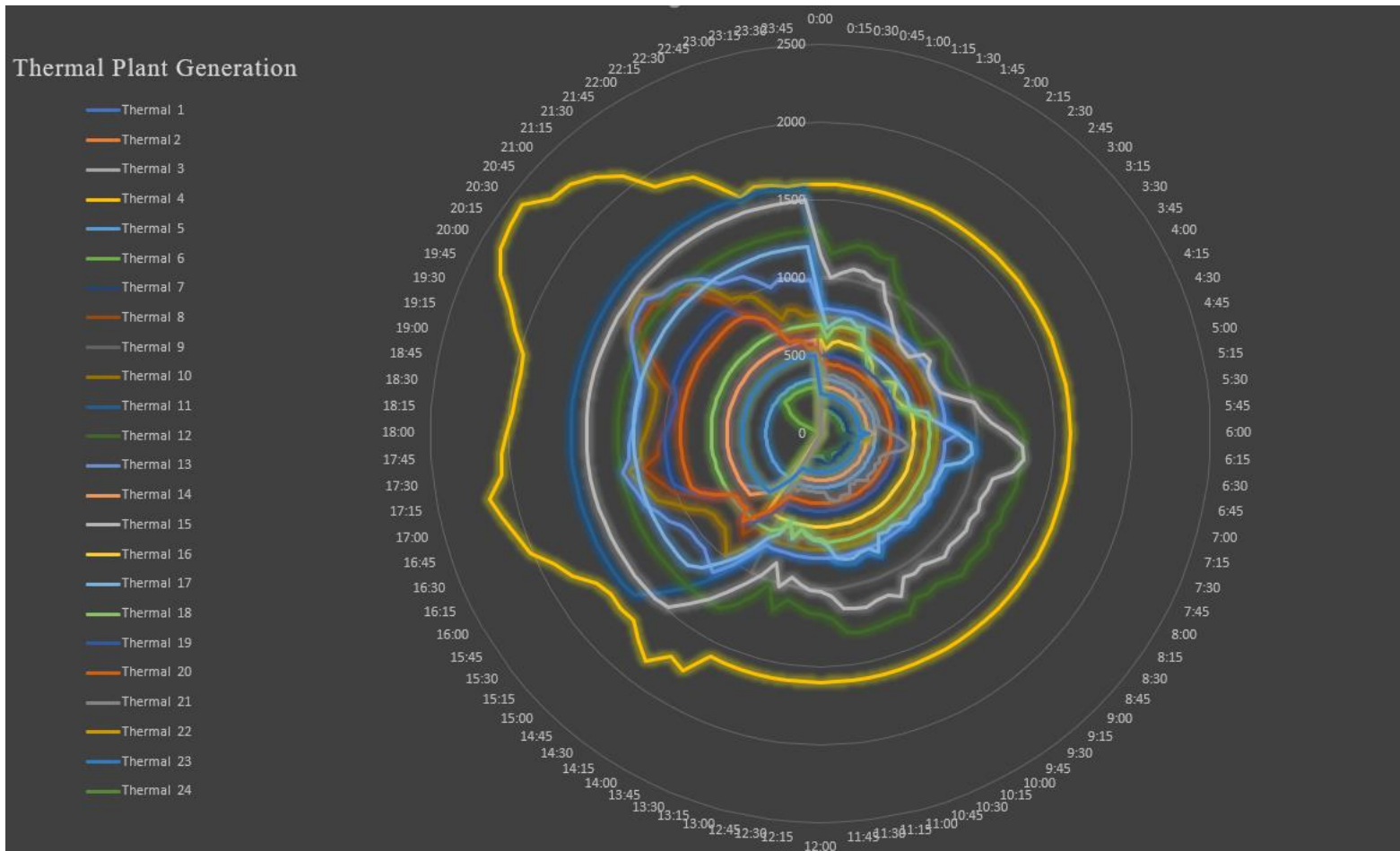


Figure 6.7: Thermal Generation Output in Province Case A (Radar Chart)

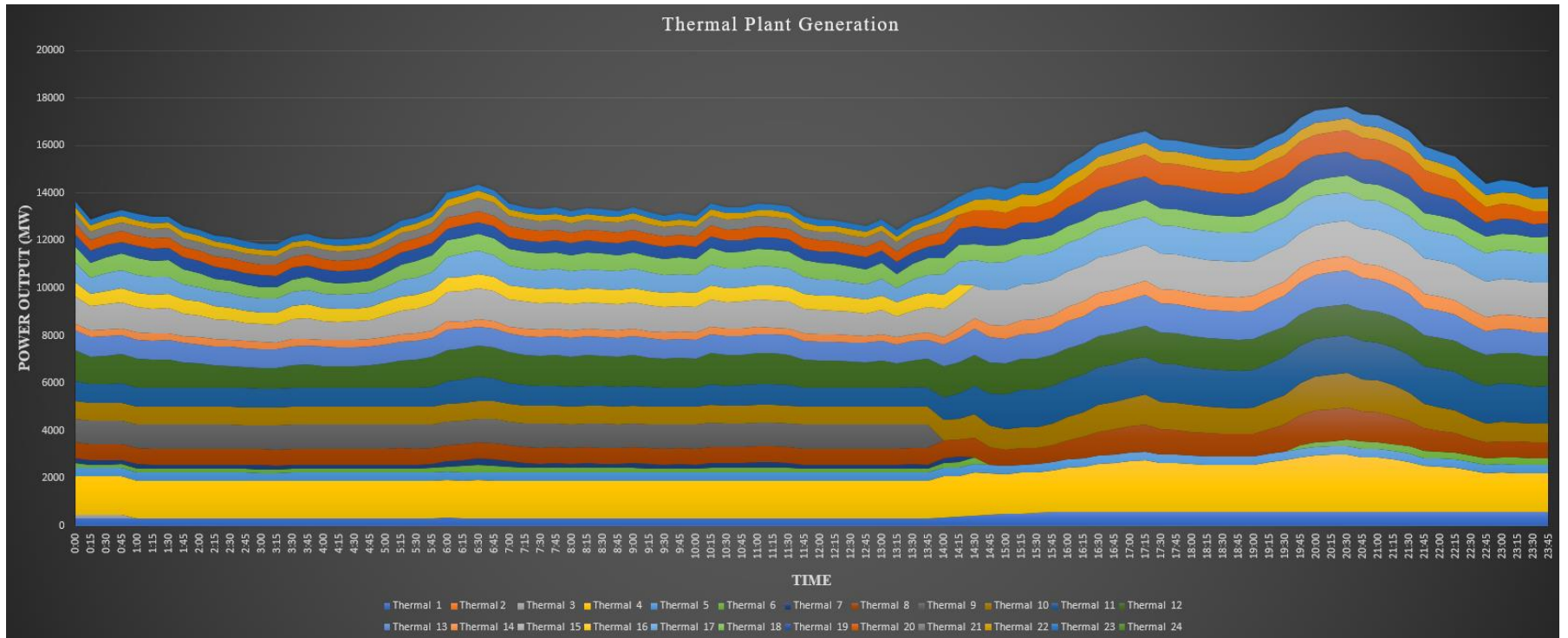
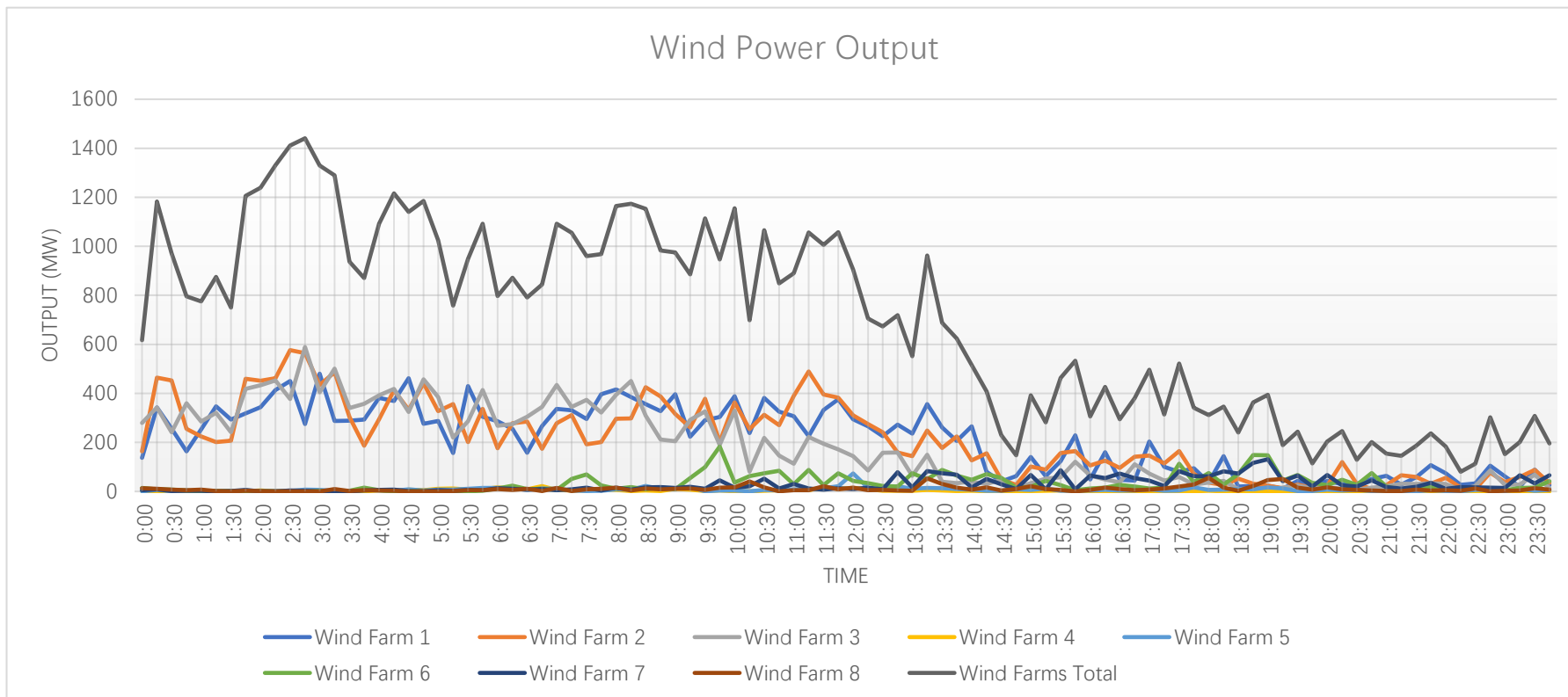


Figure 6.8: Thermal Generation Output in Province Case A (Area Chart)



*Figure 6.9: Wind Farms Output in Province Case A (Area Chart)*

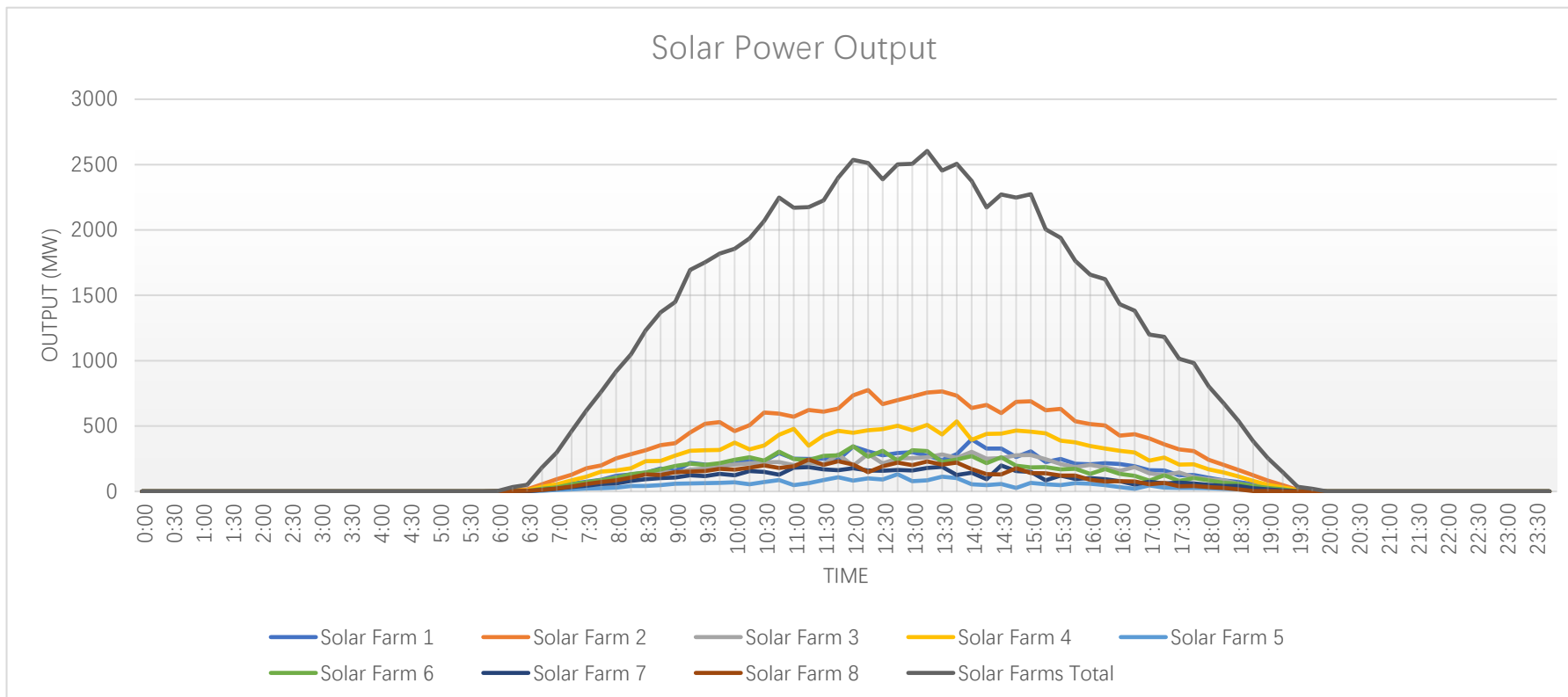


Figure 6.10: Solar Farms Output in Province Case A (Area Chart)

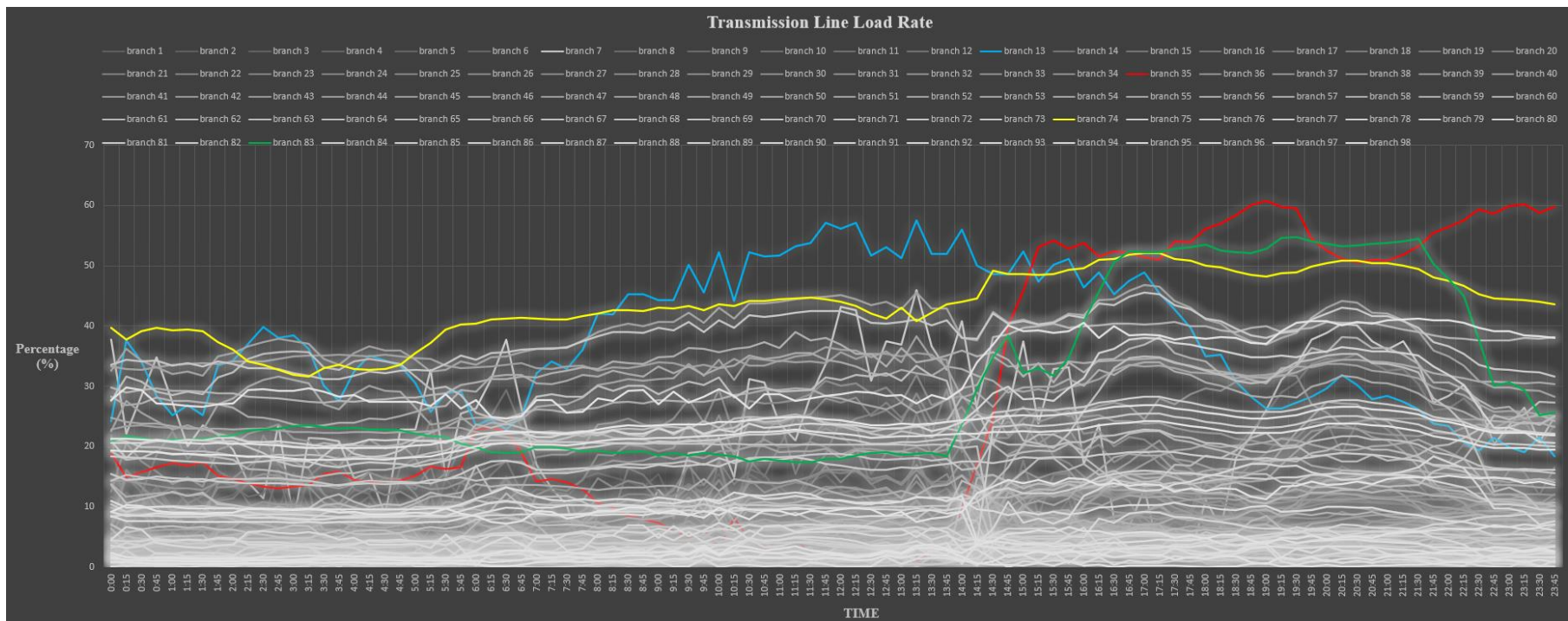


Figure 6.11: Transmission Line Load Rate in Province Case A

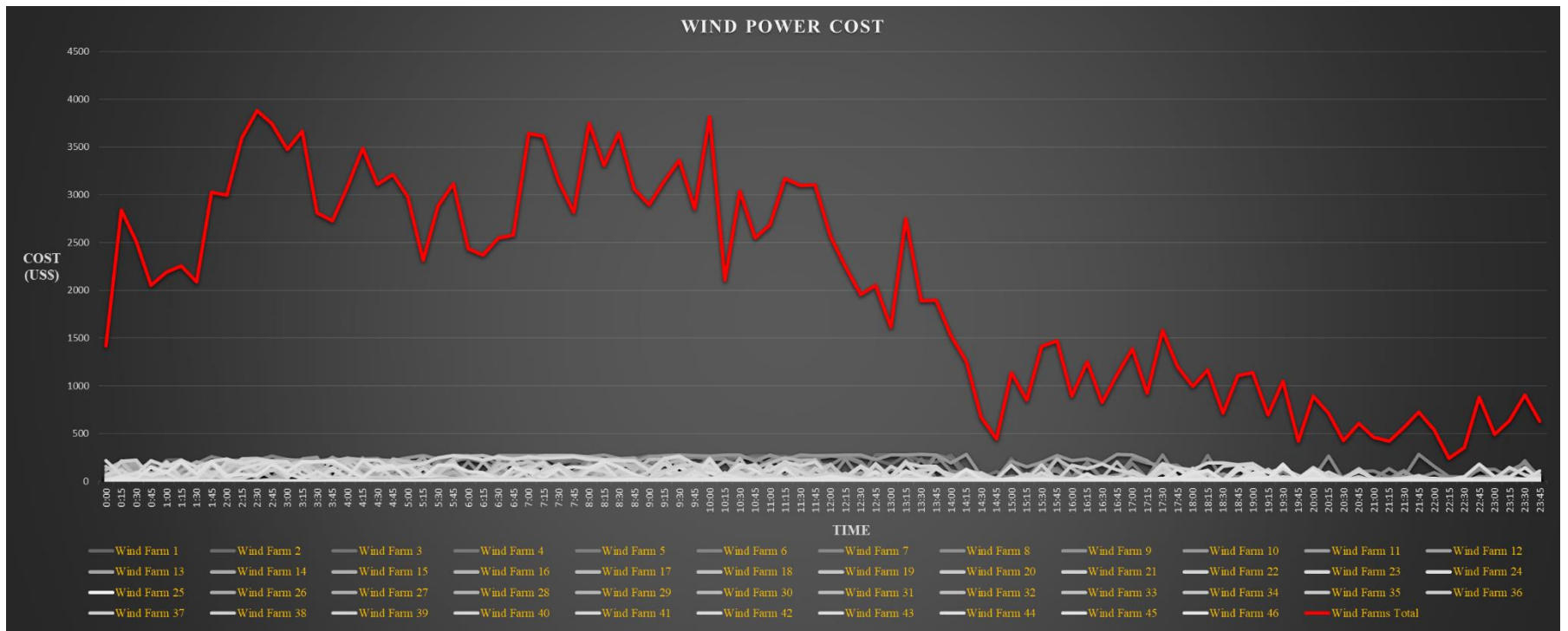


Figure 6.12: Wind Power Cost in Province Case A

Table 6-9: Solution Results of Output and Cost of All Generators in Province Case Study

Index	Case A		Case B		Case C		Case D	
output (MW) and cost (US\$)	Renewable and Emission Cost		No Renewable but with Emission Cost		Renewable and without Emission Cost		No Renewable and without Emission Cost	
	Average Output	Total Cost	Average Output	Total Cost	Average Output	Total Cost	Average Output	Total Cost
G1	415	238117	514	283202	409	183769	539	229496
G2	0	0	0	0	0	0	0	0
G3	7	6738	7	6738	7	5586	7	5586
G4	1745	892441	1690	861681	1608	705072	1631	715131
G5	349	182646	350	182959	350	137880	350	137880
G6	157	115861	275	172339	247	124958	281	137075
G7	114	85904	272	171481	247	126182	278	136640
G8	787	451865	726	418259	690	328919	736	348963
G9	583	356304	906	552769	896	442150	906	447275
G10	883	473486	841	450068	797	347382	898	390033
G11	1127	600251	1394	719036	996	464149	1291	578334
G12	1220	580965	1300	612443	1110	464744	1269	518305
G13	956	524594	973	530010	1308	506233	1526	581440
G14	418	241467	516	285582	410	186023	540	231751
G15	1215	502800	1442	597431	1104	375294	1377	471136
G16	354	224204	556	348431	22	13078	25	13992
G17	917	402961	1133	494406	1009	340218	1165	392906
G18	670	291809	700	303487	687	241109	700	245400

Index	Case A		Case B		Case C		Case D	
output (MW) and cost (US\$)	Renewable and Emission Cost		No Renewable but with Emission Cost		Renewable and without Emission Cost		No Renewable and without Emission Cost	
	Average Output	Total Cost	Average Output	Total Cost	Average Output	Total Cost	Average Output	Total Cost
G19	647	379642	631	370508	540	266581	645	311247
G20	597	353796	607	358588	501	250731	620	300767
G21	239	184502	569	368448	544	292278	596	310349
G22	352	210043	444	250557	361	167135	468	203653
G23	351	230874	375	239253	260	150298	373	196184
G24	0	0	0	0	0	0	0	0
<b><i>Thermal Total</i></b>	<b><u>14104</u></b>	<b><u>7531269</u></b>	<b><u>16221</u></b>	<b><u>8577674</u></b>	<b><u>14104</u></b>	<b><u>6119766</u></b>	<b><u>16221</u></b>	<b><u>6903543</u></b>
W1	211	51826	0	0	211	51826	0	0
W2	214	66838	0	0	214	66838	0	0
W3	184	49085	0	0	184	49085	0	0
W4	3	992	0	0	3	992	0	0
W5	7	2121	0	0	7	2121	0	0
W6	32	8445	0	0	32	8445	0	0
W7	27	9392	0	0	27	9392	0	0
W8	10	5209	0	0	10	5209	0	0
<b><i>Wind Total</i></b>	<b><u>689</u></b>	<b><u>193907</u></b>	<b><u>0</u></b>	<b><u>0</u></b>	<b><u>689</u></b>	<b><u>193907</u></b>	<b><u>0</u></b>	<b><u>0</u></b>
S1	104	45017	0	0	104	45017	0	0
S2	244	105489	0	0	244	105489	0	0

Index	Case A		Case B		Case C		Case D	
output (MW) and cost (US\$)	Renewable and Emission Cost		No Renewable but with Emission Cost		Renewable and without Emission Cost		No Renewable and without Emission Cost	
	Average Output	Total Cost	Average Output	Total Cost	Average Output	Total Cost	Average Output	Total Cost
S3	92	39681	0	0	92	39681	0	0
S4	164	70808	0	0	164	70808	0	0
S5	28	13330	0	0	28	13330	0	0
S6	92	44369	0	0	92	44369	0	0
S7	56	26924	0	0	56	26924	0	0
S8	65	34385	0	0	65	34385	0	0
<b><u>SOLAR</u></b> <b><u>Total</u></b>	<b><u>846</u></b>	<b><u>380004</u></b>	<b><u>0</u></b>	<b><u>0</u></b>	<b><u>846</u></b>	<b><u>380004</u></b>	<b><u>0</u></b>	<b><u>0</u></b>
H1	417	160160	0	0	417	160160	0	0
H2	175	100800	0	0	175	100800	0	0
<b><u>Hydro</u></b> <b><u>Total</u></b>	<b><u>592</u></b>	<b><u>260960</u></b>	<b><u>0</u></b>	<b><u>0</u></b>	<b><u>592</u></b>	<b><u>260960</u></b>	<b><u>0</u></b>	<b><u>0</u></b>
B1	-7	44587	0	0	-7	44587	0	0
B2	-2	11209	0	0	-2	11209	0	0
B3	-1	5666	0	0	-1	5666	0	0
<b><u>BESS</u></b> <b><u>Total</u></b>	<b><u>-9</u></b>	<b><u>61462</u></b>	<b><u>0</u></b>	<b><u>0</u></b>	<b><u>-9</u></b>	<b><u>61462</u></b>	<b><u>0</u></b>	<b><u>0</u></b>
<b><u>All</u></b> <b><u>TOTAL</u></b>	<b><u>16221</u></b>	<b><u>8427603</u></b>	<b><u>16221</u></b>	<b><u>8577674</u></b>	<b><u>16221</u></b>	<b><u>7016099</u></b>	<b><u>16221</u></b>	<b><u>6903543</u></b>

### **6.3.2 Discussion of Cases A, B, C and D Results**

All the solution results are calculated by modified Dynamic Programming based on selected Priority list method combining quadratic programming approach to solve this province case problem. It is selected due to its less computation time of a large-scale system and performance of the lowest cost result discussed in sub-section 4.4.5.

The simulation results in Table 6-9 show the cost impacts investigation of renewable power model and emission cost model on the operation of the thermal generation system.

In Case A, the total generation cost to meet forecasting load demand for a whole day is US\$8427603, whereas the emission cost is US\$1365120 shown in Table 6-10. In Case B, the total generation cost for a whole day is US\$8577674 and its related emission cost is US\$1562449. It can be seen that considering the cost of renewable energy power generation, the integration of renewable energy sources into the grid saves US\$150071 in expenses for the system.

In addition, at the same time emissions reduction of 51,431 tons of CO<sub>2</sub> and 21 tons of NO<sub>2</sub> were recorded for a whole day. Although the strategy of adding emissions cost consideration will put more economic pressure on companies, it will make a huge contribution to environmental protection. This also fits the emission policy of ‘carbon reduction’.

Under the optimization algorithm, the integration of renewable energy and emission costs modes reduces the utilization rate of high-consumption and high-emission thermal power units, which not only reduces the pollution emissions, but also reduces the operation costs.

Compared with Case A and Case C, it can be found that without paying the emission cost, the generation cost for a whole day is US\$7016099. And if the emission cost needs to be paid, the total cost will be US\$8455689, which is US\$28086 higher than the cost in Case A of US\$8427603. Therefore, this strategy of emission cost in Case A has contributed to the release of a total of US\$28,086 in welfare value that reduces pollution emission based on the optimum re-schedule of conventional thermal units because part of the power supplied from the highly pollution coal-fired units is shifted to the less polluted units, such as G16. However, generally, the less polluted units work with higher operation costs.

In Case D, if the payment of emissions cost is considered, the total cost should be US\$6903543 plus US\$1646165 equals US\$8549708. This total cost of US\$8549708 in Case D is US\$122105 higher than the total cost of US\$8427603 in Case A. Therefore, the integration of the renewable energy source and the consideration of emissions costs together create a relative value of US\$122105 for the system. This relative value is calculated under the current simulation pricing mechanism in the case study.

*Table 6-10: Emission Output and Cost of All Generators in Province Case Study*

Index	Case A		Case B		Case C		Case D	
Emission T (ton) and cost (US\$)	Renewable and Emission Cost		No Renewable but with Emission Cost		Renewable and without Emission Cost		No Renewable and without Emission Cost	
	Total Emission	Total Cost	Total Emission	Total Cost	Total Emission	Total Cost	Total Emission	Total Cost
CO <sub>2</sub>	355797	711595	407228	814456	375207	750413	429047	858094
NO <sub>2</sub>	145	653526	166	747993	153	689177	175	788071

Index	Case A		Case B		Case C		Case D	
Emission T (ton) and cost (US\$)	Renewable and Emission Cost		No Renewable but with Emission Cost		Renewable and without Emission Cost		No Renewable and without Emission Cost	
	Total Emission	Total Cost	Total Emission	Total Cost	Total Emission	Total Cost	Total Emission	Total Cost
Total		1365120		1562449		1439590		1646165

The use of renewable energy for power generation saves fossil fuel consumption and decreases emissions of the thermal units. From Table 6-10, it can be clearly found that the differences in pollution emission under different conditions.

For the analysis of CO<sub>2</sub>, the introduction of renewable energy sources has reduced 51,431 tons of CO<sub>2</sub> emissions for the system. The introduction of emissions costs reduced the system's CO<sub>2</sub> emissions by 19,410 tons. When these two factors are considered together, a total of 73,250 tons of CO<sub>2</sub> emissions are reduced per day for the system. It is worth noting that this value even exceeds the combined CO<sub>2</sub> emissions of 70841 tons when the two factors are considered independently. This shows that the pollution emissions can be reduced to a greater extent when integrating renewable energy sources while introducing the emission cost strategy. Therefore, they are two positive and mutually compatible strategies for each other.

Here, it is worth noting that, unlike other ED models, the operation arrangements of renewable energy generation have not changed under the different cases. This is because, under China's planned economic system, renewable energy power plants are required to generate electricity at full capacity unless safety issues occur, such as insufficient reserves of up and down ramping capacity or grid transmission congestion.

However, these situations have not occurred in this case, so Case A and Case C have the same power generation arrangement of renewable energy sources.

However, the integration of renewable energy has caused a certain amount of impact on the power generation arrangement of thermal power units, such as G9, whose power generation has been reduced by almost half. This is because of its high consumptions and high emissions. Then its parts of the power generations are shifted to renewable energy generators.

Regarding the strategy of overestimation and underestimation cost of wind turbines, although it will make the wind power generation more expensive because the extra penalty cost occurred in this additional strategy, its long-term incentive is positive under reasonable pricing. These will prompt wind farms to actively participate in wind power forecasting and power generation schedule and contribute to the security and stability of the power grid. In this case, the cost of each wind farm based on this modelling method can be observed in Figure 6.12.

Another proposal of this strategy by the author is that the cost of this strategy can be further reduced if wind farms are willing to cooperate to bear each other's forecast deviations. This is because, for example, if the forecasted power generation of each wind farm is larger than actual wind power can generate, there will be no impact on the cost difference between independent strategy and combined strategy. However, once the forecasted power generation of any wind farm is lower than actual wind power, a certain number of forecasted deviations will be offset so that the overall forecast will be more accurate and the cost to be paid will be reduced.

A model based on this strategy is created to observe the results of independent strategy and combined strategy, and it is found that this combined strategy can save a total of US\$48859 a day for the wind farms, shown in Figure 6.13. For the other

academic research, if this phenomenon of complementary characteristic is found, the combining strategy can be applied to reduce the relative speculation costs.

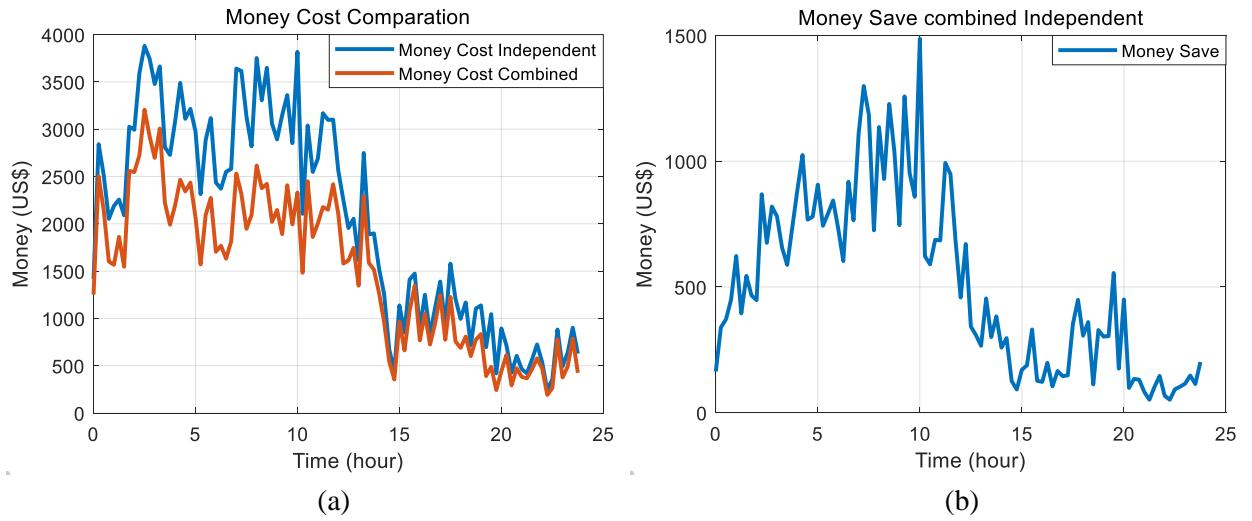


*Figure 6.13: Money Cost of Independent and Combined Strategies to Wind Farms in Province Case Study*

Figure 6.13 (a) illustrated the money cost curves of independent and combined strategies based on the rules of overestimation and underestimation of operation cost models of wind turbines. The cost difference, which means the cost saving, between these two strategies at each given time point can be observed in Figure 6.13 (b).

This part of the money saved can be returned to wind farms who made accurate forecasts to further motivate their wind power forecasting enthusiasm.

The intermittency and uncertainty of renewable energy sources sometimes make it difficult to schedule and dispatch. BESS is used to reduce the variability of renewable energy as shown in Figure 6.14. In this case, after BESS cooperative dispatching with the renewable energy source, the output deviations of the renewable energy between the predicted and the actual were reduced (the red curve in Figure 6.14 is closer to the value of zero).

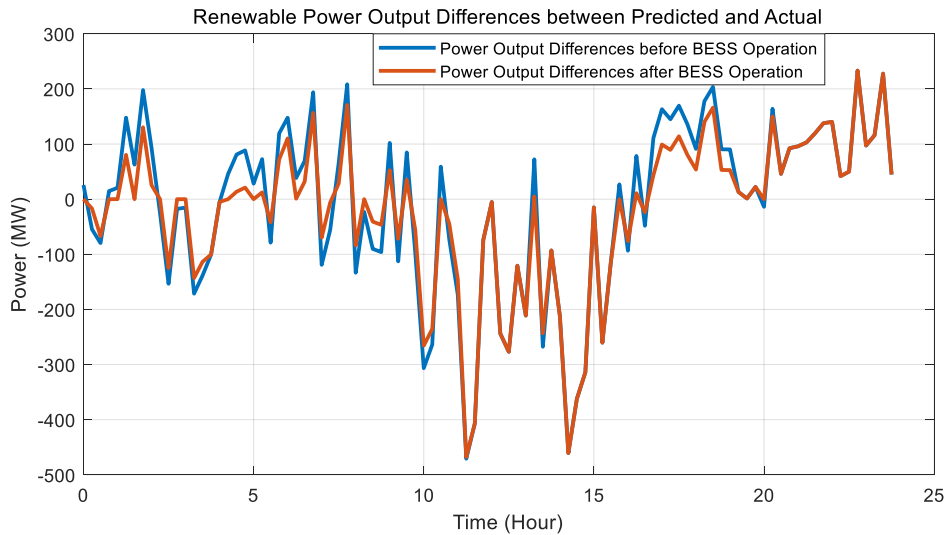


*Figure 6.14: Renewable Power Output Differences between Predicted and Actual in Province Case Study*

Figure 6.15 shows the operation situations of BES systems based on different charging and discharging strategies of Performance Priority in Figure 6.15 (a) and Lifetime Priority in Figure 6.15 (b) and Figure 6.15 (c), discussed in previous subsection 5.4.2. Figure 6.15 (d) shows the total charge and discharge summing results of the three BES systems.

The blue curves represent the current value of energy capacity of BESS in the time axis. The red columns represent how much power charge or discharge at this certain time point. The strategy of lifetime priority will only charge or discharge until it reaches the SOC upper or lower limit. And the strategy of performance priority allows BESS to change the state between charge and discharge at any time to mitigate the variability and uncertainty of renewable energy sources. However, its lifetime will reduce.

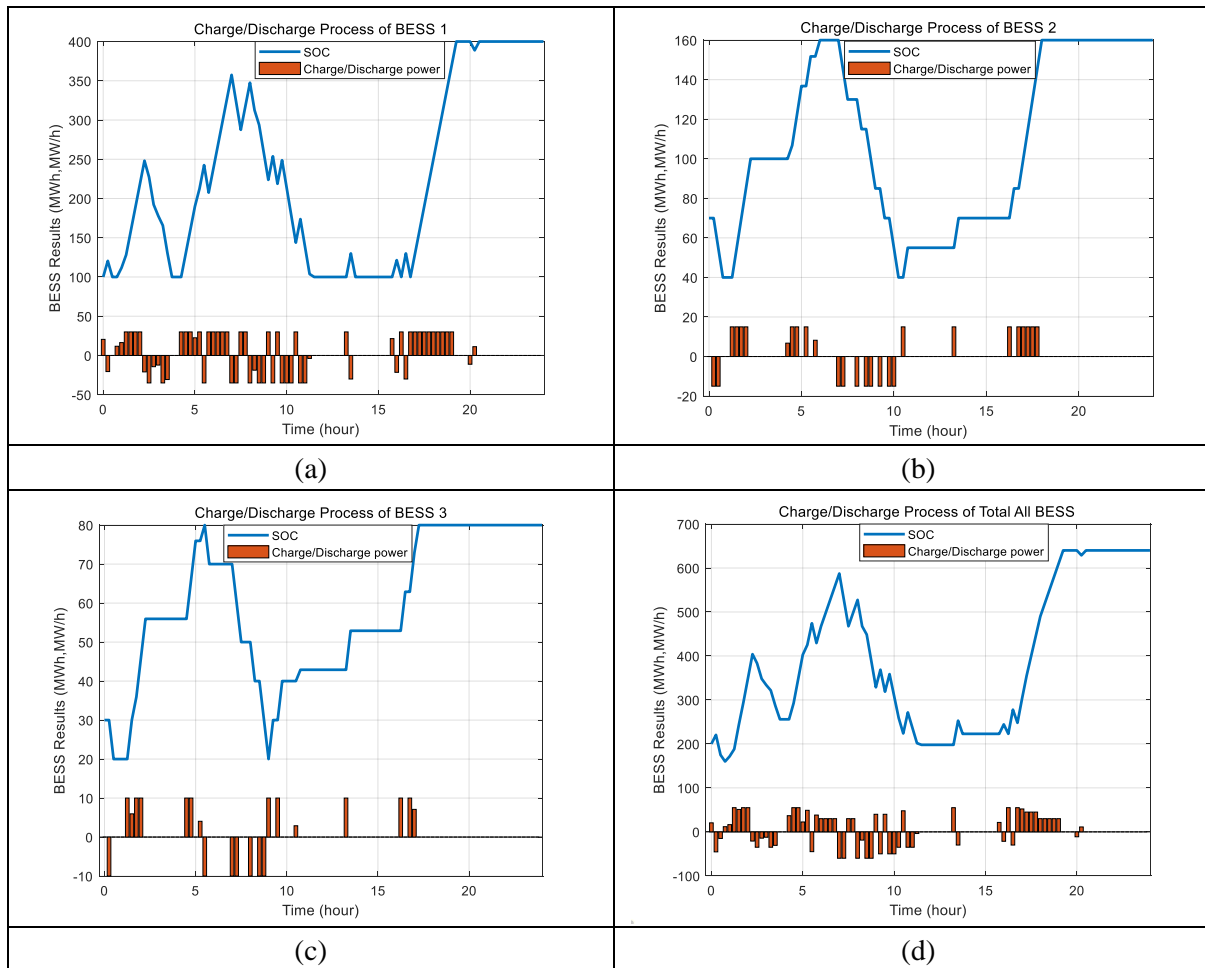


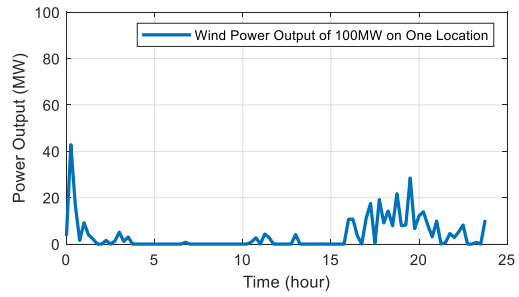
Figure 6.15: BESS Operation Situation in Province Case A (Area Chart)

Finally, when a large number of wind power generation outputs are simulated, an interesting phenomenon is found. The simulation of the output randomness of a single individual wind farm is irregular, but with the continuous increasement of the number of wind farms, the superimposition of their random output will eventually form a simulation result with universal similarity. In other words, the overall forecasting difficulties of power output variation caused by the wind power variability and uncertainty can be reduced through increasing the number of forecast individual wind farms as shown in Figure 6.16 and in Figure 6.17 by comparing the complexity of the curve. The charts (d, e, f) in the bottom of Figure 6.16 and in Figure 6.17 have simpler changes of amplitude and trends.

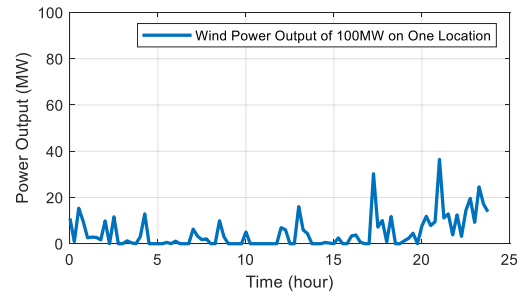
As shown in Figure 6.16, there are huge differences in the output results of stochastic simulation between one hundred 1MW rated wind turbines in different places and one 100MW rated wind turbine in a place. Figure 6.16 (a, b, c) are three simulation results of one 100MW rated wind turbine based on one set of random wind speed. And Figure 6.16 (d, e, f) are three simulation results of one hundred 1MW rated wind turbines based on 100 sets of different random wind speeds.

It is noted that their forecasting levels of difficulty are completely different. The simulations in Figure 6.16 used the same wind turbine parameters except for the rated power of wind turbine, and the wind speeds in different places are stochastically generated.

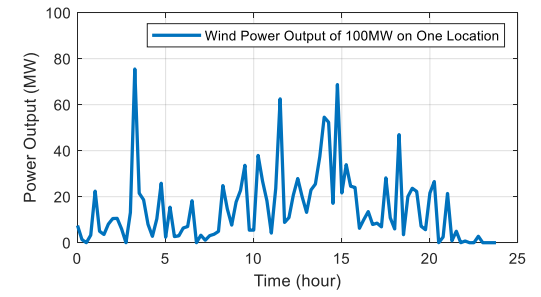
In Figure 6.16 (a, b, c), the wind power output based on the stochastic wind speed is erratic and their forecasting is difficult. However, observing Figure 6.16 (d, e, f), their wind power outputs are regular, and easier to forecast. Similarly, the output simulation of solar farms also has this same complementary characteristic, shown in Figure 6.17



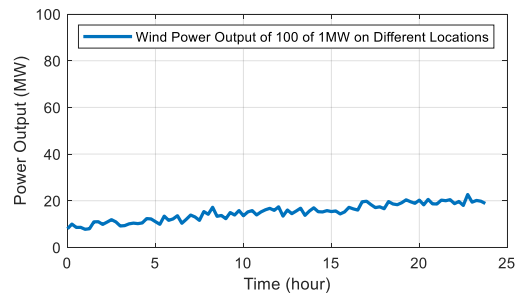
(a)



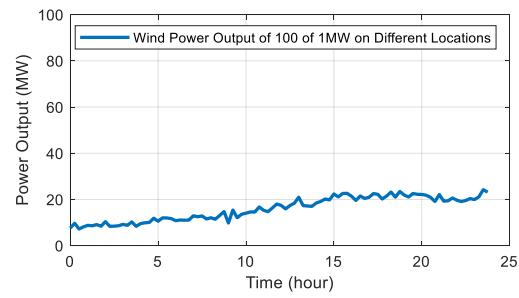
(b)



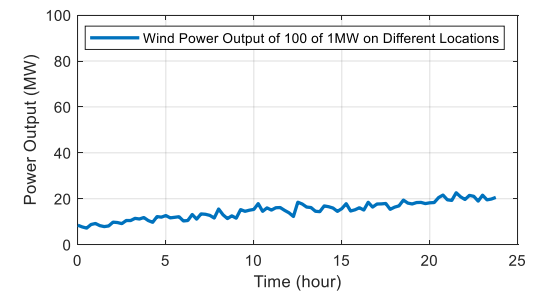
(c)



(d)

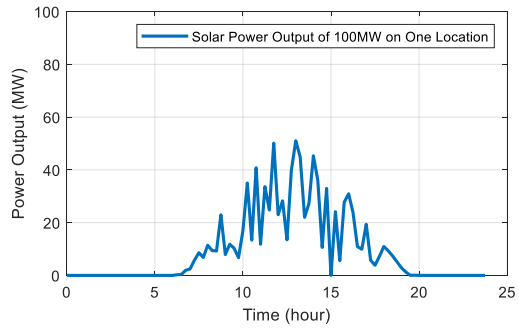


(e)

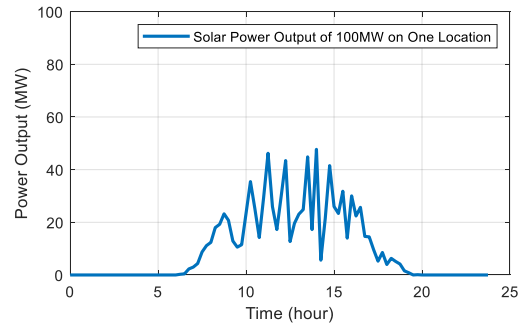


(f)

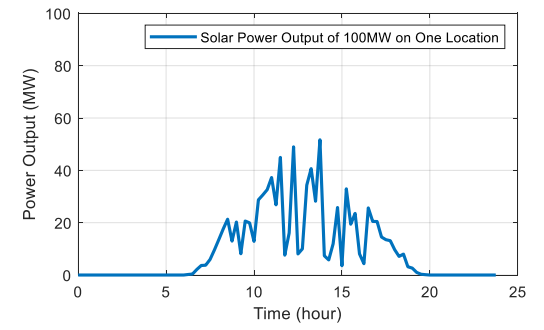
Figure 6.16: Wind Power Output Stochastic Simulation



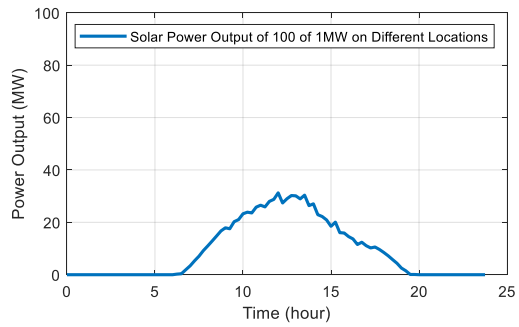
(a)



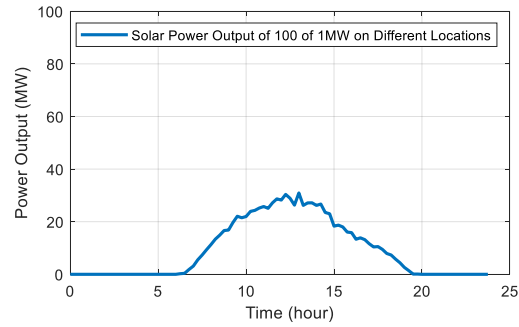
(b)



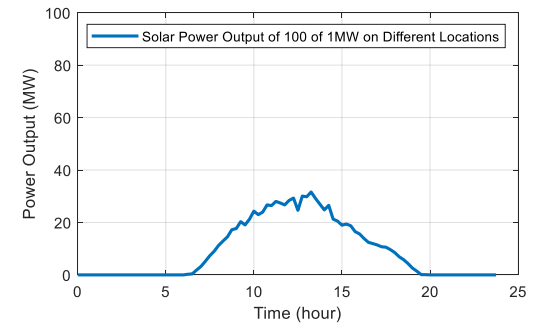
(c)



(d)



(e)



(f)

Figure 6.17: Solar Power Output Stochastic Simulation

## 6.4 Summary

A case study of a provincial power network simplified to a 58 nodes test system including thermal generators, wind farms, solar farms, and hydro plants was provided to test the modified proposed dynamic programming based on the selected Priority list method combining quadratic programming approach in order to solve problems of unit commitment and dispatching schedule.

Different test cases regarding the participation of renewable energy sources and emission cost models were studied. The results of the cost-based solution proved that after considering the cost of renewable energy power generation, BESS cost, and emission cost, the cost of system power generation in this province was reduced. At the same time, the mass of CO<sub>2</sub> emissions had also been reduced. Although the strategy of adding emissions cost consideration will increase economic pressure, it will also make a huge contribution to environmental protection.

The proposed wind power cost model not only considered the operating cost of wind power in the UC problem but also provided a new overestimation and underestimation penalty strategy, which could make each wind farm operator actively participate in wind power forecasting. The fluctuation and adjustment pressure of high penetration of renewable energy could be alleviated by the energy storage system, thereby enhancing the flexibility of the power system.

Finally, during the analysis of results, an interesting phenomenon of complementary characteristic was found that the overall forecasting level of difficulty of solar and wind power output caused by the variability and uncertainty can be reduced through increasing the number of forecast individual wind and solar units.

# Chapter 7 Conclusion and Further Work

## 7.1 Conclusion

This thesis developed an overall cost-based and 15-minute interval model of thermal units, wind farms and solar farms for resolving the day-ahead schedule problem of the power dispatch incorporating energy storage system and emission cost. This model is also compatible with the target simplified case of the actual Province Power Grid system in a semi-liberalized electricity market unique to China.

The renewable energy in the semi-liberalized electricity market of the province case should be fully integrated unless there are system constraints and grid congestions. This is different from general UC, which depends on the operation cost of each generator unit to decide the order to generate electricity and how much electricity to generate.

Detailed modelling of the generating system output (thermal, wind, and solar) and battery energy storage system had been analyzed and presented. All proposed or developed models in this thesis were built based on the well-proven software tools MATLAB 2019a and MATPOWER 7.0. The following paragraphs will conclude the key findings of this thesis based on the research contributions outlined in Chapter 1.

***Point 1:** An overall cost-based model with 15-minute interval combining thermal units, wind farms, solar power farms, and battery energy storage systems for resolving the UC problem of the day-ahead power dispatch schedule*

Most UC problems were built based on the time resolution of the one-hour or half hour interval, while the model in this thesis was developed based on 15 minutes that complied with the time interval of power market decision-making in China and also

increased the computational accuracy of operation cost calculations because the smaller time interval supports more accuracy cost result as Figure 2.1 shows. Besides this, this UC model included the emission cost problem which could affect the optimization process by considering emissions cost resulting in reducing the emission.

This model does not only consider various system constraints, which are power balance constraint, spinning reserve constraint, generator limit constraint, minimum up and down time constraints, and ramp rate constraint but also the costs of various renewable energy sources to optimize the calculation to find the minimum cost.

Without renewable energy integration, the case study based on conventional dynamic programming with all enumeration methods and sequential dynamic programming with the priority list method were demonstrated in Chapter 4. It was found that conventional dynamic programming with all enumeration method was difficult to solve the problem of a large-scale system due to the dimensionality problem. Sequential dynamic programming with the priority list approach could be used to overcome the dimensionality problem because its less CPU computing time as Table 4-15 shows. However, the priority list approach would result in a sub-optimal result due to its limited arrangement set of unit commitment combinations.

The case study with renewable energy integration based on sequential dynamic programming with the priority list method was demonstrated in Chapter 6. Based on considering the cost of renewable power generation, cost of BESS, and cost of emission, the optimum results of the UC problem for the case showed that not only the cost of system power generation was reduced but also the mass of CO<sub>2</sub> emissions that made contributions to environmental protection.

***Point 2:** A novel model of Double Cubic power curve of wind turbine is developed to express the relationship between the output power of the wind turbine with the wind speed*

The Double Cubic power curve of wind turbine is a modelling approach by combining two segments of the cubic curves based on considering the inflection point in the nonlinear portion of the wind power curve to simulate the wind power curve. The corresponding mathematical expression of this novel method was introduced in Chapter 3.

Simulation results of this novel method based on basic specification parameters of wind turbine were used to compare with other five polynomial methods, linear, quadratic, binomial, cubic, and Weibull to evaluate the simulation accuracy of power curves and the simulation results proved that the Double Cubic power curve was the most accurate model among them due to its least values of RMSE and NRMSE.

***Point 3:** A novel stochastic model of forecasting wind speed was developed by considering Weibull method with adding two types of stochastic forecasting corrections of wind speed*

The novel model of forecasting wind speed was developed to use Weibull method with adding two types of forecasting corrections modelled as the white noise generated by a random number generator to stochastically simulate forecasting wind speeds.

The advantage of combining a white noise sequence with mathematic expectation mean value of zero as the correction values to add to the base values generated by the Weibull method is that it has minimal impact to the mean value of sample space. This method will affect the overall variance value of base data of sample space a lot but just a little effect on mean value of base data of sample space.

In order to show the changing of wind speed tendency in different regions and the wind speed amplitude changings in different wind farms respectively, the first type of correction value was designed as a stochastic reference value of wind speed in different regions. The second type of correction value was designed as a stochastic deviation value of wind speed for each wind farm corresponding to that region.

Based on the design of correction values, a new method to form continuous superposition sequence was developed to generate the white noise sequence. The forecasting correction deviation values generated by this method are in line with the general characteristic of forecasting wind speed. For example, the forecasting of wind speed is relatively accurate at the beginning, but as the forecasting time increases, the forecasting deviation of wind speed will gradually becoming larger.

The random number was generated by setting their upside and downside limitation values based on the method of uniformly distributed random variables through the software MATLAB. When the limitation absolute values of upside and downside are the same, the white noise sequence consisting of random numbers will be a number sequence with a mathematical expectation of zero.

***Point 4:** The model of forecasting solar irradiance was developed based on the forecasting data extracted from the free open-source 'SOLCAST API Toolkit' by considering the more fluctuations and variations of forecasting solar irradiance*

The novel model of stochastic generation method was designed to simulate forecasting solar irradiance using the hybrid approach that combining forecast data supported by SOLCAST API Toolkit and adding stochastic forecasting corrections as the fluctuation value changes of forecasting solar irradiance. These forecasting corrections were based on uncertainty modelling techniques of the interval approach

by limiting the maximum upper and lower stochastic changes within the unit time of simulation.

The boundaries of maximum upper and lower stochastic changes were designed based on beta function that makes the stochastic generated corrections of solar irradiance fitting the distribution characteristic of solar energy in a day. For example, for the blocking effect of the same cloud layer on the solar irradiance, the influences on the solar irradiance are different in the morning and evening compared with that at noon. Generally, noon will have a greater correction change.

Based on proposed model, by adjusting the setting parameters, the patterns of solar irradiance variations in different seasons and atmospheric conditions can be simulated.

*Point 5: A model of battery energy storage system with two different proposed operation strategies, performance priority and lifetime priority, are developed to research its relative impacts on renewable energy integration and battery lifetime*

The BESS model that complies with the basic charging and discharging rules was proposed in this thesis. The functions of performance priority and lifetime priority were designed like this:

The strategy of lifetime priority will only allow to charge or discharge until it reaches the state of charge upper or lower limit. This strategy may lose renewable integration power but extend the battery lifetime. This strategy can be used in the situation which the battery replacement costs are high.

The strategy of performance priority does not require the BESS to charge or to discharge until it reaches the SOC limit. This strategy allows BESS to change the state between charging and discharging at any time to mitigate the variability and

uncertainty of renewable energy sources as much as possible between the predicted and actual power output. So, this strategy can reduce renewable energy loss in operation but lose battery lifetime due to its operation flexibility of frequently changing the state between charging and discharging.

***Point 6:** A cost-based model of wind power output is proposed to estimate their related cost*

As the share of wind power generation of electricity rapidly increases, it is necessary to include wind power operation costs in solving the electrical power systems economic dispatch problem. This proposed cost-based model of wind power output not only considered the operation cost of wind power but also provided a new penalty strategy for forecasting overestimation and underestimation.

The penalty cost for wind farm operations occurs when the forecasting underestimate or overestimate of its availability. A reasonable setting for this penalty cost can make each wind farm operator actively participate in wind power forecasting.

***Point 7:** A combined strategy of wind power operators' operation is proposed to save further penalty costs of forecasting overestimation and underestimation*

Based on the simulation results in Chapter 6, it was found that the penalty cost of forecasting overestimation and underestimation could be further reduced if wind farms are willing to cooperate to bear each other's forecast deviations.

Thus, a combined strategy and an independent strategy for each wind operator were found. For example, if all the forecasted power generations of each wind farm are larger than actual wind power, there will be no impact on the cost difference between independent strategy and combined strategy. However, once the forecasted power generation of any wind farm is lower than actual wind power, a certain number

of forecast deviations will be offset. So that the overall forecast will be more accurate and the cost to be paid will be reduced.

The money saved achieved by the combined strategy can be returned to wind farm operators who made accurate forecasts to further motivate their wind power forecasting enthusiasm.

***Point 8:** A modified generation model of a one-line 58-bus of the 330-kV test network is developed to research the China province case study*

This network of 58 nodes test system was simplified from the China province power network but because of data protection in China some of the data were not openly available. Some of the system data were supplemented from those of IEEE standard test systems and some estimated data also had to be added in the system.

The simulated model of the case simplified system including a 330-kV network, 24 thermal units, 46 wind farms, 133 solar farms, 2 hydropower plants, and 3 BESS stations was provided in Chapter 6. The 330-kV network includes 58 node buses with 98 transmission line branches.

For the unit commitment and dispatch problems to this China province case in Chapter 6, the applied solving method of sequential dynamic programming with the priority list approach was used to achieve the solutions of dispatching schedules for the system at a possible minimized operation cost. However, the priority list method will lead to a sub-optimal solution even it can reduce computational requirements.

Within this case, different test cases regarding the participation of renewable energy sources and emission cost models were studied. The optimization results of the cost-based solution proved that after considering the cost of renewable energy power generation, BESS cost, and emission cost, the total cost of system power generation in

this province was reduced because the utilization rate of high-consumption and high-emission thermal power units were reduced. At the same time, the mass of CO<sub>2</sub> emissions had also been reduced. Not only the strategy of adding emissions cost consideration will increase economic pressure, but it will also make a huge contribution to environmental protection.

## **7.2 Further Work**

This thesis contributes to develop an overall cost-based and 15-minute interval model of thermal units, wind farms and solar farms for solving the day-ahead schedule problem of the large-scale power dispatch and this model is based on unit commitment problem incorporating the energy storage system and emission cost. However, possible extensions and improvements can be applied to the methods and concepts presented in this thesis.

Firstly, in China, some provinces have gradually started trial operation of peaking balancing in the power market. It requires the operators to submit the peaking offer of ramping up cost and ramping down cost of the thermal units. So, further work can be designed to add the programming function of ramping cost into the main model in order to implement the function of optimizing dispatching cost considering the ramping cost of thermal units.

Secondly, dynamic programming has the advantage of being able to solve and manage the problems of large-scale size and to be easily modified to model characteristics of specific utilities such as adding constraints and emission cost. However, the combined function of the priority list method used in this thesis will lead to a sub-optimal solution even if it can significantly reduce computational requirements. So, if possible, a meta-heuristic method can be modified to be compatible with the target case of the actual Province Power Grid system to research

the further UC and ED results. But the problem is how to reduce the “curse of dimensionality” and guarantee convergence.

Thirdly, the problem of “curse of dimensionality” and guarantee convergence is often occurring during the large-scale programming in power system, such as the approach of complete enumeration used in sub-section 4.3.3 and 4.4.2. This approach was not used in the target case of China province because its problem of “curse of dimensionality” that the scale of power system is too large. So, an approach which can be used to reduce or control the size of the problem is required.

Fourthly, in this thesis, only once deterministic results of stochastically forecasting RES is used to determine the problems of UC and ED of thermal units in the case study. However, the produced results based on the deterministic approach with assumption input data do not fully capture the dynamics of the whole renewable energy systems, such as its fluctuation [261]. So, this study is better to move towards stochastic optimization in which the optimization considers uncertainties and probabilities of RES as different generated input samples, then repeating the simulation and calculation in the programming unit it achieved a possible best solution to evaluate this approach influence on the cost optimization results of the system.

Fifthly, in future research, with the scale of the energy storage system gradually increases, not only the economic optimization problems of BESS operation cost, but also the problem of suitable battery sizing should be considered and researched based on the proposed two different strategies, performance priority and lifetime priority.

## Appendix

### Appendix (A): Simplified network of 58 node bus system supplemented by IEEE standard test system of Case30

i) Branch data:

From bus number	To bus number	Resistance	Reactance	Total line charging susceptance	Transmission line constraints
		(p.u.)	(p.u.)	(p.u.)	(MVA)
1	2	0.02	0.06	0.03	1360
1	3	0.05	0.19	0.02	1360
2	3	0.06	0.17	0.02	1360
3	4	0.01	0.04	0	1360
3	5	0.05	0.2	0.02	1360
4	5	0.06	0.18	0.02	1360
5	6	0.01	0.04	0	1360
6	7	0.05	0.12	0.01	1360
6	8	0.03	0.08	0.01	1360
7	8	0.01	0.04	0	1360
8	9	0	0.21	0	5200
8	11	0	0.56	0	1360
8	12	0.07	0.13	0	1360
8	15	0	0.21	0	5200
9	10	0	0.11	0	1360
9	11	0	0.26	0	1360
9	13	0	0.14	0	1360
9	16	0.12	0.26	0	5200
11	13	0.09	0.2	0	1360
12	14	0.22	0.2	0	1360
12	15	0.08	0.19	0	1360
13	14	0.11	0.22	0	1360
14	15	0.06	0.13	0	1360
15	16	0.03	0.07	0	5200
15	17	0.09	0.21	0	1360
15	27	0.03	0.08	0	5200
16	24	0.03	0.07	0	5200

17	18	0.07	0.15	0	1360
17	19	0.01	0.02	0	1360
18	20	0.1	0.2	0	1360
18	25	0.12	0.18	0	1360
19	20	0.13	0.27	0	1360
19	21	0.19	0.33	0	1360
19	22	0.25	0.38	0	1360
19	28	0.01	0.02	0	1360
20	21	0.11	0.21	0	1360
20	22	0.01	0.02	0	1360
22	23	0	0.4	0	1360
23	24	0.22	0.42	0	2720
24	27	0.32	0.6	0	5200
24	28	0.24	0.45	0	1360
24	29	0.06	0.2	0.02	5200
24	34	0.02	0.06	0.01	2720
25	26	0.05	0.2	0.02	1360
25	35	0.06	0.18	0.02	1360
26	27	0.01	0.04	0	1360
27	38	0.05	0.12	0.01	1360
27	42	0.03	0.08	0.01	5200
27	45	0.01	0.04	0	1360
27	47	0	0.21	0	1360
28	29	0	0.56	0	1360
29	30	0	0.21	0	5200
29	31	0	0.11	0	1360
29	32	0	0.26	0	1360
29	33	0	0.14	0	1360
30	42	0.12	0.26	0	5200
30	50	0.07	0.13	0	1360
30	51	0.09	0.2	0	1360
31	33	0.22	0.2	0	1360
31	36	0.08	0.19	0	1360
31	54	0.11	0.22	0	1360
32	56	0.06	0.13	0	1360
33	34	0.03	0.08	0	1360
34	35	0.03	0.07	0	1360
35	43	0.07	0.15	0	1360
35	45	0.01	0.02	0	1360

36	37	0.1	0.2	0	1360
36	39	0.02	0.06	0.03	1360
36	40	0.05	0.19	0.02	1360
37	38	0.12	0.18	0	1360
37	39	0.12	0.18	0	1360
37	41	0.03	0.08	0	1360
38	41	0.03	0.08	0	1360
38	43	0.03	0.08	0	1360
39	42	0.13	0.27	0	1360
40	42	0.19	0.33	0	1360
41	42	0.25	0.38	0	1360
41	44	0.06	0.18	0.02	1360
43	45	0.11	0.21	0	1360
44	46	0	0.4	0	1360
44	49	0.22	0.42	0	1360
45	46	0.32	0.6	0	1360
45	47	0.03	0.08	0	1360
46	48	0	0.21	0	1360
46	49	0	0.56	0	1360
47	48	0.07	0.13	0	1360
49	57	0	0.21	0	1360
50	53	0	0.11	0	1360
50	55	0.22	0.42	0	2720
51	52	0.32	0.6	0	1360
51	53	0.24	0.45	0	1360
52	53	0.06	0.2	0.02	1360
52	54	0.02	0.06	0.01	1360
53	54	0.05	0.2	0.02	1360
55	56	0.01	0.02	0	1360
55	58	0.1	0.2	0	1360
56	57	0.02	0.06	0.03	1360
56	58	0.05	0.19	0.02	1360

ii) Bus data:

Bus number	Bus type	Ratio of total power demand	Bus number	Bus type	Ratio of total power demand
1	PV bus	825.0	30	PV bus	326.0
2	PQ bus	206.3	31	PQ bus	214.5
3	PV bus	206.3	32	PQ bus	214.5
4	PQ bus	206.3	33	PV bus	429.1
5	PQ bus	206.3	34	PV bus	2305.7
6	PV bus	206.3	35	PQ bus	576.4
7	PQ bus	206.3	36	PQ bus	576.4
8	PV bus	412.5	37	PQ bus	576.4
9	PQ bus	412.5	38	PQ bus	576.4
10	PQ bus	206.3	39	PQ bus	576.4
11	PQ bus	206.3	40	PV bus	576.4
12	PQ bus	464.6	41	PV bus	1152.9
13	PQ bus	232.3	42	PV bus	1152.9
14	PV bus	116.2	43	PV bus	145.7
15	PQ bus	232.3	44	PQ bus	310.0
16	PQ bus	232.3	45	PQ bus	291.4
17	PV bus	232.3	46	PQ bus	310.0
18	PQ bus	410.0	47	PV bus	291.4
19	PQ bus	135.0	48	PV bus	291.4
20	PQ bus	135.0	49	PQ bus	620.0
21	PV bus	405.0	50	PQ bus	326.0
22	PQ bus	135.0	51	PV bus	163.0
23	PV bus	820.0	52	PQ bus	163.0
24	PQ bus	820.0	53	PQ bus	163.0
25	PV bus	820.0	54	PV bus	489.0
26	Reference bus	410.0	55	PQ bus	192.2
27	PV bus	820.0	56	PQ bus	384.4
28	PV bus	1072.7	57	PV bus	192.2
29	PV bus	429.1	58	PQ bus	961.1

## Appendix (B): Exact data of case study solution results of power output dispatching of solar farms, wind farms and thermal generators in Chapter 6

### i) Solar Farms: (MW)

Time Point	1	2	3	4	5	6	7	8	9	10	11	12	13	14	15	16	17	18	19	20	21	22	23	24
Solar Farm 1	0	0	0	0	0	0	0	0	0	0	0	0	0	0	0	0	0	0	0	0	0	0	0	0
Solar Farm 2	0	0	0	0	0	0	0	0	0	0	0	0	0	0	0	0	0	0	0	0	0	0	0	0
Solar Farm 3	0	0	0	0	0	0	0	0	0	0	0	0	0	0	0	0	0	0	0	0	0	0	0	0
Solar Farm 4	0	0	0	0	0	0	0	0	0	0	0	0	0	0	0	0	0	0	0	0	0	0	0	0
Solar Farm 5	0	0	0	0	0	0	0	0	0	0	0	0	0	0	0	0	0	0	0	0	0	0	0	0
Solar Farm 6	0	0	0	0	0	0	0	0	0	0	0	0	0	0	0	0	0	0	0	0	0	0	0	0
Solar Farm 7	0	0	0	0	0	0	0	0	0	0	0	0	0	0	0	0	0	0	0	0	0	0	0	0
Solar Farm 8	0	0	0	0	0	0	0	0	0	0	0	0	0	0	0	0	0	0	0	0	0	0	0	0
Time Point	25	26	27	28	29	30	31	32	33	34	35	36	37	38	39	40	41	42	43	44	45	46	47	48
Solar Farm 1	0.6	4.3	6.0	24.9	36.1	60.2	74.3	88.7	119.8	130.4	143.3	175.1	156.2	218.0	204.8	188.6	212.0	235.9	232.8	294.0	250.1	247.6	251.1	242.5
Solar Farm 2	1.5	9.9	16.0	54.5	93.3	127.3	177.3	199.1	253.3	284.1	314.4	353.6	369.9	450.7	518.6	529.9	462.0	506.9	603.4	595.4	571.0	623.6	610.1	633.1
Solar Farm 3	0.6	3.8	5.9	21.3	27.5	45.7	64.0	83.1	107.3	95.3	133.9	161.0	141.5	166.2	175.8	196.5	206.1	215.0	223.4	225.8	200.5	219.1	207.7	281.9
Solar Farm 4	1.0	6.8	10.7	35.0	55.9	85.4	114.0	150.9	160.0	177.4	231.0	232.6	274.0	311.2	315.1	317.4	373.3	322.7	352.9	433.9	478.0	349.0	427.5	464.1
Solar Farm 5	0.0	0.7	1.1	5.9	10.9	17.0	21.9	24.1	28.4	41.0	42.6	49.3	58.3	61.8	63.9	64.6	69.3	55.8	71.8	87.7	48.4	64.1	87.1	109.2
Solar Farm 6	0.0	2.3	3.8	20.6	32.1	55.2	69.8	86.5	103.9	132.9	144.4	170.0	195.8	212.5	203.1	215.4	241.2	260.8	235.5	304.1	248.3	240.0	271.5	276.5
Solar Farm 7	0.0	1.4	2.1	11.4	19.5	32.3	43.8	57.9	60.4	81.5	92.8	102.1	106.0	123.2	116.7	135.0	124.2	156.8	150.1	128.6	182.2	186.7	167.9	162.1
Solar Farm 8	0.5	3.4	6.1	11.0	23.6	38.0	56.7	71.8	84.0	106.9	129.8	125.0	147.4	152.1	155.7	172.3	167.5	182.3	200.0	178.8	192.2	243.9	202.7	231.1
Time Point	49	50	51	52	53	54	55	56	57	58	59	60	61	62	63	64	65	66	67	68	69	70	71	72
Solar Farm 1	343.7	306.2	275.6	292.7	300.0	273.4	240.2	284.7	398.6	327.2	329.1	264.2	307.5	225.6	249.0	211.8	207.2	216.8	208.8	192.0	162.9	160.9	124.0	124.9
Solar Farm 2	734.4	775.5	669.2	698.2	726.9	755.3	764.5	732.8	638.5	662.6	598.6	685.3	690.5	620.0	630.5	536.1	515.7	503.7	428.2	437.9	405.0	359.6	322.2	308.4
Solar Farm 3	197.8	287.9	213.5	252.8	256.0	260.7	284.0	256.2	303.1	251.3	254.2	277.0	278.9	247.4	210.9	186.7	204.0	184.7	159.0	185.8	139.2	122.7	146.2	108.6
Solar Farm 4	449.1	468.0	476.7	503.5	468.9	509.1	435.9	535.9	395.1	440.7	442.6	465.0	458.0	445.1	389.4	375.4	346.5	328.0	311.8	298.0	235.6	258.3	205.4	207.2
Solar Farm 5	83.8	100.5	90.6	131.6	78.6	85.6	112.3	102.4	55.9	47.5	57.1	27.6	65.7	55.1	48.7	63.1	59.4	48.0	33.6	19.7	45.3	29.5	27.4	26.2
Solar Farm 6	345.6	266.1	310.0	236.4	314.9	309.8	224.0	244.8	269.0	216.8	261.6	196.0	183.4	185.8	169.2	172.5	133.7	171.5	134.7	120.0	82.5	124.4	80.5	102.1
Solar Farm 7	176.9	160.5	158.5	165.0	159.9	180.4	187.9	126.9	142.9	94.0	198.7	155.2	149.2	85.5	121.3	96.5	102.3	94.5	78.3	52.9	75.0	61.2	67.9	61.7
Solar Farm 8	204.9	147.1	193.0	220.8	200.9	229.9	206.0	221.3	172.1	133.1	129.5	177.5	140.4	139.6	120.6	122.0	90.2	77.0	78.1	76.1	54.1	64.8	40.7	43.0
Time Point	73	74	75	76	77	78	79	80	81	82	83	84	85	86	87	88	89	90	91	92	93	94	95	96
Solar Farm 1	104.4	85.9	72.9	53.9	33.6	19.8	5.8	3.2	0	0	0	0	0	0	0	0	0	0	0	0	0	0	0	0
Solar Farm 2	242.6	202.3	164.0	123.9	82.9	47.7	12.9	7.5	0	0	0	0	0	0	0	0	0	0	0	0	0	0	0	0
Solar Farm 3	94.5	85.1	59.8	44.2	31.1	18.2	4.9	2.8	0	0	0	0	0	0	0	0	0	0	0	0	0	0	0	0
Solar Farm 4	168.6	145.9	114.1	80.0	51.4	32.2	9.0	4.9	0	0	0	0	0	0	0	0	0	0	0	0	0	0	0	0
Solar Farm 5	24.6	19.8	15.7	11.6	9.5	4.0	0.3	0.3	0	0	0	0	0	0	0	0	0	0	0	0	0	0	0	0
Solar Farm 6	84.9	65.3	58.3	41.0	25.9	15.7	0.5	0.9	0	0	0	0	0	0	0	0	0	0	0	0	0	0	0	0
Solar Farm 7	51.4	42.7	41.4	24.8	16.8	8.6	0.6	0.5	0	0	0	0	0	0	0	0	0	0	0	0	0	0	0	0
Solar Farm 8	32.3	26.7	15.4	4.0	3.1	1.7	2.1	1.1	0	0	0	0	0	0	0	0	0	0	0	0	0	0	0	0

ii) Wind Farms: (MW)

Time Point	1	2	3	4	5	6	7	8	9	10	11	12	13	14	15	16	17	18	19	20	21	22	23	24
Wind Farm 1	137.7	342.1	256.5	163.7	252.8	347.1	293.2	318.0	343.5	414.2	450.0	274.7	480.4	287.6	288.6	293.4	381.2	368.7	461.7	275.5	287.6	157.1	429.6	305.1
Wind Farm 2	164.1	463.9	452.2	255.7	224.6	201.6	207.5	459.8	452.0	461.9	576.5	563.6	434.9	486.5	303.7	186.7	293.8	412.9	333.0	441.1	327.2	356.9	201.8	336.5
Wind Farm 3	279.5	342.5	241.1	359.5	284.9	320.9	241.2	418.0	432.7	452.4	376.6	589.0	404.6	500.6	340.0	357.9	391.4	418.3	324.8	457.1	385.1	219.7	286.6	413.8
Wind Farm 4	1.7	0.0	4.0	0.0	2.4	0.5	0.2	0.3	4.2	0.0	0.3	0.6	0.6	0.7	0.2	0.2	4.6	0.4	7.2	4.9	10.7	12.6	7.3	9.6
Wind Farm 5	0.8	6.0	1.5	3.5	0.8	1.8	2.2	0.0	1.9	1.4	2.2	7.7	6.0	3.3	0.4	6.6	4.5	3.1	9.0	4.3	7.2	7.1	11.4	13.8
Wind Farm 6	14.5	8.2	7.0	4.4	0.3	1.4	2.2	0.4	2.6	0.0	1.6	0.9	3.0	0.8	2.9	15.7	5.6	1.0	3.2	1.2	1.2	0.7	0.6	3.4
Wind Farm 7	5.2	8.9	2.3	3.0	2.5	0.0	1.9	6.3	0.0	0.0	3.6	3.1	0.0	1.1	0.6	4.0	6.5	7.7	1.7	0.1	5.3	2.4	6.3	4.7
Wind Farm 8	12.9	11.4	7.4	5.5	7.2	2.2	1.0	3.1	1.7	0.3	0.1	0.9	0.0	9.2	1.2	5.5	4.3	3.4	0.0	0.4	0.0	1.7	4.7	5.1
Time Point	25	26	27	28	29	30	31	32	33	34	35	36	37	38	39	40	41	42	43	44	45	46	47	48
Wind Farm 1	286.4	255.6	158.2	267.0	336.3	330.6	295.9	396.0	416.4	385.4	356.3	327.3	397.1	223.1	290.8	303.2	388.1	237.8	381.9	325.7	306.5	226.0	331.9	375.5
Wind Farm 2	176.4	278.2	285.3	174.2	278.0	311.3	192.5	201.0	296.9	297.9	425.1	387.5	315.6	260.6	377.8	202.4	363.6	254.2	313.2	269.7	389.9	489.9	394.8	382.7
Wind Farm 3	268.4	274.7	304.7	345.1	434.8	344.5	373.4	321.7	394.0	450.5	309.2	212.3	204.5	291.9	326.0	189.9	330.4	80.5	218.7	145.8	113.4	221.6	195.0	171.4
Wind Farm 4	17.2	10.9	8.5	21.7	5.9	4.3	4.0	6.0	6.8	1.9	4.2	1.8	11.4	7.3	2.1	3.6	0.7	0.4	2.4	4.9	6.6	5.3	17.0	11.2
Wind Farm 5	14.1	12.7	6.9	12.1	10.8	4.2	1.3	3.2	8.6	7.6	22.0	10.0	12.3	17.8	0.4	3.6	3.8	0.8	5.8	4.4	8.6	8.5	12.9	21.5
Wind Farm 6	11.6	23.0	9.4	11.4	6.6	50.6	69.5	25.0	10.7	18.0	8.7	17.2	9.1	54.6	99.0	183.0	36.4	62.5	74.5	84.2	29.1	87.3	26.3	74.0
Wind Farm 7	13.2	11.0	7.3	10.0	5.3	8.1	15.6	3.8	16.0	8.0	16.1	18.0	14.1	18.4	11.4	44.8	15.4	21.2	51.8	12.2	30.4	12.5	7.7	12.7
Wind Farm 8	10.0	6.1	10.6	2.3	13.9	1.6	8.2	11.5	15.0	4.0	11.5	9.0	11.4	12.0	5.9	15.6	16.7	41.1	16.9	1.2	5.3	5.2	20.9	8.7
Time Point	49	50	51	52	53	54	55	56	57	58	59	60	61	62	63	64	65	66	67	68	69	70	71	72
Wind Farm 1	294.5	265.9	225.7	273.1	235.9	356.6	260.6	205.7	266.2	79.8	41.1	62.2	140.7	63.1	123.0	228.6	48.7	160.5	47.1	44.7	203.9	100.2	79.6	94.5
Wind Farm 2	310.5	275.4	242.0	159.2	143.9	248.5	176.8	224.2	126.9	155.5	48.8	27.0	101.6	89.2	156.4	164.4	105.8	126.2	95.3	141.4	146.1	113.9	164.6	72.0
Wind Farm 3	144.0	85.4	157.7	159.1	63.9	150.1	39.9	34.0	39.6	30.8	47.7	12.9	34.2	52.7	57.6	120.8	64.4	49.0	37.4	110.3	73.4	44.6	58.7	28.0
Wind Farm 4	14.5	9.8	2.8	3.5	2.8	5.8	3.5	2.1	3.4	0.3	0.8	1.4	2.0	2.4	4.1	2.6	0.0	0.0	0.3	0.4	1.4	1.8	0.0	0.4
Wind Farm 5	73.5	14.8	7.7	20.9	10.9	14.5	13.5	9.6	8.0	3.2	2.7	9.0	6.9	11.7	2.7	2.6	3.6	5.9	3.8	4.4	8.1	3.1	3.7	17.1
Wind Farm 6	42.8	33.6	22.8	20.2	73.6	50.3	88.4	64.8	48.1	70.8	55.6	15.5	18.4	43.5	25.4	5.7	11.7	15.2	26.5	20.3	12.1	15.7	113.4	38.4
Wind Farm 7	9.6	15.8	8.3	78.3	17.0	82.9	74.5	67.8	16.3	51.7	28.8	9.4	66.9	8.9	87.0	8.8	64.8	54.2	73.3	54.3	44.2	22.0	81.6	62.2
Wind Farm 8	15.0	5.0	6.1	4.4	2.8	53.5	30.4	15.6	7.9	16.1	4.3	10.2	21.2	10.0	6.7	0.0	6.3	15.3	10.0	5.1	7.4	12.4	19.5	28.5
Time Point	73	74	75	76	77	78	79	80	81	82	83	84	85	86	87	88	89	90	91	92	93	94	95	96
Wind Farm 1	37.0	143.5	20.1	22.8	23.9	11.5	43.4	22.3	43.5	29.5	30.7	51.5	63.5	27.9	58.5	106.8	73.8	27.5	32.6	104.6	61.2	19.5	88.4	26.1
Wind Farm 2	36.3	25.4	52.2	31.4	23.7	12.7	28.5	14.3	24.0	119.6	31.6	9.3	25.9	65.5	58.6	31.8	55.5	15.0	9.2	76.1	38.2	58.7	87.4	34.6
Wind Farm 3	35.9	43.5	10.2	12.3	4.7	15.8	23.5	13.5	18.0	11.2	6.8	15.0	21.7	31.0	30.6	33.9	30.5	6.5	22.8	86.0	27.1	28.5	68.0	13.4
Wind Farm 4	2.9	0.7	1.1	0.4	0.4	0.0	0.0	1.5	2.0	0.3	0.0	0.0	0.2	0.0	0.0	0.0	0.0	0.0	0.0	0.6	0.0	0.0	0.0	0.0
Wind Farm 5	6.7	7.4	10.0	9.0	16.3	12.2	1.5	1.3	6.9	4.6	6.6	1.7	3.1	0.2	1.0	4.8	1.5	0.9	6.0	7.6	2.3	9.6	2.7	5.9
Wind Farm 6	75.6	27.6	70.6	148.4	147.8	44.0	66.6	34.7	25.3	47.6	27.1	74.6	20.2	6.6	10.6	21.7	5.3	9.7	14.2	11.6	4.8	14.3	15.9	42.1
Wind Farm 7	61.8	82.4	73.2	116.1	131.2	41.9	64.5	20.0	67.7	24.2	20.4	45.8	18.3	11.7	19.4	34.7	11.3	17.6	16.6	15.3	14.9	66.2	32.2	66.6
Wind Farm 8	55.7	15.8	2.5	22.7	46.5	51.1	15.8	7.3	16.9	8.7	5.9	3.9	1.9	2.0	7.2	3.6	4.9	3.0	11.7	0.2	3.3	4.5	13.7	7.4

iii) Thermal Generators: (MW)

Time Point	1	2	3	4	5	6	7	8	9	10	11	12	13	14	15	16	17	18	19	20	21	22	23	24
Thermal Generator 1	300	300	300	300	300	300	300	300	300	300	300	300	300	300	300	300	300	300	300	300	300	300	300	300
Thermal Generator 2	0	0	0	0	0	0	0	0	0	0	0	0	0	0	0	0	0	0	0	0	0	0	0	0
Thermal Generator 3	175	175	175	175	0	0	0	0	0	0	0	0	0	0	0	0	0	0	0	0	0	0	0	0
Thermal Generator 4	1600	1600	1600	1600	1600	1600	1600	1600	1600	1600	1600	1600	1600	1600	1600	1600	1600	1600	1600	1600	1600	1600	1600	1600
Thermal Generator 5	350	350	350	350	350	350	350	350	350	350	350	350	338	319	311	350	350	350	350	350	350	350	350	350
Thermal Generator 6	199	150	150	160	159	150	150	150	150	150	150	150	150	150	150	150	150	150	150	150	150	155	150	176
Thermal Generator 7	199	175	175	175	175	175	175	175	175	175	175	175	175	175	175	175	175	175	175	175	175	175	175	176
Thermal Generator 8	675	675	675	675	675	675	675	675	675	675	675	675	675	675	675	675	675	675	675	675	675	675	675	675
Thermal Generator 9	1000	1000	1000	1000	1000	1000	1000	1000	1000	1000	1000	1000	1000	1000	1000	1000	1000	1000	1000	1000	1000	1000	1000	1000
Thermal Generator 10	750	750	750	750	750	750	750	750	750	750	750	750	750	750	750	750	750	750	750	750	750	750	750	750
Thermal Generator 11	854	800	800	800	800	800	800	800	800	800	800	800	800	800	800	800	800	800	800	800	800	800	800	821
Thermal Generator 12	1299	1156	1194	1233	1232	1197	1206	1089	1039	964	935	893	871	862	966	979	929	909	921	945	1042	1150	1188	1260
Thermal Generator 13	800	800	800	800	800	800	800	800	800	800	800	800	800	800	800	800	800	800	800	800	800	800	800	800
Thermal Generator 14	300	300	300	300	300	300	300	300	300	300	300	300	300	300	300	300	300	300	300	300	300	300	300	300
Thermal Generator 15	1138	1000	1041	1077	1076	1044	1053	945	900	831	805	766	750	750	833	845	799	781	792	814	903	1005	1037	1102
Thermal Generator 16	600	538	590	600	600	600	600	600	600	571	547	511	492	485	537	584	541	525	535	555	600	600	600	600
Thermal Generator 17	814	679	722	756	755	725	733	631	600	600	600	600	600	600	600	600	600	600	600	600	600	700	718	780
Thermal Generator 18	700	620	680	700	700	700	700	627	591	536	515	485	469	462	522	547	511	497	505	522	582	642	699	700
Thermal Generator 19	500	500	500	500	500	500	500	500	500	500	500	500	500	500	500	500	500	500	500	500	500	500	500	500
Thermal Generator 20	450	450	450	450	450	450	450	450	450	450	450	450	450	450	450	450	450	450	450	450	450	450	450	450
Thermal Generator 21	434	375	375	384	383	375	375	375	375	375	375	375	375	375	375	375	375	375	375	375	375	377	375	404
Thermal Generator 22	250	250	250	250	250	250	250	250	250	250	250	250	250	250	250	250	250	250	250	250	250	250	250	250
Thermal Generator 23	250	250	250	250	250	250	250	250	250	250	250	250	250	250	250	250	250	250	250	250	250	250	250	250
Thermal Generator 24	0	0	0	0	0	0	0	0	0	0	0	0	0	0	0	0	0	0	0	0	0	0	0	0
Time Point	25	26	27	28	29	30	31	32	33	34	35	36	37	38	39	40	41	42	43	44	45	46	47	48
Thermal Generator 1	338	305	314	300	300	300	300	300	300	300	300	300	300	300	300	300	300	300	300	300	300	300	300	300
Thermal Generator 2	0	0	0	0	0	0	0	0	0	0	0	0	0	0	0	0	0	0	0	0	0	0	0	0
Thermal Generator 3	0	0	0	0	0	0	0	0	0	0	0	0	0	0	0	0	0	0	0	0	0	0	0	0
Thermal Generator 4	1600	1600	1600	1600	1600	1600	1600	1600	1600	1600	1600	1600	1600	1600	1600	1600	1600	1600	1600	1600	1600	1600	1600	1600
Thermal Generator 5	350	350	350	350	350	350	350	350	350	350	350	350	350	350	350	350	350	350	350	350	350	350	350	350
Thermal Generator 6	213	251	288	281	231	194	184	192	176	190	183	177	192	172	153	165	153	191	192	194	210	207	195	150
Thermal Generator 7	211	246	281	281	234	194	184	192	176	190	183	177	192	175	175	175	175	210	192	194	210	207	195	175
Thermal Generator 8	675	675	675	675	675	675	675	675	675	675	675	675	675	675	675	675	675	675	675	675	675	675	675	675
Thermal Generator 9	1000	1000	1000	1000	1000	1000	1000	1000	1000	1000	1000	1000	1000	1000	1000	1000	1000	1000	1000	1000	1000	1000	1000	1000
Thermal Generator 10	750	750	750	750	750	750	750	750	750	750	750	750	750	750	750	750	750	750	750	750	750	750	750	750
Thermal Generator 11	951	1003	1015	969	855	847	832	843	821	841	831	823	844	815	800	806	800	891	844	846	868	864	848	800
Thermal Generator 12	1300	1300	1300	1300	1300	1290	1273	1286	1260	1284	1271	1262	1287	1253	1221	1242	1222	1300	1287	1290	1300	1300	1292	1200
Thermal Generator 13	886	800	800	800	800	800	800	800	800	800	800	800	800	800	800	800	800	800	800	800	800	800	800	800
Thermal Generator 14	350	305	314	300	300	300	300	300	300	300	300	300	300	300	300	300	300	300	300	300	300	300	300	300
Thermal Generator 15	1204	1299	1312	1262	1139	1130	1114	1126	1102	1124	1112	1104	1127	1095	1067	1085	1067	1170	1127	1129	1153	1149	1132	1047
Thermal Generator 16	600	600	600	600	600	600	600	600	600	600	600	600	600	600	600	600	600	600	600	600	600	600	600	600
Thermal Generator 17	880	968	980	932	815	806	791	802	780	801	790	781	803	774	746	764	747	847	803	806	829	825	808	728
Thermal Generator 18	700	700	700	700	700	700	700	700	700	700	700	700	700	700	700	700	700	700	700	700	700	700	700	700
Thermal Generator 19	500	500	500	500	500	500	500	500	500	500	500	500	500	500	500	500	500	500	500	500	500	500	500	500
Thermal Generator 20	450	450	450	450	450	450	450	450	450	450	450	450	450	450	450	450	450	450	450	450	450	450	450	450
Thermal Generator 21	459	514	569	539	464	428	414	424	405	423	413	406	425	399	375	390	375	430	425	427	448	444	429	375
Thermal Generator 22	310	305	314	281	250	250	250	250	250	250	250	250	250	250	250	250	250	250	250	250	250	250	250	250
Thermal Generator 23	313	250	250	250	250	250	250	250	250	250	250	250	250	250	250	250	250	250	250	250	250	250	250	250
Thermal Generator 24	0	0	0	0	0	0	0	0	0	0	0	0	0	0	0	0	0	0	0	0	0	0	0	0

Time Point	49	50	51	52	53	54	55	56	57	58	59	60	61	62	63	64	65	66	67	68	69	70	71	72
Thermal Generator 1	300	300	300	300	300	300	300	300	338	375	412	450	487	525	562	600	600	600	600	600	600	600	600	600
Thermal Generator 2	0	0	0	0	0	0	0	0	0	0	0	0	0	0	0	0	0	0	0	0	0	0	0	0
Thermal Generator 3	0	0	0	0	0	0	0	0	0	0	0	0	0	0	0	0	0	0	0	0	0	0	0	0
Thermal Generator 4	1600	1600	1600	1600	1600	1600	1600	1600	1760	1723	1847	1769	1695	1704	1691	1731	1834	1902	2014	2052	2112	2165	2060	2048
Thermal Generator 5	350	350	350	350	350	350	350	350	350	350	350	350	350	350	350	350	350	350	350	350	350	350	350	350
Thermal Generator 6	150	150	150	150	150	150	173	155	193	230	268	0	0	0	0	0	0	0	0	0	0	0	0	0
Thermal Generator 7	175	175	175	175	175	175	175	175	210	245	0	0	0	0	0	0	0	0	0	0	0	0	0	0
Thermal Generator 8	675	675	675	675	675	675	675	675	751	704	816	752	675	685	675	713	819	889	1002	1044	1105	1161	1052	1039
Thermal Generator 9	1000	1000	1000	1000	1000	1000	1000	1000	0	0	0	0	0	0	0	0	0	0	0	0	0	0	0	0
Thermal Generator 10	750	750	750	750	750	750	750	870	885	988	923	862	870	859	892	977	1033	1126	1157	1206	1250	1164	1153	
Thermal Generator 11	800	800	800	800	800	800	817	800	930	1060	1190	1320	1450	1580	1600	1600	1600	1600	1600	1600	1600	1600	1600	1600
Thermal Generator 12	1164	1157	1121	1089	1168	1026	1133	1226	1300	1300	1300	1300	1300	1300	1300	1300	1300	1300	1300	1300	1300	1300	1300	1300
Thermal Generator 13	800	800	800	800	800	800	800	800	910	1020	1128	1088	1050	1055	1048	1069	1121	1156	1213	1232	1263	1290	1236	1230
Thermal Generator 14	300	300	300	300	300	300	300	300	350	400	450	500	550	600	600	600	600	600	600	600	600	600	600	600
Thermal Generator 15	1014	1008	975	946	1018	881	983	1071	1173	1276	1378	1481	1500	1500	1500	1500	1500	1500	1500	1500	1500	1500	1500	1500
Thermal Generator 16	600	600	600	600	600	598	600	600	600	600	0	0	0	0	0	0	0	0	0	0	0	0	0	0
Thermal Generator 17	696	691	659	631	700	600	700	750	850	950	1050	1150	1200	1200	1200	1200	1200	1200	1200	1200	1200	1200	1200	1200
Thermal Generator 18	681	677	650	627	684	604	664	700	700	700	700	700	700	700	700	700	700	700	700	700	700	700	700	700
Thermal Generator 19	500	500	500	500	500	500	500	500	578	655	732	752	675	685	671	713	791	868	946	1000	1000	1000	1000	1000
Thermal Generator 20	450	450	450	450	450	450	450	450	525	600	675	750	675	685	671	713	788	863	900	900	900	900	900	900
Thermal Generator 21	375	375	375	375	375	375	400	378	433	0	0	0	0	0	0	0	0	0	0	0	0	0	0	0
Thermal Generator 22	250	250	250	250	250	250	250	250	310	370	430	490	500	500	500	500	500	500	500	500	500	500	500	500
Thermal Generator 23	250	250	250	250	250	250	250	250	313	375	437	500	500	500	500	500	500	500	500	500	500	500	500	500
Thermal Generator 24	0	0	0	0	0	0	0	0	0	0	0	0	0	0	0	0	0	0	0	0	0	0	0	0
Time Point	73	74	75	76	77	78	79	80	81	82	83	84	85	86	87	88	89	90	91	92	93	94	95	96
Thermal Generator 1	600	600	600	600	600	600	600	600	600	600	600	600	600	600	600	600	600	600	600	600	600	600	600	600
Thermal Generator 2	0	0	0	0	0	0	0	0	0	0	0	0	0	0	0	0	0	0	0	0	0	0	0	0
Thermal Generator 3	0	0	0	0	0	0	0	0	0	0	0	0	0	0	0	0	0	0	0	0	0	0	0	0
Thermal Generator 4	2012	1981	1967	1957	1972	2070	2154	2287	2367	2390	2411	2289	2267	2194	2087	1905	1873	1832	1713	1600	1642	1626	1600	1600
Thermal Generator 5	350	350	350	350	350	350	350	350	350	350	350	350	350	350	350	350	350	350	350	350	350	350	350	350
Thermal Generator 6	0	0	0	0	0	0	0	150	188	225	263	300	300	300	300	300	300	300	300	300	300	300	300	300
Thermal Generator 7	0	0	0	0	0	0	0	0	0	0	0	0	0	0	0	0	0	0	0	0	0	0	0	0
Thermal Generator 8	1002	970	956	946	962	1062	1149	1261	1350	1350	1350	1288	1266	1190	1080	932	859	817	694	675	675	675	675	675
Thermal Generator 9	0	0	0	0	0	0	0	0	0	0	0	0	0	0	0	0	0	0	0	0	0	0	0	0
Thermal Generator 10	1124	1098	1087	1079	1091	1172	1241	1351	1417	1436	1453	1353	1335	1274	1186	1036	1009	976	877	768	819	805	762	765
Thermal Generator 11	1600	1600	1600	1600	1600	1600	1600	1600	1600	1600	1600	1600	1600	1600	1600	1600	1600	1600	1600	1581	1600	1600	1573	1577
Thermal Generator 12	1300	1300	1300	1300	1300	1300	1300	1300	1300	1300	1300	1300	1300	1300	1300	1300	1300	1300	1300	1300	1300	1300	1300	1300
Thermal Generator 13	1212	1196	1189	1184	1192	1241	1284	1352	1393	1405	1415	1353	1342	1304	1250	1158	1141	1120	1060	992	1024	1015	988	990
Thermal Generator 14	600	600	600	600	600	600	600	600	600	600	600	600	600	600	600	600	600	600	600	600	600	600	600	600
Thermal Generator 15	1500	1500	1500	1500	1500	1500	1500	1500	1500	1500	1500	1500	1500	1500	1500	1500	1500	1500	1500	1500	1500	1500	1500	1500
Thermal Generator 16	0	0	0	0	0	0	0	0	0	0	0	0	0	0	0	0	0	0	0	0	0	0	0	0
Thermal Generator 17	1200	1200	1200	1200	1200	1200	1200	1200	1200	1200	1200	1200	1200	1200	1200	1200	1200	1200	1200	1200	1200	1200	1200	1200
Thermal Generator 18	700	700	700	700	700	700	700	700	700	700	700	700	700	700	700	700	700	700	700	700	700	700	700	700
Thermal Generator 19	1000	970	956	946	962	1000	1000	1000	1000	1000	1000	1000	1000	1000	1000	898	859	817	715	612	621	604	550	553
Thermal Generator 20	900	900	900	900	900	900	900	900	900	900	900	900	900	900	900	893	859	817	718	620	621	604	550	553
Thermal Generator 21	0	0	0	0	0	0	0	0	0	0	0	0	0	0	0	0	0	0	0	0	0	0	0	0
Thermal Generator 22	500	500	500	500	500	500	500	500	500	500	500	500	500	500	500	500	500	500	500	500	500	500	500	500
Thermal Generator 23	500	500	500	500	500	500	500	500	500	500	500	500	500	500	500	500	500	500	500	500	500	500	500	500
Thermal Generator 24	0	0	0	0	0	0	0	0	0	0	0	0	0	0	0	0	0	0	0	0	0	0	0	0

## References

1. Matti Supponen, X.Q., CHEN Qixin and JIANG Nan, *Electricity markets and systems in the EU and China*. 2020.
2. Administration, N.E., *Statistics on the power industry in 2020*.
3. Dudley, B., *BP statistical review of world energy*. BP Statistical Review, London, UK, accessed Aug, 2020.
4. Muyi Yang, X.S., *EMBER Global Electricity Review 2021*. 2021, EMBER COAL TO CLEAN ENERGY POLICY.
5. Qian, Y., *How reform worked in China*. Available at SSRN 317460, 2002.
6. Zeng, M., et al., *The power industry reform in China 2015: Policies, evaluations and solutions*. Renewable and Sustainable Energy Reviews, 2016. **57**: p. 94-110.
7. CEC, *Analysis of National Electricity Market Transaction in the 4th Quarter of 2018*. 2021, China Electricity Council.
8. Wang, Q. and X. Chen, *China's electricity market-oriented reform: from an absolute to a relative monopoly*. Energy Policy, 2012. **51**: p. 143-148.
9. Ho, M.S., Z. Wang, and Z. Yu, *China's power generation dispatch*. Resources for the Future (RFF): Washington, DC, USA, 2017.
10. Shang, Y., *In 2020 the total amount of transaction power in power exchange sectors of the State Grid are 480.11 billion kWh*. 2021, State Grid News.
11. Zhou, J., *Annual Development Report of China Power Industry 2021*. 2021, China Electricity Council.
12. Serreze, M.C. and J. Stroeve, *Arctic sea ice trends, variability and implications for seasonal ice forecasting*. Philosophical Transactions of the Royal Society A: Mathematical, Physical and Engineering Sciences, 2015. **373**(2045): p. 20140159.
13. Transformation, G.E., *A Roadmap to 2050*. International Renewable Energy Agency, Abu Dhabi, 2018.
14. Baldick, R., *The generalized unit commitment problem*. IEEE Transactions on Power Systems, 1995. **10**(1): p. 465-475.
15. Li, C.-A., R.B. Johnson, and A.J. Svoboda, *A new unit commitment method*. IEEE Transactions on Power Systems, 1997. **12**(1): p. 113-119.
16. Xiong, S., Y. Wang, and C. Zhang, *Achievement of Carbon Peak Goals in China's Road Transport—Possibilities and Pathways*. 2022.
17. Ciwei, G. and L. Yang, *Evolution of China's power dispatch principle and the new energy saving power dispatch policy*. Energy Policy, 2010. **38**(11): p. 7346-7357.
18. Cherni, J.A. and J. Kentish, *Renewable energy policy and electricity market reforms in China*. Energy Policy, 2007. **35**(7): p. 3616-3629.

19. Yiyao Cao, J.C., Bingqi Liu, *Zero Carbonization of Electricity Growth (2020–2030): China's Only Way to Achieve Carbon Neutrality*. 2021, ROCKY MOUNTAIN INSTITUTE.
20. Council, C.E., *Basic Statistics Data of China Electricity Industry in 2018*. 2019.
21. Yadav, A. and A. Rani. *GEPSO Tuned NN MPPT Control of PV System*. in *2021 IEEE Bombay Section Signature Conference (IBSSC)*. 2021. IEEE.
22. deLlano-Paz, F., et al., *The European low-carbon mix for 2030: The role of renewable energy sources in an environmentally and socially efficient approach*. *Renewable and Sustainable Energy Reviews*, 2015. **48**: p. 49-61.
23. Chang, W.-Y., *A literature review of wind forecasting methods*. *Journal of Power and Energy Engineering*, 2014. **2**(04): p. 161.
24. Foley, A.M., et al., *Current methods and advances in forecasting of wind power generation*. *Renewable energy*, 2012. **37**(1): p. 1-8.
25. Wang, X., P. Guo, and X. Huang, *A review of wind power forecasting models*. *Energy procedia*, 2011. **12**: p. 770-778.
26. Varanasi, J. and M. Tripathi. *A comparative study of wind power forecasting techniques—A review article*. in *2016 3rd International Conference on Computing for Sustainable Global Development (INDIACom)*. 2016. IEEE.
27. Li, J., et al., *Review of uncertainty forecasting methods for renewable energy power*. *High Volt. Eng*, 2021. **47**: p. 1144-1157.
28. Moore, R.E., R.B. Kearfott, and M.J. Cloud, *Introduction to interval analysis*. 2009: SIAM.
29. Ramakrishna, R., et al., *A model for joint probabilistic forecast of solar photovoltaic power and outdoor temperature*. *IEEE Transactions on Signal Processing*, 2019. **67**(24): p. 6368-6383.
30. Zadeh, L.A., *Fuzzy sets as a basis for a theory of possibility*. *Fuzzy sets and systems*, 1978. **1**(1): p. 3-28.
31. Carta, J.A., P. Ramirez, and S. Velazquez, *A review of wind speed probability distributions used in wind energy analysis: Case studies in the Canary Islands*. *Renewable and sustainable energy reviews*, 2009. **13**(5): p. 933-955.
32. Chang, T.P., *Performance comparison of six numerical methods in estimating Weibull parameters for wind energy application*. *Applied Energy*, 2011. **88**(1): p. 272-282.
33. Fyrrippis, I., P.J. Axaopoulos, and G. Panayiotou, *Wind energy potential assessment in Naxos Island, Greece*. *Applied Energy*, 2010. **87**(2): p. 577-586.
34. Chang, T.P., *Estimation of wind energy potential using different probability density functions*. *Applied Energy*, 2011. **88**(5): p. 1848-1856.
35. Brown, B.G., R.W. Katz, and A.H. Murphy, *Time series models to simulate and forecast wind speed and wind power*. *Journal of Applied Meteorology and Climatology*, 1984. **23**(8): p. 1184-1195.

36. Kamal, L. and Y.Z. Jafri, *Time series models to simulate and forecast hourly averaged wind speed in Quetta, Pakistan*. Solar Energy, 1997. **61**(1): p. 23-32.
37. Yunus, K., T. Thiringer, and P. Chen, *ARIMA-based frequency-decomposed modeling of wind speed time series*. IEEE Transactions on Power Systems, 2015. **31**(4): p. 2546-2556.
38. Billinton, R., H. Chen, and R. Ghajar, *Time-series models for reliability evaluation of power systems including wind energy*. Microelectronics Reliability, 1996. **36**(9): p. 1253-1261.
39. Erdem, E. and J. Shi, *ARMA based approaches for forecasting the tuple of wind speed and direction*. Applied Energy, 2011. **88**(4): p. 1405-1414.
40. Ozay, C. and M.S. Celiktas, *Statistical analysis of wind speed using two-parameter Weibull distribution in Alaçatı region*. Energy Conversion and Management, 2016. **121**: p. 49-54.
41. Seguro, J. and T. Lambert, *Modern estimation of the parameters of the Weibull wind speed distribution for wind energy analysis*. Journal of wind engineering and industrial aerodynamics, 2000. **85**(1): p. 75-84.
42. Bidaoui, H., et al., *Wind speed data analysis using Weibull and Rayleigh distribution functions, case study: five cities northern Morocco*. Procedia Manufacturing, 2019. **32**: p. 786-793.
43. Jowder, F.A., *Weibull and Rayleigh distribution functions of wind speeds in Kingdom of Bahrain*. Wind Engineering, 2006. **30**(5): p. 439-445.
44. Safari, B. and J. Gasore, *A statistical investigation of wind characteristics and wind energy potential based on the Weibull and Rayleigh models in Rwanda*. Renewable Energy, 2010. **35**(12): p. 2874-2880.
45. Baran, S. and S. Lerch, *Log-normal distribution based Ensemble Model Output Statistics models for probabilistic wind-speed forecasting*. Quarterly Journal of the Royal Meteorological Society, 2015. **141**(691): p. 2289-2299.
46. Akpinar, S. and E.K. Akpinar, *Estimation of wind energy potential using finite mixture distribution models*. Energy Conversion and Management, 2009. **50**(4): p. 877-884.
47. Celik, A., A. Makkawi, and T. Muneer, *Critical evaluation of wind speed frequency distribution functions*. Journal of renewable and sustainable energy, 2010. **2**(1): p. 013102.
48. Poggi, P., et al., *Forecasting and simulating wind speed in Corsica by using an autoregressive model*. Energy conversion and management, 2003. **44**(20): p. 3177-3196.
49. Torres, J.L., et al., *Forecast of hourly average wind speed with ARMA models in Navarre (Spain)*. Solar energy, 2005. **79**(1): p. 65-77.
50. Gomes, P. and R. Castro, *Wind speed and wind power forecasting using statistical models: autoregressive moving average (ARMA) and artificial*

- neural networks (ANN)*. International Journal of Sustainable Energy Development, 2012. **1**(1/2).
51. Wang, J. and J. Hu, *A robust combination approach for short-term wind speed forecasting and analysis—Combination of the ARIMA (Autoregressive Integrated Moving Average), ELM (Extreme Learning Machine), SVM (Support Vector Machine) and LSSVM (Least Square SVM) forecasts using a GPR (Gaussian Process Regression) model*. Energy, 2015. **93**: p. 41-56.
  52. Suyono, H., et al. *Forecasting of Wind Speed in Malang City of Indonesia using Adaptive Neuro-Fuzzy Inference System and Autoregressive Integrated Moving Average Methods*. in *2020 International Conference on Technology and Policy in Energy and Electric Power (ICT-PEP)*. 2020. IEEE.
  53. Yazhou, L., W. Weisheng, and Y. Yonghua, *Wind power penetration limit calculation based on chance constrained programming*. PROCEEDINGS-CHINESE SOCIETY OF ELECTRICAL ENGINEERING, 2002. **22**(5): p. 32-35.
  54. Lei, Y., et al., *Optimal real power flow in wind power integrated system*. Power System Technology, 2002. **26**(6): p. 18-21.
  55. Jangamshetti, S.H. and V.G. Rau, *Site matching of wind turbine generators: a case study*. IEEE Transactions on Energy Conversion, 1999. **14**(4): p. 1537-1543.
  56. Suresh, H.J. and R. Guruprasada, *Optimum sitting of wind turbine generators [J]*. IEEE Trans on Energy Conservation, 2001. **16**(4): p. 8-13.
  57. Zárate-Miñano, R., M. Anghel, and F. Milano, *Continuous wind speed models based on stochastic differential equations*. Applied Energy, 2013. **104**: p. 42-49.
  58. Johnson, P., S. Howell, and P. Duck, *Partial differential equation methods for stochastic dynamic optimization: an application to wind power generation with energy storage*. Philosophical Transactions of the Royal Society A: Mathematical, Physical and Engineering Sciences, 2017. **375**(2100): p. 20160301.
  59. Wang, Y., et al., *Approaches to wind power curve modeling: A review and discussion*. Renewable and Sustainable Energy Reviews, 2019. **116**: p. 109422.
  60. Villanueva, D. and A. Feijóo, *A review on wind turbine deterministic power curve models*. Applied Sciences, 2020. **10**(12): p. 4186.
  61. Yun, E. and J. Hur, *Probabilistic estimation model of power curve to enhance power output forecasting of wind generating resources*. Energy, 2021. **223**: p. 120000.
  62. Kusiak, A., H. Zheng, and Z. Song, *Models for monitoring wind farm power*. Renewable Energy, 2009. **34**(3): p. 583-590.

63. Shokrzadeh, S., M.J. Jozani, and E. Bibeau, *Wind turbine power curve modeling using advanced parametric and nonparametric methods*. IEEE Transactions on Sustainable Energy, 2014. **5**(4): p. 1262-1269.
64. Lydia, M., et al., *Advanced algorithms for wind turbine power curve modeling*. IEEE Transactions on sustainable energy, 2013. **4**(3): p. 827-835.
65. Sohoni, V., S. Gupta, and R. Nema, *A critical review on wind turbine power curve modelling techniques and their applications in wind based energy systems*. Journal of Energy, 2016. **2016**.
66. Thapar, V., G. Agnihotri, and V.K. Sethi, *Critical analysis of methods for mathematical modelling of wind turbines*. Renewable Energy, 2011. **36**(11): p. 3166-3177.
67. Teyabeen, A.A., F.R. Akkari, and A.E. Jwaid. *Power curve modelling for wind turbines*. in *2017 UKSim-AMSS 19th International Conference on Computer Modelling & Simulation (UKSim)*. 2017. IEEE.
68. Deshmukh, M. and S. Deshmukh, *Modeling of hybrid renewable energy systems*. Renewable and sustainable energy reviews, 2008. **12**(1): p. 235-249.
69. Sainz, E., A. Llombart, and J. Guerrero, *Robust filtering for the characterization of wind turbines: Improving its operation and maintenance*. Energy Conversion and Management, 2009. **50**(9): p. 2136-2147.
70. Villanueva, D. and A.E. Feijóo, *Reformulation of parameters of the logistic function applied to power curves of wind turbines*. Electric Power Systems Research, 2016. **137**: p. 51-58.
71. Liu, X., *An improved interpolation method for wind power curves*. IEEE Transactions on Sustainable Energy, 2012. **3**(3): p. 528-534.
72. Lydia, M., et al., *Wind resource estimation using wind speed and power curve models*. Renewable energy, 2015. **83**: p. 425-434.
73. Khatib, T., et al., *Modeling of daily solar energy on a horizontal surface for five main sites in Malaysia*. International Journal of Green Energy, 2011. **8**(8): p. 795-819.
74. Atwa, Y., et al., *Optimal renewable resources mix for distribution system energy loss minimization*. IEEE Transactions on Power Systems, 2009. **25**(1): p. 360-370.
75. Soroudi, A., M. Aien, and M. Ehsan, *A probabilistic modeling of photo voltaic modules and wind power generation impact on distribution networks*. IEEE Systems Journal, 2011. **6**(2): p. 254-259.
76. Angstrom, A., *Computation of global radiation from records of sunshine*. Ark. Geofys.:(Sweden), 1956. **2**.
77. Chineke, T.C., *Equations for estimating global solar radiation in data sparse regions*. Renewable Energy, 2008. **33**(4): p. 827-831.
78. Sopian, K. and M.Y.H. Othman, *Estimates of monthly average daily global solar radiation in Malaysia*. Renewable Energy, 1992. **2**(3): p. 319-325.

79. Yohanna, J.K., I.N. Itodo, and V.I. Umogbai, *A model for determining the global solar radiation for Makurdi, Nigeria*. *Renewable Energy*, 2011. **36**(7): p. 1989-1992.
80. Benson, R., et al., *Estimation of daily and monthly direct, diffuse and global solar radiation from sunshine duration measurements*. *Solar energy*, 1984. **32**(4): p. 523-535.
81. El-Sebaili, A., et al., *Global, direct and diffuse solar radiation on horizontal and tilted surfaces in Jeddah, Saudi Arabia*. *Applied energy*, 2010. **87**(2): p. 568-576.
82. Collares-Pereira, M. and A. Rabl, *The average distribution of solar radiation-correlations between diffuse and hemispherical and between daily and hourly insolation values*. *Solar energy*, 1979. **22**(2): p. 155-164.
83. Tuller, S.E., *The relationship between diffuse, total and extra terrestrial solar radiation*. *Solar Energy*, 1976. **18**(3): p. 259-263.
84. Li, H., et al., *Estimating monthly average daily diffuse solar radiation with multiple predictors: a case study*. *Renewable energy*, 2011. **36**(7): p. 1944-1948.
85. Mohandes, M., S. Rehman, and T. Halawani, *Estimation of global solar radiation using artificial neural networks*. *Renewable energy*, 1998. **14**(1-4): p. 179-184.
86. Al-Alawi, S. and H. Al-Hinai, *An ANN-based approach for predicting global radiation in locations with no direct measurement instrumentation*. *Renewable Energy*, 1998. **14**(1-4): p. 199-204.
87. Dorvlo, A.S., J.A. Jervase, and A. Al-Lawati, *Solar radiation estimation using artificial neural networks*. *Applied Energy*, 2002. **71**(4): p. 307-319.
88. Reddy, K.S. and M. Ranjan, *Solar resource estimation using artificial neural networks and comparison with other correlation models*. *Energy conversion and management*, 2003. **44**(15): p. 2519-2530.
89. Hontoria, L., J. Aguilera, and P. Zufiria, *An application of the multilayer perceptron: solar radiation maps in Spain*. *Solar energy*, 2005. **79**(5): p. 523-530.
90. Şen, Z., *Fuzzy algorithm for estimation of solar irradiation from sunshine duration*. *Solar Energy*, 1998. **63**(1): p. 39-49.
91. Khatib, T., A. Mohamed, and K. Sopian, *A review of solar energy modeling techniques*. *Renewable and Sustainable Energy Reviews*, 2012. **16**(5): p. 2864-2869.
92. Bivona, S., et al., *Stochastic models for wind speed forecasting*. *Energy conversion and management*, 2011. **52**(2): p. 1157-1165.
93. Roulston, M.S., et al., *Using medium-range weather forecasts to improve the value of wind energy production*. *Renewable Energy*, 2003. **28**(4): p. 585-602.

94. Leung, D.Y. and Y. Yang, *Wind energy development and its environmental impact: A review*. Renewable and Sustainable Energy Reviews, 2012. **16**(1): p. 1031-1039.
95. Nemati, M., M. Braun, and S. Tenbohlen, *Optimization of unit commitment and economic dispatch in microgrids based on genetic algorithm and mixed integer linear programming*. Applied energy, 2018. **210**: p. 944-963.
96. Fossati, J.P., *Unit commitment and economic dispatch in micro grids*. Memoria de Trabajos de Difusión Científica y Técnica, 2012. **10**: p. 83-96.
97. Papavasiliou, A., S.S. Oren, and B. Rountree, *Applying high performance computing to transmission-constrained stochastic unit commitment for renewable energy integration*. IEEE Transactions on Power Systems, 2014. **30**(3): p. 1109-1120.
98. Jiang, R., J. Wang, and Y. Guan, *Robust unit commitment with wind power and pumped storage hydro*. IEEE Transactions on Power Systems, 2011. **27**(2): p. 800-810.
99. Chen, C.-L., *Optimal wind-thermal generating unit commitment*. IEEE transactions on energy conversion, 2008. **23**(1): p. 273-280.
100. Venkatesh, B., et al., *Fuzzy MILP unit commitment incorporating wind generators*. IEEE Transactions on power systems, 2008. **23**(4): p. 1738-1746.
101. Johnson, R., H. Happ, and W. Wright, *Large scale hydro-thermal unit commitment-method and results*. IEEE Transactions on Power Apparatus and Systems, 1971(3): p. 1373-1384.
102. Wood, A.J., B.F. Wollenberg, and P. Generation, *Operation and Control*, John Wiley & Sons. New York, 1984.
103. Snyder, W.L., H.D. Powell, and J.C. Rayburn, *Dynamic programming approach to unit commitment*. IEEE Transactions on Power Systems, 1987. **2**(2): p. 339-348.
104. Abujarad, S.Y., M.W. Mustafa, and J.J. Jamian, *Recent approaches of unit commitment in the presence of intermittent renewable energy resources: A review*. Renewable and Sustainable Energy Reviews, 2017. **70**: p. 215-223.
105. Singh, R.L.R. and C.C.A. Rajan, *An Efficient and Improved Artificial Neural Network Algorithm to Solve Unit Commitment Problem with Cooling Banking Constraints*. European Journal of Scientific Research, 2011. **61**(4): p. 561-571.
106. Sheblé, G.B. and T.T. Maifeld, *Unit commitment by genetic algorithm and expert system*. Electric Power Systems Research, 1994. **30**(2): p. 115-121.
107. Kazarlis, S.A., A. Bakirtzis, and V. Petridis, *A genetic algorithm solution to the unit commitment problem*. IEEE transactions on power systems, 1996. **11**(1): p. 83-92.
108. Swarup, K. and S. Yamashiro, *Unit commitment solution methodology using genetic algorithm*. IEEE Transactions on power systems, 2002. **17**(1): p. 87-91.

109. Sood, Y.R., N.P. Padhy, and H. Gupta, *Discussion of " Optimal power flow by enhanced genetic algorithm"*. IEEE Transactions on Power Systems, 2003. **18**(3): p. 1219.
110. Sisworahardjo, N. and A. El-Keib. *Unit commitment using the ant colony search algorithm*. in *LESCOPE'02. 2002 Large Engineering Systems Conference on Power Engineering. Conference Proceedings*. 2002. IEEE.
111. Ting, T., M. Rao, and C. Loo, *A novel approach for unit commitment problem via an effective hybrid particle swarm optimization*. IEEE transactions on power systems, 2006. **21**(1): p. 411-418.
112. Zhao, B., et al., *An improved particle swarm optimization algorithm for unit commitment*. International Journal of Electrical Power & Energy Systems, 2006. **28**(7): p. 482-490.
113. Yuan, X., et al., *An improved binary particle swarm optimization for unit commitment problem*. Expert Systems with applications, 2009. **36**(4): p. 8049-8055.
114. Mori, H. and T. Usami. *Unit commitment using tabu search with restricted neighborhood*. in *Proceedings of International Conference on Intelligent System Application to Power Systems*. 1996. IEEE.
115. Saneifard, S., N.R. Prasad, and H.A. Smolleck, *A fuzzy logic approach to unit commitment*. IEEE Transactions on Power Systems, 1997. **12**(2): p. 988-995.
116. Mantawy, A., Y.L. Abdel-Magid, and S.Z. Selim, *Unit commitment by tabu search*. IEE Proceedings-Generation, Transmission and Distribution, 1998. **145**(1): p. 56-64.
117. Sen, S. and D. Kothari, *Optimal thermal generating unit commitment: a review*. International Journal of Electrical Power & Energy Systems, 1998. **20**(7): p. 443-451.
118. Ma, H. and S. Shahidehpour, *Unit commitment with transmission security and voltage constraints*. IEEE transactions on power systems, 1999. **14**(2): p. 757-764.
119. Rudolf, A. and R. Bayrleithner, *A genetic algorithm for solving the unit commitment problem of a hydro-thermal power system*. IEEE Transactions on Power Systems, 1999. **14**(4): p. 1460-1468.
120. Li, T. and M. Shahidehpour, *Price-based unit commitment: A case of Lagrangian relaxation versus mixed integer programming*. IEEE transactions on power systems, 2005. **20**(4): p. 2015-2025.
121. Abujarad, S., M. Mustafa, and J. Jamian. *Unit commitment problem solution in the presence of solar and wind power integration by an improved priority list method*. in *2016 6th International Conference on Intelligent and Advanced Systems (ICIAS)*. 2016. IEEE.
122. Alizadeh, M.I., M.P. Moghaddam, and N. Amjady, *Multistage multiresolution robust unit commitment with nondeterministic flexible ramp considering load*

- and wind variabilities*. IEEE Transactions on Sustainable Energy, 2017. **9**(2): p. 872-883.
123. El-Saadawi, M., M. Tantawi, and E. Tawfik, *A fuzzy optimization-based approach to large scale thermal unit commitment*. Electric Power Systems Research, 2004. **72**(3): p. 245-252.
  124. Wu, H., M. Shahidehpour, and A. Al-Abdulwahab, *Hourly demand response in day-ahead scheduling for managing the variability of renewable energy*. IET Generation, Transmission & Distribution, 2013. **7**(3): p. 226-234.
  125. Damousis, I.G., A.G. Bakirtzis, and P.S. Dokopoulos, *A solution to the unit-commitment problem using integer-coded genetic algorithm*. IEEE Transactions on Power systems, 2004. **19**(2): p. 1165-1172.
  126. Farhat, I. and M. El-Hawary, *Optimization methods applied for solving the short-term hydrothermal coordination problem*. Electric Power Systems Research, 2009. **79**(9): p. 1308-1320.
  127. Pang, C., G.B. Sheblé, and F. Albuyeh, *Evaluation of dynamic programming based methods and multiple area representation for thermal unit commitments*. IEEE Transactions on Power Apparatus and Systems, 1981(3): p. 1212-1218.
  128. Pang, C. and H. Chen, *Optimal short-term thermal unit commitment*. IEEE Transactions on Power Apparatus and Systems, 1976. **95**(4): p. 1336-1346.
  129. Ouyang, Z. and S. Shahidehpour, *An intelligent dynamic programming for unit commitment application*. IEEE Transactions on power systems, 1991. **6**(3): p. 1203-1209.
  130. Rong, A., H. Hakonen, and R. Lahdelma, *A variant of the dynamic programming algorithm for unit commitment of combined heat and power systems*. European Journal of Operational Research, 2008. **190**(3): p. 741-755.
  131. Singhal, P.K. and R.N. Sharma. *Dynamic programming approach for solving power generating unit commitment problem*. in *2011 2nd International Conference on Computer and Communication Technology (ICCCT-2011)*. 2011. IEEE.
  132. Zavadil, R., *Wind integration study for public service company of colorado*. May, 2006. **22**: p. 2006.
  133. Yang, Y., et al., *Modelling and optimal energy management for battery energy storage systems in renewable energy systems: A review*. Renewable and Sustainable Energy Reviews, 2022. **167**: p. 112671.
  134. Stephan, A., et al., *Limiting the public cost of stationary battery deployment by combining applications*. Nature Energy, 2016. **1**(7): p. 1-9.
  135. Yang, Y., et al., *Battery energy storage system size determination in renewable energy systems: A review*. Renewable and Sustainable Energy Reviews, 2018. **91**: p. 109-125.
  136. Hao, J., et al., *Optimal unit commitment based on ant colony optimization algorithm*. Power system technology, 2002. **26**(1): p. 26-31.

137. Othman, M., et al., *Solving unit commitment problem using multi-agent evolutionary programming incorporating priority list*. Arabian Journal for Science and Engineering, 2015. **40**(11): p. 3247-3261.
138. Yamin, H.Y., *Review on methods of generation scheduling in electric power systems*. Electric Power Systems Research, 2004. **69**(2-3): p. 227-248.
139. Kerr, R., et al., *Unit commitment*. IEEE Transactions on Power Apparatus and Systems, 1966(5): p. 417-421.
140. Guy, J.D., *Security constrained unit commitment*. IEEE Transactions on Power apparatus and Systems, 1971(3): p. 1385-1390.
141. Saravanan, B., et al., *A solution to the unit commitment problem—a review*. Frontiers in Energy, 2013. **7**(2): p. 223-236.
142. Catalao, J., et al. *Profit-based unit commitment with emission limitations: A multiobjective approach*. in *2007 IEEE Lausanne Power Tech*. 2007. IEEE.
143. Ruzic, S. and N. Rajakovic, *A new approach for solving extended unit commitment problem*. IEEE Transactions on Power Systems, 1991. **6**(1): p. 269-277.
144. Cohen, A.I. and S. Wan, *A method for solving the fuel constrained unit commitment problem*. IEEE Transactions on Power Systems, 1987. **2**(3): p. 608-614.
145. Rajan, D. and S. Takriti, *Minimum up/down polytopes of the unit commitment problem with start-up costs*. IBM Res. Rep, 2005. **23628**: p. 1-14.
146. Wang, C. and S. Shahidehpour, *Effects of ramp-rate limits on unit commitment and economic dispatch*. IEEE Transactions on Power Systems, 1993. **8**(3): p. 1341-1350.
147. Muralikrishnan, N., L. Jebaraj, and C.C.A. Rajan, *A comprehensive review on evolutionary optimization techniques applied for unit commitment problem*. IEEE Access, 2020. **8**: p. 132980-133014.
148. Bruninx, K., et al., *Optimization and allocation of spinning reserves in a low-carbon framework*. IEEE Transactions on Power Systems, 2015. **31**(2): p. 872-882.
149. Moussouni, F., et al., *Optimization methods*. Exhaustive Enumeration (EE) method, EC Lille, France, 2007.
150. Lee, F.N., *The application of commitment utilization factor (CUF) to thermal unit commitment*. IEEE Transactions on Power Systems, 1991. **6**(2): p. 691-698.
151. Senjyu, T., et al., *Emerging solution of large-scale unit commitment problem by stochastic priority list*. Electric Power Systems Research, 2006. **76**(5): p. 283-292.
152. Lee, F.N., *Short-term thermal unit commitment-a new method*. IEEE Transactions on Power Systems, 1988. **3**(2): p. 421-428.

153. Tingfang, Y. and T. Ting. *Methodological priority list for unit commitment problem*. in *2008 international conference on computer science and software engineering*. 2008. IEEE.
154. Handschin, E. and H. Slomski, *Unit commitment in thermal power systems with long-term energy constraints*. IEEE Transactions on Power Systems, 1990. **5**(4): p. 1470-1477.
155. Redondo, N.J. and A. Conejo, *Short-term hydro-thermal coordination by Lagrangian relaxation: solution of the dual problem*. IEEE transactions on power systems, 1999. **14**(1): p. 89-95.
156. Sudhir, V., et al., *Implementation of a Lagrangian based unit commitment problem*. IEEE Transactions on Power System, 1989. **4**(4): p. 1373-1380.
157. Logenthiran, T. and D. Srinivasan. *Formulation of unit commitment (UC) problems and analysis of available methodologies used for solving the problems*. in *2010 IEEE International Conference on Sustainable Energy Technologies (ICSET)*. 2010. IEEE.
158. Guan, X., Q. Zhai, and A. Papalexopoulos. *Optimization based methods for unit commitment: Lagrangian relaxation versus general mixed integer programming*. in *2003 IEEE Power Engineering Society General Meeting (IEEE Cat. No. 03CH37491)*. 2003. IEEE.
159. Chen, C.-L. and S.-C. Wang, *Branch-and-bound scheduling for thermal generating units*. IEEE transactions on energy conversion, 1993. **8**(2): p. 184-189.
160. Cohen, A.I. and M. Yoshimura, *A branch-and-bound algorithm for unit commitment*. IEEE Transactions on Power Apparatus and Systems, 1983(2): p. 444-451.
161. Dillon, T. and G. Egan, *The application of combinatorial methods to the problems of maintenance scheduling and unit commitment in large power systems*. IFAC Proceedings Volumes, 1976. **9**(3): p. 39-50.
162. Taylor, B., *Integer programming: The branch and bound method*. module-C, 2001.
163. Land, A.H. and A.G. Doig, *An automatic method for solving discrete programming problems*, in *50 Years of Integer Programming 1958-2008*. 2010, Springer. p. 105-132.
164. Viswanath, A., L. Goel, and W. Peng. *Mixed integer programming formulation techniques and applications to Unit Commitment problem*. in *2012 10th International Power & Energy Conference (IPEC)*. 2012. IEEE.
165. Chang, G., et al. *A practical mixed integer linear programming based approach for unit commitment*. in *IEEE Power Engineering Society General Meeting, 2004*. 2004. IEEE.

166. Ghadirianari, R., M. Rashidinejad, and M. Fotuhi-Firuzabad, *A mixed integer linear programming based approach for unit commitment in smart grid environment*. Journal of Engineering Research, 2014. **2**(3): p. 1-28.
167. Van den Bergh, K., et al., *A mixed-integer linear formulation of the unit commitment problem*. WP EN2014-07, 2014.
168. CASTILLO, E. and E. ALVAREZ, *Uncertainty methods in expert systems*. Computer-Aided Civil and Infrastructure Engineering, 1990. **5**(1): p. 43-58.
169. Ouyang, Z. and S. Shahidehpour, *Short-term unit commitment expert system*. Electric power systems research, 1990. **20**(1): p. 1-13.
170. Li, S.-h., S. Shahidehpour, and C. Wang, *Promoting the application of expert systems in short-term unit commitment*. IEEE Transactions on Power Systems, 1993. **8**(1): p. 286-292.
171. Venkatesh, B., T. Jamtsho, and H. Gooi, *Unit commitment—a fuzzy mixed integer linear programming solution*. IET Generation, Transmission & Distribution, 2007. **1**(5): p. 836-846.
172. Sasaki, H., et al., *A solution method of unit commitment by artificial neural networks*. IEEE Transactions on Power Systems, 1992. **7**(3): p. 974-981.
173. Kalogirou, S.A., *Applications of artificial neural-networks for energy systems*. Applied energy, 2000. **67**(1-2): p. 17-35.
174. Kurban, M. and U.B. Filik. *Unit commitment scheduling by using the autoregressive and artificial neural network models based short-term load forecasting*. in *Proceedings of the 10th International Conference on Probabilistic Methods Applied to Power Systems*. 2008. IEEE.
175. Goldberg, D.E. and J.H. Holland, *Genetic algorithms and machine learning*. 1988.
176. Borghetti, A., et al. *Lagrangian relaxation and tabu search approaches for the unit commitment problem*. in *2001 IEEE Porto Power Tech Proceedings (Cat. No. 01EX502)*. 2001. IEEE.
177. Tang, H. and E. Miller-Hooks, *A tabu search heuristic for the team orienteering problem*. Computers & Operations Research, 2005. **32**(6): p. 1379-1407.
178. Padhy, N.P., *Unit commitment-a bibliographical survey*. IEEE Transactions on power systems, 2004. **19**(2): p. 1196-1205.
179. Selvi, V. and R. Umarani, *Comparative analysis of ant colony and particle swarm optimization techniques*. International Journal of Computer Applications, 2010. **5**(4): p. 1-6.
180. Sum-Im, T. and W. Ongsakul. *Ant colony search algorithm for unit commitment*. in *IEEE International Conference on Industrial Technology, 2003*. 2003. IEEE.

181. Gaing, Z.-L. *Discrete particle swarm optimization algorithm for unit commitment*. in *2003 IEEE Power Engineering Society General Meeting (IEEE Cat. No. 03CH37491)*. 2003. IEEE.
182. Sriyanyong, P. and Y. Song. *Unit commitment using particle swarm optimization combined with Lagrange relaxation*. in *IEEE Power Engineering Society General Meeting, 2005*. 2005. IEEE.
183. Mori, H. and K. Ohkawa. *Application of hybrid meta-heuristic method to unit commitment in power systems*. in *2008 IEEE Canada Electric Power Conference*. 2008. IEEE.
184. Victoire, T.A.A. and A.E. Jeyakumar, *A tabu search based hybrid optimization approach for a fuzzy modelled unit commitment problem*. *Electric Power Systems Research*, 2006. **76**(6-7): p. 413-425.
185. Zhang, X., J. Zhao, and X. Chen. *A hybrid method of lagrangian relaxation and genetic algorithm for solving UC problem*. in *2009 International Conference on Sustainable Power Generation and Supply*. 2009. IEEE.
186. Chang, W. and X. Luo. *A solution to the unit commitment using hybrid genetic algorithm*. in *TENCON 2008-2008 IEEE Region 10 Conference*. 2008. IEEE.
187. Su, C.-C. and Y.-Y. Hsu, *Fuzzy dynamic programming: an application to unit commitment*. *IEEE transactions on power systems*, 1991. **6**(3): p. 1231-1237.
188. Ouyang, Z. and S. Shahidehpour, *A hybrid artificial neural network-dynamic programming approach to unit commitment*. *IEEE Transactions on Power Systems*, 1992. **7**(1): p. 236-242.
189. Pelletier, F., C. Masson, and A. Tahan, *Wind turbine power curve modelling using artificial neural network*. *Renewable Energy*, 2016. **89**: p. 207-214.
190. Raj, M.M., M. Alexander, and M. Lydia. *Modeling of wind turbine power curve*. in *ISGT2011-India*. 2011. IEEE.
191. Schlechtingen, M., I.F. Santos, and S. Achiche, *Using data-mining approaches for wind turbine power curve monitoring: a comparative study*. *IEEE Transactions on Sustainable Energy*, 2013. **4**(3): p. 671-679.
192. Liu, Z., *Global energy interconnection*. 2015: Academic Press.
193. Peake, S., *Renewable energy-power for a sustainable future*. 2018: Oxford university press.
194. IRENA, *Renewable capacity statistics 2020*. 2020.
195. Layke, J., et al., *5 Things to Know About the IEA's Roadmap to Net Zero by 2050*.
196. IEA, *Net Zero by 2050*. 2021, IEA: Paris.
197. Taylor, M., P. Ralon, and A. Ilas, *The power to change: solar and wind cost reduction potential to 2025*. International renewable energy agency (IRENA), 2016.
198. IRENA, *Renewable Power Generation Costs in 2020*. 2021, International Renewable Energy Agency.

199. Madsen, H., J.M. Morales, and P.-J. Trombe, *Wind resource assessment and wind power forecasting*, in *DTU International Energy Report 2014: Wind energy—drivers and barriers for higher shares of wind in the global power generation mix*. 2014, Technical University of Denmark. p. 72-78.
200. Thygesen, J. and A. Agarwal, *Key criteria for sustainable wind energy planning—lessons from an institutional perspective on the impact assessment literature*. *Renewable and Sustainable Energy Reviews*, 2014. **39**: p. 1012-1023.
201. Anahua, E., et al. *Stochastic analysis of the power output for a wind turbine*. in *Proceedings of the European Wind Energy Conference-EWEC in London*. 2004.
202. Luo, G., et al., *Why the wind curtailment of northwest China remains high*. *Sustainability*, 2018. **10**(2): p. 570.
203. Barthelmie, R., F. Murray, and S. Pryor, *The economic benefit of short-term forecasting for wind energy in the UK electricity market*. *Energy Policy*, 2008. **36**(5): p. 1687-1696.
204. Liu, Z., et al., *A combined forecasting model for time series: Application to short-term wind speed forecasting*. *Applied Energy*, 2020. **259**: p. 114137.
205. Taylor, D., *Wind energy*. *Renewable Energy: Power for a sustainable future*, 2004: p. 244-293.
206. Philibert, C., H. Holttinen, and H. Chandler, *Technology Roadmap: Wind Energy*. International Energy Agency France2013, 2013.
207. Hasan Ali, M., *Wind energy systems: solutions for power quality and stabilization*. 2012: Crc Press.
208. Menezes, E.J.N., A.M. Araújo, and N.S.B. da Silva, *A review on wind turbine control and its associated methods*. *Journal of cleaner production*, 2018. **174**: p. 945-953.
209. Zhang, J., et al. *Pitch angle control for variable speed wind turbines*. in *2008 Third International Conference on Electric Utility Deregulation and Restructuring and Power Technologies*. 2008. IEEE.
210. Senjyu, T., et al., *Output power leveling of wind turbine generator for all operating regions by pitch angle control*. *IEEE Transactions on Energy conversion*, 2006. **21**(2): p. 467-475.
211. Arnalte, S., J. Burgos, and J. Rodriguez-Amenedo, *Direct torque control of a doubly-fed induction generator for variable speed wind turbines*. *Electric power components and systems*, 2002. **30**(2): p. 199-216.
212. Bakouri, A., et al. *Direct torque control of a doubly fed induction generator of wind turbine for maximum power extraction*. in *2014 International Renewable and Sustainable Energy Conference (IRSEC)*. 2014. IEEE.

213. Yingcheng, X. and T. Nengling, *Review of contribution to frequency control through variable speed wind turbine*. Renewable energy, 2011. **36**(6): p. 1671-1677.
214. Ela, E., et al., *Active power controls from wind power: Bridging the gaps*. 2014, National Renewable Energy Lab.(NREL), Golden, CO (United States).
215. Causebrook, A., D.J. Atkinson, and A.G. Jack, *Fault ride-through of large wind farms using series dynamic braking resistors (March 2007)*. IEEE Transactions on power systems, 2007. **22**(3): p. 966-975.
216. Ela, E., et al. *The evolution of wind power integration studies: Past, present, and future*. in *2009 IEEE Power & Energy Society General Meeting*. 2009. IEEE.
217. Khosravi, A., S. Nahavandi, and D. Creighton, *Prediction intervals for short-term wind farm power generation forecasts*. IEEE Transactions on sustainable energy, 2013. **4**(3): p. 602-610.
218. Yuan, T.-j., et al., *Short-term wind power output forecasting model for economic dispatch of power system incorporating large-scale wind farm*. Proceedings of the CSEE, 2010. **30**(13): p. 23-27.
219. Tapia, G., A. Tapia, and J.X. Ostolaza, *Proportional–integral regulator-based approach to wind farm reactive power management for secondary voltage control*. IEEE Transactions on Energy Conversion, 2007. **22**(2): p. 488-498.
220. Tarnowski, G.C. and R. Reginatto. *Adding active power regulation to wind farms with variable speed induction generators*. in *2007 IEEE Power Engineering Society General Meeting*. 2007. IEEE.
221. Zhao, J., Y. Fu, and D. Li, *Reactive power optimization in distribution network considering reactive power regulation capability of DFIG wind farm*. Automation of Electric Power Systems, 2011. **35**(11): p. 33-38.
222. Abbey, C. and G. Joos. *Effect of low voltage ride through (LVRT) characteristic on voltage stability*. in *IEEE Power Engineering Society General Meeting, 2005*. 2005. IEEE.
223. Conroy, J. and R. Watson, *Low-voltage ride-through of a full converter wind turbine with permanent magnet generator*. IET Renewable power generation, 2007. **1**(3): p. 182-189.
224. Lee, C.-T., C.-W. Hsu, and P.-T. Cheng, *A low-voltage ride-through technique for grid-connected converters of distributed energy resources*. IEEE Transactions on Industry Applications, 2011. **47**(4): p. 1821-1832.
225. Carrillo, C., et al., *Review of power curve modelling for wind turbines*. Renewable and Sustainable Energy Reviews, 2013. **21**: p. 572-581.
226. Ragheb, M., *Optimal rotor tip speed ratio*. Lecture notes of Course no. NPRE, 2014. **475**.
227. ENERCON, *ENERCON product overview*. 2015, ENERCON GmbH. p. 15.

228. Elmabruk, A.M., F.A. Aleej, and M.M. Badii. *Estimation of wind energy in Libya*. in *2014 5th International Renewable Energy Congress (IREC)*. 2014. IEEE.
229. Shcherbakov, M.V., et al., *A survey of forecast error measures*. World Applied Sciences Journal, 2013. **24**(24): p. 171-176.
230. Silbernagl, M., M. Huber, and R. Brandenberg, *Improving accuracy and efficiency of start-up cost formulations in MIP unit commitment by modeling power plant temperatures*. IEEE Transactions on Power Systems, 2015. **31**(4): p. 2578-2586.
231. Gao, D.W., *Energy storage for sustainable microgrid*. 2015: Academic Press.
232. Abdou, I. and M. Tkiouat, *Unit Commitment Problem in Electrical Power System: A Literature Review*. International Journal of Electrical & Computer Engineering (2088-8708), 2018. **8**(3).
233. Bellman, R. and R. Kalaba, *Dynamic programming and statistical communication theory*. Proceedings of the National Academy of Sciences of the United States of America, 1957. **43**(8): p. 749.
234. Giri, B.C., *Dynamic programming*. 2004.
235. Al-awaji, S.H., *Investigation and comparison of solution methods of the unit commitment problem for thermal units*. 1990, University of Strathclyde.
236. Fröhlich, C. and J. Lean, *The Sun's total irradiance: Cycles, trends and related climate change uncertainties since 1976*. Geophysical Research Letters, 1998. **25**(23): p. 4377-4380.
237. Smith, R.L., *Efficient Monte Carlo procedures for generating points uniformly distributed over bounded regions*. Operations Research, 1984. **32**(6): p. 1296-1308.
238. Polo, J., et al., *A simple approach to the synthetic generation of solar irradiance time series with high temporal resolution*. Solar Energy, 2011. **85**(5): p. 1164-1170.
239. Fatemi, S.A., A. Kuh, and M. Fripp, *Parametric methods for probabilistic forecasting of solar irradiance*. Renewable Energy, 2018. **129**: p. 666-676.
240. Jain, R., *Exploring NJWxNet Solar Radiation Observations*. 2020.
241. Hetzer, J., C.Y. David, and K. Bhattarai, *An economic dispatch model incorporating wind power*. IEEE Transactions on energy conversion, 2008. **23**(2): p. 603-611.
242. Boyle, G., *Renewable energy: power for a sustainable future*. Vol. 2. 2004: OXFORD university press Oxford.
243. Mahmood, F.H., A.K. Resen, and A.B. Khamees, *Wind characteristic analysis based on Weibull distribution of Al-Salman site, Iraq*. Energy reports, 2020. **6**: p. 79-87.
244. Justus, C., et al., *Methods for estimating wind speed frequency distributions*. Journal of Applied Meteorology (1962-1982), 1978: p. 350-353.

245. Stevens, M. and P. Smulders, *The estimation of the parameters of the Weibull wind speed distribution for wind energy utilization purposes*. Wind engineering, 1979: p. 132-145.
246. Carrillo, C., et al., *An approach to determine the Weibull parameters for wind energy analysis: The case of Galicia (Spain)*. Energies, 2014. **7**(4): p. 2676-2700.
247. Khalili, A. and K. Kromp, *Statistical properties of Weibull estimators*. Journal of materials science, 1991. **26**(24): p. 6741-6752.
248. Minami, F., et al., *Estimation procedure for the Weibull parameters used in the local approach*. International journal of fracture, 1992. **54**(3): p. 197-210.
249. Arslan, T., Y.M. Bulut, and A.A. Yavuz, *Comparative study of numerical methods for determining Weibull parameters for wind energy potential*. Renewable and Sustainable Energy Reviews, 2014. **40**: p. 820-825.
250. De Andrade, C.F., et al., *An efficiency comparison of numerical methods for determining Weibull parameters for wind energy applications: A new approach applied to the northeast region of Brazil*. Energy conversion and Management, 2014. **86**: p. 801-808.
251. Xuesong, Z., L. Ji, and M. Youjie. *Review on wind speed model research in wind power systems dynamic analysis*. in *2009 International Conference on Sustainable Power Generation and Supply*. 2009. IEEE.
252. Li, W. and B. Zhang, *Reliability impacts of large scale utilization of wind energy on electric power systems*. PROCEEDINGS-CHINESE SOCIETY OF ELECTRICAL ENGINEERING, 2008. **28**(1): p. 100.
253. Yichun, W., D. Ming, and L. Shenghu, *Reliability assessment of wind farms in generation and transmission systems*. Transactions of China Electrotechnical Society, 2004. **19**(11): p. 72-76.
254. Li, D.-d. and C. Chen, *Wind speed model for dynamic simulation of wind power generation system*. PROCEEDINGS-CHINESE SOCIETY OF ELECTRICAL ENGINEERING, 2005. **25**(21): p. 41.
255. Manwell, J.F., J.G. McGowan, and A.L. Rogers, *Wind energy explained: theory, design and application*. 2010: John Wiley & Sons.
256. Sun, J., *Research on wind farm modeling and simulating*. Beijing: Tsinghua University, 2004.
257. Welfonder, E., R. Neifer, and M. Spanner, *Development and experimental identification of dynamic models for wind turbines*. Control Engineering Practice, 1997. **5**(1): p. 63-73.
258. Observatory, H.K. *Winds at King's Park Meteorological Station*. 2021; Available from: <https://www.hko.gov.hk/en/wxinfo/aws/kpwind.htm#>.
259. Li, Q., et al., *On the determination of battery energy storage capacity and short-term power dispatch of a wind farm*. IEEE Transactions on Sustainable Energy, 2010. **2**(2): p. 148-158.

260. Runyon, J., *New solar is cheaper to build than to run existing coal plants in China, India and most of Europe*. 2021.
261. Altıntaş, O., et al., *Bi-objective optimization of a grid-connected decentralized energy system*. International Journal of Energy Research, 2018. **42**(2): p. 447-465.